Cooperative Connected Intelligent Vehicles and Infrastructure for Road Safety Applications

STEVEN ALAN KNOWLES FLANAGAN

Doctor of Philosophy

ASTON UNIVERSITY

January 2022

ASTON UNIVERSITY

Cooperative Connected Intelligent Vehicles and Infrastructure for Road Safety Applications

by Steven Alan KNOWLES FLANAGAN

Doctor of Philosophy, 2022

Abstract

Connected Vehicles (CV) and Autonomous Vehicles (AV) are two of the most promising modern vehicular technologies to tackle road safety challenges with advanced communications, sensor and Artificial Intelligence (AI) technologies. The primary motivation for this thesis is a study into the design and evaluation of connected and autonomous vehicles (CAVs) technologies for cooperative road safety applications.

As vehicular communication plays a critical role in CAV networks and road safety applications, this thesis designs, improves and evaluates a software-defined radio (SDR) based vehicle to everything (V2X) platform. It provides a scalable and more cost-effective solution for Dedicated Short-Range Communications (DSRC) and V2X research. Experiment results show the SDR-based DSRC can perform to the standards of commercial DSRC systems with high reliability of over 99%, low latency of 2.89 milliseconds and a communication range suitable for Vehicle to Vehicle (V2V) which is measured up to 250 metres. It maintained high performance whilst mobile and is proven capable of transmitting video data. This improved SDR-Based DSRC is an invaluable academic tool for the research community.

Furthermore, the V2X communication reliability and its impact on road safety are investigated. This is essential for modelling safety with communication capabilities. New algorithms for collision avoidance with V2V communication are designed and developed. V2V communication packet losses are measured and modelled. Its impact on stopping and safety distance is investigated. Simulation results show that V2V can effectively reduce vehicle reaction time, which decreases the stopping distance needed, and that the density of CV networks has a more significant impact on safety distance than the V2V communication distance. These investigations show significant impacts to safety when consecutive packet losses are incurred, leading to increased numbers of collisions.

Lastly, cooperative sensing among the CAVs and connected road infrastructure is investigated to improve road safety. As the sensors of AVs have inherent shortcomings, cooperation among CAVs and the infrastructure could help enhance the perception of the driving environment and make safe driving decisions. A novel Cooperative connected Road-infrastructure and Autonomous Vehicles (CRAV) framework is designed and developed with a scalable and flexible simulation approach. Various use cases with CRAV are studied to investigate the vulnerable road users (VRU) collision warning. A new approach to utilising the Responsibility-Sensitive Safety (RSS) model and CRAV is also designed to provide an appropriate safety distance to facilitate collision avoidance. Results show that with the support of Roadside Units(RSU), vehicles can be alerted to the presence of VRUs much earlier than

when using local sensors, up to a maximum of 80 metres. RSS with CRAV integration can significantly reduce road collisions, which is highly significant for reducing road fatalities and the results show collisions are reduced with the incorporation of these new algorithms for speeds up to 31 metres per second.

To sum up, this thesis presents an improved SDR based DSRC communication tool for academic research into V2X, an extensive investigation and creation of new algorithms for stopping distance and a novel CRAV framework simulation that compiles many areas needed for V2X into one complete system. The approaches taken in this thesis show significantly improved safety for road users.

Future work will be an extension of the SDR-based DSRC in large scale field tests and an incorporated automatic gain control. In addition, CRAV will be further developed to consider an expanded amount of safety scenarios and an investigation into the impacts of CRAV on road capacity.

Keywords: Collision Avoidance, CRAV, CAV, SDR, DSRC, Connected Vehicle

Dedicated to my family, Vincent
and Jay (RIP).
¡Hala Madrid! Y nada más

Acknowledgements

First and foremost, I would like to offer my sincerest thanks to my supervisors Dr. Zuoyin Tang and Dr. Jianhua He for their expertise, support and patience during the years towards PhD. My gratitude to Dr. Xiaohong Peng for his support throughout the initial stages of this study and for his guiding words.

I would like to thank Aston University, EPSRC and COSAFE for the studentship to conduct this thesis. A further thank you to Highways England and Phillip Proctor.

I would also like to express my appreciation for Dr. Irfan Yusoff (Ifrit) and Mala Sadik (Binder Buddy) for their assistance and support for the last few years, and for a cherished time which I will never forget.

To my family, Vincent and girlfriend, my sincerest thanks, for the support and encouragement that drove me to complete my thesis, without their understanding and patience, I would not have been able to complete my studies.

Finally, I would like to thank my brother Sam for being there through the good and bad times. M.C.I.D.

"So when the saints go marching in
They won't be singing for your sins
They just hope to Hell you've learned something
Living and breathing
Four walls in this prison
But I can still see the river
Four walls in this prison
Lies to poison your decisions in life, take note"

-While She Sleeps (2015)

Contents

List of Figures

List of Tables

List of Acronyms

AD	Autonomous Driving
ADAS	Advanced Driving Assistance Systems
AI	Artificial Intelligence
AV	Autonomous Vehicles
AWD	Actual Warning Distance
BPSK	Binary Phase Shift Keying
BSM	Basic Safety Message
CAM	Cooperative Awareness Message
CAV	Cooperative And Autonomous Vehicles
CRAV	Connected Road Infrastructure And AV
CV	Connected Vehicles
C-V2X	Cellular Vehicle to Everything
dB	decibel
dBm	decibel-milliwatts
DENM	Decentralized Environmental Notification Message
DSRC	Dedicated Short Range Communication
E2E	End to End
ETSI	European Telecommunications Standards Institute
FPGA	Fried Programmable Gate Array
FSPL	Free Space Path Loss
GHz	Gigahertz
GPS	Global Positioning System
Hz	Hertz
IPG	Inter Packet Gap
IS	Industry Standard
ITS	Intelligent Transport System
Kbps	Kilobit per Second
KBps	Kilobyte per Second
LAN	Local Area Network
LIDAR	Light Detection and Ranging
LoS	Line of Sight
LTE	Long Term Evolution
LTE-V	Long Term Evolution for Vehicles
M2M	Machine to Machine
MAC	Medium Access Control
MATLAB	Matrix Laboratory
Mbps	Megabit per Second
MBps	Megabyte per Second

MHz	Megahertz
mph	miles per hour
ms	millisecond
m/s	metres per second
NLoS	Non-Line of Sight
NTP	Network Time Protocol
OCB	Out-of-the Context-of-a Base-station/Basic-service-set
OFDM	Orthogonal Frequency-Division Multiplexing
PER	Packet Error Rate
PHY	Physical layer
PLR	Packet Loss Rate
PPS	Packets per Second
PRR	Packet Receive Rate
RADAR	Radio Detection and Ranging
RSS	Responsibility-Sensitive Safety
RSSI	Received Signal Strength Identifier
RSU	Road Side Unit
RTT	Round Trip Time
Rx	Receiver
s	Second
SDR	Software Defined Radio
SNR	Signal-to Noise Ratio
TCP	Transmission Control Protocol
TTC	Time to Collision
Tx	Transmitter
UE	User Equipment
UDP	User Datagram Protocol
USRP	Universal Software Peripheral
UWB	Ultra-Wide Band
V2D	Vehicle to Device
V2I	Vehicle to Infrastructure
V2P	Vehicle to Pedestrian
V2V	Vehicle to Vehicle
V2X	Vehicle to Everything
VANET	Vehicular Ad-hoc Networks
VC	Vehicular Communication
VLC	VideoLAN Client
VRU	Vulnerable Road User
WAVE	Wireless Access in-the Vehicular Environment
WLAN	Wireless Local Area Network
µs	microsecond

Chapter 1

Introduction

1.1 Introduction

Safer roads and safer driving are primary concerns that need addressing, and this can be achieved with the implementation of vehicular communication. Road accidents and congestion are some of the main issues for safety and are contributing factors leading the way to find solutions towards a safer and more efficient road system. The World Health Organization (WHO) reported that more than 1.2 million people suffered fatal road accidents in 2015 [1] and this rose to over 1.3 million in 2021 [2], with more than half of all road deaths being vulnerable road users. In the UK alone, the national statistics for 2019 state that approximately 2000 road-related fatalities occurred with a further 28000 serious injuries [3]. In addition to this, it has been reported that traffic congestion will lead to the loss of 90 billion hours per year spent in a vehicle, and this leads to an increase in pollution [4]-[5]. Inrix, a traffic data firm, has also reported that an average UK driver will lose 178 hours yearly due to congestion, which in turn leads to a loss to the UK economy of £7.9 billion [6]. In addition to these issues, congestion increases air pollution with the excessive wastage of fossil fuels; by improving efficiency, less time is spent idling on roads.

However, both Autonomous Vehicles (AV) and Connected Vehicles (CV) have been shown to have limitations currently. For example, AV relies on primarily sensing technologies. The problems can be highlighted with the fatal accident examples of the autopilot Tesla failure in 2016 [7], a self-driving Uber in 2018 [8], Waymo driverless cars being involved in 18 accidents [9] and the Tesla autopilot failure in 2021 resulting in two fatalities [10]. CV technologies rely upon the exchange of messages between communicating nodes, such as vehicles, and the impact of this technology is hindered because of the lack of market penetration, high cost and non-commercial availability [11]. In recent years the requirements for V2X have grown, such as with the evolving needs for more efficient and robust Advanced Driver Assistance Systems (ADAS) techniques and autonomous vehicle technologies, thus increasing the requirement for efficient, robust and low latency vehicular

communications that can support a multitude of ADAS techniques whilst supporting autonomous driving capabilities.

Cooperative and Autonomous Vehicles (CAVs) are changing how transportation is perceived, used and operated. As road traffic accidents and traffic congestion continue to be challenging issues in the global transport sector, it is hoped that CAV technologies can improve general road safety and reduce traffic congestion. Most of the current research is conducted on public roadways. It involves many corporations such as Uber with their self-driving taxis, Amazon with automated fleets and Tesla with their autopilot features. Safety in the CAV environment is highly critical and is one of the fundamental concepts that need to be addressed. The increase in safety has a tumble effect of consequences such as reducing road fatalities, less time spent on the road, reducing fossil fuel usage and easing the economy's loss due to hours spent on roads.

The future of vehicles is significantly changing, from being a combustion-powered machine used to get from one place to another to an electric, autonomous, fully connected device. This new generation of vehicles will offer many benefits such as fossil fuel reduction, a safer mode of transport and offering a more enjoyable travelling experience via additional in-vehicle services. A critical part of this is the adoption of wireless communication capabilities. Whether between vehicles, vehicles to infrastructure, vehicles to pedestrians or vehicles to the global network, forming a fully connected vehicle network is not just adding a component to vehicles. It is changing the definition of vehicles from mere transport to a globally connected transportation device. Communication is a crucial component towards reaching the full potential of autonomous vehicles, and it will be vitally important in forming Intelligent Transport Systems (ITS) [12]-[13]. There are many concerns about the adoption of this technology, as with any emerging enhancements, for example, 5G [14]-[15]. Therefore, the system selected and incorporated must have some key features, and these features are to enable user comfort, ensure robust connectivity, offer reliable communication and provide road user safety [16].

1.2 Research objectives

Safety is vitally important in the evolution and adoption of CAVs and still requires extensive testing and development. CV will be an essential tool and discovering the advantages and disadvantages of this technology is of high importance and the subject of many research projects. There are two leading competing technologies to be the standard used; these are known as 802.11p/DSRC/ITS-G5 [17]-[18] and 4G/5G Cellular Vehicle-to-Everything (C-V2X) [19]-[20]. These different technologies are

currently still being researched, developed, standardised and tested, and as such, there is still a debate about which will be adopted for CV or AV.

DSRC is based upon IEEE standards and is considered as the forerunner for Vehicle to Vehicle type communication and as many safety-based operations take place between vehicles [21]-[22]. This technology is vastly maturing, but most research is focused on the performance parameters of the devices rather than the application and practical usage. Existing technologies for DSRC are proprietary systems capable of only operating to the original manufacturer specifications, which reduces the reconfigurability and adaptability. Further works are concerned with developing connectivity instead of focusing on the application of the technology and critically analysing the most critical aspects of its application [23]. Collision avoidance is a massive part of vehicular safety, and many of the works concerning this focus solely on simulated analysis [24], [25], [26], [27]. Real-world testing is also essential to analyse the system and learn how it performs in the environment [28]-[29]. Currently, it is not yet standardised entirely. Much work still needs to be performed in the research towards vehicular communication and which technology will be used. Therefore, it is highly advantageous to analyse DSRC relating to safety over an extensive range of quantifiable areas and prove how this technology performs and its advantages.

This study aims to investigate the performance of vehicular safety-related concepts such as collision avoidance and stopping distances, focusing on identifying how communication will improve the development of safety systems that rely on different types of communication. An SDR-based DSRC transceiver has been developed to investigate the performance of DSRC and conduct measurements linked to real-world scenarios analytically over a variety of different performance aspects. The investigations are aimed towards safety-related performance and how it is applied to assist in collision avoidance. The DSRC transceiver will be built utilising a technology known as Software Defined Radios (SDR) which is beneficial for research purposes and will form the basis of a V2X platform. The platform is significantly more scalable than traditional DSRC, due to high cost of multiple devices and a more cost-effective solution for further V2X research.

Secondly, DSRC is incorporated into a collision avoidance scenario to compare the performance of stopping and safety distances with and without communication capabilities. V2X communication reliability is then considered, and the impacts on road safety are investigated. Novel algorithms are developed for collision avoidance. Additionally, V2X packet losses and measured and modelled for different loss scenarios, with their impacts on safety distance quantified.

Lastly, cooperative sensing and communications will be used to identify how

they can also increase safety. This investigation is performed in a Cooperative connected smart Road-infrastructure and AV (CRAV) framework to assess the impact of data fusion, pre-defined deep learning techniques and RSU information sharing and this done to show the difference between non CRAV enabled vehicles and CRAV enabled vehicles for detecting various safety occurrences. Various scenarios are designed to study the implications of safety for vulnerable road users (VRU) and AVs. In addition, a novel approach with Responsibility-Sensitive Safety (RSS) and a newly developed Actual Warning Distance (AWD) model are proposed to provide more accurate and appropriate safety distances. The implications of CRAV are to assess the safety benefits offered with and without RSU assistance for vehicles and different types of vulnerable road users.

1.3 Contribution

The availability of commercial DSRC devices is limited to expensive systems currently mainly used in automotive research and development by leading automotive vendors, such as Tesla, BMW, Audi and Ford [30], [31], [32]. Through design and development, SDR-based DSRC has been achieved with the modification of an existing open-source project [33] previously used to create a DSRC compliant transceiver. This modified SDR-based DSRC is based on Software Defined Radios, that can be used to emulate a traditional DSRC. The SDR implementation has been thoroughly examined, and various experiments performed to show the capabilities, disadvantages and advantages. SDR devices are a cheaper alternative to commercial DSRC, which is highly beneficial for the research community and offer many more benefits. They are also flexible in how they can be operated, allow on the fly configuration changes, are interoperable with open-source software and are highly scalable. Further to this, the adoption of vehicular communication could potentially be split between 5G, 4G, DSRC or other future technologies, and the network will not be fully connected if the V2X protocol differs per vehicle. SDR is fully adaptable, and thus the network selection can be altered on the fly, allowing SDR technology to operate as all V2X network types. However, SDR also has disadvantages such as it can be limited by the user's expertise, can be time consuming to initially configure, and features no direct interface to a vehicle.

Mathematical algorithms for stopping and safe distances are developed from the results of the experiments, and further simulated tests were performed. Pre-defined deep learning techniques for object detection and recognition and cooperative communications techniques for additional assistance are investigated, particularly for relaying vision detected obstacles or when in Non-Line of Sight (NLoS) conditions.

The research methodology initially investigates the fundamentals and background research relating to CAVs, Vehicular Ad-hoc Networks (VANET), infrastructure and the components of such systems. The research findings highlight areas that have not yet been fully utilised, such as using communication for safety distance maintenance, designing and developing algorithms for safety, simulation of various forms of consecutive packet loss and their impacts and cooperative relaying of information from video/deep learning. We then look at related research, highlighting the areas focused on safety and stopping distance. The focus then shifts to identify other associated technologies that have attempted to create DSRC implementations and show how the technologies could not meet the standards required for robustness, reliability and quality. We then show how we chose our system and the components, with further descriptions of our experiments and findings. Infrastructure communication is explored, developing a new framework towards cooperative, connected infrastructure and intelligent vehicles for the vehicle's safety and vulnerable road users.

This thesis has primary contributions which can be summarised into two categories:

1.3.1 Research contributions

The following list is a breakdown of each of the contributions made overall.

- Design and development of an SDR-based DSRC/802.11bd/p platform. SDR-based DSRC is flexible, scalable and a better approach for research and development whilst maintaining performance equal to the standards that are required for commercial DSRC systems such as the Cohda MK5. With high reliability, low latency and a communication range suitable for V2V. These findings are then applied for stopping distance for collision avoidance.
  - the design allowed easy customisation and adaptability and was created by improving an existing open-source project and then applied to V2V rear-end collision avoidance through the development of stopping distance algorithms. The SDR approach was taken as commercial devices may be adopted from different vendors with the same communication capability. On the other hand, SDR may be configured to adapt to use many communication types such as cellular and Wi-Fi. Performance attributes for DSRC are measured relating to robustness, latency, reliability, data rate, packet loss rate and throughput. These performance statistics are applied to stopping distance for vehicles and show the significant benefit for CAV by reducing stopping distance.

- Safety and stopping distance algorithms to improve collision avoidance
  - Algorithms have been designed and evaluated for both stopping and safety distances to show the increase in safety provided by communication capabilities. The algorithms are applied to field test results with related tests providing analysis and key performance aspects. The tests highlight how the usage of DSRC reduces the distance needed to allow a safer driving experience. In addition, the test evaluates the distance-based performance factors and data rate performance. This study gives new insights into vehicle communications for how data can be used and shared towards improving safety performance.
  - Field test data concerning various levels of losses is and categorised; distance independent, distance dependant and density based. These losses directly impact communication reliability, which concerns safety-related reliability. These losses are proposed with various algorithms to assess the impact on stopping and safety distance. Various tests are shown between fieldwork and simulations.
- Cooperative CRAV for intelligent vehicles and safe driving
  - A CRAV framework is designed and developed in a software-based form. Such an approach is novel as to the best of knowledge, connected smart road infrastructure and autonomous vehicles for safe driving has not been fully investigated. A decoupled framework is proposed in software, which can be used offline and easily adapted and modified. This framework is used to investigate the impacts of a connected roadside infrastructure with vehicles, and various use cases with CRAV are studied to investigate the VRU collision warning.
  - CRAV is used to show the advantages of sharing data between vehicles and infrastructure with cooperative models. The impact on RSU location to avoid potential collisions is evaluated under different sensor configurations. Local sensor data is compared with RSU data gathered through pre-trained deep learning and shared with CAV nodes. This investigation is performed over a wide range of scenarios and shows the inherent advantages of cooperative CRAV to identify the existence of VRUs on the road that are blocked from direct vision.
  - A novel approach to use RSS for safety in CRAV has been designed, with algorithms developed for safety and stopping distances to reduce collisions between vehicles and VRUs and rear-end vehicle collisions. In

addition, a novel method of identifying vehicle locations is produced to solve identified issues in other works when the location of a vehicle is a GPS coordinate, disregarding vehicle dimensions.

- an analysis of cooperative communication and the ability to relay information in the vehicular environment is provided and solves issues for NLoS. Highlighting the use for safety-related scenarios and giving new insights on delivering safety broadcasts to surrounding vehicles.
- CRAV is proposed for development in collision avoidance using different speeds. The effectiveness of CRAV is shown to reduce collisions between vehicles when appropriate spacing is used; the developed algorithms and infrastructure can provide that.

1.3.2 List of academic publications

This thesis is based on the following list of peer-reviewed publications and each has been specified to a chapter.

- Chapter 3
  - S. Knowles Flanagan, J. He, and X. H. Peng, "Improving Emergency Collision Avoidance with Vehicle to Vehicle Communications," Proc. - 20th Int. Conf. High Perform. Comput. Commun. 16th Int. Conf. Smart City 4th Int. Conf. Data Sci. Syst. HPCC/SmartCity/DSS 2018, pp. 1322–1329, 2019.
  - S. Knowles Flanagan, X. H. Peng, I. Yusoff, and J. He, "Empirical Investigation of SDR-based DSRC Communication," IEEE Veh. Technol. Conf., vol. 2020-May, pp. 0–4, 2020.
- Chapter 4
  - S. Knowles Flanagan, Z. Tang, J. He, and I. Yusoff, "Investigating and Modelling of Cooperative Vehicle-to-Vehicle Safety Stopping Distance," Future Internet, vol. 13, no. 3, p. 68, Mar. 2021.
- Chapter 5
  - Z. Tang, J. He, S. K. Flanagan, P. Procter, and L. Cheng, “Cooperative Connected Smart Road Infrastructure and Autonomous Vehicles for Safe Driving,” Proc. - Int. Conf. Netw. Protoc. ICNP, vol. 2021-November, 2021.

- Investigating the Safety Impacts of Cooperative CRAV for Safe Driving - Currently in Preparation
- Implications of Cooperative Connected Smart Road Infrastructure and Autonomous Vehicles for Road Safety - Currently in Preparation for Submission to the IEEE Network Magazine

1.4 Structure of thesis

The remainder of the thesis has been organised into five chapters, each pertaining to a different aspect. Chapter 2 is dedicated to a literature and background review into CAVs and related concepts, with further detail on communication technologies used and brief descriptions on the operation of each. There is also a short description of the fundamentals of the types of wireless communication and related attributes, which serve as the basis of the thesis works and will help emphasise the motivation behind the thesis and how the contributions are relevant.

Chapter 3 presents the development and investigation of DSRC via using SDR devices. The development and calibration procedure for SDR-based DSRC is shown. The tools used are introduced, explaining the testing and measurement scenarios performed to assess the reliability and quality of the performance and connectivity, particularly concerning V2V. Results are then presented with their impacts and relevance for CAVs, focusing on QoS and reliability. Each scenario is described for how measurements are taken and how they could improve safety for collision avoidance.

Chapter 4 utilises the results gathered in chapter 3 to enhance collision avoidance performance, focusing on developing real-world scenarios and related performance measurements, through an analytical model methodology. A new algorithm is designed as a tool for measuring and ensuring safety distance is maintained for V2V. The impacts of the consecutive losses identified in chapter 3, are explored in various scenarios. Mathematical processes, field tests and simulated proofs are used to assess the losses. These results are used to create models for differing types of safety distance, depending on the environment.

Chapter 5 presents cooperative, smart road infrastructure and CAV with the application of pre-defined deep learning techniques toward collision avoidance and intelligent vehicles. CRAV is a decoupled framework used to investigate scenarios to compare local sensors to those with RSU assistance. We also show an example of cooperative communication with and without pre-defined deep learning for object recognition, to share application-specific data. An assessment is also performed to analyse the performance for NLoS safety applications using cooperative relaying

systems using a newly developed set of algorithms. These algorithms are an evolution of RSS for CRAV and Actual Warning Distance (AWD) to highlight the difference between received data and real-world data. This process differs from chapters 3 and 4 and uses vehicle communication and V2I with RSU assistance.

Finally, in chapter 6, the thesis is summarised and discussed. The thesis is then concluded, and future directives are speculated.

This research project has received funding support from the European Union's Horizon 2020 research and innovation programmes under the Marie Skłodowska-Curie grant agreement No 824019 and grant agreement No 101022280.

This research was also supported by funding through Aston University, Engineering and Physical Sciences Research Council award 1957348, and Highways England.

Chapter 2

Background on Vehicular Communications

2.1 Introduction

Wireless communication has been a vital component of modern communication for many years. Starting from a simple radio transmission by Marconi in 1896 [34], to wireless transmission of data known as SMS [35], satellite communication [36] and to the modern technology of today enabling wireless internet connectivity in many forms [37]. Wireless communication has evolved and continues to do so at a rapid pace. The capability to transmit and receive information over wireless is an enthralling achievement, which continues to reach new capabilities. The elimination of the need for a physical medium to connect allows for communication in many forms. Examples are streaming information from Device-to-Device (D2D), body area networks through Bluetooth and ubiquitous connectivity for mobile phones and smart devices that allow interconnections between many more devices to interoperate and work together. This connectivity forms what is known as the Internet of Things (IoT). IoT is shifting focus from an individual being connected to having everything connected, wherever and always. One vital component of the next generation of wireless connectivity is the connected vehicle concept.

Vehicles are a quintessential component of everyday life, and to fulfil the goal of fully connected smart cities, it is vitally important that vehicles are always fully capable of being connected [38]. The research and development going into this goal continue at a fast pace, making vehicle transport into an intelligent transport system. The concept of a connected vehicle is to enable a safer, more efficient and comfortable experience for the user. For instance, the increase in safety will lead to fewer accidents and congestion, which has the ripple effect of reducing the usage of fuels leading to a reduction in pollution. For the user, safety is critical but not at the expense of comfort and experience; this must be achieved together. Figure 2.1

shows a mind map containing some vital features to vehicular communication. The centre of the mind map shows the core component enabling CV connectivity in red. The following essential features can be directly connected from the core and are the three crucial factors of user experience, capacity and safety in orange. The enabling components can be seen in yellow and green, which are the least important factors; however, they are essential for CV.

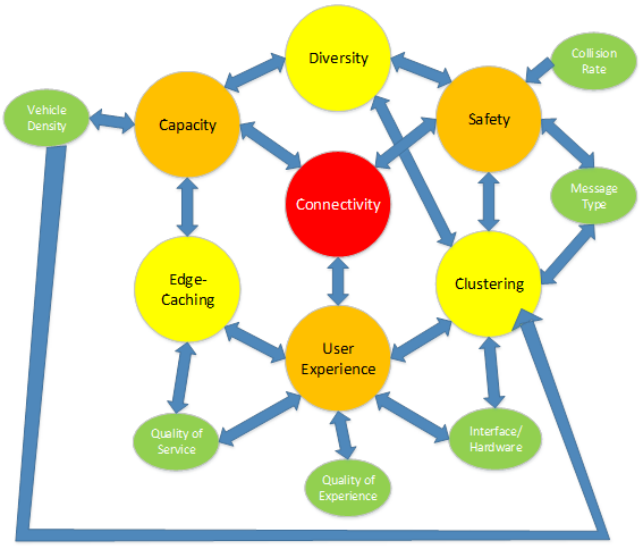

FIGURE 2.1: Mindmap of vehicle communication

One goal of the smart vehicle is fully autonomous driving, referred to as CAVs. CAVs are the combination of technologies and techniques to allow vehicles to communicate, share information and have heterogeneous knowledge of one another, although this is not strictly limited to vehicles. This cooperative collaboration will lead to a safer and more efficient road system and is currently an ongoing development for traditional Wi-Fi-based and cellular-based technologies, both used in conjunction with sensors. Wireless and vehicle communication fundamentals will be discussed to understand the debate for the candidate technologies, with further work shown in the current research area.

2.2 Wireless communication fundamentals

Wireless communication characteristics are determined by the choice of technology used. There are many variations of the technique ranging from earlier systems such as radio to the latest technologies such as cellular 5G and Wi-Fi 6, with further evolutions still in development. Depending on the type of technology used determines

their use case, many vital aspects must be considered when developing and selecting the appropriate solution. Wireless communication is a type of connection that allows data to be shared without a physical connection, and it enables far more options than those of wired networks. The basic principle of wireless is to utilise a source and destination system. The transmission medium is the channel, and the transmitter or receiving device is equipped with an antenna. An example is seen in Figure 2.2. This figure gives a general overview of wireless communication and an example scenario of a laptop accessing a server.

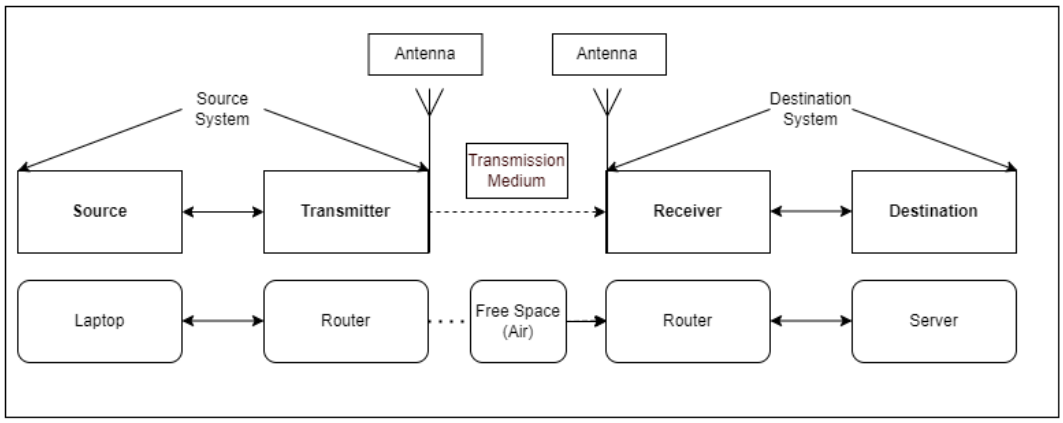

FIGURE 2.2: Block diagram of wireless communication basics

Wireless communication is a form of radio propagation at its core. With this comes the theory of free space being the channel, which is the environment between sender and receiver in clear Line of Sight (LoS) conditions, where there are no obstacles in the signal path. Wireless communication is the most used network type worldwide [39] There are continually newly emerging standards and technologies to enhance further and strengthen their performance. There are many forms of wireless communication, and along with this, there are many metrics used to measure performance.

There are multitudes of wireless communication available such as Bluetooth, infrared, ultra-wideband, cellular, Wi-Fi and many more. However, not all these types of communication suit the specific needs of vehicular communication. The specified technologies that are the primary contenders for the usage in CAVs are Wi-Fi-based and cellular [18], as they are the most mature and available options. This brief section will give an overview of many related wireless communication parameters that are used for testing wireless capabilities.

2.2.1 Wireless communication attributes

Wireless communication has many attributes used to measure different components as wireless is used in many different types of devices such as television, mobile phones, watches and vehicles. An understanding must be given for various terms used to describe the attributes used to describe and measure these communication types. The following section defines the most important aspects commonly used in wireless communication and will be used throughout the thesis.

Signal-to Noise Ratio (Power)

SNR is a measurement of power used to indicate the strength of a signal compared to background noise or a ratio between the information signal and unwanted signals. It is an important measurement that determines the ability of a receiver to distinguish between information and noise [40]. This is represented in Equation 2.1.

$$SNR(dB) = \frac{P_{Signal}}{P_{Noise}} \; or \; SNR(dB) = 10log_{10}(P_{Signal}) \tag{2.1}$$

Data rate

The data rate measures the transmission speed, or the number of bits/bytes transmitted per second [41]. Represented in Equation 2.2.

$$Data\ Rate\ (bps) = Packets\ Sent * Packet\ Size \tag{2.2}$$

Range

The range is a measurement of distance used to denote the maximum distance that communication can be transmitted over. This is commonly determined by the signal strength and calculated by the SNR. In the case of wireless communication, the range is determined to be the communication range, which dictates how far a signal can be propagated and received. This measurement is usually taken in metres or kilometres.

Reliability

Reliability is a term used to emphasise how reliable a communication link is. This is often a ratio between the number of packets received and the number of lost packets. This can be represented as either being packet error rate (PER), packet loss rate (PLR) or packet success rate (PSR) [42]. Represented in Equation 2.3 for PER.

$$PER(\%) = Packets\ lost / Packets\ sent \tag{2.3}$$

Path loss

Path Loss is an exponent used in communication, and one form most commonly used in wireless is Free Space Path Loss (FSPL). It measures the losses incurred by a signal through the air where the path is free from any impediments such as obstacles. The measurement of FSPL is classified as propagation loss due to signal attenuation[43]. FSPL is represented in Equation 2.4.

$$FSPL, or, L_f\ (dB) = \left(\frac{4 * \pi * f * d}{c}\right)^2 \tag{2.4}$$

Where c represents the speed of light, d is used for the distance between antennas and f denotes the frequency being used.

Latency or delay

Latency is a measurement of time used to represent the interval between the information sent by a transmitter and the information received at the receiver. It can be measured as the end to end latency from transmitter or receiver or round-trip latency/time. This time is split into two types,

- the queueing or processing delay: the time taken for the packet to reach the transmission medium, this is the most critical delay in wireless communication, as it is the delay incurred by the hardware and software components. Shown in Equation 2.5. Where L represents packet length and R represents transmission rate.
- the propagation delay: the time taken for the packet to travel across the transmission medium to the destination. Shown in Equation 2.6. Where d represents the distance between nodes and c represents the speed of light.

$$T_T(s) = L/R \tag{2.5}$$

$$T_P(s) = \frac{d}{c},\ c = \text{speed of light} \approx 2.9 \times 10^8 \tag{2.6}$$

2.3 Vehicular communication fundamentals

The modern vehicle is vastly different from previous decades, where vehicles relied mostly on mechanical features to control and operate the vehicle. Electric vehicles have become more common, and autonomous vehicles are the next trend [15].

Vehicular communication is the term given to represent the concept of communication and networking when relating to a connected vehicle or vehicular network. There are many forms of this type of communication. It is not solely limited to vehicles communicating with one another, but rather a vehicle communicating with another 'thing', known as Vehicle to Everything (V2X) [44]. As the technology and techniques are continually evolving toward wireless communication for vehicles, the fast rate and growth emphasise the need for supporting technologies and infrastructures capable of meeting the high requirements of this worldwide system. Two main competitors are the options for the Intelligent Transport System (ITS) future. They utilise different types of communication and are defined differently depending on the country or continent they are being developed for [45]-[46].

2.3.1 Connected and Autonomous Vehicles (CAVs)

CAVs are a future goal, with fully connected automated self-driving vehicles. They will form what is known as the ITS [47]-[48]. CAVs utilise many communication techniques to form a network between vehicles (V2V) and infrastructure (V2I), amongst other such types. A prominent component of CAVs that holds a great potential to build vehicular cooperation and mutual awareness is the Vehicular Ad-hoc Network or VANET. Two main competitors are the options for the future of ITS/CAVs, and they utilise different types of communication. Firstly, the two competing technologies are a traditional Wi-Fi-based system adapted for vehicular needs with an improved standard known as 802.11p/DSRC [49] or ITS-G5. The second technology is cellular networks, with slight amendments known as 4G LTE-V2X and future 5G/C-V2X[50]-[51]. A vast amount of research is invested in the growing area of vehicular communications, leading to fully Autonomous Driving (AD). Technology and communications must continue to evolve for AD to meet the needs of this highly complex communication network to enable efficient data dissemination. The ITS refers to all types of transport being connected, via ad-hoc, infrastructure or other such devices, and CV is primarily focused on the communication of road vehicles [52]. There are many types of communications systems that are in the field of CV, and the two most prominent and researched are Vehicle to Vehicle (V2V) and Vehicle to Infrastructure (V2I), which form a part of V2X.

There are six stages to this plan ranging from zero (no autonomy) to five (full autonomy) and DSRC is an enabling component of autonomy; these stages are shown in Figure 2.3 and are based upon the Society of Automotive Engineers (SAE) international standard J3016 [53] and the Organisation Internationale des Constructeurs d'Automobiles (OICA) levels of automated driving [54]. This research whilst not contained to a level, the need for communication will be a core component of reaching level five.

SAE Level	Name	Narrative Definition	Execution of Steering and Acceleration/ Deceleration	Driving Environment Monitoring	Fallback Performance of Dynamic Driving Task	System Capability (Driving Modes)
Human driver monitors the driving environment						
0	No Automation	Human driver performs full time performance of all conditions of *dynamic driving tasks*, even with the use of warning and intervention systems	Human Driver	Human Driver	Human Driver	n/a
1	Driver Assistance	Driver assistance system performs *driving mode* specific actions, either steering or acceleration/deceleration utilising driving environment information, human driver performs all other *dynamic driving tasks*	Human Driver and System	Human Driver	Human Driver	Some driving modes
2	Partial Automation	Driver assistance system performs *driving mode* specific actions with the use of one or more systems, of both steering and acceleration/deceleration utilising driving environment information, human driver performs all other *dynamic driving tasks*	System	Human Driver	Human Driver	Some driving modes
Automated driving system monitors the driving environment						
3	Conditional Automation	Automated driving system performs all *driving mode* specific actions relating to the *dynamic driving task*, with the human driver expected to respond appropriately when *requested to intervene*	System	System	Human Driver	Some driving modes
4	High Automation	Automated driving system performs all *driving mode* specific actions relating to the *dynamic driving task*, even if the human driver does not respond appropriately when *requested to intervene*	System	System	System	Some driving modes
5	Full Automation	Automated driving system performs full time all *driving mode* specific actions relating to the *dynamic driving task* under all road and environment conditions that can be managed by the human driver	System	System	System	All driving modes

FIGURE 2.3: The six levels of autonomous driving [55]

CAV technology is currently under scrutiny to determine which wireless communication will be utilised. Currently, the most mature options are 802.11p or DSRC, LTE-V2X or a hybrid heterogeneous network [56]-[57]. DSRC is one of the most researched types and is the only technology currently commercially available. It is formed as part of the IEEE 802.11 standards and operates via an on-board communication device used for communicating with other vehicles on the 5.9GHz band. The DSRC device is used for message exchange, and the core message defined by the SAE is the basic safety message (BSM). This message contains data about the vehicle location, speed, brake operation, direction heading and safety-related messages [58]-[59]. This message broadcasts situational data to local vehicles [60].

Sensing is an important aspect of the development of CAVs. They can supply efficient information to the vehicle, which can be used by the vehicle with the sensors or relayed to other vehicles for cooperative collaboration. A review of sensing and

communication factors has been performed in [61], and they analyse different types of sensing available and the benefits or drawbacks they will offer CAVs. Radio Detection and Ranging (RADAR), Light Detection and Ranging (LIDAR), camera and acoustic sensors are some of the reviewed sensors, and they propose a fusion of sensors and communication will be the greatest advantage for CAV development. This approach is further highlighted in [62], where the authors propose a LIDAR and positioning sensor fusion algorithm used with V2V will be the optimal safety solution; they detail the advantages this will provide and state this must be realised in future. They show an example scenario with a rover equipped with a Global Positioning System (GPS) and LIDAR that significantly increases position accuracy when both systems are used instead of just one.

Finally, in [63], they propose using V2V as a sensor for cooperative driving. The authors propose that V2V can relay information, combine the supplied information, and share it with other drivers. This approach effectively renders V2V as a sensor communication device. They do, however, note the application logic will have to be significantly sophisticated at dealing with and fusing large and varied data amounts.

2.3.2 Vehicle to Everything (V2X)

Vehicle to everything is a term that groups all types of communication in this area under one term; there are, however, many different branches to V2X. These branches enable different communication types to occur and relay information between any parties involved for many multiple different reasons. V2X can be split into many types of communication, for example; Vehicle to Vehicle (V2V), Vehicle to Infrastructure (V2I), and can also include Vehicle to Pedestrian (V2P) and Vehicle to Network (V2N), the use of these various techniques is to enable autonomous driving.

The origin of V2X communication is based upon the concept of Device to Device (D2D). However, non-proprietary V2X suffers many issues relating to inter-cell interference, high latency and poor reliability[64]-[65]. This concept led to an increased interest in research and the evolvement of hardware designed for these use cases. Though originally envisaged for use with safety applications, the technology has been expanded to include enhancements for traffic efficiency, provide the ability to use infotainment services and increase user quality of experience [66].

2.3.3 Vehicle to Infrastructure (V2I)

Vehicle to infrastructure is a node to node exchange of information, usually from vehicles to roadside units. This method enables communication to be used anywhere in the surrounding area or even countrywide. The capabilities provided by

V2I are continually expanding and highly important within the automotive sector, and it has been theorised that 80% of accidents can be avoided using this technology. Problems that can be avoided include traffic congestion, parking spot locating, and fuel wastage at traffic stops, all of which can be mitigated with V2I assistance [67].

Primarily the usages again are for the information to be used for safety or traffic management, via information being passed to road agencies or even emergency services. For example, if a vehicle sees a crash, the information will be sent to an RSU node and passed along anywhere necessary. An added benefit to V2I is the ability to allow road surveys from vehicles, allow governments to plan new roads, plan road development, and even for traffic companies to analyse road conditions.

A future implementation of V2I is to reduce the use of road signage and instead use roadside sensors for advertising roadside information to the driver. However, a problem with V2I will be if other vehicles are not connected, as they will appear invisible to V2I structures.

Signal Phase and Timing (SPaT) is the biggest type of V2I investigation, which incorporates vehicle information over time to optimise vehicular patterns and adequately manage traffic flow in areas. SPaT also helps vehicle owners by optimising time and providing fuel economy.

Nwiziege et al. propose that the key challenges for V2I are achieving high mobility and high data rates whilst maintaining the use of 802.11 standards to maintain a high quality of service. They recommend the use of a Rate Adaptation Algorithm (RAA) to control and manage these factors [68].

With a complete ITS framework, V2I will perform real-time data transmission, allowing infrastructure data to be processed and used for services non-local. V2I includes things such as paying toll systems [69], identifying car parking spaces, avoiding congestion and providing real-time travel advice to passengers [70].

Lin et al. compare 802.11a and 802.11p for V2I communication [71], and they analyse the throughput over a distance from 25-475 metres. The results show that 802.11p has a significant advantage due to the lack of authentication required, and thus throughput and connection time are much higher.

2.3.4 Vehicle to Vehicle (V2V)

Vehicle to vehicle is one of the most important technology concepts to arise in vehicular communications technology. However, it is also one of the most challenging. The main concept of V2V is an automobile technology designed to allow communication between vehicles on the road. Usually, this is with an ad-hoc connection or VANET utilising DSRC/C-V2X technology. This communication is a wireless

exchange of data, providing many types of information, with one of the core information sources relating to safety.

This type of vehicular communication is a necessity for the primary area of safety. Vehicles will pass along known information from other vehicles, advertising their locations via GPS information, direction, speed, and other information relating. Further areas of V2V are accident avoidance and detection, advertising road conditions, share route information and traffic information.

A V2V approach taken by Tian of Beijing University is to produce a self-adaptive system via SDR. [72]. Their proposal will include the DSRC and WAVE standards associated with V2V, and the platform is based upon a Linux OS. The system comprises a self-written program adapted to both a host and router side. The system then analyses many performance factors emulating driving conditions to test viability.

V2V applications

Further works have been investigating the use of broadcast communication in V2V scenarios, such as in [73], where the work models broadcasting schemes for V2V using a self-designed vehicle module using ultrasonic sensors. The sensors record information for object detection and relay the information to the driver. However, their results only prove that the system will detect obstacles, with no definition between what is sensed and how it can be broadcast and shared with others.

Platooning is another area of CV and V2V that uses the beacon message. The work in [74] uses a simulation platform to analyse the impact of 802.11p communication on the performance of platooning. Their simulation framework was used to monitor how the acceleration and spacing between vehicles are impacted using 802.11p to supply the data from the following and lead vehicles. The results showed a significant increase in performance when using communication to relay data cooperatively; however, they note that performance significantly decreases when the platoon size grows larger. This decrease can be mitigated by limiting the platoon size, bit error rate and packet arrival rate. With these inclusions, the robustness required for V2V can be satisfied.

A similar study for platooning has been completed by a joint effort between Nokia and Vodafone, and they analysed the performance of highway platooning using V2V with both C-V2X and 802.11p solutions [75]-[76]. Their simulation was conducted using a simulated ten vehicle platoon and a lead vehicle known as a jammer. They monitor the inter-vehicle spacing and use latency and reception rate as the measurement metrics. Their results show that 802.11p is suitable to provide day one safety services and their measurements show it meets requirements. They

also show that C-V2X meets these standards and will be more applicable for future scenarios.

A survey was also conducted for DSRC V2V truck platooning scenarios, with the evaluation being performed in a test track filed test [77]. They used metrics such as latency, packet delivery ratio, message losses and pairwise delivery ratio to analyse the performance of V2V and used various antenna positions on the truck vehicle to analyse how different locations alter performance. Their findings show that up to 78 metres DSRC maintains a 100% delivery ratio and that high data rates and large message sizes lead to a lower successful delivery ratio. The findings relating to antenna position show that non-parallel truck alignment can lead to a low delivery ratio, but this can be improved when the terrain leads to reflected signals. Their final noteworthy point is that the message broadcast is mostly impacted by low layer components, such as hardware rather than the environment.

Road safety is a primary concern of these technologies. As can be seen in Table 2.1 the details briefly describe the types of alerts that will be used as signals within vehicles and have been collated in a vehicular networking survey [78]-[79].

2.3.5 Vehicle to Device (V2D)

Vehicle to device is not such a key area for this project however should be explained. V2D is a term used for connecting vehicles to devices, and this can be either Bluetooth devices, keyless entry devices, mobile phones or even cellular services. However, this is mainly used for recreational purposes rather than to offer any safety reasoning.

A few reasonable uses for the V2D are vehicle tracking systems, anti-theft devices, keyless entry, mobile broadband hotspot and mobile phone connectivity. However, the most prevalent usage is mobile phone application integration, aiming to provide a wider variety of information to passengers such as locational information, traffic updates and even application aiming to improve safety [70].

2.3.6 Vehicle to Pedestrian (V2P)

Vehicle to pedestrian is another area currently being investigated, especially by the United States Department of Transport (USDOT). This area will not be greatly explored as the usage is out of this project's scope; however, it will be briefly detailed. The main idea is that a detection system can be implemented into the ITS infrastructure or directly use pedestrians. This approach is achieved via the use of vehicles systems based on V2V but adjusted for the sensing of pedestrians. The approach can also be with pedestrians carrying handheld devices, such as a mobile phone.

TABLE 2.1: Road safety alerts.

Type of Alert	Intended Action
Intersection Collision Warning	A warning that is given to vehicles at intersections about collisions that have been detected
Lane Changes	Vehicles are alerted when a vehicle in a blind spot is changing lanes.
Overtaking vehicle warnings	Vehicles send an alert to others that they are performing an overtaking manoeuvre.
Head-on Collisions	Warnings are sent as a broadcast to vehicles travelling in the opposite direction. This may be just a general warning or warning not to overtake slower vehicles.
Rear Collision	Warns following drivers of intent to slow down due to problems.
Collision warning	This type of warning is issued cooperatively by other vehicles informing drivers of an accident and to use alternative routes.
Emergency vehicle alerts	information is broadcast from emergency vehicles to other vehicles in a specific area to clear space and make room for their passing or entry.
Pre-crash sensing/warning	A warning that an unavoidable crash is about to occur. Nodes will share information, and with statistical evidence, crashes will be predicted. Life-saving equipment and actions can be deployed.
Merging assistance	Vehicles merging into the same lane can alert each other and cooperate to achieve this without collision.
Emergency brake alert	If a vehicle needs to perform an emergency braking manoeuvre, other drivers will be alerted of this.
Stationary vehicle	A warning will be emitted from a stationary vehicle informing neighbouring nodes that it is immobile either due to an accident or mechanical breakdown.
Traffic conditions	Varied traffic circumstances and events will be alerted to other nodes in the area.
Signal violation	Roadside units will alert drivers of potential situations where vehicles have intentionally or unintentionally ignored traffic control, such as driving through a red light.
Collision risk	Roadside nodes will detect collisions between vehicles that cannot warn other vehicles, such as legacy cars without smart capabilities.
Hazardous location warnings	Warnings to advertise hazards such as black ice, obstacles, accidents, debris or road works.
Control loss alerts	A warning issued that a vehicle driver could lose certain instruments such as indicators or lights.

The utilisation of this will vary, but some of the more advanced applications are applications for pedestrians with disabilities that will alert vehicles drivers of their presence at blind turns or road crossings. Another use is the application of automated technologies developed to brake a vehicle to avoid striking a pedestrian automatically. This system will be known as pedestrian crash avoidance and mitigation system [80]. The belief is that these systems, when implemented, will be possible to eliminate up to 46% of unimpaired pedestrian accidents.

2.4 Vehicular communication technologies

The following section outlines the main competing technologies used for vehicular communication. Detailing the standard, they represent, how they work and current research involved.

2.4.1 DSRC/Automotive WLAN IEEE 802.11p

DSRC is one technology used for vehicular communications and is based on the IEEE 802.11 standard amendment. This standard is 802.11p [81] and has been built from the 802.11a standard with incorporations for QoS from 802.11e [22]. More recently, it has been designated as 802.11bd [82]-[83] with even more changes to the standard [84]-[85], which are aimed towards high reliability, low latency and high throughput. This standard is also designated as DSRC [86] in America and ITS-G5 in Europe [87]-[88]. Although commercial devices are proprietary and expensive, it is available currently, limiting the research community's availability.

The usage of DSRC stems from the short-range radio technologies and, more particularly, the wireless LAN. 802.11p is based on the 5.9GHz frequency band with a 75MHz bandwidth split into seven 10MHz channels with one channel reserved for control at 5MHz. The 10MHz channels are half of those of 802.11a and were specified to eliminate the interference evident in the vehicular communications environments [71],[89]. However, in 2020 the allocation in America was reduced, with 45MHz at the lower end reallocated due to slow deployment [90]. 802.11p standard has had two main extensions to make it applicable for vehicular communications. The first is the operation in the 5.9GHz frequency ITS bands, and the second is an amendment to the MAC layer. This change to the MAC is 802.11OCB and means Outside the Context of a Base Service Set (OCB) [91], which allows vehicles to communicate without being involved in a BSS, however, with reduced functionality. The approach is geared towards vehicles as it omits the need for authentication or association procedures, such as the handshake procedure and instead uses pre-defined

parameters to communicate information. This method can be applied as a wildcard called broadcast communication, whereby all vehicles within a communication range can receive a message [84], [92].

This extension is also known as IEEE WAVE (Wireless Access in Vehicular Environment) in the US [93],[94] and ETSI C-ITS in Europe [47]. They are a higher layer protocol dedicated to regulating and standardising the 802.11 standards in their respective continents. These standards are predominantly the same; however, they have some differences, such as the message types used, but are both based on 802.11p.

ITS is the European ETSI standardised higher protocol stack implemented for vehicular communication and is similar to the IEEE WAVE in that it uses the 802.11p as a fundamental. However, it has some amendments to fit the European ECC regulations and is known in technical terms as ITS-G5 [70], [95]. The use of ITS-G5 does not adopt a single transceiver system, and it instead uses two transceivers with one permanently in the safety control channel. In this thesis, the use of DSRC/802.11p/ITS-G5 will refer to the basics of the application rather than higher-level region changes.

The most recent amendment to the 802.11 vehicular WLAN has been given the standard as 802.11bd and is an enhancement towards the next generation of V2X. As the need continues to share information between vehicles, it has been clear that this needs to be reliable and low latency to support safe use scenarios. In [83], they discuss the current limitations of 802.11p and the difficulty it has in supporting a high level of autonomy, and they present 802.11bd evolutions such as the use of the 60GHz range, support for speeds up to 500km/h and higher performance such as a much lower bit error rate. However, they note that interoperability between .11p and .11bd could be an obstacle and instead suggest a coexistent model.

The reliability of .11bd has also been reported in [85]. They give an overview of the composition of .11bd detailing the PHY and MAC changes; they also show research that highlights the effect of Doppler shift as the most prevalent detractor in .11bd performance. Further simulated work has been done comparing .11bd and .11p, with coded models for each tested for packet reception ratio, bitrate and latency [83]. They find that .11bd outperforms .11p in every category, with PRR most significant at 88% in .11bd and 75% in .11p.

The premise of V2X is to use the different communication types to provide efficient and robust road safety, traffic efficiency and infotainment. Two types of messages are considered for V2X. These messages are taken from the ETSI specification and are classified below. They are split into two categories; Cooperative Awareness Message (CAM) [96],[97] and Decentralized Environmental Notification Messages (DENM) [97].

Cooperative Awareness Messages - CAM

CAMs are effectively a beacon message type, transmitting at a specified time-frequency such as 1 second. It takes the form of a short message broadcast to all neighbours providing information relating to location, presence, positioning, kinematics, telematics and basic status. They have various use cases such as emergency vehicle warnings [98], indicating a slow-moving vehicle, collision warnings, motorcycle awareness messages and speed limit notification. Multiple studies have recognised this message type as the message used for V2V communication, utilising a one-hop broadcast transmission [99].

The CAM messages are broadcast from a transmitting node to any receiving node. It should be stated, however, that there is a limit to the distance that the CAM message can be transmitted; the transmit power decides this, usually a few hundred meters; this can be classified as an awareness range [60]. Below is a list of the specifications for CAM type messages:

- Frequency: 1-10 Hz
- Max Latency: 100 ms
- Length: 800 bytes

Decentralized Environmental Notification Messages - DENM

DENMs are an event-driven triggered message type, which is again a short broadcast but different to CAMs as it is event triggered, meaning it is also broadcast when triggered by a pre-defined set of rules. This message will be formed of largely the same information as the CAM; the purpose differs as this message type is used solely for safety-related and hazard warning messages. The use cases of a DENM are shown in Table 2.2 and is taken from a whitepaper report by Ericsson [100].

DENM messages are another broadcast message type, but this message will be sent to both other vehicles and the infrastructure for the information to be shared somewhat locally.

Below is a list of the specifications for DENM type messages:

- Max latency: 100 ms
- Length: Shorter than CAM

2.4.2 Cellular-V2X (4G/5G)

The 3GPP mobile broadband initiative governs cellular networking standards, and this body is responsible for the various releases attaining cellular standards and

TABLE 2.2: DENM use cases

Use Case	Triggering Cause	Terminating Conditions
Emergency Brake Light	Hard Braking	Automatic after expiry time
Collision risk warning	Detection of Turning/crossing/merging collision by RSU	End of collision risk
Stationary vehicle due to accident	eCall Triggering	Vehicle involved in an accident is removed
Stationary vehicle due to breakdown	Vehicle hazard or breakdown warnings	vehicle is removed from road
Traffic jam warning	traffic jam detection	end of traffic jam
Road work warning	signalled by road station	end of road work
Adverse weather conditions	Detection of weather (Rain/Snow)	Detection of end of situation
Road adhesion (Ice)	Detection of slippery road conditions	Detection of end of situation

specifications [101],[102],[103]. Initial use of cellular technology started with 4G LTE and LTE-A. However, the latest specified release, LTE-V2X, has been significantly altered to enable vehicular communications before the move in the future to 5G.

LTE-V2X, or in China previously known as LTE-V, is a standard released by 3GPP for the primary concern of vehicular communication and aims to address the shortcoming that rendered the previous release of LTE unsuitable. LTE-V2X was a candidate technology, and many studies have investigated its usage with vehicle type communications and benefits or deficiencies it may have. However, LTE-V2X is seen as only a precursor and can only be considered for partial automation and driver assistance [104]. Due to the high cost of practical fieldwork, no current large capacity systems have been implemented. Therefore, significant simulations have been completed with varying results. Such findings prove the capability in terms of latency and capacity to meet ITS requirements. Other studies find that the network can become overloaded without a connectivity model adequate for management [105]-[18].

5G is the future of mobile communication but is also seen as a part of the future for vehicular communication too [106]. For this to happen, however, certain standards and requirements must be met and proven before this can be implemented worldwide. The current standards that need to be met are listed in Table 2.3 and can be found in [20], [107].

TABLE 2.3: 5G standards.

Attribute	Requirement
Peak Data Rate	Downlink: 20 Gbps, Uplink: 10 Gbps
Latency	1 ms for AV
Connection Density	1 million devices per square km
Mobility	Operate at relative speeds of 0 km/h to 500 km/h
Energy Efficiency	Low energy and low energy power save
Spectral Efficiency	Assuming 8x8 MIMO, Downlink: 30 bits/Hz, Uplink: 30 bits/Hz

2.4.3 Enabling technology for C-V2X

Building upon the context of individual message types for V2V and V2I messages, C-V2X utilises an individual interface associated with each individual, and these interfaces are known as the PC5 and Uu interfaces [108].

PC5 Interface

PC5 is used for direct mode communications and is built upon the LTE-direct or Sidelink device-to-device concept, with standards adjusted and created solely for vehicular usage, with amendments for adaptability at higher speeds, doppler reduction, high-density, low latency and rapid synchronisation. The PC5 interface is built for proximity communication, making it the viable candidate for V2V. PC5 can operate in and out of cell tower range, meaning communication will still occur without connection to Radio Base Station (RBS)/cellular towers [109].

Uu Interface

Uu interface is used for network communications and is built upon common cellular/LTE concepts, in a manner like that of mobile devices, but with adaptations to enable critical vehicular messages. This concept is achieved using LTE broadcast utilising roadside units, V2X servers, and cellular networks. These components make cellular the ideal candidate for V2I communication. The range of this component has a wide reach as it is not governed via proximity. Rather this covers wide area networks, utilising the infrastructure in place via cellular networks [110].

2.5 Developments in vehicular communication

The following section will be used to outline the most recent developments in the field of vehicular communication.

2.5.1 Modern state of vehicular communication research

802.11p technology and concepts are continually developing, and the tools used to research and develop are also evolving. Many research works are conducted regarding the standardisation of vehicular communication in both cellular and WLAN domains. Various vehicular communication surveys delve into different aspects that give overviews of the many aspects that need to be developed for the technology to be considered mature and viable and an overview can be found in A summary of the survey standards can be seen in Figure 2.4 which shows how the IEE standards are divided for transportation. A summary of related work can be found in Table 2.4.

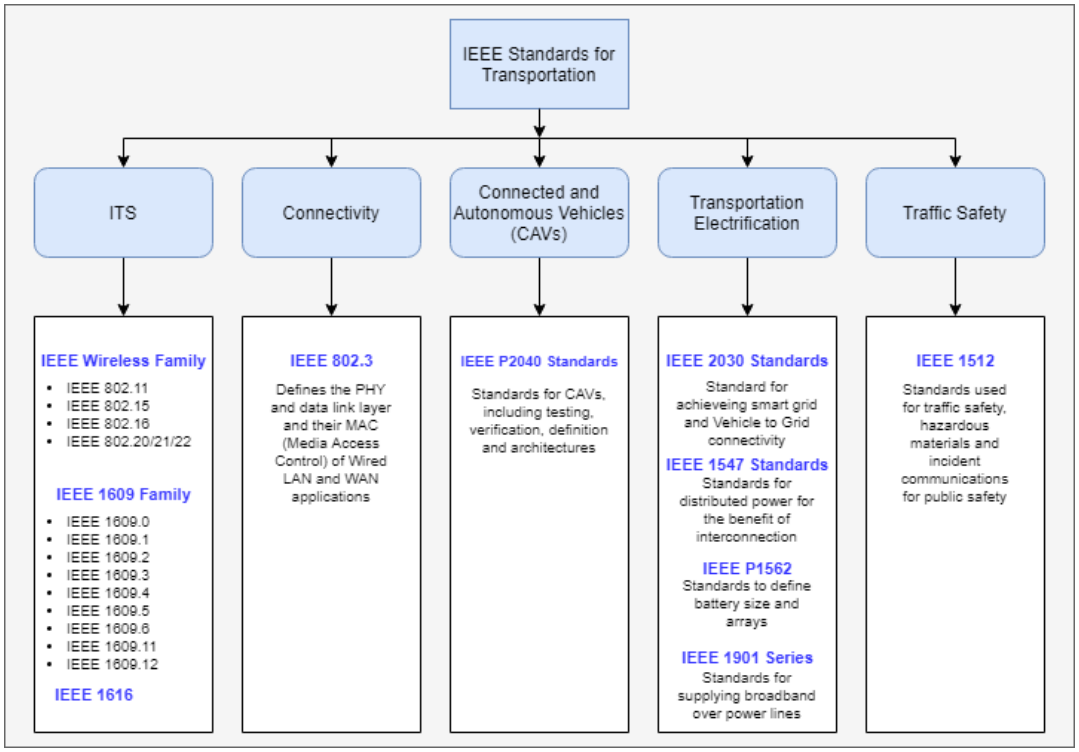

FIGURE 2.4: ITS standards summary

TABLE 2.4: Vehicular Communication

Author	Key Findings	Reference
Festag	802.11p, WAVE and 5G are discussed regarding the standards and their implications. The discussion consider the usage of the technology and operation.	[13][111]
Kenney	Describes DSRC standards with a focus towards the US standardisation in regards to the structure of the DSRC message and the operating modes, paying particular focus on the OCB mode.	[17][92]
Jiang et al.	Detail the improvements that need to be made for DSRC and WAVE, showing that the receiver will need significant performance improvements when operating in adjacent channels, known as cross channel interference.	[81]
Campolo et al.	The authors find issues in receiver performance similarly. They identify a solution to counter this issue, which is the use of channel congestion control algorithms.	[112]
Choi et al. Liu et al.	Authors approach channel congestion but with a focus towards message control in vehicular safety. The works help identify an issue: many field tests focus on transmit performance and not enough on the implications of a full system loop.	[113] [114]
Kloc et al.	Transmitter performance is analysed without a full system loop, to monitor how the received information is utilised for channel congestion.	[115]
Papadimitratos Zeadally et al. Wang et al.	Tutorial surveys detailing the entire systems used in vehicular communication, the applications of V2V, the requirements, architectures and the types of technology and their implications.	[116] [117] [118]
Singh et al.	Authors detail state of the art and future directions for vehicular communications and they foresee interest in the software-defined nature of networking and technology, the field of Named Data Networking (NDN) and vehicle prediction intelligence for safety.	[119]
Matolak at al. Vehicular Comm. Ghori et al.	Survey articles relating to the networking, routing and communication environments of vehicular communication, with a focus predominantly on VANETs and their implementations.	[120] [121] [122]

2.5.2 Vehicular Communication Testing

As Vehicular communication standards are being finalised, they must be tested to assess their performance. There are many ways that industries and academics are testing vehicular solutions, simulation for larger-scale testing and field tests for real-world scenarios. A summary of related work can be found in Table 2.5.

TABLE 2.5: Vehicular Communication Testing

Author	Key Findings	Reference
Balador et al. Abdelsamee	Research lacks real deployment, testing is completed in simulation environments such as MATLAB and OMNET++.	[123] [124]
Jafari et al.	Authors focussed on communication with emergency service vehicles and a simulation on connectivity probability over different distances.	[125]
Baloch and Reggiana et al.	A simulation framework using Simulation of Urban MOBility (SUMO) that monitors the effects of velocity on packet loss. They find that increasing the vehicle's velocity has a 15% increase in packet loss from 5 to 45 mph.	[126]
Kim et al.	Authors propose a new QoS scheme and find the new scheme has a higher packet delivery ratio and much smaller delay.	[127]
Wang et al.	V2X testing is surveyed, and they have encountered a lack of end-to-end testing of a CV system.	[128]
Chen et al.	A C-V2X test in China, they do test 802.11p vs C-V2X. While the cellular variant outperforms .11p at longer distances, the performance is nearly identical up to approximately 400 metres.	[19]
Xu et al.	A C-V2X test in China, The findings in this work show that DSRC can hit the latency requirement for CV, but with C-V2X, the latency is higher and suffers far more variation at higher speeds.	[18]
Kosilo et al. Sjoberg et al.	Safespot is a cooperative system for road safety projects, and their SP4 document outlines the findings for V2V testing. They detail various scenarios and highlight the benefits that can be seen in safety scenarios.	[129] [130]
Botte et al. InterCor Project	In Europe, a project known as InterCor was designed using roadway corridors for cooperative intelligent transport systems and had various field tests.	[106] [131]
InterCor Project	The UK based testbed was used to test a hybrid combination of both technologies and cross-country interoperability between two different ITS systems.	[132]
Intercor Project	The testbed in Belgium was a joint effort between the Intercor countries and aimed to analyse Day-1 services of C-ITS using ITS-G5.	[133][134]
He et al. Chen et al.	Cooperative Connected Intelligent Vehicles for Safe and Efficient Road Transport (COSAFE) is a research endeavour in the Horizon 2020 project. This project is aimed towards cooperative Connected Intelligent Vehicles.	[26][38] [135]

2.5.3 Vehicular Communication Analysis

Many works for CV are interested in the channel models for vehicles when nonstationary, as the movement is a contributing factor to performance degradation. For

instance, Bernado et al. [136] are concerned with the effects of channel models for connectivity and the probability of success. They also perform tests in simulation to monitor the effects on signal performance. Similarly, the investigation into the performance of the technology is also vital, and [88], [121] assess both 802.11p and ITS-G5. Both works are completed in simulation environments and are testing the latency, throughput, and packet loss depending on the number of vehicles or distance between vehicles; however, they recommend a field test is essential for further testing.

Similarly, in [137] a study is conducted on reliability using 802.11p, and the same conclusions are drawn regarding field testing. However, this test was a function of losses observed over speed, and findings show a higher speed difference leads to more losses. Further to this, an analysis by Anwar et al. [85] is a recent investigation into the newly formed 802.11bd, which includes the new renovations and spectrum losses of 802.11p.

One vital component to DSRC is the use of beaconing and broadcast messaging. These messages are used to propagate messages to any vehicle within the vicinity of the transmitting vehicle. The messages periodically exchange information with neighbouring vehicles, and they utilise the control channel in 802.11p. The message type is BSM or CAM depending on the region of use and is commonly referred to as beacons. The information contained in the messages relates to the current vehicle status such as speed, heading, brake operation and general vehicle attributes such as weight of vehicle, and these messages are often used in safety-related aspects [138]. A summary of beaconing and broadcast can be found in Table 2.6.

The following is the equation by [142] found in Table 2.6.

$$P_r = \frac{P_T}{(4\pi)^2(d/\lambda)^\gamma}\left[1 + \eta^2 + 2\eta + 2\eta * cos\left(\frac{4\pi * h^2}{d\lambda}\right)\right] \tag{2.7}$$

Where, P_t denotes transmitter power, d represents distance, λ is used to show the wavelength of the signal, γ represents a path loss exponent variable, η represents a phase shift, and h expresses antenna height.

TABLE 2.6: Beaconing and Broadcast

Author	Key Findings	Reference
Sepulcre et al.	The optimum data rate for a beacon is simulated, with the findings showing that higher data rates can reduce channel load compared to lower data rates with the increase in transmission time.	[139]
Tomar et al.	Study on beaconing showing the busy channel time is lower with a higher data rate, and thus beacon delivery success is higher.	[140]
Mahipal et al.	Authors suggest the usage of a new contention window timing, as opposed to the legacy version. Their findings show an increased packet reception rate up to 500 metres, which is an acceptable safety range for V2V.	[141]
Stibor	An evaluation of broadcast messaging, where the approach was taken to use 802.11p and monitor the performance over distance with a two-ray model to calculate received power. Equation 2.7.	[142]
Shaikh et al.	Authors propose a robust broadcast V2V scheme with the use of a wireless sensor network. However, they propose a framework and no results are presented to propose any benefits.	[143]
Lei and Rhee	Propose an enhancement for beaconing using NS-3 simulation with a random contention window selection based on MAC control. They validate by simulating a random number of nodes that random window selection is better than the constant contention window's standard.	[144]
Campolo et al. Gonzalez et al.	Two works have simulated and characterised packet loss in WAVE/802.11p vehicular networks Both works state that the increasing number of nodes leads to an increase in packets lost.	[145] [146]
Lyu et al.	Authors find Simulate losses and find most losses occur when there are 25-150 nodes, with the hidden terminal causing an exponential rise as nodes increase.	[147]
Sikdar et al.	They use broadcast for passing information locally from an RSU to all vehicles in the range. The findings show that frequency splitting is the dominant technique in most cases.	[148]

2.5.4 DSRC performance evaluations

As with any wireless communication system, the performance attributes are an essential part that must be thoroughly investigated, developed and measured. These can be performed in simulated and fieldwork trials and are useful procedures further to understand the hardware and software limitations. Many research works have been conducted into the performance of V2X systems, and they cover a wide area of analysis. Early work compared 802.11a and 802.11p and was used to show the benefits gained with the standard changes between the amendments [71]. The

results of this work covered various metrics such as loss rate in line of sight and non-line of sight conditions and throughput using different modulation schemes. In the findings, they discover that, as previous works show, the lack of authentication means that connections are established much faster and that in both LoS and NLoS, 802.11p performs better than 802.11a. They also report that the higher modulation level decreases throughput performance as distance increases. Binary Phase Shift Keying (BPSK) can maintain a steady connection for distances up to 150 metres. In a similar work, the authors monitor the performance of throughput again but also measure end-to-end ($E2E$) latency [149]. They also provide results that find lower modulation schemes can maintain a more stable connection at higher distances and show that the $E2E$ latency is lower at smaller packet sizes, with a difference of 300-byte size having 0.5 ms latency and 1500 bytes having 1.6 ms latency.

Two similar works can be found regarding DSRC. The works are similar in that they are both a performance assessment of the ad-hoc nature of V2V in the DSRC standards. The first work is a simulation of V2V monitoring the channel and measuring the sensing range, and the number of packets dropped [150]. Though this work is tailored to V2V, the authors chose to measure a large sensing ranges of 500 metres, which is a higher than the needed range for V2V communication, especially for safety usage. Similarly, the second work monitors V2V; however, the authors chose to use a field test to monitor performance and used commercial off the shelf devices capable of operating over 802.11p and traditional Wi-Fi devices to compare performance [151]. This field test was a measurement campaign to monitor data loss, throughput, and jitter. The results show that 802.11p has a lower throughput and higher packet loss and jitter when stationary. However, when the vehicles move, .11a is outperformed by .11p in all measurements.

Another field test was performed using 802.11p again, but this test was designed to monitor safety-related application performance [152]. This article studied five key performance metrics, UDP goodput, TCP goodput, RTT, Jitter and packet delivery ratio. They report their findings using three different devices, Arduino Yun, Laptop PCs and MikroTik; however, these devices are not capable of operating at the 802.11p specified frequencies of 5.9 GHz, but the latter two do operate at 5.8 GHz. They analyse the devices at short to medium distances, which is preferable for safety situations and state that correct transmission power is a fundamental requirement to guarantee timely and successful delivery of messages. They also show that latency remains low even in challenging environmental conditions, and transmissions never failed, although they did degrade. Reliability is a key issue for safety and has been approached in many works such as [94], [137], [153], with all the three-research

works finding similar results in the field tests. They note that key safety performance attributes are packet delivery ratio, and in almost all cases, they observe an 80% or more rate. In work by Bai and Krishnan [154], a measurement procedure was carried out to analyse the performance of BSM. The authors used 802.11p hardware compliant devices and monitored latency and RSSI, both key attributes although they are basic. They find latency is at most 600 ms over 75 metres, and RSSI drops at 20 metres from above 70 to 50, then a gradual decrease to 30 at 100m.

Huang et al. [155] performed a study on DSRC using data gathered from a safety pilot held in Michigan, USA. They characterised DSRC using three main metrics; Packet delivery ratio (PDR), maximum range (MR) and effective range (ER). They conclude that the biggest factor to PDR and MR is the effect from NLoS conditions, closely followed by antenna positioning. They also discover that weather has little influence on performance. It shows that performance is not degraded when up to six consecutive transmitting devices are used.

Quality of service (QoS) is a key component for safety in DSRC as this determines the level of service the user receives. A poor QoS would result in dropped packets, which is especially vital when cooperative communication is used. A recent article has approached QoS with the use of cooperative communication using diversity which aims to enhance reliability [156]. The concept is to find the most reliable transmission between V2I using V2V links. The authors propose an algorithm for this, which is a useful way of communicating V2I information and effectively reduces the issues faced by intermittent V2I connections. However, the author does not indicate this usage, such as how the result would apply.

As mentioned, safety messages are important in 802.11p, and the effective dissemination of these messages are of utmost importance when safety-critical factors are involved. Various constraints must be met for the vehicular network safety messages, such as ensuring the full range, not overloading the network, and delivering reliable messages in highly dense networks. Recently a method has been designed to enhance message dissemination with an approach called MORS [157]. The MORS method reduces the broadcast storms caused by message broadcasts and adjusts the high-speed topology changes to reduce network disconnects. They find that the MORS system is better than traditional broadcasting in terms of E2E latency and packet reception rate, which has solved two main issues.

One major cause of negative influence to wireless systems is the effect of interference; in a vehicular environment with many communicating vehicles, this is a predominant issue. This interference was extensively reviewed and explained in [158], where the authors discussed the issues that interference will have for vehicular communication and, in addition, how this will impact safety factors. A simulation was

developed that modelled the effect of interference, and the results are highlighted regarding the effects when a channel is at maximum load.

2.5.5 DSRC with Software Defined Radio (SDR)

Wireless communication is continually advancing, and communication technologies need to evolve to meet the requirements of consumers and networks. Wireless communication has rapidly become an essential part of daily life for consumers, ranging from mobile phones, smart devices, television and electronic payments. With the emergence of the Internet of Things (IoT), the predicted number of devices will reach 27.1 billion in 2025, with an estimated 24 billion needing some form of wireless connectivity [159]. The number of wireless protocols is also increasing to develop new, faster, efficient and robust methods of communication. These vary from ZigBee, Bluetooth, 5G, Wi-Fi 6, D2D and Machine to Machine (M2M) communication. These technologies all have different requirements. Hence, the technology used is built with a clear and defined purpose to support a particular technology and its requirements are pre-set such as frequency, modulation scheme, channel selection, and digital signal processing. As wireless standards continue to change, research and development must accommodate the requirements and specifications to handle multiple protocols. A flexible, robust, reconfigurable and programmable framework for hardware and software is fundamental to achieving this.

Software-Defined Radios (SDRs) are capable of meeting and overcoming wireless communication requirements, if they are programmed and compiled correctly. They are freely programmable hardware devices that allow users to configure and build the entire communication framework, including the entire communication stack. The option includes currently available protocols and future protocols in development. The technology of SDR is based on software-defined protocols rather than non-flexible hardware. SDR is beneficial for proof of concept and rapid prototyping as the software implementation can be changed and updated immediately. Some modern uses of SDR are available such as with consumer devices such as WLAN or 4G/5G, where the hardware chips are known to be updated and reconfigured through firmware updates or the Tesla autopilot, which is capable of over the air updates [160].

The SDR consists of different architectures such as GPP-based, DSP-based, FPGA-based or a hybrid design. FPGA based offers the advantages of higher bandwidths, minimal latencies and deterministic timings, which allow for the implementation of modern state of the art communication protocols. GPP-based architecture is an easier to use implementation as most of the processing is done using a high-end PC, offering more flexibility but are not capable of the same level of performance as

FPGA. Hybrid approaches are the current trend as they combine the advantages of both, where the GPP computation is used in conjunction with an accelerated FPGA [161]. The configuration is all compiled within the software and written to the device. SDR is a useful tool for research communities as it allows for rapid prototyping and allows the software to be continually updated and altered.

There have been attempts to create SDR implementations of wireless communication previously, such as the works by Chao et al. [162] where an SDR measurement platform was created and utilised to monitor wireless networks. However, this work focused on monitoring 802.11 as a whole and not for communication but rather as an analysis tool.

Attempts have also been made to operate the DSRC 802.11p framework on non-802.11p intended devices. The work conducted by Vandenberghe [163] modified 802.11a to 802.11p system using commercial off the shelf devices. This work successfully modified certain aspects of .11a to .11p, such as the contention window parameters, AIFS, SIFS and slot time. However, the system could not replicate the distance required by DSRC and suffered a less robust signal. They speculate that due to the low Effective Isotropic Radiated Power (EIRP), two milli-watts instead of the needed 2 watts. For this reason, a more powerful device is needed.

Similar work to this was implemented on SDR devices and low-cost processors in [164]. The SDR device in this project is the well-known HackRF [165], and the project was the creation of an 802.11a/g/p implementation. The work initially draws attention to the state of the art SDR implementations before their own implementation on GNURadio is tested. They perform measurements on software performance and comparisons between the capabilities in terms of processing and software. They, however, fail to use the device in meaningful field tests correlating the hardware performance with vehicular scenarios.

In work by Peng et al. [166], the authors created an open-source platform used for experimentation prototyping for the ITS-G5 European version of DSRC. The platform allows real-world tests as the package links to a vehicle OBD-II connector. However, the system is much more complicated than an SDR and requires many expensive pieces of equipment to be used but did perform well with commercial devices such as Cohda MK5 DSRC device and could receive data.

More recent works have focussed on the implications of latency in SDR platforms, such as in [167],[168] where the authors used GNURadio and Ettus peripherals to monitor the performance of multiple different SDR devices. The works were concerned with finding where the highest point of latency was found, whether due to the software, hardware or processing, with the findings highlighting that the host

machine's processing is most culpable. The work conducted by Gandhiraj and Soman [169] consisted of USRP devices to create a system capable of modern digital communications. They utilise USRP1 and recreate a capable of performing OFDM transmission and RDS communication systems, a cheaper and configurable alternative to commercial products.

Research has also been performed in the area of SDR for cellular networks. Engelhardt proposed [170] the first 5G D2D testbed and in-band communication, and they provide the open-source code after validating performance with multiple User Equipment (UE). Similarly, Asadi et al. [171] created a 5G D2D testbed; however, this implementation is for out-band communication. More recently, a work conducted for C-V2X using CARLA simulator was performed for autonomous driving [172]. The authors used USRP devices and SUMO to generate traffic, analysed a platooning simulation, and validated the communication of vehicle status information.

The vehicular communications research community has also assessed the use of SDR devices as DSRC devices. National Instruments, which are also manufacturers of SDR peripherals, have also passed V2X performance themselves, creating a system that can be used adhering to the standards. However, this is quite an expensive software component costing approximately $4000. The package supplied by National Instruments (NI) is a combination of communication, simulation, validation and measurement components and is operated with LabView software.

Many projects have focussed on open source software variations for DSRC to combat the price inhibitors. The works in [173] create a GNURadio implementation capable of transmitting 802.11p standard frames, and they model the transmission power and test transmission performance. This work, however, does not include receiver or transceiver operation and, as such, is a one-way system. In [174], V2V is implemented on USRP and LabVIEW. They note how real-time throughput and reliability have not been evaluated, alongside the hardware imperfectness factors that have not been reported yet. However, this system is based on the LTE framework and does not consider any practical scenarios, taking lab measurements only.

Further research has been performed to use SDR with 802.11p. However, this research uses tailored experiments to one issue. Agostini et al. [175] used 802.11p enabled SDR devices to monitor PER for different packet sizes, noting that larger packets had less error. Whilst Vlastaras et al. [176] stress-tested an SDR for PER and found that larger packet sizes have a higher number of errors, and this is due to increased time of transmission.

The work by Bloessel et al. [33], [177], [178], [179], [180], is the most complete, open-source and capable 802.11p transceiver available. The project was created by a team in Paderborn and is the WiME Project. They developed a fully functional

802.11p transceiver using USRP and GNURadio, capable of performing to the standards of 802.11p, with frames fully compliant and providing access to the entire project for the enablement of changing and altering the code. The project has been used in simulated scenarios and tested with interoperability with commercial devices, finding both possible and successful. The project was also field-tested with simple transmit and receive procedures, and they note the transceiver is not subject to random errors but can suffer in multipath environments.

In addition to this work, a second work utilised the WiME project to accelerate the performance in [181]. They detail improving the project by profiling the existing blocks and noting the slowest performing blocks. They implemented improvements and noted a performance increase in the CPU and the effective transfer rate within the SDR. The results while effective at showing an increased SDR speed, failed to consider any extra processing incurred by the computing device. This could be mitigated with a fully offline implementation that can be run upon power on, however this loses one of the key advantages of SDR, in that it can be adjusted at any time.

2.5.6 V2X safety and collision avoidance

As mentioned, safety is of critical importance for the adoption and heterogeneous usage of CAVs and their technology. One of the most important areas is the use of collision avoidance (CA). CA uses information shared between various V2X sources to reduce road accidents and increase users' safety when using vehicles on the roads and highways. Collision avoidance has been developed to reduce vehicular accidents, one of the most severe problems associated with vehicular transport. Therefore, it is advisable to develop methods and techniques by which accidents can be significantly reduced. Collision avoidance uses on-board vehicle systems that can send information containing GPS location, vehicular travelling direction, and speed, amongst other data. This data is passed to other vehicles to advertise the vehicle's intentions. Other dangers can also be detected and advertised, such as pedestrians and imminent collisions. These transmitted messages are received and then, dependent on the system, they are either relayed to the driver or automatically acted upon, such as automatic braking.

Collision avoidance

Collision avoidance has been a hot topic since the inception of CAVs. It is often split into two categories being active or passive systems, with passive systems being airbags, seatbelts, eCall, and rescue systems. These are typically used to reduce injury to passengers and alert local authorities. Active systems, however, are typically

used to avoid accidents or predict them using on-board sensors and communication capabilities, for example, rear-end collision warnings [182] or pre-crash sensing [183]. These systems allow the driver to know of emerging safety scenarios and autonomous enabled cars allow the vehicle to take control and engage in pre-emptive measures. A review of this has been published in [28], and the article details essential technologies for collision avoidance systems. Traditionally, sensors provide vehicle safety systems; however, this limits the range for vehicles to see neighbours and judge their intentions; hence, the systems can be ineffective. Conversely, it can be enabled with DSRC, which has a much larger range than sensors, allowing vehicles to communicate further and receive data at larger distances. A summary of some important collision avoidance research can be can be found in Table 2.7.

An approach for collision avoidance was proposed by [27], where various algorithms are considered for a kinematic approach using the laws of motion to trigger reactions or a perceptual approach where triggers are activated based on predefined thresholds. The kinematic approach is based on the stopping distance of vehicles, where triggers are used when a vehicle has a distance that is minor or equal to the vehicle leading. The perceptual approach is based upon the time to collision (TTC). Equation 2.8 [27] defines this algorithm, and various other algorithms have since been developed, such as the Honda algorithm and the Hirst and Graham algorithm.

$$TTC = (X_F - X_L - L_F)/(V_F - V_L) \tag{2.8}$$

where X_{F} is used to show following vehicle position, X_{L} represents lead vehicle position, L_{F} shows the lead vehicle length, V_{F} denotes following vehicle velocity and V_{L} denotes lead vehicle velocity.

$$DTC_a = \frac{-V_r - \sqrt{Vr^2 + 2a_{lv}r}}{a_{lv}} V_{fv} \tag{2.9}$$

where,DTC_{a} is the resultant detected time to collision, V_{r} denotes relative velocity, a_{lv} represents lead vehicle acceleration, r is used for range between vehicles and V_{fv} is used to show following vehicle velocity.

$$D_s = vt_{p-r+v^2}/2ug \tag{2.10}$$

where, D_{s}, is minimum safety distance, g represents gravity, v shows vehicle current speed, $t_{\mathrm{p\text{-}r}}$ denotes perception reaction time and u represents the friction factor. velocity.

A recent article published was research on a forward-collision warning system using V2V communication via 802.11p, TTC and Collision Avoidance Range (CAR)

TABLE 2.7: Collision Avoidance

Author	Key Findings	Reference
Herard et al.	A recent study has compared the various solutions for collision avoidance with simulations based on the various solutions. They conclude that the testing results are complex for active safety solutions, that performance safety indicators are a key attribute, and that metrics must be developed for this need.	[184]
Wang et al.	Investigated DSRC throughput and delay in the context of highway capacity. They found that with DSRC communication enabled, capacity can be increased by up to 491% in perfect circumstances.	[185]
Mahmud	*TTC* and other such indicators have been extensively reviewed , where the research is focussed on proximal temporal indicators, distance-based proximal indicators and deceleration-based indicators. The different indicators are reviewed and analysed, and they have provided extensive advantages and disadvantages, with applications for each considered.	[186]
Liu and Gao	Propose a vehicle collision warning system that has been designed using V2V communication. The authors use a Cohda MK5 DSRC unit and analyse the reaction time of drivers at different speeds and weather conditions to create an android terminal that can be used to warn drivers to slow down.	[187]
Hosny et al. Yousef et al.	Use a warning system comprised of a GPS, Raspberry Pi and a display monitor in conjunction with a collision avoidance algorithm, shown in Equation 2.9 to demonstrate vehicle collision avoidance with warnings generated by shared acceleration profiles.	[58] [188]
Agrawal and Varade	Propose a collision detection and avoidance system using Equation 2.10 and a buzzer alarm. Their results are limited but show that a driver can have increased reaction time with warnings provided by ultrasonic devices.	[189]
Gluhakovic et al.	A method of detecting vehicles through the use of object detection is used in.	[190]
Laurenza et al.	Authors propose using an obstacle detection algorithm to simulate the probability of a crash depending on actions taken.	[191]
Yakusheva et al.	Pedestrian collision avoidance via GPS/INS system is used, where they propose to predict pedestrian movements to avoid colliding with them.	[192]

[193]. The proposed solution is a system that calculates the distance to give warnings if a vehicle is in danger of a collision. The system was monitored in a field test with results showing 0.7 metres positioning accuracy error and latency of 5.5

ms. The authors did not implement any other sensing technology to measure the distance to increase the accuracy. In the field tests, they acknowledge that this was capable of meeting requirements but could be improved, in their recommendation the inclusion of radar systems.

Rear-end collision avoidance

There are many works solely dedicated to rear-end collision avoidance. These works can be split into communications for data or communications for distance maintenance. Data is essential for CA and some related studies for rear end collision avoidance can be seen in Table 2.8.

Lyu et al. [147] propose adaptive beaconing for rear end collision avoidance, where the beacons or put into an ABC scheme and compared with the traditional 802.11p and LIMERIC system. The proposed system has improved reliability over the other two systems, but they provide no usage in safety scenarios; however, this reliability can be speculated to offer increased safety. Recent work has focused on creating an effective model to monitor the vehicles' distance towards collision avoidance or collision detection. In [27], [194], [195], various algorithms are discussed, such as Mazda, Berkeley and PICUD, and then extensions and improvements are made to the algorithms. These alterations are used to offer an increased accuracy reading for distance monitoring. These algorithms are based on the speeds of vehicles and distance measuring devices. However, in [196], the article considers hardware implementations to offer sensor-based automatic braking. They utilise an alert system to notify drivers when 3 metres between vehicles is approaching and apply the brakes if the driver does not stop the warning. This approach offers various issues, such as giving the driver another device to monitor, countering the intended usage and causing crashes. They also observed that three metres is a short distance and is inadequate to avoid collisions effectively.

Another approach to collision avoidance provided in work by Javed and Khan [197] is the usage of a safety zone. In this approach, the transmitter's power for the CAM message is limited to only propagating messages to a certain range. This range eliminates the overloading of the safety channel due to the periodic broadcast nature of safety messages. The usage of the safety zone vastly reduces packet losses and channel utilisation. This safety zone can be achieved when the range is set to a certain level meaning fewer vehicles are transmitting to one another. Vehicle density rather than a range show this. The safety zone approach is also used in [198]. However, the authors instead use a verification algorithm to eliminate unnecessary messages based on proximity to the vehicle. This approach eliminates any unwanted messages, such as messages that are not directly going to influence the safety of the

vehicle of interest. The authors state that this method lower inter-message delay and reduces packet losses, leading to a more comprehensive overview of neighbouring nodes or increasing awareness of the local vicinity. It would be useful for the ideas to be used in conjunction as errors in discarded packets could lead to needed packets being lost and therefore reducing safety.

Cooperative awareness

Cooperative awareness has been previously discussed and is a method of data communication that CAVs use to gain enhanced knowledge of their surrounding environments, such as neighbouring vehicles, intentions, and environment. A performance study has been conducted on cooperative awareness for 802.11p and C-V2X in [204], [205], and the authors compare and review both candidate technologies, their advantages and disadvantages. They compare some essential attributes for cooperative awareness, such as awareness range and vehicle density, with both having to meet standardised QoS requirements. The results show that 802.11p can have a trade-off depending on the MCS, where the better performance or longer range can be applied. They also note that .11p is robust at distances up to a few hundred metres and can support a vehicle every 10 metres. After the range of 300 metres is approached, the performance starts to degrade due to the hidden node problem. This method is different to C-V2X, where the technology performs poorer at shorter distances and better at larger distances. They recommend .11p for short distances, as it is well suited for collision avoidance and rear-end collision avoidance.

Cellular based collision avoidance is also further investigated in [26], with an enhanced system for broadcast communication over LTE. This method uses CAM messages containing vehicle information to build cooperative awareness for vehicle safety applications. These messages have been enhanced with the use of an enhanced message collision avoidance scheme to minimise the collisions of packets. The results from the simulation show that with this system, packet received rate is improved over distances from 0-500 metres and are improved with a larger vehicle density compared to a basic system. Li et al. [206] have also used LTE-V for collision avoidance strategies. The authors consider automated systems avoiding collisions based on V2V communication in this research. They find that low distances suffer a relatively low amount of communication lag and that improving collision avoidance depends highly on latency.

Many works consider the impacts of latency for 802.11p and the importance of safety and CA. The most widely speculated latency has been reported in many works as 100 ms [97], [143] for BSM/CAM. Researchers have also deemed that this

TABLE 2.8: Rear End Collision Avoidance

Author	Key Findings	Reference
Ye et al.	Investigate use of V2V to propagate an Emergency Warning Message (EWM) for rear-end CA in a platoon. The usage of this message is to prevent a chain event of rear-end collisions. The requirements are low latency and maintaining inter-vehicle spacing between vehicles. The authors use a modified MAC to achieve this, and they highlight specifically for safety that delay or latency is a vital component.	[199]
Tang et al.	Latency is further evaluated, with an analysis on collision avoidance timings for DSRC enabled vehicles. The authors investigate the timings for vehicles to stop, the latency for emergency warnings to be used, and how this latency impacts the collision avoidance probability. They note that intersections have the most stringent latency requirements.	[200]
Manwar et al.	Intersection collision avoidance is investigated. This work also studies latency requirements between two types of safety messages; broadcast periodic messages and event-driven safety messages. Their findings show that safety message throughput is higher in their algorithm than typical 802.11p usage but do not state the vital reliability findings.	[24]
Rakesh and Belwal	Data is used to procedurally generate the shortest and most efficient route to the driver's destination. The data communication is used to inform drivers of any situations on the route and receive data from other vehicles whilst on the route. They produced an example using an emergency vehicle that avoids vehicles that had already collided on their route to a destination.	[201]
Metzner et al.	Authors exploit V2V for enhanced situational awareness and the results show that using data can allow vehicles to create a grid of vehicles along with the locations of the vehicle, but only provide this example on a highway exit ramp.	[60]
Patel et al.	authors produce simulations where the study is based on a "Misbehaving vehicle" performing unexpected manoeuvres. The shared data in the CAV group can allow vehicles to collaborate to avoid the vehicle and prepare a joint action and decisions together.	[202]
Yang et al.	Data communication was also used in a forward collision avoidance approach for CA. The authors' demonstrate that the efficient usage of data shared via V2V leads to an 8997.67% correct warning rate to avoid collisions compared to a TTC based system, a 6.34% increase.	[203]

will not be adequate and will instead need to be 50 ms [207], especially when used for pre-crash sensing.

The range for 802.11p is vitally important for safety, and it is standardised that this range can be in up to 1000 metres for 802.11p, which has been stated in recent works [22], [208]. However, other research speculates that for certain safety scenarios, a distance of 100-300m is necessary and sufficient [97].

2.6 Summary and conclusions

In this chapter, the wireless communication attributes have been briefly presented, and then a thorough literature review into vehicular communications and the current state of the art has been discussed. The modern concept of a vehicle is far more advanced than previous generations. It will now include many features to enable them to be connected and eventually fully automated driving. The use of these technologies is still being debated, but DSRC is considered a more mature and ready option for V2V. The demands of vehicle networks are high, requiring high reliability, low latency and always available connectivity. Wireless communication in the road infrastructure will allow many benefits, and continued research into this area will enable faster adoption and implementation of features that will allow a safer, quicker, and better-quality driving experience.

Software-defined radios are a promising technology for research on connected vehicles. They have helped make strides towards many different areas that are increasingly useful for the research community. In addition, the currently available projects can perform to the high standards detailed for DSRC.

Collision avoidance is a primary safety concern and will be a highly beneficial area in future to provide safety for vehicle drivers and vulnerable road users. The inclusion of infrastructure via V2I/I2V will allow data to be cooperatively shared with other road users out of the communication range. This approach will allow an entire data network to be shared, leading to more efficient travelling systems, mainly when autonomous vehicles are present.

Through this extensive literature review, various issues have been outlined. One large issue is the availability of a complete and modifiable DSRC implementation available for the research community. There have been many approaches taken, however, they are all tailored towards a specific use case or do not utilise the complete DSRC protocol. In addition to this, vehicular communication is assessed in various safety methods, however, the consideration for safety distances between vehicles based on communication is significantly lacking research.

Robustness in terms of reliability is of importance, however, there is a lack of investigation for this considering how it may affect the safety between vehicles or other road users. V2I is also under investigation and a complete simulation environment is not yet available that has all features of a complete vehicular network, such as communication, mobility, roadside units, camera vision with deep learning for object detection and complete V2X profiling. This would be of great benefit to assess various safety features and allow further research into the interactions between road users, and the implications of these interactions. This development is of importance for autonomous vehicle research.

Chapter 3

Vehicular Communication with SDR based DSRC

3.1 Introduction

Future connected and autonomous vehicles (CAVs) will be equipped with many sensors and communication devices to enable a more efficient and safer global transport system for both vehicle drivers and general road users. These devices will allow the gathering and sharing of appropriate information in a heterogeneous vehicular network. Important areas that CAVs will address are to increase road safety for road users, reduce road accidents, ensure road use is more efficient and ease the problem of traffic congestion [209]-[210]. Collaborative road safety is based upon V2V broadcasting, whereby vehicles share data to build up a mutual understanding of themselves and awareness of other road users. However, V2V can suffer from significant delays, poor channel performance, substantial packet loss rate and collisions due to the random channel access of broadcasting. There are many forms of communication to share vehicular information, and this chapter will focus on one of these areas, known as V2V.

Various approaches have been made to create an alternative to commercial DSRC devices for the research community, such as [166] who created an 802.11p transmitter using GNURadio. However, the author acknowledges that their work was only used to generate and packetize 802.11p compliant frames without an adequate receiver's complete design and testing. Similar work to this [211] also created an 802.11p transmitter for a Hardware in the Loop (HIL) embedded system for simulation and evaluation of vehicular type messaging. The SDR only operates in the 2.4GHz frequency band in the HIL system, which is not the area of the spectrum DSRC has been designated.

Further work on V2V utilises a Universal Software Peripheral (USRP) based platform [212], but this project has been based on the 5G framework with some adjustments to represent C-V2X closely. They analysed this system via an evaluation of real-time throughput and hardware imperfectness.

Two more research works have been investigated regarding 802.11p with SDR, but these two works had a similar goal. In [181] the authors mainly focused on accelerating the performance of the 802.11p transceiver by aiming to speed up hardware operation. The second is a platform created for measuring wireless networks based on SDR architecture [162], which again does not fit into the area of DSRC.

After analysing various DSRC projects, the option selected was to use a well-established and proven DSRC project, an 802.11 a/g/p SDR-based Transceiver developed via GNURadio and is known as the WiME Project [180], which is an open-source software implementation that can be uploaded to an SDR device. WiME is the most established open-source project researched and found readily available. The project has been created to represent DSRC accurately and proven operational with commercial devices while adhering to the 802.11p/DSRC standard protocol. This project has been made available to the research community to continue and assist research into vehicular communication. A modified and improved version is developed, through manipulation of the core block coding to incorporate an open UDP channel, that is capable of receiving modified data, and will form the basis of this chapter to establish an SDR-based DSRC transceiver that has been improved to enable V2V. WiME has already been extensively tested via simulations and a field test to monitor interoperability with commercial DSRC devices. The previous evaluations confirmed the operation to be appropriately capable of adhering to standard DSRC protocols, but no investigation for V2V was explored, as the authors created this SDR implementation as a tool for further research. Therefore, their experiments were tailored towards operating on the 802.11p channel, ensuring that communication was established, and performance statistics met those of DSRC.

The WiME project was chosen and, through development, modifications to the code will allow an improvement to offer V2V and will allow the option for customisable configurations depending on the scenario needed. The modified transceiver was used for SDR-based DSRC V2V, and results are generated to enable utilisation in real-time and real-world scenarios. The SDR-based DSRC project was used to assess vehicular communication capabilities for safety. The SDR-based DSRC transceiver was subjected to a real-world field test, where analysis was conducted.

This chapter aims to develop a fully functioning SDR-based DSRC device that can be used in future to increase road safety via the cooperation and communication of V2V information. This device is designed to operate as a V2V transceiver and is

investigated in scenarios for these purposes.

The survey conducted in [28] gives us an insight into the use cases and scenarios that consider collision avoidance and help identify the performance attributes needed. This survey also details the types of data and alerts that can be propagated by V2V systems allowing further knowledge on the approach needed to create and propagate messages relating to different scenarios. The approach was to create a modified version of an existing DSRC project and incorporate this into a platform capable of field-testing in a lab or outdoor environment, on roads and in various traffic scenarios. To create a platform capable of meeting the requirements specified, three main features needed to be met; easily portable, relatively low-cost, and performing to DSRC standards. For these reasons, SDR devices were chosen to perform the communication and laptop devices to create data packets and for result processing.

This chapter aims to design and establish a novel SDR-based DSRC for V2V that is proven capable of DSRC standard communication whilst gaining a key understanding regarding the performance aspects and capabilities of a non-commercial DSRC communication kit. This research is focused on the quality of service and robustness of the communication types and the capability it must have to support road safety applications and assist cooperative awareness in future smart cities. SDR's prime feature is that they allow reconfigurability and adaptability to suit all communication types. When V2X is fully adopted, there may be discrepancies between vehicle vendors over which protocol to use. The technology choice could be split between cellular-based or DSRC based, and SDR has the advantage to operate as all.

An SDR-based DSRC platform has been designed and investigated over various scenarios. The relevant results have been gathered, compiled and evaluated. The layout and composition of the platform will be outlined and detailed. The various testing scenarios will be explained in experiment scenarios, with their importance and meaning discussed. The experiments are tailored to give insights into the fundamental challenges of how different technologies such as SDR and V2V communications can effectively address the practical driving safety issues.

In section 3.2, an overview is shown for the development and design of the SDR-based DSRC transceiver, showing how the process is taken from open-source WiME to a newly modified adaptable transceiver. Section 3.3 details the initial scenarios used to monitor the performance of V2V using the SDR in a field-tested evaluation. Section 3.4 shows some extended investigations with SDR-based DSRC to show advantages and capabilities for V2V. Section 3.5 gives a summary and conclusion.

3.2 Software Defined Radio

Due to the inherent advantages provided by SDR, it is an ideal candidate for developing and implementing V2X communication protocols. The SDR has an advantage because the technology for V2X is still under debate, such as proprietary systems, WLAN, cellular, sensing technologies, and the possibility of future developments are still open options. V2X may become a system using multiple options such as a hybrid system with all protocols available or potentially vendor specific. Legacy cars may potentially have the opportunity to purchase a 'V2X upgrade kit' that may enable communication capabilities under certain situations. SDR is a flexible system capable of being all of these technologies through the simple alteration of the software protocol stack and can even be installed to legacy vehicles and reprogrammed when updates or adjustments are needed. This ability makes SDR a prime candidate for the development of V2X and the investigations of the capabilities or shortcomings.

3.2.1 SDR-based DSRC transceiver setup

The SDR-based DSRC platform needed to be relatively low cost and operated outside of the confines of a laboratory environment to accommodate in-vehicle testing. With these requirements known, the option chosen was to use a low-cost SDR device that does not require mains power and can be operated on the fly. The Ettus Universal Software Radio Peripheral (USRP) B210 software-defined radios and Lenovo ThinkPad laptops were selected for these reasons. They are relatively low cost compared to commercial DSRC devices, and the laptop allows for monitoring and recording results. The B210 was chosen over the N210, as the N210 requires a mains power supply that is impossible within a vehicle without incurring additional cost. The B210 was selected as higher functioning, and faster USRP devices cost significantly more to ensure the low-cost specification. This expense can be seen with the B210 at approximately £1000 per device. In contrast, the N210 costs £2500+ with an additional daughterboard also needed to be purchased at approximately £700. Commercial DSRC systems cost upward of £4000, such as the Cohda MK5 [213].

The WiME project was created using GNURadio software, and the complete transceiver project has been made available open-source for the research community [214]. Amendments have been made to the software flow graph to allow the ability to transmit both UDP or TCP packets via a python code, which will then be packetized into a complete 802.11p/DSRC frame and transmitted via the USRP device. This differs to WiME as they use a preconfigured message interface within GNURadio. The Python coding will enable configuring and adjusting packets for different

requirements. Figure 3.1 is a small part of the GNURadio block flow-graph, that shows the additional blocks that enable UDP/TCP access to the flow-graph and, with correct settings, allow the control and modification of data to be used in the datagram. A full GNURadio block chart flow graph can be seen in appendix A. This control uses correct port numbers and addresses parameters configured within the GNURadio and python coding. The use of python allows further options, including the transmission and readings of device power, transmit levels and the option to send more than just message data, such as pre-recorded or live video.

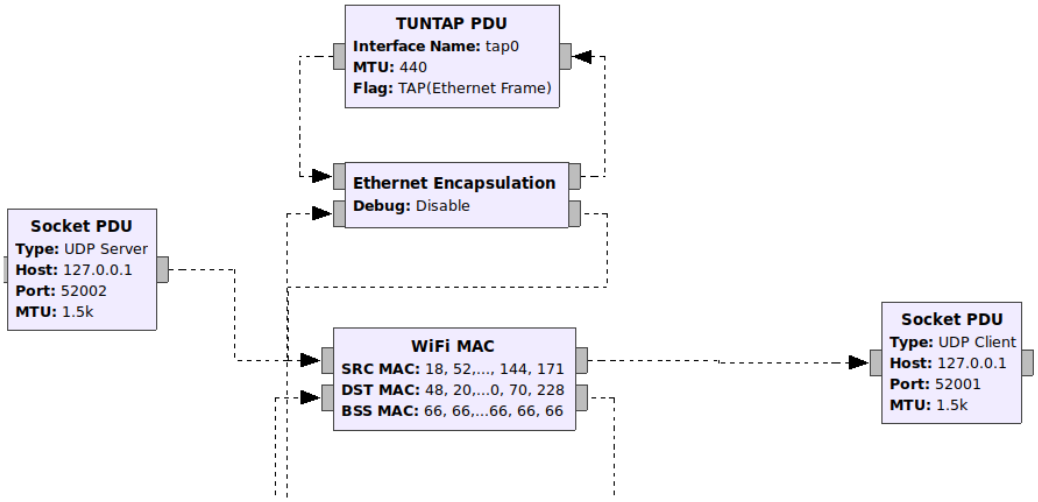

FIGURE 3.1: GNURadio UDP socket block diagram

UDP was chosen as the message protocol because broadcast communication is considered. With UDP, the connection between hosts does not need to be established; thus, TCP is not a viable option. UDP is not the typical standard used for broadcast; however, it allows the closest alternative and suits broadcasting capabilities. Theoretically, this should decrease processing latency, but the reliability could be compromised as data is not reported as lost as there is no packet reception confirmation. The UDP code developed allows the manipulation and configuration to adapt codes to various use cases. The options utilised are power transmission level, transmitter and receiver gain levels, packet content manipulation, packet size alteration, the interval of sending or Inter Frame Spacing (IFS) and the number of messages. These options are critical for calibrating the USRP as it allows the option to display the received power accurately and record results into separate files for processing.

An SDR-Based DSRC platform has been developed that consists of two or more

FIGURE 3.2: USRP B210 ports

FIGURE 3.3: USRP B210 with Taoglas antenna attached

software-defined radios: the Ettus/National Instruments USRP B210 devices. Figure 3.2 and Figure 3.3 show the platform, with one showing the physical antenna ports and the other showing the device with antenna attached. In most experiments, each device was configured as a transceiver; however, each was operated as a transmitter or receiver. For this reason, a single omnidirectional antenna from Taoglas was used per device, which can be seen in Figure 3.3. Omnidirectional antennas were chosen as the radiation pattern emits almost equally in all directions, suiting the needs of a broadcast. This is opposed to directional where the transmission is only propagated in one direction. The radiation pattern for the Taoglas antenna can

be seen in Figure 3.4, which is taken from the specification sheet and can be identified with the 5850Mhz label. The Antenna height was kept to 1.2 metres on tripods for most of the testing, and the antenna is kept with vertical alignment with the line of sight maintained where possible. The USRP and antenna were placed on the vehicle dashboard in vehicles tests, and the height was vehicle dependent. Figure 3.5 shows the SDR testbed in a block diagram with more details on internal system configuration, and Figure 3.6 shows a physical example of the SDR-based DSRC testbed in an outdoor environment.

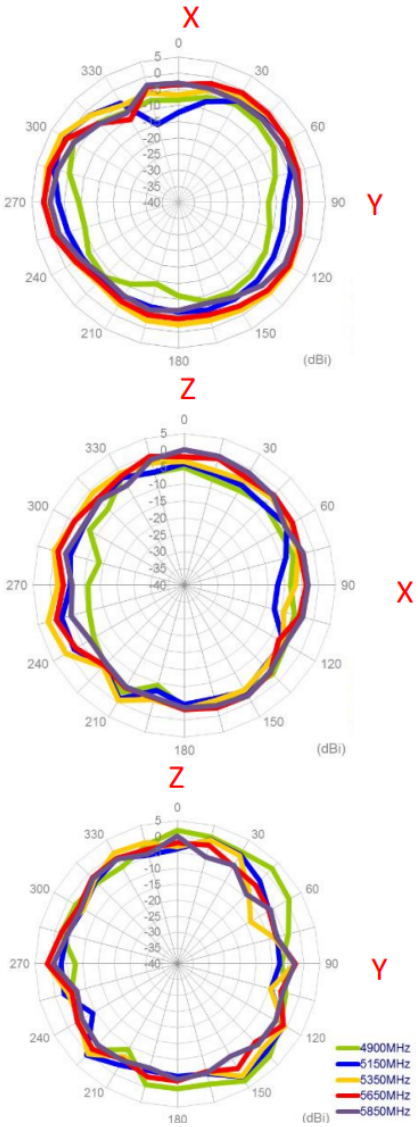

FIGURE 3.4: Taoglas radiation pattern [215]

The USRP transmitter device is configured to transmit according to the DSRC

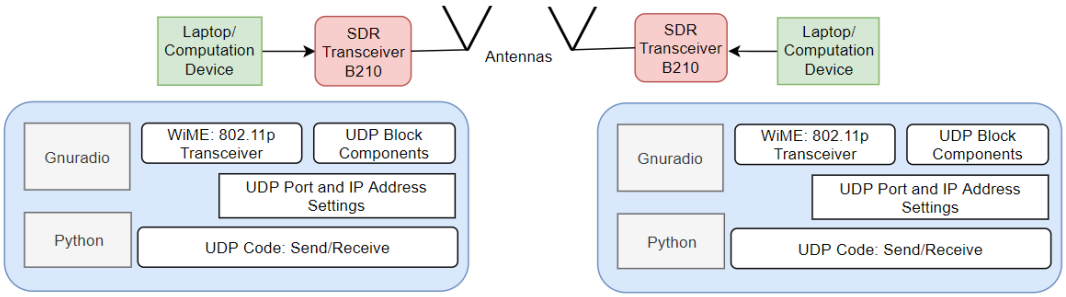

FIGURE 3.5: SDR-based DSRC block diagram

FIGURE 3.6: Physical example of SDR testbed

standard. The frequency was set to 5.89 GHz (channel 178), with a Bandwidth at 10KHz, an absolute gain value between 0 and 89dB and the tests were conducted with BPSK 1/2 modulation. The USRP was then connected to a Lenovo ThinkPad laptop via USB 3.0 high-speed connection for the generation of signals, UDP messages and processing. The receiver device followed the same main setup; however, the absolute value was between 0 and 76dB. These absolute values are taken from the Ettus datasheet accordingly [216]. An overview of the testbed components can be seen in Table 3.1.

Most experiments have been conducted using two nodes. However, an option to incorporate a third or more is available. The concept is to simulate vehicular nodes broadcast messages such as safety-related messages. The basic message would be a Basic Safety Message (BSM) in the American standards [217] or a Cooperative Awareness Message (CAM) in the European standard [218]. The insights gained from the performance analysis will allow further testing to evaluate its impact on V2V collision avoidance. Table 3.2 shows some of the more important testbed settings.

TABLE 3.1: Testbed details

Component	Detail
Operating System	Ubuntu Linux 18.04.2 LTS
Python Version	2.4/3
SDR	Ettus USRP B210
Frequency	5.89 GHz
Bandwidth	10 MHz
Laptop	Lenovo ThinkPad
Modulation Scheme	BPSK 1/2
Laptop	Lenovo ThinkPad
Processor	Intel i5 8th Gen
RAM	8 GB DDR4
HDD	256GB SSD

TABLE 3.2: Testbed settings

USRP Settings	
USRP Device	Ettus B210
USRP Tx Gain	0-89dB absolute, 0-1 normalized
USRP Rx Gain	0-76dB absolute, 0-1 normalized
Sample Rate	10 Million Samples per second
Antenna	Taoglas TG.35.8113
Software	GNURadio and Python Terminal
Coding Settings	
Type of Code	Python

GNURadio is used to create the correct waveform and signal generation for 802.11p/DSRC standard, adhering to the correct frequencies and bandwidth as required. Python application codes have been individually written and programmed for each device, which is different for transmitter and receiver whilst also interchangeable for any devices running in alternate terminals. The use of python coding enables the creation of a different code for any experiment, which will allow individual monitoring and result gathering for the parameter results needed. All coding can be modified to allow collaboration into a comprehensive code when required.

3.2.2 Calibration of SDR-based DSRC

The supplier does not calibrate the Ettus USRP B210 devices; therefore, the devices will need to be calibrated to represent accurate power levels and compensate for measurement errors. The calibration was completed using an Agilent vector signal analyser, a data sheet for the USRP, and was conducted in a laboratory environment. A sample of power readings was recorded, and linear curve fitting was applied, with the resulting formula used to create a calibrated power value. The calibration for the transmitter was completed with the setup shown in Figure 3.7. The gain was selected as a standard value of 53.88dB and then incrementally raised to get a

TABLE 3.3: Calibration results

Tx Gain (dB)	Tx absolute (dB)	Tx Power (dBm) @2.4	Tx Power (dBm) @ 5.9
1	89.8	-6.02	-8.02
0.9	80.82	-12.33	-14.33
0.8	71.84	-21.13	-23.13
0.7	62.86	-29.92	-31.92
0.6	53.88	-38.94	-40.94
0.5	44.9		
0.4	35.92		
0.3	26.94		
0.2	17.96		
0.1	8.98		

calibrated value for each gain level in dBm values. From these readings, a selection is made for the value of the transmitter. It then is used for correct calibration of the receiver device based upon the known and calibrated transmitter value.

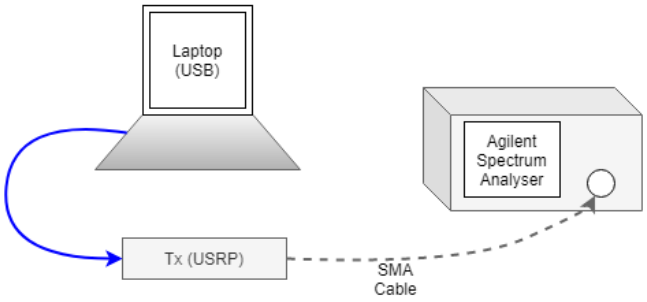

FIGURE 3.7: Calibration procedure block diagram

The transmitter is programmed to emit a continuous signal at a chosen frequency and gain setting. The signal analyser is used to measure the signal received, which was then recorded and tabulated for each gain level. The initial measurement was to take a power reading at 2.4 and 5.89 GHz using the USRP devices to find the power received without calibration. The USRP was then connected to the signal analyser using SubMiniature version A (SMA) cables to minimise losses. The initial test has been conducted using a transmitter set to 53.88 dB absolute power. The results of this experiment show a 2dBm difference is shown between 2.4 and 5.89 frequencies, with the respective values being -38.94 dBm and -40.94 dBm and can be seen in Table 3.3.

The transmitter was then connected to the receiver via direct SMA cable without any attenuation, and the power was then recorded at the receiver and compared to the tabulated values. A block diagram of this connection can be seen in Figure 3.8, with power readings taken and evaluated. A small sample of readings was

recorded, and linear curve fitting was applied, using the resulting formula to create a calibrated power value. The formula used for curve fitting is shown below in Equation 3.1, with x being the gain value to be calibrated. Figure 3.9 and 3.10 show before and after calibration for all gain values.

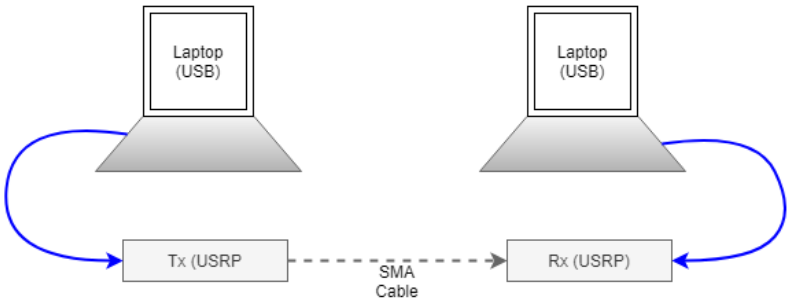

FIGURE 3.8: Block diagram of the calibration procedure with Tx/Rx

$$y = 0.9957 * x - 65.41 \tag{3.1}$$

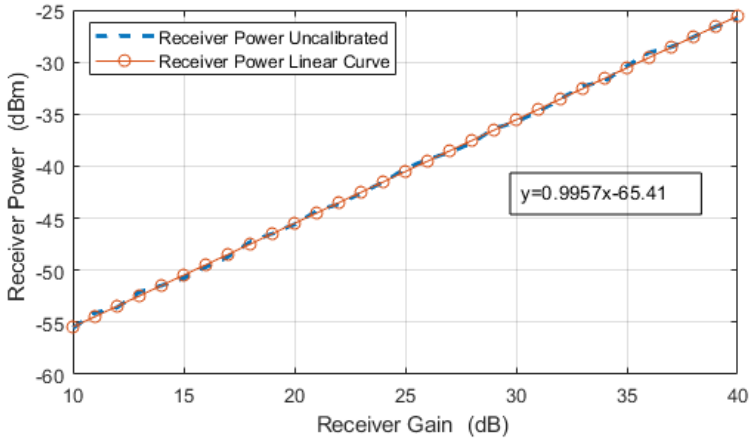

FIGURE 3.9: Uncalibrated power graph

Figure 3.10 shows that the received power is very close to the initial readings taken from the USRP; However, calibration is necessary to produce an exact value for each gain level. The calibration allows accurate power measurements in future experiments to show the difference between transmitted and received. This approach allows recording the Received signal strength indicator (RSSI).

The calibrated results can indicate the difference between the power chosen to transmit and the value received. This will indicate any outside noise from fading

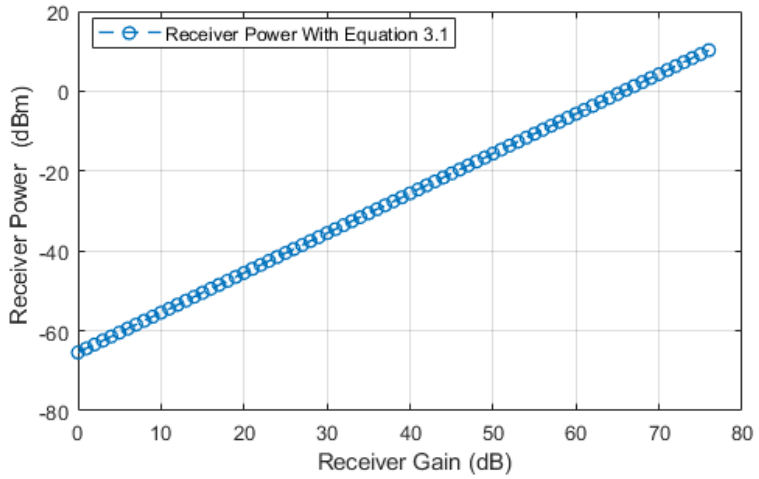

FIGURE 3.10: Calibrated power graph

or reflection that is present in a real-world transmission, showing how the power will be reduced in the environment. Minimal fading is seen in the calibration as low attenuation cables are used. With calibration performed, the difference between the USRP devices is evaluated. This calibration can be shown by choosing an example transmitter gain and then taking the calibrated values, and the differences can be compared as shown in Equation 3.2.

$$Gain = G(Tx) - G(RxCalibrated) \tag{3.2}$$

The difference is shown in gain when the transmitter is set to 0.6 gain value or -40.94 dBm at 5.9 GHz, and the receiver values can be seen along with the respective difference in power in Figure 3.11. This figure highlights the difference in the power received by the receiver, and it can also be seen that when the gain is higher, the difference in power becomes positive. The final calibration stage accounts for the antenna gains, which are taken from the information on the antenna specification sheet. The antenna gains will be detailed in a later section.

The difference shown in Figure 3.11 relates to the gain value chosen at the receiver and the power that is received from the transmitter. This allows to see the exact value that is received based on the transmitted signal after calibration, when different gain values are chosen.

3.2.3 SDR transceiver measurement set-up and scenarios

The following section will describe the performance and measurements tests carried out with the SDR-based DSRC transceiver to gather information on the base

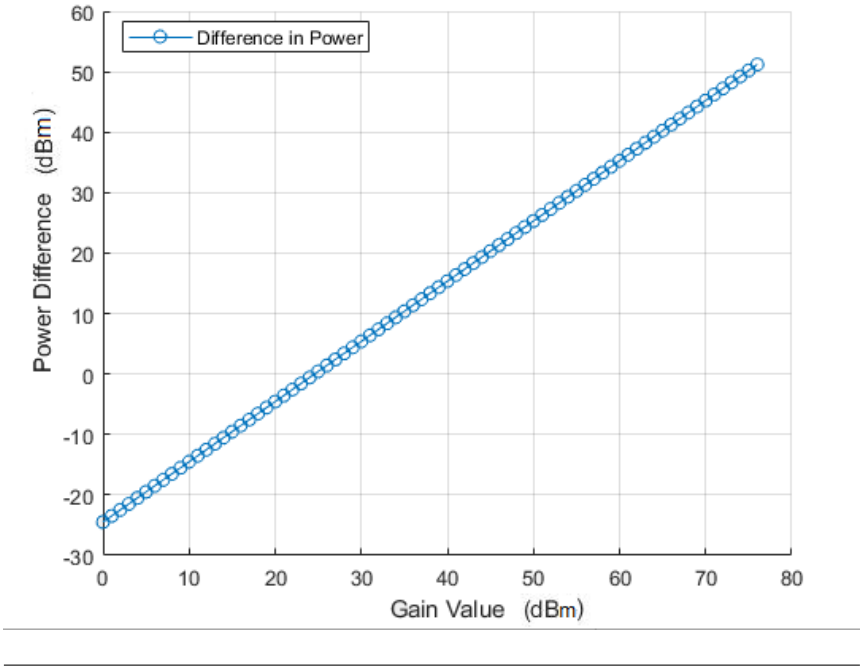

FIGURE 3.11: Power difference graph

performance statistics and how they convey to safety scenarios. Each test will be summarised and related to V2V, identifying the key performance characteristics and how SDR functions with broadcast communication. It should also be noted that unless otherwise specified, all packets are used at a maximum of 1500 bytes which is the maximum defined for DSRC [219] An exception is scenario three, where a 500-byte packet size is used. Each USRP has been configured as a transceiver but only uses one antenna. This antenna will be attached to the transmit or receive port, depending on the requirement. The USRP devices have both been configured to 5.895 GHz with a 10MHz channel as is standard for DSRC [220]. The USRP was also set to a gain level of 69dBm at the transmitter and 76dBm at the receiver.

To adequately assess the performance of SDR-based DSRC, a series of measurement campaigns were designed and have been tailored with a specific code. Each measurement campaign scenario has been developed to gather results for a specific performance attribute, and the scenarios will be outlined along with the parameters to be analysed. This procedure is designed to analyse different performance aspects to understand better the physical limitations the SDR may have.

First Measurement campaign: The first scenario used to investigate the SDR-based DSRC is designed to measure received power and packet delivery ratios. The received power was sampled 50 times at 10-metre intervals from 10-250 metres, with an additional test performed at 300 and 400 metres. Secondary samples were also

taken, and these were recorded whilst moving from each test point to the next whilst moving approximately 3-3.5 mph. The packet delivery ratio was measured the same way; however, the samples were taken over 10 to 450 metres. P_s represents stationary power, and P_m represents moving power.

Second Measurement campaign: Then, the second scenario was used to measure the data rate/throughput and latency simultaneously. The samples in this experiment were taken with direct connection using no antennas to eliminate channel losses and outside interference. Throughput was sampled to find maximum packets transmitted in a second without any losses, and then a calculation was used to find the maximum rate that could be achieved theoretically.

Throughput and goodput equations are also used, based on the packet losses previously measured, to find the actual data transmitted against the theoretical maximum that could be possible. This equation shows the transmitter's data compared to the usable data.

Latency or delay was measured using SMA cables to measure the processing time. A calculated value of propagation time was used to find total latency; the equation used to calculate End to End processing latency ($E2E_{PL}$) is shown in Equation 3.3. Round-Trip Time (RTT) was recorded between transmitter time (T_S) and receiver time (T_R). 3000- time samples were recorded and used to calculate the mean value and standard deviation to create a normal distribution bell curve to give the min, max and average latency values. Propagation time was then calculated separately, and the two latency values were used to estimate the end to end total latency.

$$E2E_{PL} = \frac{(T_R - T_S)}{2} \tag{3.3}$$

Third Measurement campaign: The final scenario determines the quality of service (QoS) or reliability. The QoS is vital in CAVs as safety messages must have almost guaranteed delivery or at least 99.9% [221], and this is especially important for collision avoidance where missed packets are highly likely to lead to avoidable collisions. This scenario is used to extract relationships between reliability, distance (metres), and data rate in packets per second (pps). The formula in Equation 3.4 is used for calculating the successful packet delivery ratio (Pa_D).

$$Pa_D = \frac{P_R * 100}{P_{ID}} \tag{3.4}$$

Packet ID (Pa_{ID}) is a value inserted into each packet payload at the transmitting side, from 1 to 7500 in this experiment. This is used to identify the number of packets sent from the source. The number of packets received (Pa_R) is a receiver value incremented when each packet is received. These two values can then be used to

calculate the total packet delivery ratio, which is essentially the ratio of packets that have been received at the destination to the number of packets sent at the source. Each test was performed three times, and results were recorded.

This test was conducted over 5-25 metres in 5-metre intervals and extended to 100 metres at 25-metre intervals. The analysis was conducted up to a maximum distance of 100 metres because in previous work relating to vehicular stopping distance [222], it was calculated that without the communication capability, stopping distance is 96 metres when travelling the UK speed limit of 70 mph. In addition, it was chosen to analyse data rate from 10-140 packets per second which is the maximum limit found later in Chapter 3, with the number of packets being sent set to 7500 as this is an efficient point between manageable data and time taken to transmit. For this experiment, to accurately represent a cooperative awareness message (CAM) or basic safety message (BSM) [95], a smaller packet size was chosen of 500 bytes, as is the standard size for these message types.

3.3 SDR-based DSRC experiment results and analysis

The following section will give extra detail specifically tailored to the measurement scenarios and the relevant results gathered during each measurement campaign.

3.3.1 Distance power measurement

This initial experiment monitored the performance over short to long distances and how received power changes over distance. This experiment took 100 samples at each distance and was completed over the full distance range at 10-metre intervals. In addition, three measurements of 100 samples are also taken whilst moving to each distance point, which was done at a brisk walking pace of approximately 3.5 mph. The recorded samples have then been averaged for both cases. In this experiment where V2V will be considered, 250 metres is categorised as a longer distance communication, as typically vehicles will not exceed this range for V2V type communication.

The results for this experiment can be seen in Figure 3.12 and 3.13, with the first figure showing both uncalibrated and calibrated results and the second focusing on the calibrated results. The figures display the received power being approximately -84dBm at its lowest point. They also show that from 0 to 250 metres, the power drops considerably by approximately 20dBm. P_m represents power when moving, and P_s represents power when stationary they can be seen in Figure 3.12, which represents the trend of received power and distance. These results have also been

estimated through curve fitting. The formula representing each curve can be seen in Equation 3.5 (P_s) and Equation 3.6 (P_m).

$$P_s(dBm) = -5.088ln(x) - 55.039 \tag{3.5}$$

$$P_m(dBm) = -5.5153ln(x) - 55.863 \tag{3.6}$$

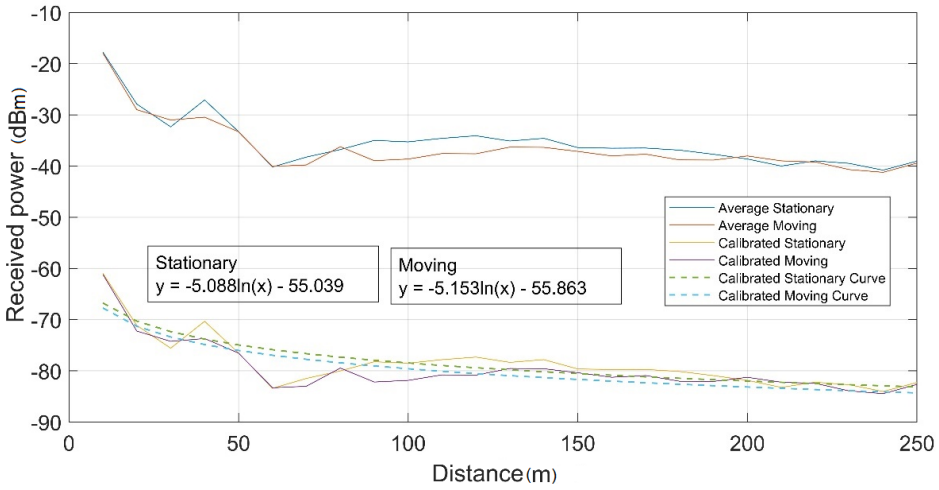

FIGURE 3.12: Receiver power over distance

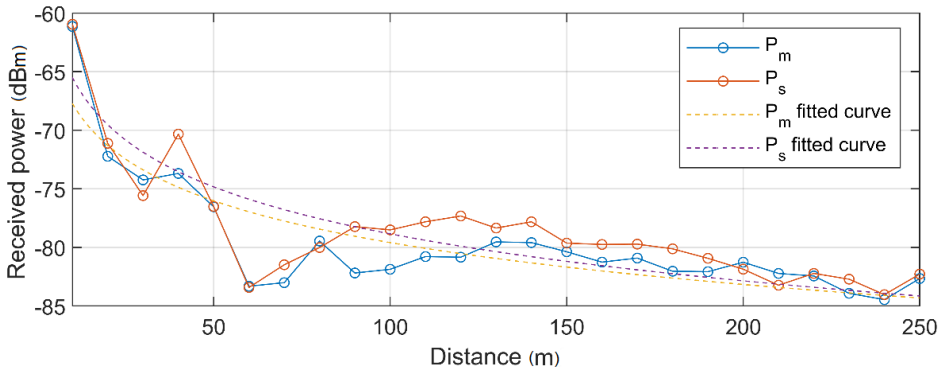

FIGURE 3.13: Calibrated receiver power over distance

The only significant results to see in Figure 3.12 is that the calibrated results can be seen shifted to a lower value of power received which is a more accurate representation of the power that is received by the SDR device, which highlights to the user that the power is not accurately represented by default.

3.3.2 Path loss measurements

The next section of this test analysed the calibrated power received and produced a theoretical path loss model based on the recorded results, therefore this calculation will represent the path loss potentially observed in the field test and the which has been used in the path loss formula in Equation 3.7 represents this. Free space path loss is used in this instance as it was observed there had been no blockage to the line of sight during the experiment. The results were used to produce a curve fitting formula for the path loss calculated. It should also be stated that the antenna used has a peak gain of 2.55 dBi. The antenna gain is measured in dBi as this is the standard measurement for forward gain in an isotropic antenna.

$$FSPL = Tx_p - Rx_p - Tx_G - Rx_G \tag{3.7}$$

Where FSPL represents resultant free space path loss, Tx_p represents transmitter power, Rx_p represents receiver power, Tx_G is used to show transmitter antenna gain and Rx_G denotes receiver antenna gain.

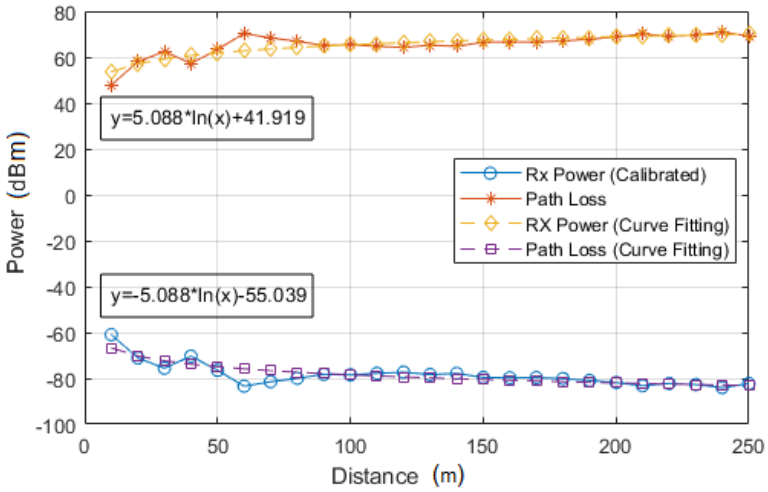

FIGURE 3.14: Path loss

The result in Figure 3.14 shows an expected result, that path loss will follow the same trend as the received power but will be almost completely inverse. The results of received power and path loss show that from approximately 75 to 250 metres, there is not a lot of variance in the recorded values. The result shows the USRP SDR is capable of operating at these distances. In a V2V scenario for object detection or maintaining stopping distances, 250 metres will be an adequate distance to operate over as safety distances between vehicles do not typically exceed this value.

(A) SDR side profile

(B) SDR front profile

FIGURE 3.15: Dashboard of vehicle, SDR set-up

TABLE 3.4: Vehicle on road power

Distance	Average Power received (dBm)	RX Power calibrated (dBm)
10	-21.1175718	-64.3551718
20	-28.54562352	-71.78322352
30	-33.43328825	-76.67088825
40	-35.76543987	-79.00303987
50	-38.73738324	-81.97498324
60	-33.14888791	-76.38648791
70	-42.13624254	-85.37384254
80	-40.53155063	-83.76915063
90	-42.35360801	-85.59120801
100	-41.44789598	-84.68549598

3.3.3 On-road mobility field test

A field test was conducted to analyse the performance whilst having two cars equipped with the SDR setup without tripods. An example set-up can be seen in Figure 3.15 and Figure 3.16. The SDR and antenna were placed on the dashboard, and the power performance was monitored on a 100-metre road. Secondly, the packet loss and power received were separately recorded whilst travelling for 15 minutes in normal traffic conditions. The average speed during the second test was approximately 30 mph. Packets were sent at 100 packets per second, and power was recorded approximately once every second.

For the initial roadside test, the results can be seen in Table 3.4 and Figure 3.17. In the results, it can be observed that a sharp increase in power is recorded at 60 metres. This reading occurred as a large vehicle entered the communication range of the SDR devices at the roadside, which shows that this large vehicle could have amplified the omnidirectional antenna via reflection of the signal.

FIGURE 3.16: Dashboard of vehicle, SDR and laptop set-up

The second test was conducted on a stretch of roads near Birmingham, Aston University campus; the route can be seen in Figure 3.18.

This route is approximately 2.6 miles, travelling through the middle of Birmingham to a reservoir and the journey time is approximately 14 minutes. The experiments utilised the same configuration as previously with two SDR devices mounted to the vehicle's dashboard. The configuration for the SDR has two separate code procedures; on the transmitter side, a code was utilised to send ten packets per second to the receiving vehicle, along with power transmission values sent every second. The receiver was coded to receive the normal packets, record an overall packet reception percentage, and record the power received from the transmitter. Initially, the vehicles were approximately 10 metres apart upon initialising the code within

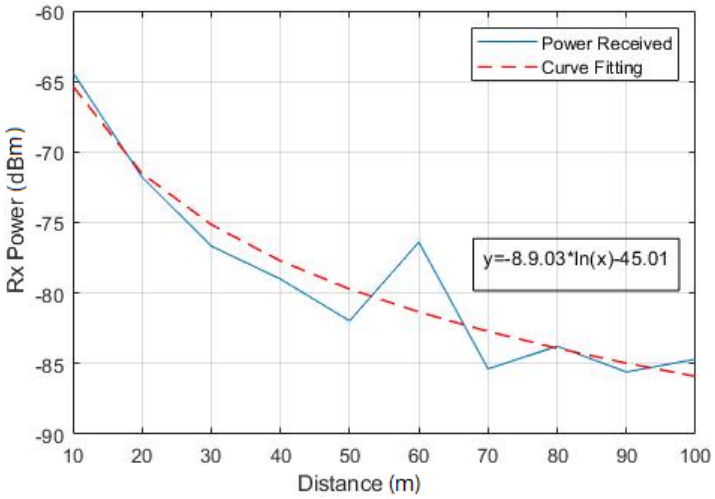

FIGURE 3.17: Calibrated power for road test

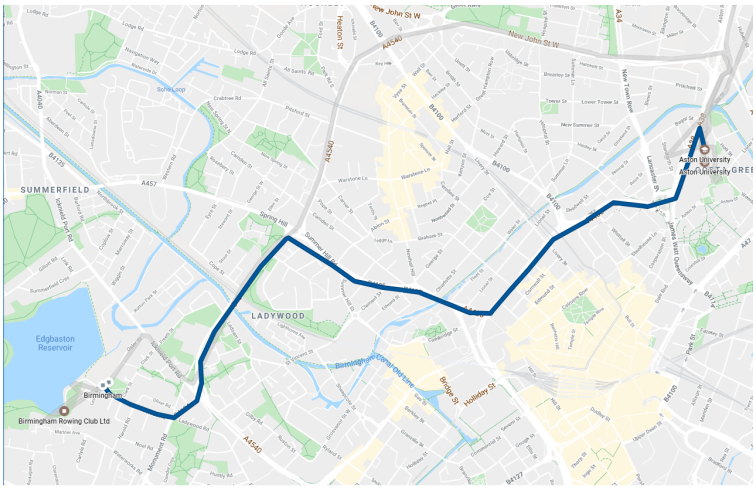

FIGURE 3.18: On road test route

a crowded car park. After leaving the car park, the lead vehicle followed GPS to the reservoir and was equipped with the sending node, while the following vehicle followed the route set by the lead and was equipped with a transmitter. The experiment was conducted in normal daytime conditions and a typical UK road system following normal road rules. The results for this test can be seen in Figure 3.19.

In Figure 3.19 the received power is displayed for the full journey time displayed in seconds. Initially, the received power is reading high, and this is because the vehicles are within proximity, located in the car park starting location, approximately 10 metres spacing. As the test continues, it can be seen that gradually the received

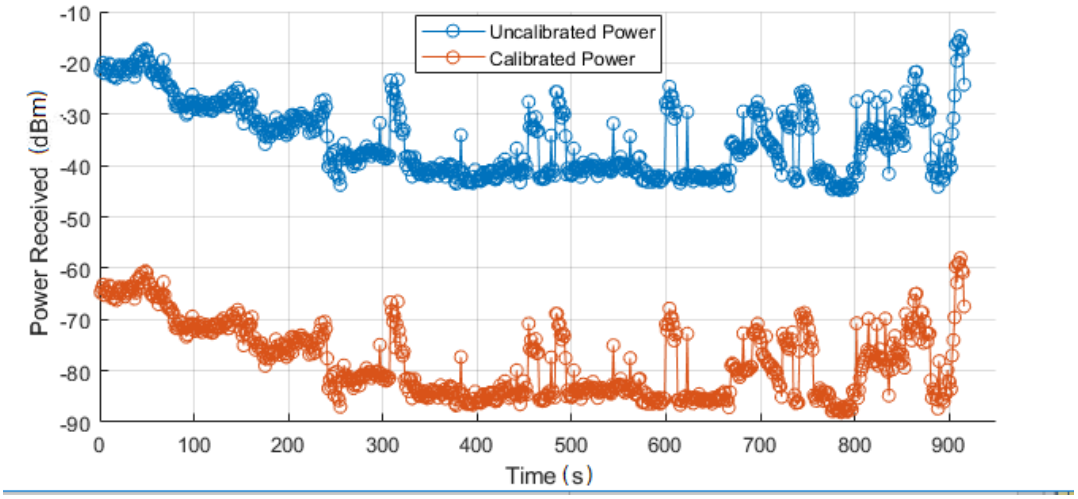

FIGURE 3.19: On road test route, calibrated power

power after about 300 seconds approaches to -85dBm. Then for the rest of the test, this is the baseline power reading. This result can be noted as the reading taken once vehicles have separated by a safe distance, usually approximately two car lengths. The results and map were investigated, and the readings that raise in value back up to -70 dBm would be the junctions and traffic lights where the distance between vehicles is reduced. At around 700 seconds, the two vehicles were separated by an emerging heavy goods vehicle, which produced a scattered power reading, hence the signal would have been reflected towards the receiver, increasing power. The final point to note through the test is the rapid variations between 800 and 900 seconds. At this time, vehicles were entered a busy residential area and the two vehicles return to a 5-metre distance gap between each other when parked in a residential street. Therefore, the signal is amplified, as distance reduces, but the signal is also scattered due to obstructions and channel fluctuations, causing scattering and reflections. This result shows that the SDR devices maintained a high level of communication throughout the experiment; however, it highlights the previous finding of power decreases over significant distances and gives further insight into the effects when LoS is compromised.

Figure 3.20 further proves the results in 3.19, however, the x-axis are different representations, and the results are calculated using Equation 3.4. In this test the number of packets are used to represent the results, instead of a time measurement. However, the main difference to be seen is that when the scattered signals occur, power received can increase due to reflections, but this interference also cause significant losses. For comparison, the results can be correlated with circumstances

explained previously. At points 1200, 2000, 3000, 3800 and 4100, slight reductions can be seen that are packet losses, these are the points at which the previously mentioned junctions were exited, and the distance increased. It can also be due to the increase in vehicles waiting at the junction, causing additional interference to the communication. At the 5000 packets transmitted point, a decline of 4% losses occurs; this is the same location as the power scatter loss. As the vehicle cleared this obstacle, the packet success began to rise, but in the last part of the test, it can be seen the rate reduced gradually again as the vehicles entered the residential area.

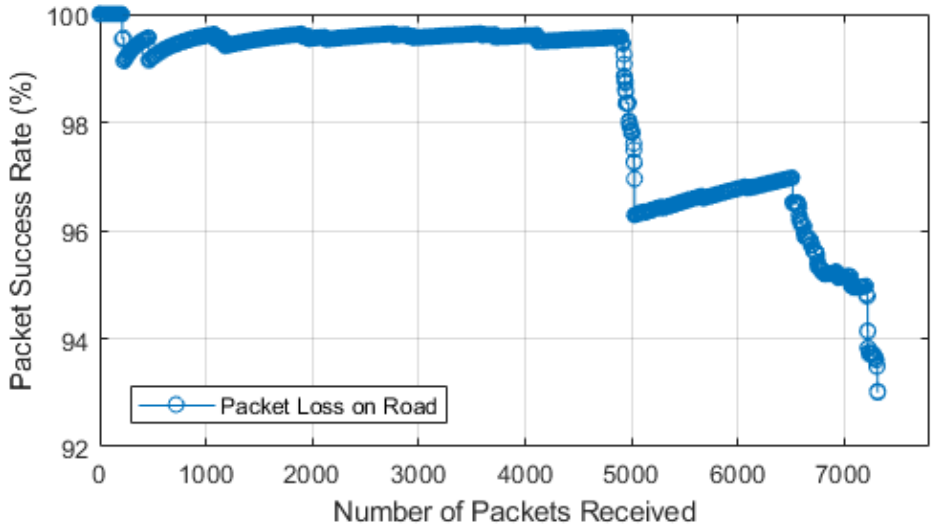

FIGURE 3.20: On road test route, packet loss

3.3.4 Throughput and latency

This test was used to theoretically prove the throughput that could be achieved using UDP over SDR-based DSRC. It was found that the maximum number of packets that could be sent within a second via UDP was approximately 140 packets. This information is used to produce a theoretical throughput for each number of packets. The range used is between a minimum of 1 packet per second and a maximum of 140 packets per second and is outlined in Table 3.5.

The data rate is especially important in networking as it measures how much data can be transmitted over a certain amount of time. As mentioned, it was discovered that the maximum rate of packets per second is 140, and a maximum packet size of 1500 is given for DSRC. This result gives a maximum theoretical data rate of 1.68 Megabits per second. The minimum specified data rate for DSRC with BPSK modulation is given as 3 Mbps [139] and as can be seen at the highest with the UDP

TABLE 3.5: Throughput

Send Rate (seconds)	pps	Packet Size(Bytes)	KBps
1	1	1500	1.5
0.1	10	1500	15
0.04	25	1500	37.5
0.02	50	1500	75
0.013333333	75	1500	112.5
0.01	100	1500	150
0.008333333	120	1500	180
0.007142857	140	1500	210

scheme, it can reach just over half of this. However, this is tailored towards high complex systems. In the case of this platform, the limitations are placed on the processing power of the laptops. For this scenario, 140 pps is acceptable but further analysis will need to be shown in terms of packet loss.

Throughput and goodput

The goodput was also analysed to monitor the SDR in various field tests rather than just the theoretical value of throughput. This was achieved in a field test outside of the vehicle rather than inside, to mitigate the effect of the windscreen of the vehicle. The following equations were used, and the previous result information from testing. The equations can be expressed in two forms.

The first representation can be seen in Equation 3.8. Let N denote the total number of transmitted packets (data rate), let N' denote a total number of lost packets (Loss rate) and N'' will represent a total number of received packets (Goodput).

$$N'' = N - N' \tag{3.8}$$

Or secondly, it may be expressed as Equation 3.9, where R denotes the total number of transmitted packets (data rate), P represents the packet loss rate, and η denotes the goodput or usable data. In this equation two cases are outlined; these cases show that goodput will be less than or equal to the data rate and cannot be higher. The two cases will depend upon the value of P, if P is 0 there is no loss rate the values of R and η will be equal. If P is above 0, η and R will be equal.

$$\eta = R - P \text{ and } \eta \leq R \begin{cases} \eta < R \text{ when } P \neq 0 \\ \eta = R \text{ when } P = 0 \end{cases} \tag{3.9}$$

Goodput at distances from 10 to 100 metres is measured, and coding was placed in the script to ensure each packet received was not corrupted. The packet loss rate at each distance has been recorded to show this result, and then this is calculated into a quantity of goodput using Equation 3.9. The results can be observed in Figure 3.21 and show almost identical results to those of throughput and not much difference between all data rates used.

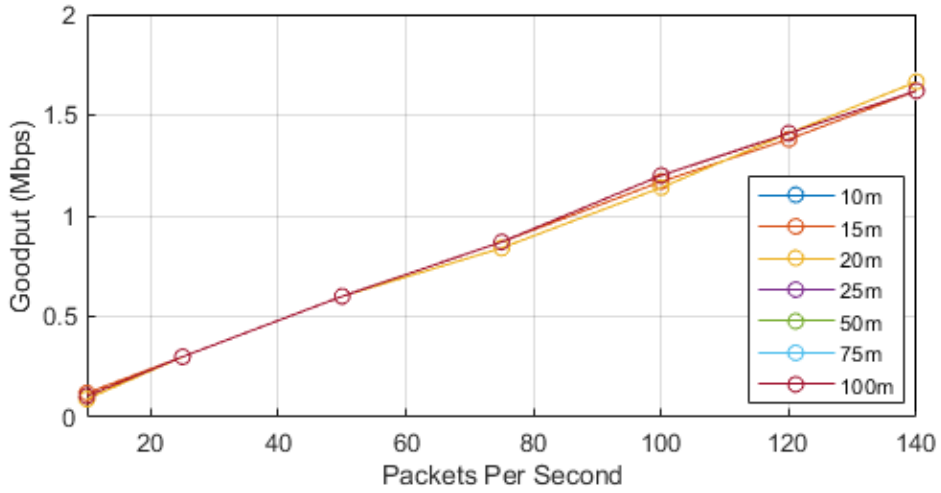

FIGURE 3.21: Goodput vs. distance

Latency or end to end delay

The next area chosen for analysis was the latency of the SDR-based DSRC with UDP. Many attempts were made to make this an end to end measurement, but the NTP server chosen could not synchronise the times accurately enough. Instead, a round trip time measurement would be an alternative but highly accurate option. The same setup was replicated as previous tests; however, instead of using the Taoglas antennas, SMA cables were used to measure the round-trip time. The cables are used as they eliminate any propagation time that is incurred and will more accurately represent the processing time incurred at the transmitter and receiver. This method allowed the measurements to be focused on the processing time and the propagation time was later calculated and added. As the calculation is completed theoretically the calculation be used for any distance, but the maximum measured was 450 meters. The formula can be found in Equation 3.10.

Latency is a critical factor of CAVs as this measurement dictates how a message can be sent, received, and processed so appropriate action can be taken. The Round-Trip Time (*RTT*) was recorded using a python code that captured the internal time

as each packet was sent from the transmitter. The receiver will receive the packet and send it back to the original transmitter device via its transmitter. The transmitter would then receive a packet containing its original time and then print via another python code when it receives the packet back. The values generated by these codes will be used in Equation 3.10 to produce an estimated, one-way end to end latency timing.

$$\text{Approximate E2E Latency}(s) = \frac{\text{Time Received Back - Initial Send Time}}{2} \tag{3.10}$$

Approximately 3000-time samples were taken and used to calculate the mean value and standard deviation. The samples are then used to create a normal distribution bell curve of the recorded time values, and this is seen in Figure 3.22. This finding will help identify the latency range from min to max and to identify where average or mean latency is situated on the curve.

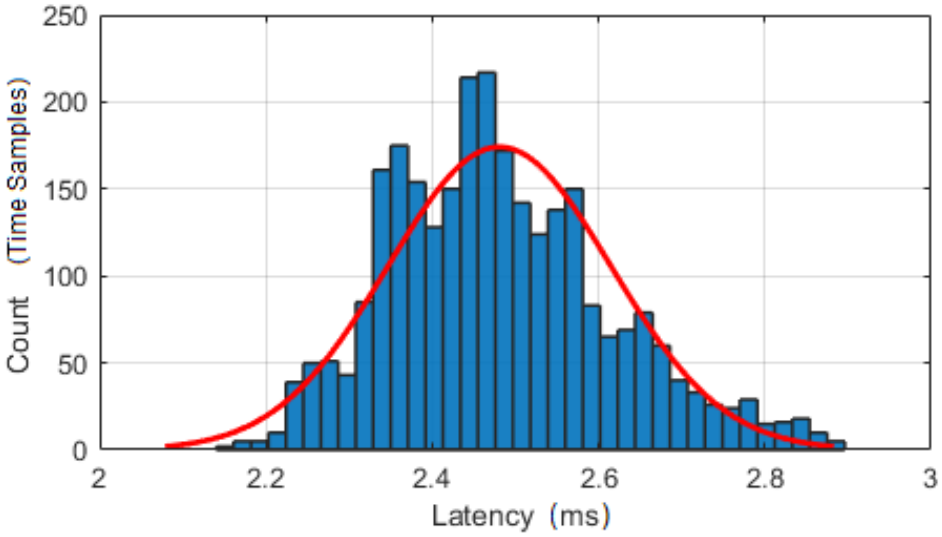

FIGURE 3.22: End to End latency distribution

The resultant curve shows that the latency ranges between 2.1 and 2.9 ms, and the mean is 2.48 ms. The result shows the latency is very low and is lower than the speculated time of DSRC at 100 ms and even less than the predicted value for pre-crash sensing, which is 50 ms; it is higher than the 1 ms requirement 5G CAVs. However, one point to note is that this experiment has taken place through cable connected devices, and a more accurate representation will be needed when the propagation time is included. This result is relative, and it can be speculated that the increase would be based on sensing information to be passed to DSRC and then

further processing time.

As mentioned, the propagation time is also calculated and used in addition to the measured processing time and this addition will present a more accurate timing example for the SDR. It was estimated that the mean is the most appropriate value to represent this result. As can be seen in Figure 3.23, the difference between 10 and 450 metres is less than 0.146 μs. The formula for propagation time can be seen in Equation 3.11 and is used to give theoretical values of latency over different distances, which can then be used in addition with the processing time previously measured to give a representation of full end to end latency.

$$T_P(s) = \frac{d}{c},\ c = \text{speed of light} \approx .2.9 \times 10^8 \tag{3.11}$$

Where, T_P represents propagation time, d represents distance between nodes and c represents speed of light.

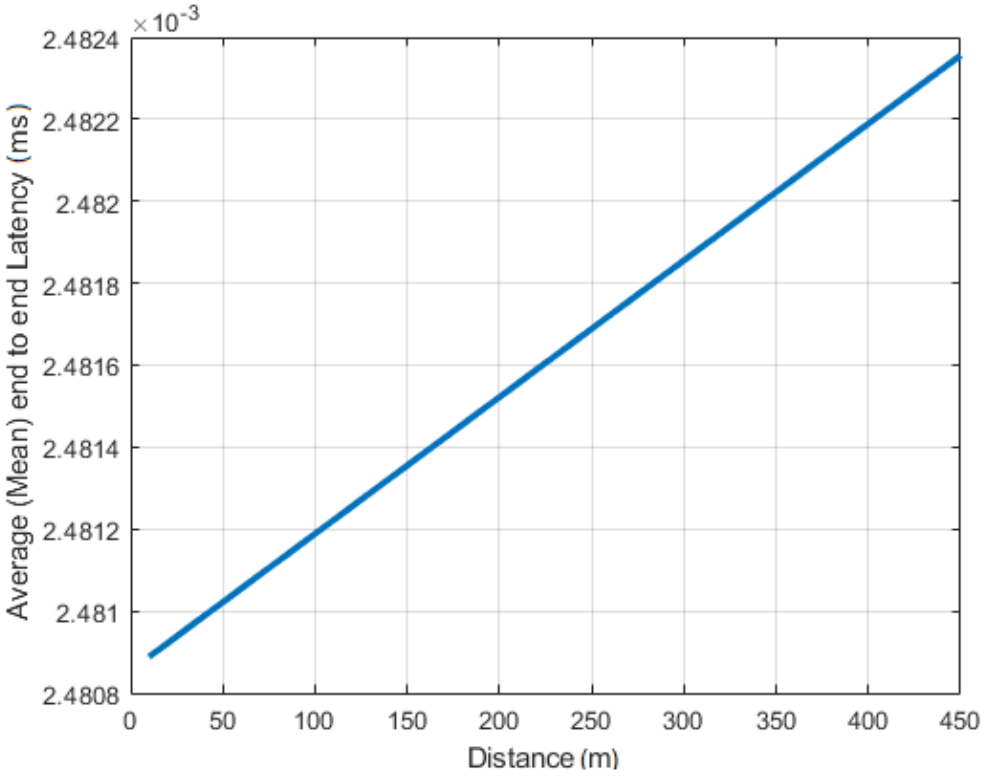

FIGURE 3.23: Mean end to end latency vs. distance

From the results, most of the latency in the SDR-based DSRC can be attributed to processing time at both transmitter and receiver and not the propagation time. The

latency measured is considered information freshness if used in a collision avoidance or safety scenario. This result is expected, as propagation is equivalent to the speed of light and latency would be expected to be slower. However, it is also shown that the latency mean value is 2.48 ms and is between 2.1 and 2.9 ms at every test conducted. This result identifies a lower latency than expected, even for a simple packet of 1500 bytes. When added, the propagation time produces a minimal effect, and the difference between 10 and 450 metres is less than 0.146 μs.To summarise, a 2-3 ms latency is adequate for many scenarios, such as lane merging, emergency collision warning, and stopping distance maintenance when considering collision avoidance.

3.3.5 Reliability and packet loss rate

The final experiments are the most important, determining the QoS or communication reliability. This set of experiments is used to test relationships between reliability in terms of the packet loss ratio, distance in meters and data rate in packets per second. The QoS is vital in CAVs as safety messages must have almost guaranteed delivery or at least 99.9%. This investigation is especially important for collision avoidance, where missed packets lead to avoidable crashes and accidents.

Initially, a field test was used to monitor packet losses over large distances. Three instances of 1000 packets were sent and recorded whilst stationary at each interval from 10 to 450 metres to measure the packet losses. The packet delivery ratio was then averaged at each of the specified distances, but it was found that such a small number of packets yielded a 0% loss. Due to a reception rate of 100%, it was necessary to repeat this test with a higher packet number but smaller distances. This is to find and identify a baseline of performance which can be used to predict the trend of packet losses at larger distances and can also minimise the losses incurred by external factors such as temperature, humidity and outside interference. However, this test highlights that the range of SDR-based DSRC can exceed 450 metres in meeting V2V requirements.

The initial setup for the redesigned field test was the same as previous experiments and was conducted within an indoor laboratory environment. This experiment was achieved using a short distance with a high quantity of packets, and an example equipment setup is shown in Figure 3.24.

The same range of 10 to 140 packets per second is used and set to send 7500 packets. The experiment is measured over 5 to 25 metres. With the packet size also kept to 1500 bytes, it is determined that 10.5 million bytes will be sent for each test. For each stage of this test, line of sight was maintained, and two python codes were used for receiver and transmitter. The transmit python code injects a value chosen

FIGURE 3.24: Laboratory Equipment set-up

and set, starting from 1 to the desired value, into the data payload of the sent packet. The receive python code displays the number of packets captured as a percentage and a counter that displays the total received packets. This packet manipulation is achieved in the physical layer. The formula in Equation 3.12 is used for calculating the packet success percentage. Packet number (P_N) is a value inserted into each packet payload at the transmitting side, from 1 to 7500 in this experiment. The number of packets received (P_R) is the value that the receiver adds to each time a packet is received. The value of 100 is used to represent 100%. The result is also displayed as the total packets successfully (P_S) received in number format.

$$P_S(\%) = \frac{P_R * 100}{P_N} \tag{3.12}$$

Initial calculations were performed to determine packet size, bytes sent and related statistics. The initial results can be seen in Table 3.6. This table contains the baseline statistics used for each test over every distance chosen to measure.

The formula in Equation 3.13 and Figure 3.25 are used to show how the equation for packet loss is derived. Where N denotes the total number of transmitted packets, N' represents the total number of lost packets (loss rate), N'' denotes a total number

TABLE 3.6: Packet size statistics

Data Rate(pps)	Interval(s)	Number of packets	Time(Seconds)	Total Bytes(Mb)
1	1	7500	7500	11.25
10	0.1	7500	750	11.25
25	0.04	7500	300	11.25
50	0.02	7500	150	11.25
75	0.013	7500	100	11.25
100	0.01	7500	75	11.25
120	0.0083	7500	62.5	11.25
140	0.0071	7500	53.571	11.25

of received packets, R is used to show the throughput, P denotes packet loss rate, η signifies goodput, and T represents total transmission time.

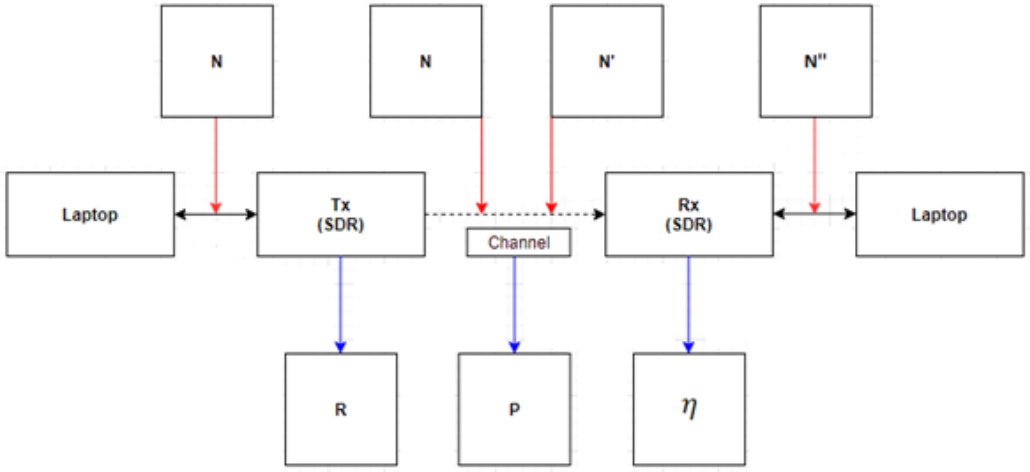

FIGURE 3.25: Packet loss equation block

$$
\begin{aligned}
P &= \frac{N'}{N}\% \\
P &= \frac{N - N''}{N} = N'' \\
N = R * T, \quad \text{so,} \quad R &= \frac{N}{T}\text{packets/s} \\
N'' = \eta * T, \quad \text{so,} \quad \eta &= \frac{N''}{T}\text{packets/s} \\
P = R - \eta = \frac{N}{T} - \frac{N''}{T} &= \frac{N - N''}{T}\text{packets/s}
\end{aligned}
\tag{3.13}
$$

An initial test was conducted using an increased number of packets of 75000,

TABLE 3.7: Experiment results at 5 metres

Data Rate(pps)	Data Rate(B/s)	Packets Sent	Packets Lost	Success%	Loss%
10	15000	7500	2	0.9997	0.0002
25	37500	7500	1	0.9998	0.0001
50	75000	7500	1	0.9998	0.0001
75	112500	7500	4	0.9994	0.0005
100	150000	7500	5	0.9993	0.0006
120	180000	7500	5	0.9985	0.0006
140	210000	7500	2	0.9997	0.0002

but it was found that the time taken for each test was far too high with an excessive number of packets. For example, with ten packets per second, each test would take two hours, and the amount of data transmitted was 562.5 million bytes.

For the 7500-packet test, an instance was performed at every distance three times and recorded the lost packets and packets success rate. The results were tabulated to show packet loss rate, percentage loss rate per 1000 packets and the approximate number of bytes lost. An example of the tabulated results will be included for the experiment conducted at 5 meters in Table 3.7. The table will also include the overall packet loss rate, distance and data rate relationship. Table 3.7 shows the packet losses are relatively low, over 99.8% at 5 metres and the largest loss being 0.6 packets per 1000.

Figure 3.26 shows the results for packet loss rate versus data rate, the results for each distance are plotted and include the initial test result with the increased 75000 packet example and this is done to show similarity and confirm the decision to reduce packet quantity. The results show that all distances are very close in packet loss rate being approximately 1 or 0 per 100 packets. The exception is the 25-metre test, where a significantly higher loss at 120 and 140 pps can be seen, respectively. This finding can be attributed to the system not handling high messages or channel conditions. It is deemed a rate of up to 100 pps for future testing is suitable for collision avoidance. The results show that data rates up to 100 pps over each distance maintain an average error of less than one packet in each instance. It can also be seen that from 10 to 50 pps, the packet losses are very low, but after 50, the losses start to increase slightly. The final point of notice is that the increased packet test of 75000 packets at 5 metres, yielded a larger packet loss at 140 pps compared to the other tests. This could be due to time taken and fluctuating environment conditions such as humidity or temperature. TCP may be considered in future investigations to decrease packet losses but may suffer increased latency.

Figure 3.27 is a plot showing the relationship between packet loss rate and distance for each data rate. The second figure is used to show assumptions are correct based on the first figure shown in Figure 3.26.

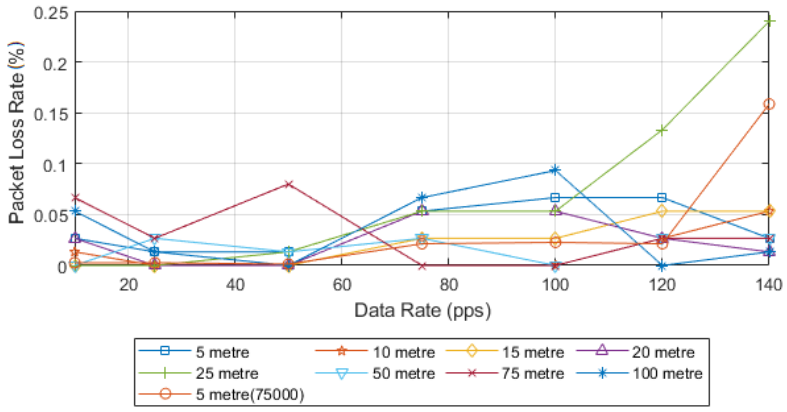

FIGURE 3.26: Packet loss rate vs. data rate

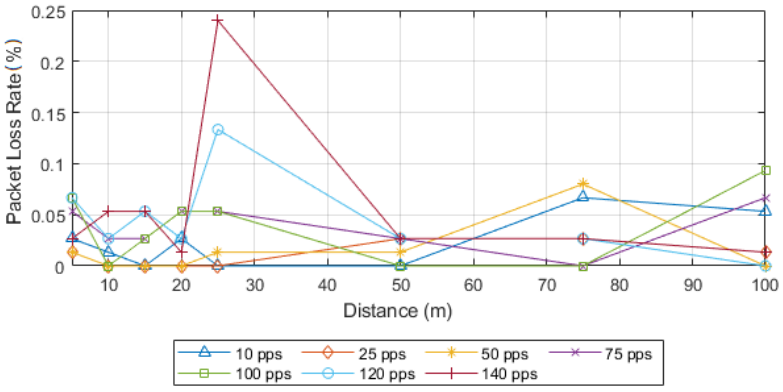

FIGURE 3.27: Packet loss rate vs. distance

As previously shown, the highest data rate of 120 and 140 pps are the points at which the packet loss increases at 25 meters. This figure also emphasises that all other data rates are uniform across all distances, with only a slight rise in 100 at 25 metres and a significant increase at 25 metres. However, the error is approximately 2.4 errors per 1000 packets and occurred at the longest distance with the highest number of packets per second. A significant point can be seen in the 140 pps test, where a significant increase in loss can be seen at 25 metres. This can be attributed to outside factors, such as interference from outside sources such as temperature or interference from people passing by.

The final section of this experiment analyses the tests that operated for a long period. This result helps to indicate how the system copes when used for extended periods or for such cases of V2I, which could be a potential usage. One of the previous tests was conducted using 75000 packets, as has been discussed and was also

TABLE 3.8: Extended experiment results at 5 metres

Data Rate (pps)	Interval(s)	Number of packets	Time, Hours	Loss%
1	1	75000	20.83333333	6.66667E-05
10	0.1	75000	2.083333333	2.66667E-05
25	0.04	75000	0.833333333	2.66667E-05
50	0.02	75000	0.416666667	1.33333E-05
75	0.013333333	75000	0.277777778	0.000213333
100	0.01	75000	0.208333333	0.000226667
120	0.008333333	75000	0.173611111	0.000213333
140	0.007142857	75000	0.148809524	0.001586667

tested with one packet per second, which took 20 hours. The results for that test can be seen in Table 3.8. As can be observed, these results show no significant change from running the tests over an extended period.

Two other tests were performed similarly, with one taking 18 hours at 100 pps and the second for 2 hours with ten packets per second. The results for the first were a loss of 5600 packets from 6480000, meaning a loss ratio of 0.0008. The results for the second are a loss of 22 from 72000 a loss rate of 0.0003. These results show a slight increase in loss, but not much higher than previous tests.

3.3.6 Regression analysis

Regression analysis is used to investigate the relationship between the power and packet losses and predict the signal to noise ratio (SNR). This result is achieved using the estimated values for packet loss and received power. The SNR has been extracted using a linear regression-based method based on the packet loss linear regression curve estimation and the power received regression curve. The signal to noise ratio is then computed from the power estimation result and the noise floor result, measured at -100dBm.

Three layers of regression known as multiple linear regression were applied. The previously generated field test results provide estimations, and predictions can give useful insights into performance. The first use of regression is to create a distance against packet loss estimation using previous data. This result can be plotted using different variations of data rates, with the example used of 140 pps.

Figure 3.28 shows the packet losses recorded in a field test, over a distance at 140 pps, from 10 to 100 metres, and this also has the linear trendline associated with the data. This experiment was performed ten times and the average is used for the curve fitting. The equation for the trendline is shown in Equation 3.14. The losses incurred at points 30 and 70 are attributed to reflections of the signal causing increased interference. and in ideal circumstances losses would be minimal.

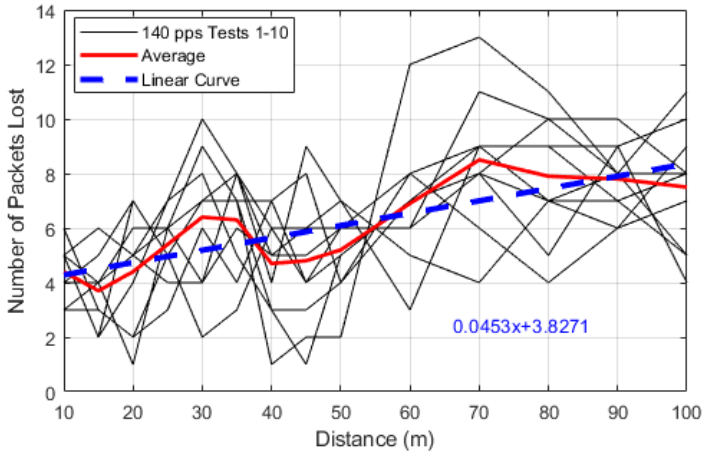

FIGURE 3.28: Regression at 140 pps, packet loss rate vs. distance

$$Y = 0.0453x + 3.8271 \tag{3.14}$$

This equation can then be applied to a chosen selection of distances to produce a packet loss estimation. The results are shown in Figure 3.29 and represent the predicted number of lost packets from 0 to 500 metres, however it should be noted that this is only a preliminary estimation and does not represent accurate results, rather offers an insight of predicted losses.

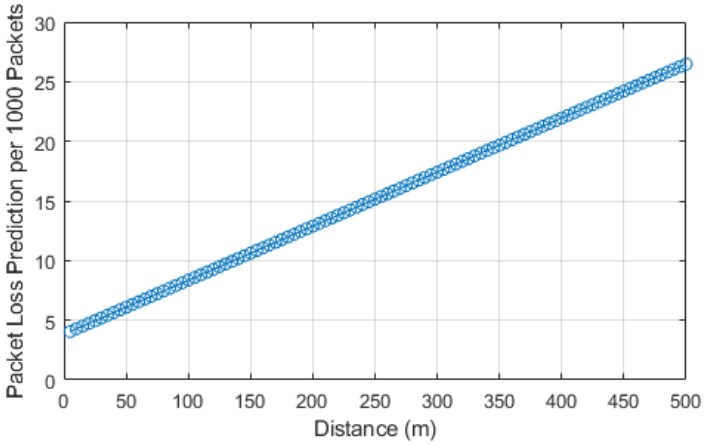

FIGURE 3.29: Regression prediction to 500 metres

The trendline calculation and the resulting values at each distance can produce a power estimation correlation using these values. Figure 3.13 shows the original plot for the power measured in a field test, with the curve fitting following a logarithmic

scale for the larger amount of data acquired. The power equation used is seen in Equation 3.15.

$$Y = -5.088 * ln(x) - 55.039 \tag{3.15}$$

From the equation for power plotted and the data from the packet losses, a power estimation can be plotted to show the relationship and produce a power estimation trend based on the number of packets that have been lost. This result can be seen when replacing the value for packet loss at each distance into the power loss estimation equation, and the results can be seen in Figure 3.30. This figure shows how packet loss and power correlate and identifies further the relationship, that lower power leads to an increase in the number of packets lost.

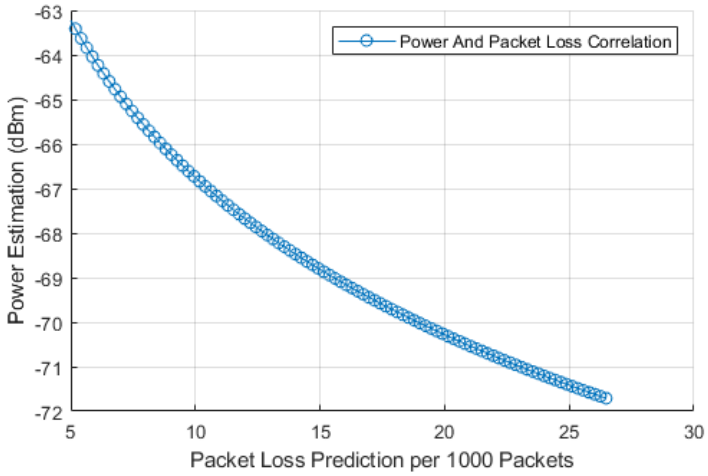

FIGURE 3.30: Power vs. packet loss correlation to 500 Metres

The noise floor is the sum of all noise sources and signals that are not being monitored and discovered to be -100dBm. The signal to noise ratio can be calculated, and, in this case, it is a simple equation shown in Equation 3.16.

$$SNR(dB) = PowerEstimation(dB) - NoiseFloor(dB) \tag{3.16}$$

SNR can also be calculated in another way if the requirement is to be in non-dB form and is shown in Equation 3.17.

$$SNR = P_{Signal} / P_{Noise} \tag{3.17}$$

The SNR can now be plotted using regression and the formulas for each distance. SNR can be shown for any distance range and is calculated up to 500 m. Figure 3.31

and 3.32 represent both linear and log form respectively.

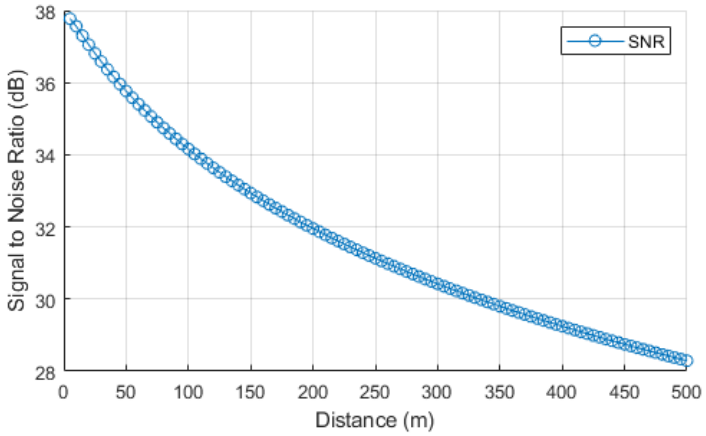

FIGURE 3.31: Linear signal to noise ratio to 500 metres

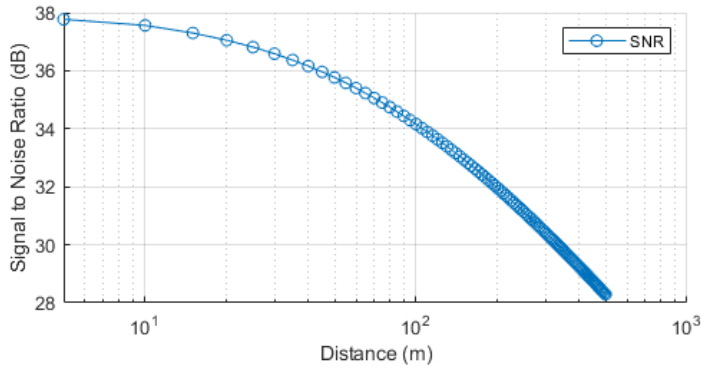

FIGURE 3.32: Logarithmic signal to noise ratio to 500 metres

These results show that up to a maximum distance of 500 metres using the regression-based analysis, that distance impacts the packet loss ratio, which can be caused by the change in the SNR ratio, where the signal power can be seen decreases and this decrease leads to increased packet losses.

3.4 Further field testing

The following experiments are used for further analysis and are tests where certain performance aspects have been analysed. These tests were used to identify further opportunities for SDR in V2V scenarios not yet investigated. However, they are smaller in scope.

TABLE 3.9: Two transmitter reliability results

Test	Total Received	Total Lost	Packet Loss rate %
1	19998	2	0.01
2	20000	0	0
3	19997	3	0.015
4	19991	9	0.045
5	19988	12	0.06
6	19994	6	0.03
7	19981	19	0.095
8	19999	1	0.005
9	19990	10	0.05
10	19998	2	0.01
Average	19993.6	6.4	0.032

3.4.1 Receiver reliability with two transmitters

Analysis was also performed, showing how the receiving device would cope with two transmitters sending at the same time to one receiver. The same setup was used but included an extra replicated transmitter setup. Ten tests were performed in this setup, with a mid-range chosen of 50 packets per second with 10,000 packets sent per device, and this means it would be expected to receive 20,000 at the receiver side. The setup for this was with each transmitter spaced on either side of the receiver at approximately 10 metres.

The experiment results in Table 3.9 show an average loss of 6.4 packets per 20,000 packets sent, and this is highly similar to the results obtained with one transmitter. Overall, this indicates that even with two transmitters, the receiver is robust enough to operate whilst receiving from at least two devices. This finding shows that inclusion into rear-end collision avoidance is possible.

3.4.2 Video transmission with SDR-based DSRC

The final experiment conducted using the SDR-based DSRC was a simple experiment to explore the concept of object detection with the transmission of video data showing the potential safety hazard. For this, it was chosen to transmit a video file in real-time through the SDR to the receiving devices. This experiment was conducted in a lab environment using the existing UDP block additions and an open-source video player stream via UDP incorporated. The readily available and free to use VLC Media Player was used.

The setup with this test was also using three SDR devices. The transmitting device was placed centrally (Tx1), and two other devices were placed in different locations; one was positioned 10 metres away with clear LoS (Rx1), and the second was positioned 10 metres away without clear LoS (Rx2). A second scenario was

used that operated as a cooperative relay system, where Rx2 was programmed as a transceiver, where each of the Tx and Rx ports operated with different port schemes. The scenarios can be seen in Figure 3.33.

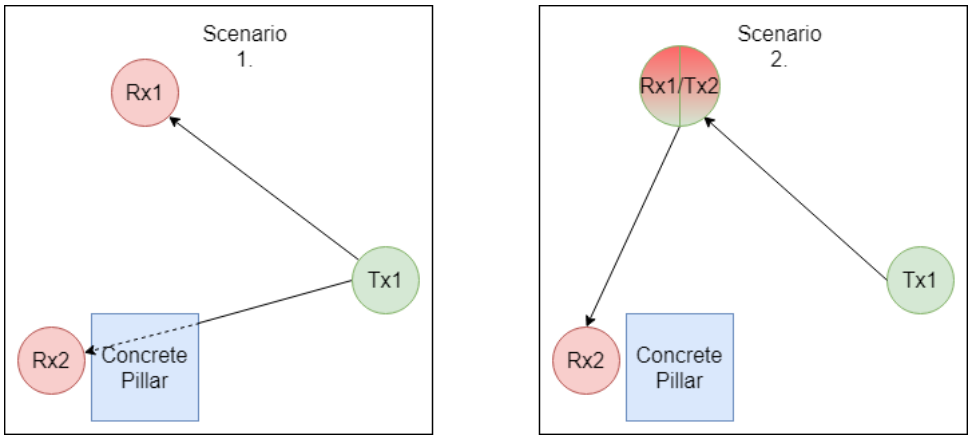

FIGURE 3.33: Video transmission scenarios, 1. LoS vs. NLoS and 2. Cooperative relay

The VLC program had to be prepared to be compatible with the SDR compilation, which required separate setup configurations on the Tx and Rx, respectively. The Transmitter configuration can be seen in the following set of Figures. Figure 3.34 shows the address configuration within the SDR code for a UDP client. The Wi-Fi MAC block is used to show the correct addressing used for broadcast communication.

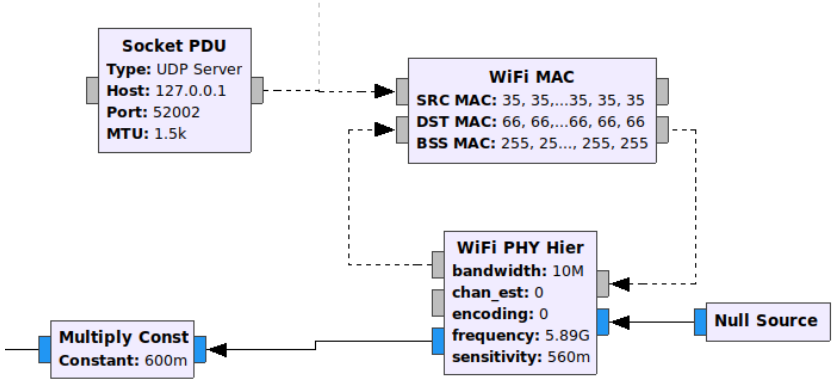

FIGURE 3.34: Tx configuration in Gnuradio

Figure 3.35 shows the configuration inside the VLC suite, detailing the process of creating a UDP stream profile and addressing matching the client and the video

setting parameters, with a data rate matching those calculated in previous experiments.

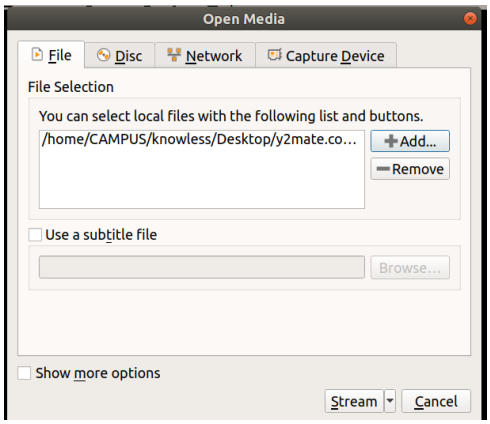

(A) Select video source file

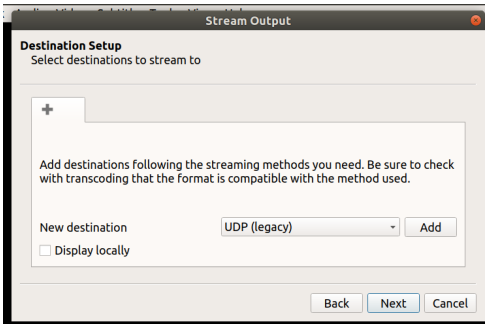

(B) Select video broadcast destination

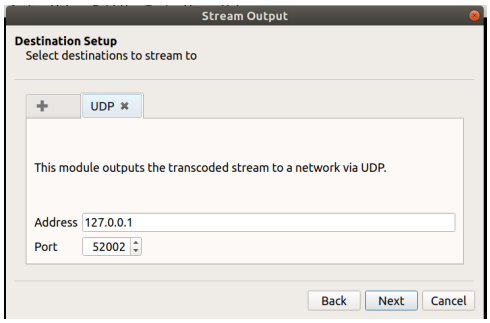

(C) Set address and port

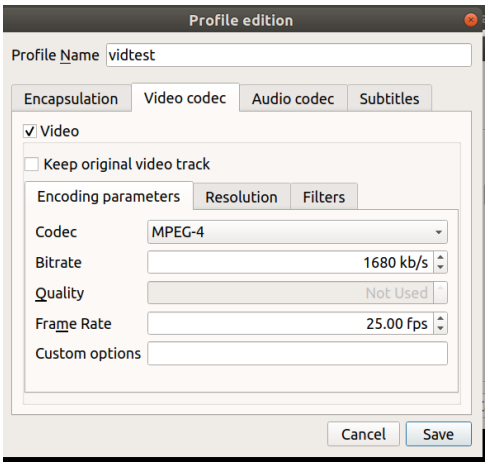

(D) Set video codec

FIGURE 3.35: VLC settings on Transmitter

On the Receiver side, the same process is followed. Figure 3.36 shows the addressing in the GNURadio suite for a UDP client and the matching address configured in VLC.

Figure 3.37 shows the output of the streamed content from transmitter to receiver via the SDR devices. The addressing scheme and image quality can be seen in the figure. The video broadcast in this test was a 480p standard definition image, and it is easily discernible to see the road and vehicles.

The video transmission experiment allowed us to stream video and audio content through the SDR-based DSRC testbed. The receiving side received the data and streamed the video and audio with almost identical quality. However, a small error was observed, with some pixels missing or freezing images, which was very

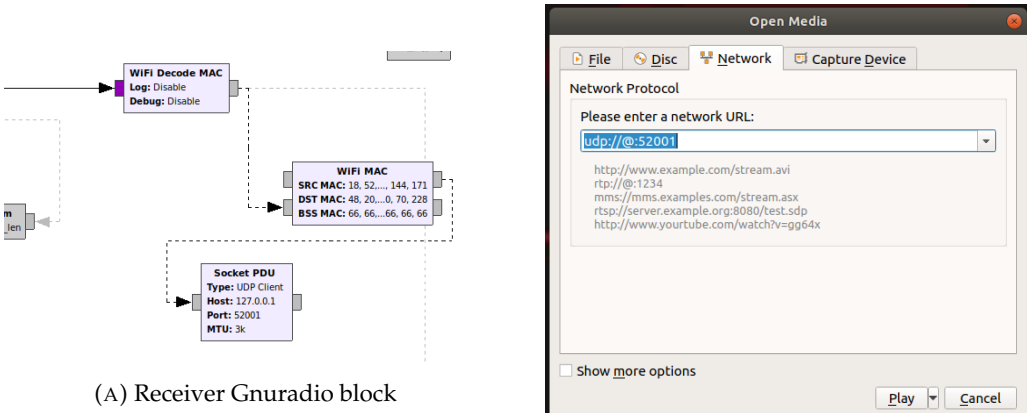

(A) Receiver Gnuradio block

(B) Set VLC video stream address

FIGURE 3.36: VLC settings on receiver

low. The longer the stream continued, the more reliable the quality and connection became.

This experiment proves it will be possible to use video capturing to detect an object and stream the information or even a warning message advertising the problem encountered to other vehicles in the vicinity. This concept is used to recognise pedestrians or bicycles on the road or even measure distances through continued training and inference with a deep learning algorithm.

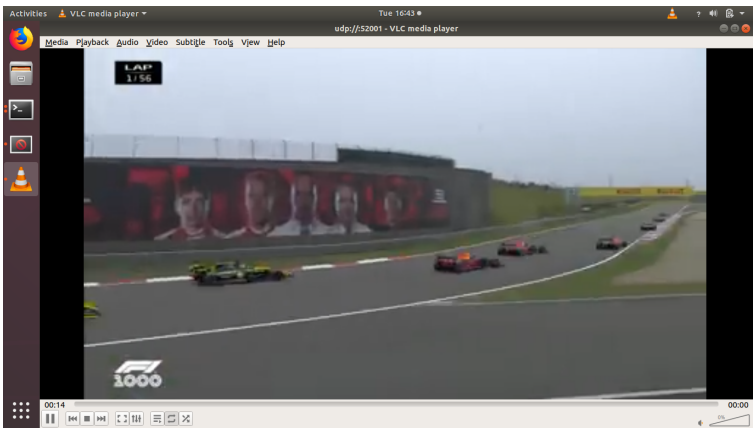

FIGURE 3.37: Screenshot of video received at Rx

3.5 Summary and conclusions

In this chapter, an SDR-based DSRC platform for V2V was designed, developed and analysed. The capabilities were presented along with the performance attributes being measured. Various parameters were shown and extracted through robust testing in various environments and simulations. Knowledge is gained on the performance relating to the impacts of power on SDR-based DSRC performance. In addition, regression analysis has allowed the extraction of further components such as the SNR and the relationships between packet loss and received power.

The SDR-based DSRC was shown to perform to a standard capable of traditional DSRC communication, observing that the biggest impact is seen with longer distances. However, it can also be noted that in terms of packet losses, the SDR-based DSRC does not meet the 99.9% requirement and instead approximately 99.75% at its lowest. The SDR platform was investigated over a large distance to analyse the performance. It then was subjected to a measurement campaign within a vehicle, demonstrating the performance is not significantly affected whilst moving. Still, the reduction of the line of sight had a more significant impact.

Robustness was also proven to support vehicular communication, with testing scenarios showing steady data rates, short latency and a high packet success ratio. These components also proved that the SDR-based DSRC could perform real-time video transmissions using a UDP-based stream of pre-recorded content. The receiver received this data and played it with acceptable quality and sound.

Further testing using regression has enabled the prediction and modelling of packet losses, received power and signal to noise ratio, with extracting linear and logarithmic curve fitting to enable the parameters to be further used in future.

This investigation provides a deep understanding of the developed SDR-based DSRC performance related to the modified DSRC project and the physical limits of the SDR device. Further evaluation concerning collision avoidance and the performance in scenarios closer to those in the real-world environment can be investigated. This development will enable further experimentation to develop the performance and be compatible with further incorporated technologies and techniques.

Chapter 4

Reliable V2V communication for Collision Avoidance

4.1 Introduction

The continuing evolution and adaptation of vehicular technology are needed to support autonomous driving. The needs of autonomous driving vary but have a specific set of fundamental requirements for many different applications. The requirements encompass various attributes such as reliability, latency, robustness, efficiency, high capacity, and stability. Examples are in-car entertainment which requires a steady data throughput with less stringent demands on latency or safety that requires low latency and high reliability. ADAS systems to support AV have high reliability and Quality of Experience (QoE) requirements, which requires regularly updated information via V2I or V2V. The safety of vehicle operators and other road users is a paramount concern for ADAS and AV.

Safety for CAVs is vital for the emergence of the future of connected vehicle. Essential to this will be the application of the various technologies and techniques developed and utilised in modern vehicles. With the emergence of CAVs, there has been a significant increase in research and development for concepts and technologies that can enable and enhance information sharing. CAV safety aims to address the nature of what it is to drive [223] to allow a safer and more efficient worldwide transport system that is achieved by reducing collisions, easing congestion, and enabling a safer road system for all road users. Facilitating communication between vehicles, infrastructure, pedestrians, and the network will also decrease air pollution by traffic efficiency. This effect can be attributed to the tumbling effect of increasing safety; fewer accidents mean less congestion, and less congestion means fewer vehicles spending time on the road.

Safety is a critical component for CAVs, and this area must be continually addressed. Critical factors such as reduced road fatalities, less time spent on the road,

and reduced lost hours spent in congested roadways will all be somewhat impacted by increased road safety procedures. In the UK, the number of road accidents with casualties is reported to be 115,584 with 1460 fatalities in the year 2020 [224] and the WHO reported a worldwide estimate of 1.35 million road accident-related deaths in 2021 [2].

The application of vehicular communication into safer driving is one of the primary goals with CAVs and DSRC is a candidate technology for V2V communication. In this chapter, DSRC is shown to improve the safety performance for vehicles through the analysis of stopping distances. V2V reliability via DSRC is then investigated via the implications of consecutive losses. This investigation identifies how stopping distance reduction can be impeded by packet losses in terms of distance and density-based losses.

Firstly, a model is created using SDR-based DSRC to reduce stopping distance via V2V communication. Then the analysis was further developed into a novel scenario for collision avoidance via adherence to a stopping distance, which is based on the DSRC capabilities previously measured in Chapter 3. The stopping distance algorithm developed also shows an advantage over traditional methods and shows that with SDR-based V2V communication, the stopping distance required can be reduced with communication. Secondly, this model is subject to different categories of burst losses, and the implications are evaluated. This evaluation is achieved with the design of a model for the remaining stopping distance. This model is used with different speeds and packet rates to analyse the impacts of losses in different scenarios. Finally, this model is developed and compared with other available models to show the increase in performance.

In section 4.2, initially, an investigation into V2V collision avoidance with SDR-based DSRC is produced, showing the two main advantages of incorporating CAVs and how safety will be increased. Then secondly, an investigation is made into communication assisted stopping distances and algorithms are developed for distance measurements. Section 4.3 is used to show the impact of consecutive losses, with a model designed and developed for distance independent and distance dependant losses. In section 4.4, density-based losses are investigated, with a safety distance algorithm developed with SDR-based DSRC and a simulation of node density. Finally, section 4.5 proposes a joint loss system, and 4.6 summarises and concludes the chapter.

4.2 Collision avoidance with V2V

The following section is used to design and investigate the application of SDR-based DSRC in V2V collision avoidance scenarios. The scenarios will be shown with algorithms developed for each respectively. Results will be developed to highlight the advantages of non-communication assisted collision avoidance.

4.2.1 Stopping distance with V2V communication

Stopping distance is a critical component for rear-end collision avoidance towards increasing safety. It measures the distance a vehicle will take to come to a complete stop. If correct procedures aren't followed, collisions can occur when a lead vehicle brakes in an emergency and the following vehicle is unaware. Safety issues can potentially be reduced with vehicle communication. The concept of using the SDR-based DSRC is investigated to show the capabilities of emitting a safety broadcast message or beacon. The SDR-based experiments previously investigated will be used to develop this novel idea, and the most vital statistic to be used in the latency between sending and receiving nodes. The idea is that the lead vehicle can alert the following vehicle, and braking can be applied more efficiently and quickly, especially in an autonomous vehicle rather than a vehicle operated by a human driver.

The time taken for a broadcast message to be received will be classified as the delay or message latency, and a distance will be travelled during this time, which will be discussed further. The latency usage can be classified as the time for a message sent by a transmitting node and received at its endpoint. In this case, it can be assumed to be a broadcast type communication, advertising the braking status. As the receiver sees a change in braking status, it too can apply automatic braking.

A clarification will show how stopping distance is measured in this scenario.

- Stopping Distance: The total distance traversed until a vehicle comes to a complete stop and comprises the following measurements.
  - Reaction Time (s): Time is taken for the driver/system to apply the reaction to a problem, such as applying brakes.
  - Thinking Distance (m): Distance travelled during a driver to notice a problem and initiate a reaction.
  - Braking Distance (m): Distance travelled by a vehicle after the reaction has been made, such as brakes being engaged and the vehicle coming to a full stop.

In this procedure, these values will be broken down into separate measurements, and the reaction time will be replaced with either the human standard reaction time

or the SDR-based DSRC latency, which can be classified as AV or ADAS. Thinking distance will be omitted due to comparisons with an autonomous system where automatic braking will not require any action by the human, therefore is taken as zero to keep the results consistent.

Stopping distance can be calculated as shown in Equation 4.1, where D_S is stopping distance, D_R is reaction distance and D_B is braking distance. Additionally, in the equation, μ is used for the coefficient of friction, and g represents the gravitational acceleration (9.80m/s^2). The coefficient of friction used in dry conditions and average tyres is 0.8 and can be found in [225]. Research suggests that the reaction time of an average driver is approximately 1.5 seconds [226] but has also been cited to be 0.67 seconds. T_R will be used to represent the reaction time, and is specified in three formats, each representing a different time. T_{R1} represents a reaction time of 1.5 seconds, T_{R2} is used for 0.67 seconds and T_R represents the latency of the SDR at 2.89 milliseconds. In addition, V is used to represent vehicle velocity.

$$\begin{aligned} D_{\mathrm{S}}(m) &= D_{\mathrm{R}} + D_{\mathrm{B}} \\ D_{\mathrm{R}}(m) &= V * T_{\mathrm{R}} \\ D_{\mathrm{B}}(m) &= \frac{V^2}{2g\mu} \end{aligned} \tag{4.1}$$

Using the latency measured in Chapter 3 in place of the human reaction time will show the reduction in stopping distance that is produced when using V2V broadcast assistance. This result will be shown for both estimated human reaction times and the V2V reaction time (latency), at speeds from 4.5 to 45 m/s, and the results can be seen in Table 4.1 and Figure 4.1. This figure is used to show the difference in stopping distances when comparing human reactions against autonomous reactions, which can be given by the latency from the SDR. In addition, the decrease gained by using the SDR latency over the human reaction time can be seen in Figure 4.2 and this figure shows how much distance is saved by using T_R as reaction time compared to both human based reactions. This is produced by finding the difference between the results and showing the reduction at each speed. For instance, at 30 m/s T_R will offer 20 metre reduction compared to T_{R2}.

Using the latency of the SDR-based DSRC transceiver reduces the reaction time significantly. However, this value could be increased slightly due to mechanical processing. The results show that stopping distance is reduced substantially with this SDR implementation compared to human driver reactions. The distance saved would be between 20 and 46 metres at 32 m/s (70 mph). This distance is a considerable reduction, and thus collision avoidance would be reduced with the advanced

TABLE 4.1: Stopping distance comparison

v (m/s)	D_B	D_S at T_R1=1.5s	D_S at T_R2=0.67s	D_S at T_R=2.89ms	Decrease in D_S from T_R1	Decrease in D_S from T_R2
4.5	1.46	8.16	4.45	1.47	6.69	2.98
8.9	5.83	19.24	11.82	5.85	13.38	5.96
13.4	13.11	33.22	22.09	13.15	20.08	8.95
17.9	23.30	50.13	35.28	23.36	26.77	11.93
22.4	36.41	69.94	51.39	36.48	33.46	14.91
26.8	52.43	92.67	70.40	52.51	40.15	17.89
31.3	71.37	118.31	92.33	71.46	46.85	20.88
35.8	93.22	146.86	117.18	93.32	53.54	23.86
40.2	117.98	178.33	144.93	118.09	60.23	26.84
44.7	145.65	212.71	175.60	145.78	66.92	29.82

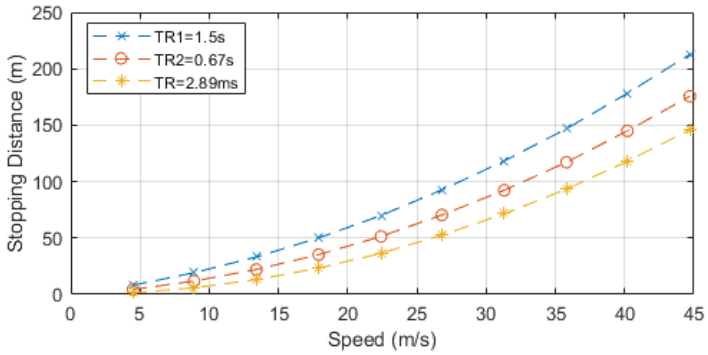

FIGURE 4.1: Comparison of stopping distance using SDR-based DSRC

warnings provided by V2V.

The information can be shared cooperatively via V2V over large distances to warn others of obstacles or accidents ahead. The information passing via multiple V2V nodes will provide this warning hundreds of meters in advance, depending on the communication range and power profile specified.

4.2.2 Beaconing with V2V reaction time

A secondary scenario for applying the SDR-based DSRC communication would be to emit a beacon periodically to make drivers aware of situations. This scenario would have various applications, and two will be briefly explained.

Emergency services are an integral part of daily road usage. Currently, the only method to alert road users of their presence is with the combination of audible sirens and visible lights. Still, this method is not always practical for drivers with disabilities, loud music or obscured vision. The novel approach proposed here is the use

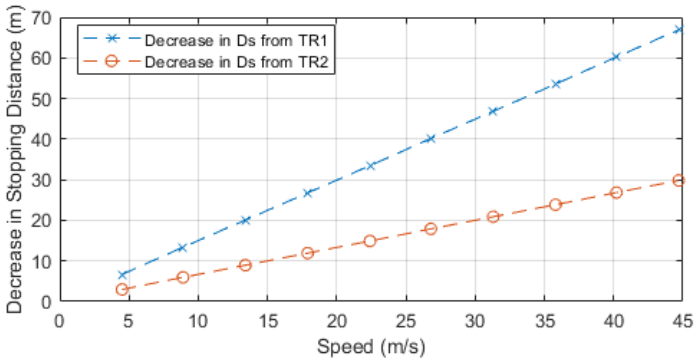

FIGURE 4.2: Comparison of decrease in stopping distance using SDR-based DSRC

of an emergency service broadcast. This broadcast will be used to alert lead drivers on the same route to an approaching emergency service vehicle, which would allow them to make appropriate collision avoidance manoeuvres. This warning would mean that emergency services would arrive at their locations sooner and prepare life-saving capabilities more efficiently.

The proposition of the system can be extended to more at-risk, vulnerable road users, such as bicycles or motorcycles, that can potentially be equipped with a communication device, warnings from other vehicles or through object detection. This system would emit a broadcast to receiving vehicles, and they will have an alert light on the dashboard or an audible alert informing them that a two-wheeled vehicle is near. The location information from Global Positioning Systems (GPS) can improve effectiveness when linked to distance and displayed to the drivers. This warning would assist in identifying the distance to the broadcasting vehicle.

The designed system would implement a directive broadcast from a vehicle. The directive broadcast will be received, and the message relayed to the vehicle driver. The broadcast message will be sent periodically using a regular broadcast to all nodes in range advertising a two-wheeled vehicle in the detection range and an approximate distance measurement to the location of the vulnerable road user.

The experiments show that up to 500 metres are possible in the SDR range. This distance can be converted into time for different speeds and offer drivers the additional time to be aware of a motorcycle or leave adequate space for emergency vehicles to pass. This system would be potentially lifesaving and would avoid many collisions with VRUs. The results in Figure 4.3 show the awareness time that would be given at different speeds and various communication ranges. This has been achieved with Equation 4.2, where T_A represents awareness time, D represents distance and T_R denotes the reaction time.

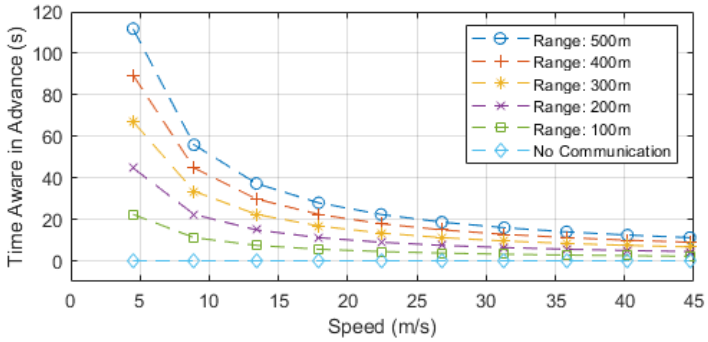

FIGURE 4.3: Awareness Time that can be offered with SDR-based DSRC

$$T_A = \frac{D}{T_R} \tag{4.2}$$

4.2.3 Comparison to laptop-based DSRC

Previous work utilised a different DSRC testbed based upon Linux laptop nodes that act as DSRC devices. Following earlier experiments with the SDR and laptop variations, the SDR-based DSRC has superior performance in every area. However, the cost is significantly more expensive, although still less than commercial DSRC. The implementation of the SDR-based DSRC is taken from Chapter 3, and uses the 2.89 ms reaction time.

The laptop implementation achieved approximately 100 metres in broadcast distance, but the SDR can exceed 450 metres. The delay and data rate have also improved, with previous measurements being 18 ms and 56 Kilometres per second, respectively. The SDR implementation can provide a latency between 2.1-2.9 ms and a data rate of 210 KB/s.

The QoS has also improved for both packet loss rate and the number of collisions when operating with two receivers. The packet loss rate in the laptop-based had a value of 1.6% at 10 metres, whereas the SDR could maintain a loss rate of 0.06% at the same distance. This result can also be compared with the smaller number of packets test where a 0% loss rate at 450 metres was measured with the SDR. In comparison, the laptop version had a 30% loss at 110 metres. Collisions of two transmitters and one receiver have decreased from 6.6% loss to 0.095%.

The final comparison that can be made is with the decrease in stopping distance gained from the SDR. Previous work analysed the laptop-based DSRC reduction when used for stopping distance purposes. The latency of 18 ms is compared to a human reaction time of 1.5 seconds, and the stopping distance can be reduced at 70

mph, from 96.01 metres to 75.26. Utilising the SDR-based DSRC, it can be concluded that the stopping distance would be reduced to 74.76 metres. This result can be seen in Figure 4.4 where the slight decrease can be seen in the SDR-based DSRC. This figure is used to show the difference between a laptop based and SDR-based DSRC, where the slightly lower reaction time produced by the SDR also leads to a slightly lower stopping distance needed.

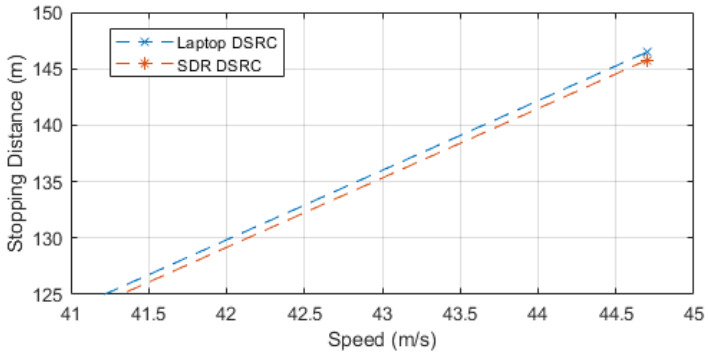

FIGURE 4.4: Comparison of stopping distance between laptop and SDR-based DSRC

4.2.4 Communication assisted stopping distance

The SDR-based DSRC used in Chapter 3 has also been used in this chapter. The empirical measurements evaluate the capabilities and show performance to meet 802.11p/DSRC standards. With this SDR-based DSRC established, it was then used in more direct scenarios concerned with vehicular safety scenarios.

One of the most important areas highlighted in the literature is rear-end collision avoidance [182], [221], [227], [228], and is classified as a collision by the following vehicle to a leading vehicle, commonly occurring for not having enough space between vehicles. Stopping distance is the term used for the distance a vehicle will take before it comes to a complete stop. This distance includes the time taken for a driver to react to an emerging situation, the distance that is travelled during this time, and the distance taken before the vehicle completely stops from the initial operation of the brakes to the point the vehicle is entirely stopped, and velocity is 0. This stopping distance is commonly split into three categories, which can be found in section Section 4.2.1.

These different categories will be explained and discussed in later stages. Still, it should be stated that in the investigations, the reaction time will be replaced and substituted with SDR-based DSRC communication time or latency. This latency will be the DSRC system latency and a perceived computational time.

The following sections make use of the developed SDR-based DSRC and utilise some of the results that have been taken from previous measurement campaigns. In this first area considering rear-end collisions and stopping distance, the value used is the value for latency. This latency is observed in the previous experiments highlighted in Chapter 3 and is the measured E2E latency between sender and receiver as shown in Equation 3.10 and 3.11. Latency is a critical component for CAVs. It is a measure of time taken for nodes to communicate important data to each other so that appropriate actions may be taken. This investigation is vital for safety scenarios. The latency of the SDR-based DSRC can be seen in Chapter 3, Figure 3.22. As mentioned, this latency measurement is measured, and, in this case, the logical processing was ignored as it is negligible. The latency was measured to be in the range of 2.1 and 2.9 milliseconds with a mean of 2.48 milliseconds.

Two different methods are typically used in the literature to calculate the stopping distance in the vehicular environment. The first equation is the more commonly used formula used in physics to calculate braking distance [129], [229], [230]. However, this method is not based upon the vehicle's mass and uses a deceleration rate from 0 to max. The formula is shown in Equation 4.1 where g is the gravitational acceleration ($9.81 m/s^2$), v is the current velocity of the vehicle, μ represents

TABLE 4.2: Coefficient of friction

Road Type	Coeff of Friction With ABS	Without ABS
Asphalt - Dry	0.8-0.9	0.75
Asphalt - Wet	0.5-0.7	0.45-0.6
Concrete - Dry	0.8-0.9	0.75
Concrete - Wet	0.8	0.7
Snow	0.2	0.15
Ice	0.1	0.07

the coefficient of friction. This equation is paired with an equation for thinking distance to calculate the total stopping distance. Thinking distance is calculated using velocity and reaction time; in this experiment, reaction time is represented with T_{E2E} when using SDR related measurements.

The coefficient of friction is a variable that is allocated to measure the friction between a vehicles rubber tyres and the road surface. Depending on the road type and condition, this can have a different impact on the coefficient of friction. Table 4.2 represents some road types and weather conditions, highlighting the different values for the average coefficient of friction associated [228]. In this experiment, 0.8 is chosen for the coefficient of friction as this is the standard for normal-dry road conditions.

The second equation is found in many research papers due to the more detailed parameters involved in discerning the conditions of vehicle information used [228], [231], [232], [233]. This equation discerns more detailed parameters on the type of vehicle, road conditions, air conditions, and other parameters and can be seen in Equation 4.3 that is split into three individual parts used to equate the total D_S. The components of the equation have been detailed in Table 4.3 and it shows the typical ranges used in other research along with the value chosen in this experiment specifically.

$$\begin{aligned} D_{\mathrm{B}}(m) = \frac{W}{2gC_{\mathrm{ae}}} ln(1 + \frac{C_{\mathrm{ae}}V^2}{\eta_{\mathrm{b}}\mu W + f_{\mathrm{r}}cos\theta + Wsin\theta}) \\ C_{\mathrm{ae}} = (p * Af * Cd)/2 \\ D_{\mathrm{S}}(m) = D_{\mathrm{B}} + D_{\mathrm{R}} \end{aligned} \tag{4.3}$$

A prediction can be made using equations and the SDR-based DSRC maximum communication latency as the reaction time recorded as 2.92 milliseconds. This time will be used instead of the typical driver reaction time, which is suggested to be between 0.67 seconds and 2 seconds. The reaction time depends on the driver state, such as age, driver experience and state of mind. In this investigation, 1.5 seconds

TABLE 4.3: Equation parameter values

Value	Meaning	Range	Chosen Value
W	Weight Of Vehicle	N/A	1800kg (Citroen DS3)
g	Gravitational Acceleration	N/A	9.8 (m/s^2)
p	Air Density	N/A	1.35
Af	Projection Area	Height * Width	2.562
Cd	Air Drag Factor	0.15-0.5	0.4
V	Velocity (m/s)	N/A	(mph/2.237)
η_b	Brake efficiency	0.8-1.0	0.7
μ	Friction Factor	N/A	0.8
θ	Road Slope	N/A	0
f_r	Roll Factor	0.012-0.015	0.015
C_{ae}	Air Resistance (kg/m)	N/A	(p*Af*Cd)/2

is chosen as the reaction time as this is the time reported in a study conducted by Brake to accurately represent most drivers [226], [234]. The travelling speed has also been displayed in both kilometres per hour (km/h) and miles per hour (mph).

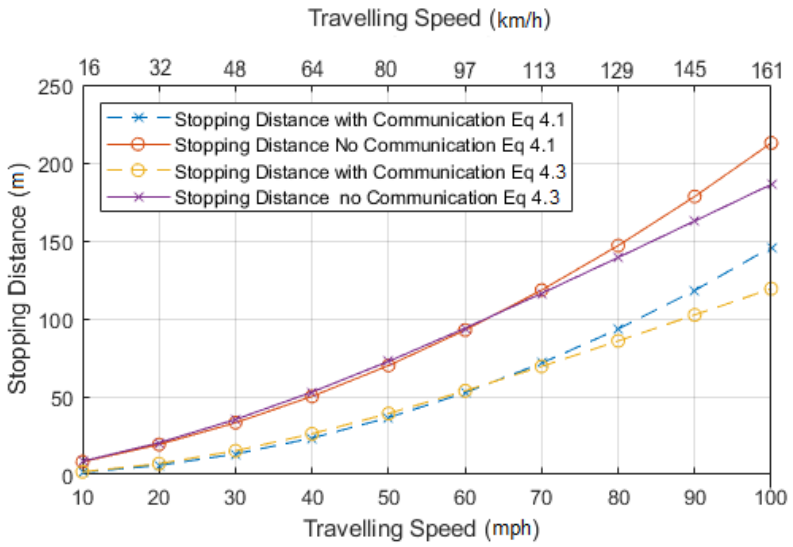

FIGURE 4.5: Comparison of stopping distance using different equations, Equation 4.1 and Equation 4.3

Figure 4.5 highlights the stopping distance reduction that could be observed when using communication assistance systems or automatic braking systems. The results show the distance saved using the communication system and the difference between each method for calculating stopping distance. It can be seen that the second more detailed method has a slight reduction in the distance needed when tailored towards a specific vehicle. Secondly, the figure shows the vast reduction in

TABLE 4.4: Stopping distance reduction

mph	Km/h	Stopping Distance Reduction (m)	Decrease (%)
10	16.09	6.69247	81.9962
20	32.18	13.3849	69.5796
30	48.27	20.0774	60.4289
40	64.36	26.7699	53.4053
50	80.45	33.4624	47.8444
60	96.54	40.1548	43.3324
70	112.63	46.8473	39.5980
80	128.72	53.5398	36.4563
90	144.81	60.2322	33.7764
100	160.90	66.9247	31.4635

stopping distance needed when using communication in both examples compared to the traditional distance needed to brake for unassisted drivers.

The application of this system can be used when critical braking scenarios are required, such as debris on the road causing an emergency braking situation, a vehicle breaking down, a crash occurring, or sudden braking by the lead vehicle. This concept can be further highlighted in the results in Table 4.4. The stopping distance reduction is shown for each travelling speed, assuming a 100% receive rate. At the minimum, the inclusion of communication assisted stopping distance has a 30% reduction over normal braking. The use of the two different methods to calculate stopping distance can both be deemed accurate; however, Equation 4.3 uses more details on environment and vehicle choice, so it is deemed to give a more accurate representation for the studied vehicle. This equation is variable and can be altered and adjusted for the studied vehicle. For these reasons, this equation was chosen moving forwards.

4.3 Impact of consecutive losses on stopping distance

Reliability is an essential factor for safety systems in vehicles as missed or lost packets may lead to important messages and data being lost. These missed packets could cause the following vehicles to receive alerts too late and would mean reaction time would be compromised, and accidents that could have been avoided would occur. However, the impact of singular losses is not a cause for concern if the data rate is high enough. The reliability issue can be seen with consecutive losses, such as a burst of packet losses. A field test is conducted using the SDR-based DSRC and monitors and records the burst losses, packet reception rate, and the number of total losses. The losses observed and recorded in the field test are quantified as either a single loss or a consecutive (burst) packet loss. Burst losses can occur for many reasons or circumstances such as channel fluctuations, obstacles blocking LoS, weather changes or the hidden node problem. The use of UDP transmissions means there is no acknowledgement of a packet received, and therefore if a packet is lost, the sender is not aware of this. UDP will also allow communication to occur more efficiently as no relationship needs to be built between the nodes, eliminating the time-consuming process of the handshake procedure. UDP is the closest representation of a broadcast type communication, and TCP is considered for future work, due to its increased reliability. Broadcast communication is used for CAMs/BSMs, though it is not specifically UDP. However, work by Santa et al. [97] also propose UDP for CAMs.

This test is used to identify the reliability requirements in DSRC and the importance of high levels of reliability in safety scenarios. The tests conducted have been performed with different data rates to monitor the inter-packet gap (IPG) impact. The number of losses chosen will be shown later, but it should be stated that these losses are based upon real-world field tests conducted with the existing SDR-based DSRC.

4.3.1 Impact of consecutive loss on stopping distance: model design and development

A developed model will show the theoretical loss to stopping distance that consecutive packet loss will produce in a vehicular environment. The model was designed based on the stopping distance analysis formula and an equation to calculate the loss of stopping distance per missed packet. This equation includes the interval between packet sending or IPG. The IPG will be abbreviated to T_{PI} which is the packet interval time. Equation 4.4 shows the developed model formula, and Table 4.3 and Table 4.5 show the classification for each parameter. It should also be noted that T_{E2E}

TABLE 4.5: RSD parameters

Component	Detail
T_{E2E}	End to End Latency or Reaction Time
V	Velocity (m/s)
g	Gravitational Acceleration
μ	Coefficient of friction
PaL	Number of Packets Lost (Consecutive)
PT_{E2E}	Processing Time Latency at Receiver (s)
T_{PI}	Packet Interval Time(s)

is used to represent reaction time.

$$R_{SD} = \Big\{(T_{E2E}V) + [\frac{W}{2gC_{ae}} ln(1 + \frac{C_{ae}V^2}{\eta_b \mu W + f_r cos\theta + W sin\theta})]\Big\} - \Big\{V[PaL(T_{E2E} + T_{PI})]\Big\} \tag{4.4}$$

However, this initial model does not consider the next packet after the burst losses are successfully received and processed. The omission of this packet would mean that no packet would be transmitted, successfully received, processed, and appropriate action to be taken after the consecutive packet losses. The reception of this data would be a vital component in autonomous systems where communication would be essential to maintaining appropriate distances and maintaining mutual awareness. To counter this, an extra iteration of processing, RTT, and T_{PI} would have to be included that will be used to represent the successful packet being received and processed. This fundamental change can be seen in Equation 4.5, the newly developed model formula. This model is a simulation based on real world data and the reaction time is represented by T_{E2E}, for autonomous vehicles no human reaction is used.

$$\begin{aligned} R_{SD} = &\Big\{(T_{E2E}V) + [\frac{W}{2gC_{ae}} ln(1 + \frac{C_{ae}V^2}{\eta_b \mu W + f_r cos\theta + W sin\theta})]\Big\} \\ &- \Big(\Big\{V[PaL(T_{E2E} + T_{PI})]\Big\} + \Big[V(T_{E2E} + T_{PI} + PT_{E2E})\Big]\Big) \end{aligned} \tag{4.5}$$

The second model in Equation 4.5 is used as this simulation focuses on how packet loss will alter the stopping distance when relying on communications and highlights that impact. The model works by utilising the normalised stopping distance and subtracting the distance lost via consecutive losses. The losses can be seen in the second part of Equation 4.5. The resulting information will leave the distance remaining till a collision occurs or the stopping distance remaining between vehicles. After consecutive losses, it is known that the vehicle will still need to stop. However, if the sign is switched in the second part of Equation 4.5, This would then

represent the stopping distance plus the distance lost through consecutive loss to leave us with total stopping distance. In this case, the model shows how to lead and follow autonomous vehicle communication, with the following vehicle adhering to a communication assisted stopping distance. This model allows the analysis of how stopping distance is impacted by consecutive packet loss and is shown for different speeds and data rates. The results show the stopping distance when zero packets are lost, and then they show how the stopping distance is reduced with each consecutive loss. This result highlights how the reduction in reliability leads to reduced stopping distance and hence a higher chance of collisions with the lead vehicle. As the reduction value reaches zero, it can be deemed that this to be the point at which the lead and follow vehicle will be occupying the same space or that a collision may have occurred. In addition, a negative value can be calculated, meaning the following vehicle has gone past the lead vehicle, and this would be classified as a collision, which is shown to identify the impact of reliability.

4.3.2 Investigation into consecutive losses observed in field testing

The results can further investigate the impacts of consecutive loss in the field test experiments. The results will be analysed in two ways; the first is a distance independent instance, where theoretical analysis is conducted to see how consecutive losses will affect stopping distance at different distances, with a range of losses monitored. The second is a distance-dependent analysis based on packet losses measured during field test trials. This scenario is measured up to 100 metres and will use varied data rates and travelling speeds.

4.3.3 Impact of distance independent consecutive packet loss on stopping distance

A measurement campaign was carried out in the field to measure and record consecutive losses in 3000 samples when measuring the packet loss rate. For the independent distance analysis, 100 metres was chosen as the baseline as typical stopping distances up to 70 mph fall within the 100-metre range. The result was achieved by attaching a number inside each packet that could be extrapolated and compared at the receiver allowing the extraction of the number losses seen consecutively. The samples are taken at 100 metres, and a normal distribution plot is compiled, highlighting the spread of consecutive losses. This spread can be seen in Figure 4.6 which shows the distribution of losses and highlights that most consecutive losses are from 0 to 11 per 1000 packets. Most of the tests yielded a packet loss rate of 0 packets per 1000; for the sake of testing the impact of consecutive losses, a range of values has

TABLE 4.6: Remaining stopping distance (m) at 30 mph (48.27km/h)

Consecutive packet loss	Eq. 4.4 Remaining SD (m)	Eq. 4.5 Remaining SD (m)
0	13.1474	13.1474
1	11.7675	10.3488
2	10.3876	8.96891
4	7.62782	6.20911
6	4.86803	3.44932
8	2.10823	0.68952
9	0.72833	-0.6903
11	-2.0314	-3.4501
13	-4.7912	-6.2099
15	-7.5510	-8.9697
17	-10.3108	-11.7295
18	-11.6907	-13.1094

been selected through 1-18, as 1 is the minimum consecutive loss and 18 was the highest. Results are produced for 30, 40, 50, 60 and 70 mph for the full range of data rates, from 10 to 140 packets per second.

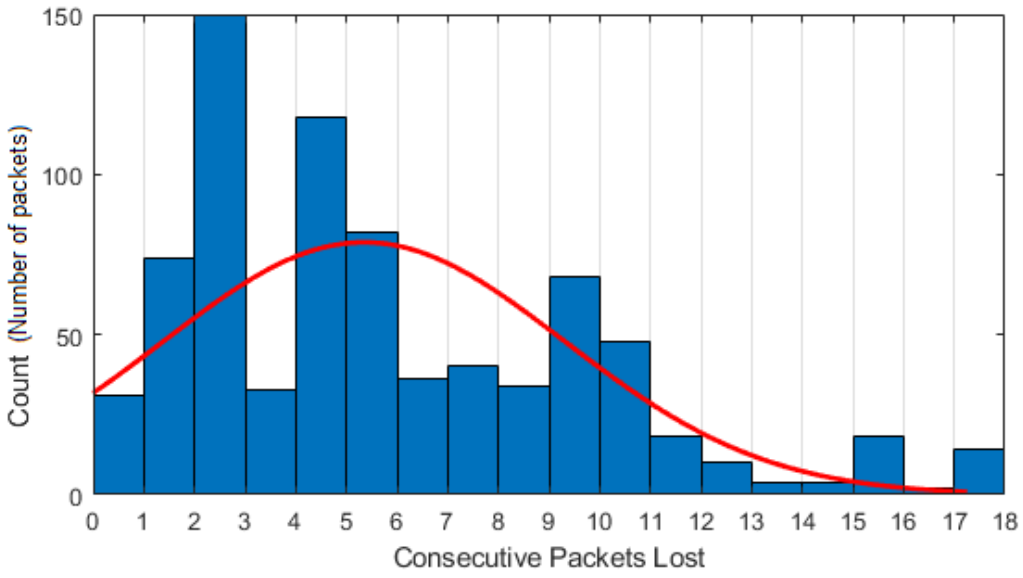

FIGURE 4.6: Distribution chart of consecutive packet loss

An example of the impact of the consecutive loss can be seen in Table 4.6, which shows the results for 30 mph after the application of the models developed for *RSD*. The results are compiled using 10 pps and 30 mph and give an example of the model application.

As shown in the table at 0 losses, the full stopping distance is needed at 30 mph.

As the consecutive losses increase on the left side of the table, the remaining stopping distance gradually decreases, which can be seen on the right. It can also be seen that 11 packets and higher than the value becomes negative, which would indicate that the vehicles have either collided or overtake has been performed. This result highlights the importance of reliability for safety scenarios such as communication assisted stopping distance, especially as autonomous vehicles become more widespread on the road.

The following figures are used to show the results for each different speed, and it should also be stated that there are three different variables in the model which will be shown;

- Consecutive losses, which have been set to – 0, 1, 4, 6, 8, 9, 11, 13, 15, 17, 18
- Data rate in packets per second (pps), which is configured as - 10, 25, 50, 75, 100, 120, 140
- Speed in mph (km/h), which is configured as – 30 (48.27), 50 (80.45), 70 (112.63)

These Results are attained through the use of Equation 4.5 and in the results a negative or minus result would indicate a collision has occurred. at this point the results could potentially maintain a zero value, however the negative value is maintained in order to show how significant the collision would be and how much extra braking would have been required to avoid a collision.

As shown in Figure 4.7 and Figure 4.8, the results show an evident pattern from the consecutive losses, in that as expected with more losses, the stopping distance decreases. However, it can be observed that at lower speeds in the 30, 40 and 50 mph simulation, the higher levels of packet losses can cause crashes, as evidenced by the negative recorded values. Another highly useful observation is when the different data rates are examined. For each experiment, 50 pps and above doesn't reach a level to cause collisions and, at most, reaches a 50% decrease in the slowest velocity test. The initial packet loss of 1 consecutively shows that not much impact is observed in all scenarios. Extending this to 6 packets consecutively lost, using Equation 4.5 has minimal impact, other than at a 10 pps rate, which can be deemed unsuitable for this scenario, which would be expected. It can be assumed that for each case, after minimal losses, vehicles would be able to adjust their position in motorway scenarios; however, on-road scenarios, in some cases, would lead to unavoidable crashes.

In all figures, the 120 and 140 pps rates have a very small distance reduction for each speed, even in the largest case being 30 mph and a 4.5-metre reduction, which is the average length of a vehicle and hence leaving enough space to take emergency action. When considering the maximum consecutive packet loss, the

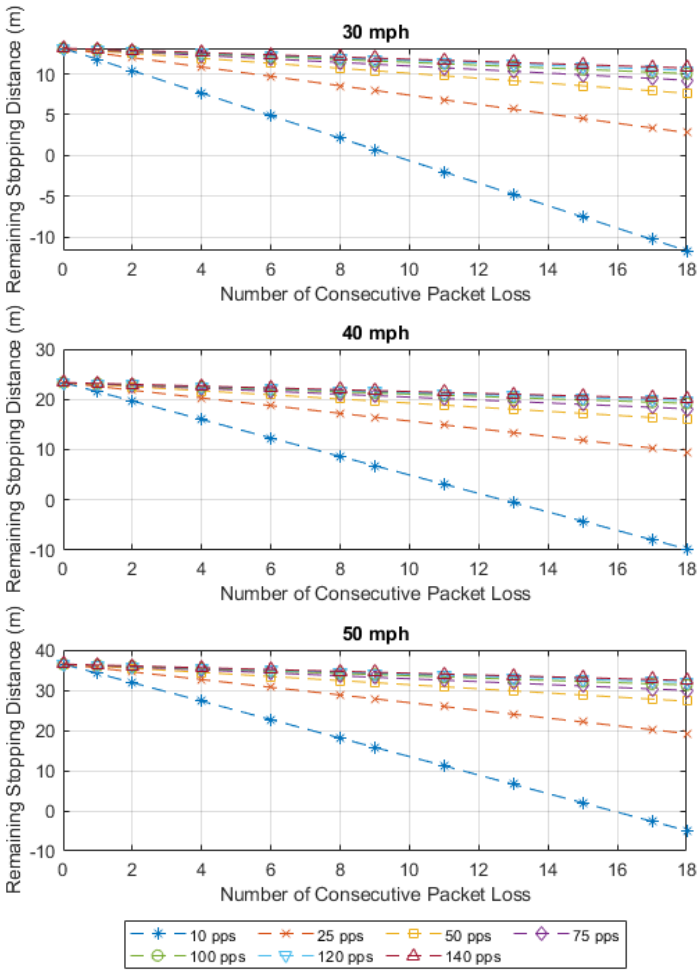

FIGURE 4.7: Remaining stopping distance after consecutive losses at 30, 40 and 50 mph

minimum data rate that would provide adequate time to respond would be above 75 pps per second in the 50 mph experiments, as seen in Figure 4.7. Anything lower than this and the stopping distance is reduced by 50-75%, which is deemed a short distance to react. In the 70 mph example in Figure 4.8, 25 pps would reduce less than 40%, and the higher data rates with consecutive loss degrade the stopping distance by approximately 10%. However, in the 60 mph test, a 50 pps and above data rate would reduce the stopping distance by 20% maximum, and for 70 mph, 25 pps would also have a less than 40% reduction and this distance would be large enough to take emergency action.

A conclusion can be drawn from the results that at lower speeds, the consecutive packet loss has much more of an impact than at higher speeds, even at low levels

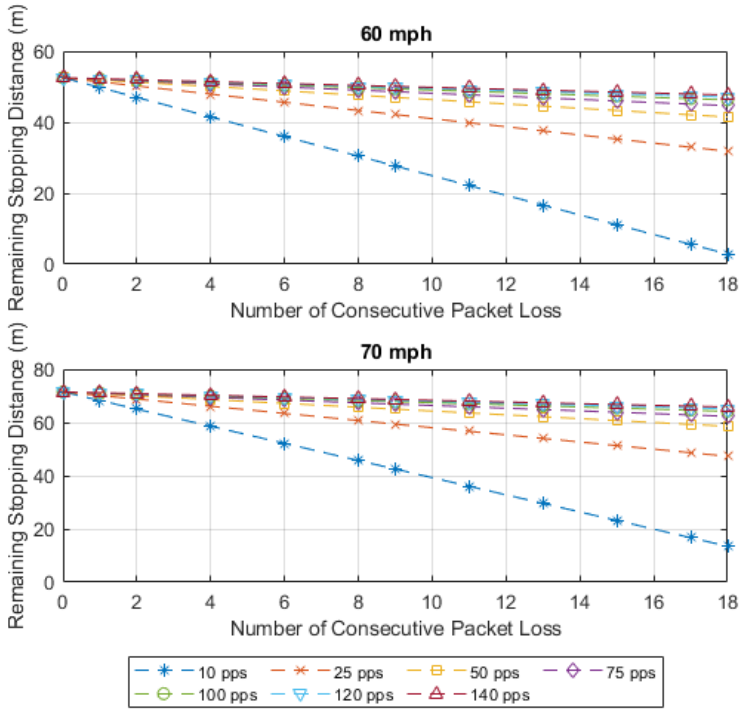

FIGURE 4.8: Remaining stopping distance after consecutive losses at 60 and 70 mph

of consecutive loss. As the stopping distance is smaller, less distance to receive the delayed or lost communication message is given, but the results in Figures 4.7 and 4.8, show that with high data rates, the packet losses are less detrimental. As more packets are sent the losses are less consequential due to receiving more messages in a short amount of time. It is also concluded that data rates are as essential as reliability in safety scenarios. With reduced reliability, higher data rates can assist in getting more messages transferred to increase the packet reception rate. In turn, actions can be made from the messages received. This result identifies a three-way relationship that safety would rely on, reliability, data rate and latency. This meaning that all three factors play an important role, latency and data can be high but with low reliability, messages will be missed. Reliability and data rate can have high rates, but with low latency messages will be received too late. Reliability and latency can be high, but with a slow data rate, the messages may have too long between them, meaning distance will be significantly reduced between them.

4.3.4 Impact of distance dependent consecutive packet loss on stopping distance

A second scenario analysed was to monitor consecutive packet losses observed at each distance or distance dependant losses. In this field test experiment, the packet losses have been recorded at every 10-metre interval from 10 to 100 metres. The losses have been recorded like the distance independent. Each test has a number injected into each packet to monitor the max number of consecutive losses at each distance and data rate. This test monitors the different distances from the lead vehicle to the vehicle of interest, how packet loss rate differs at different communication ranges and how stopping distance is impacted according to real-world measurements. In Figure 4.9 the power over distance is shown for each of the distances in the SDR-based DSRC field test, then in Figure 4.10 the number of packets recorded consecutively are shown at the distances and each data rate. These results are taken with the SDR-based DSRC setup in a field test, with the distances measured between transmitter and receiver. This result gives insights into the packet losses and how they differ and change over the distances chosen.

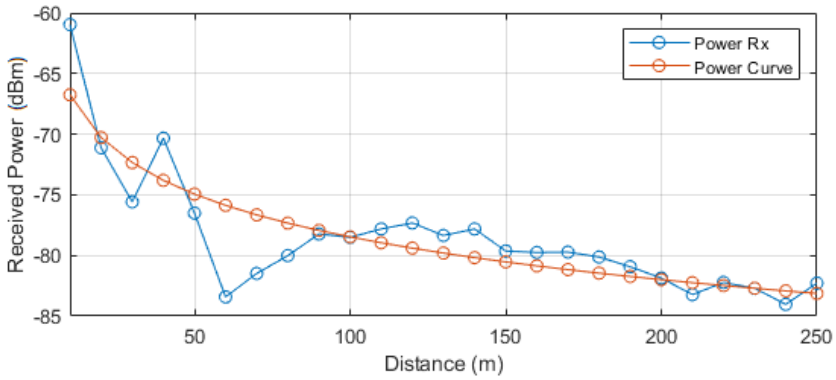

FIGURE 4.9: Receiver power from SDR-based DSRC

These initial figures show that at distances of 30 metres and between 60 to 90 metres, packet losses are significantly increased at both 120 and 140 pps curves. This result is due to power drops seen in Figure 4.9 and are due to the fading nature of the channel. The receiver suffers degradation at these distances. It can be assumed to attribute these losses to channel overloading caused by the high number of packets being transmitted in a harsher environment. Therefore, the fading nature at these specific distances coupled with high data rates impacts the packet reception ratio rather than the distance itself.

Following this, a figure will be plotted for each speed showing how these distance dependant losses impact the remaining stopping distance, such as previously

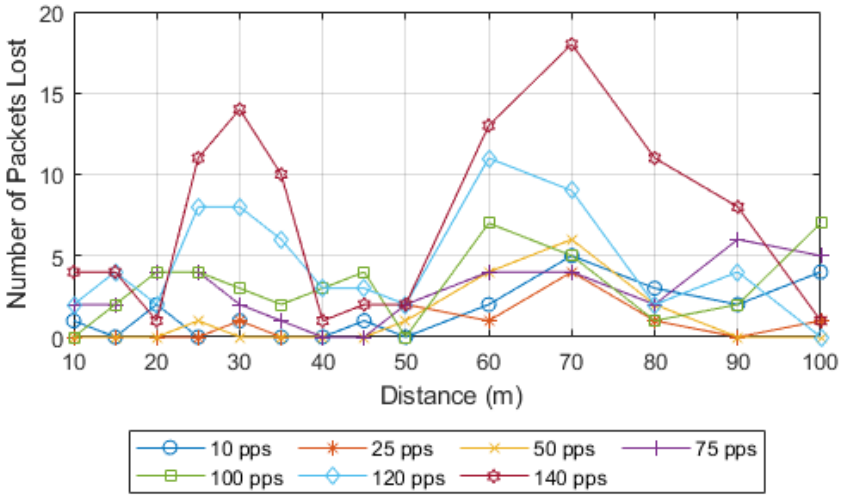

FIGURE 4.10: Distance dependant packet loss distribution

shown. The same formula will be applied as in previous examples and applied to the recorded losses seen in these experiments, and this will be shown for the same speeds and data rates as used previously. The results are presented in Figure 4.11, Figure 4.12 and Figure 4.13.

The main conclusions drawn from the distance dependant experiments are that a high data rate must be used to maintain enough reaction time to mitigate the effects of consecutive losses in safety scenarios. This result is highlighted by the 10 pps scenarios with the highest stopping distance reduction due to packet losses. The results show that a 99.9% reliable system is possible in almost all scenarios. Figure 4.11, Figure 4.12 and Figure 4.13 show that the loss of two packets or 0.1% has a minimum effect.

The highest loss to stopping distance is seen in the 30 mph test, and this loss is at the lowest data rate and suffers at max a 50% loss which can be seen in Figure 4.11. All other data rates at 30 mph suffer only a few metres of reduction, showing the importance of high data rates. This trend is followed in the other speed tests, but the reduction is not as severe as slower speeds due to the increase in stopping distance. This finding is especially prevalent for 60 and 70 mph, respectively, where every data rate other than 10 pps has approximately less than 10% reduction, based on actual measurements.

The lower speed data rates suffer more loss at higher distances. However, the losses cause more substantial degradation to stopping distance at lower distances, and a primary example of this can be seen in the 30 mph tests in Figure 4.11. It can

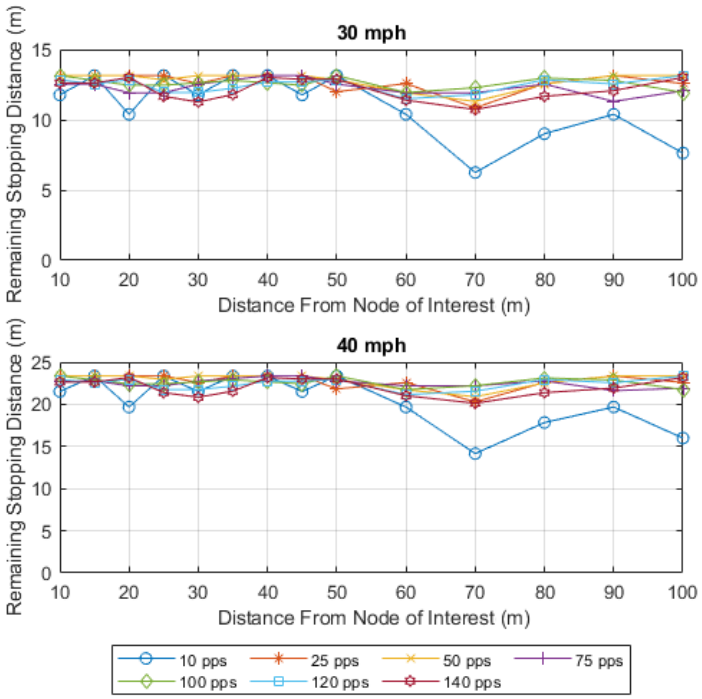

FIGURE 4.11: Remaining stopping distance after distance dependant consecutive losses at 30 and 40 mph

also be seen that as the distance increases, the packet losses have less of an impact exponentially. Figure 4.9 showing the power highlights the reason for this, the figure shows received power levels at distances up to 250 metres, but the focus is only to 100 metres. It also shows the fading characteristics indicated at the lower distances by the rapidly changing power levels, hence the higher losses seen at lower distances. Figure 4.9 also highlights that the power levels for lower distances suffer fading but that 100 metres has a lower power level but does not suffer the same level of packet losses. This loss can be attributed to the fading characteristics of the channel and the gain settings on the SDR. It can also be seen that at 60 metres, a significant level of fading is observed.

4.4 Impact of vehicle density on safety distance

There are other implications other than the distance to consider in wireless vehicular networks when the concept of safety is concerned. The second important aspect is the density of the roadway or the number of vehicles on the road within the communication range. This section investigates the connotations of consecutive losses incurred by the density of the vehicles on the road network. This loss can be deemed

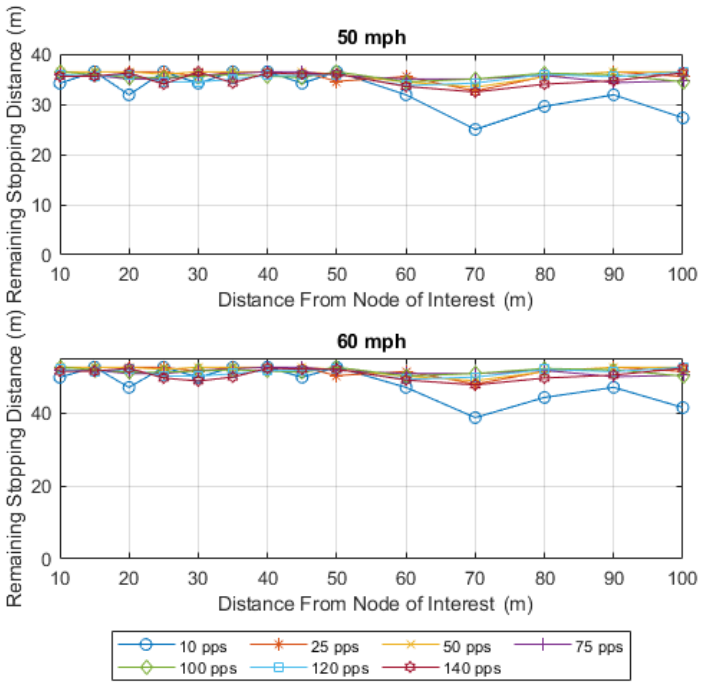

FIGURE 4.12: Remaining stopping distance after distance dependant consecutive losses at 50 and 60 mph

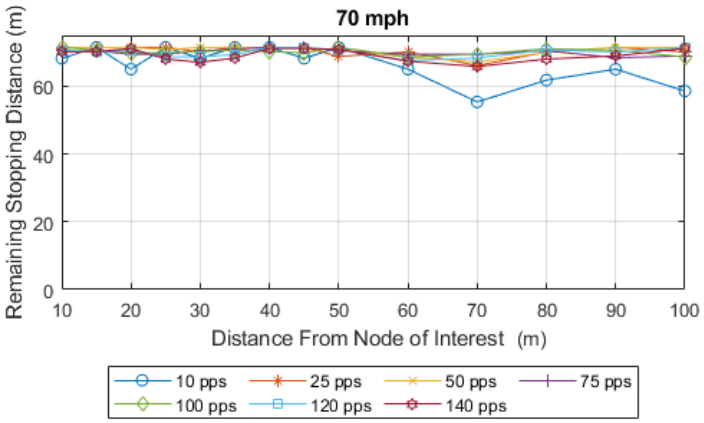

FIGURE 4.13: Remaining stopping distance after distance dependant consecutive losses at 70 mph

the number of packet losses incurred by the receiver caused by an increased number of vehicles transmitting simultaneously.

This investigation is essential to measure the losses incurred in-vehicle networks

and how reliability will be affected by a vast number of vehicular nodes transmitting their safety messages. The effects of this message dissemination will adversely impact reliability. The approach taken is the creation of a simulation of a vehicular scenario based on several nodes within the communication vicinity and relate this to the number of packets lost and the effect on safety distances. The experimental simulations prove the use of communication will reduce reaction time. With this reduction in reaction time, there is a decrease in both; nodes in communication range and the range needed for safety distance.

4.4.1 Investigating consecutive losses versus vehicle density

In this section, a simulation is designed to monitor the packet losses in the network when considering a varied number of nodes in a three-lane highway environment. It can be assumed that the opposite flowing traffic will be eliminated via location-based broadcast, which is the preferred method for cooperative collision avoidance (CCA) [199]. The initial step is to approximate the number of nodes within the broadcast communication range. This range is chosen to incorporate automatic gain control (AGC) [235], which is used to alter the gain depending on the speed being travelled. Lower gains are used at lower velocities to create a reduced and lower communication range.

The first step of this section is to identify the communication range classified in this investigation as safety distance. The safety distance is the distance left between vehicles to provide enough distance or time to react to a situation without crashing. In the case of this experiment, this will be approximately the same as the reaction time for a human driver or DSRC/advanced driver assistance systems (ADAS) device and is approximately 1.5 seconds without the SDR-based DSRC and 2.92 milliseconds with the developed SDR-based DSRC Chapter 3. For the consideration of safety distance, the separate measurement of braking distance is not required because, as described previously, stopping distance is the combination of braking distance and reaction distance. In this scenario, safety distance is considered reaction distance or reaction time. In this investigation, the measurement to be calculated is the safety distance or minimum required gap between vehicles depending on the speed being travelled.

When using a full functioning ADAS system, a suitable approach must be made to calculate braking distance, as, without this, chain reaction collisions would be prevalent. This simulation represents an example of the safety distance with communication and the impacts of node density. It can be shown that the safety distance D_S is directly affected by; the time taken for a reaction to being made by the driver or

ADAS system T_R and the acceleration coefficient of the vehicle (a). This relationship can be shown in Equation 4.6 as;

$$D_{\mathrm{S}} = a * T_{\mathrm{R}} \tag{4.6}$$

In the case of the SDR-based DSRC reaction time, there must also be a consideration for the delay within the hardware system due to the received information processing and the mechanical delay introduced when activating the brakes. It will be assumed that this is equal across all acceleration speeds and has set this value as 0.25 seconds and will be specified as reaction processing time (T_{RP}). This is shown for human driver in Equation 4.7 and ADAS in Equation 4.8. In this example T_{R1} represents human reaction time and T_R represents the ADAS reaction time. Although the formula is longer for the ADAS vehicle, the reaction time of the human is significantly larger.

$$D_{\mathrm{S,h}} = a * T_{\mathrm{R1}} \tag{4.7}$$

$$D_{\mathrm{S,a}} = a * (T_{\mathrm{R}} + T_{\mathrm{RP}}) \tag{4.8}$$

The difference between the two safety distances, human driver/ADAS, according to the travelling speed, can be shown and, in addition, also show the results of various stopping distance algorithms used in literature and other research work. These algorithms are the Mazda algorithm [27], the Stop Distance Algorithm (SDA) [27], and a more recent variation, known as the PATH (Berkeley) algorithm [27], [194], [195]. The PATH algorithm is a modified version of the well-established Mazda algorithm and is used to show safety distance calculation or to equate critical warning distance.

The results for the various algorithms can be shown. The deceleration of a vehicle is assumed to be at maximum for both following and leading vehicles, as is common practice. This is taken from a study conducted into various vehicles [195], [236], [237]. For this interpretation of the algorithms, the deceleration rate for a standard petrol car is used to keep compatibility with the type of vehicle used previously. The deceleration can also be calculated using a formula and the initial calculated braking distance without reaction time.

Deceleration (á) can be calculated using two different methods and is shown in Equation 4.9 and Equation 4.10; with S_f representing the final speed, S_i representing the initial speed, t denotes time component, and d is a distance of braking.

$$\acute{a} = (\frac{s_f - S_i}{t}) \tag{4.9}$$

$$\acute{a} = (\frac{S_f^2 - S_i^2}{2d}) \tag{4.10}$$

For this scenario, Equation 4.10 is used as the braking distance has already been calculated. The deceleration will then be modelled to represent the rate of deceleration ($\acute{a}_R$). This model is taken from Ro et al. [195] and is a validated model representing the reality of braking via the CarSim simulator. The formula Equation 4.11 is a linear equation representing an approximation of deceleration rate and is used to simplify the vehicle braking dynamics. Where á is the max rate of deceleration, and the mechanical delay is (T_{RP}).

$$\acute{a}_R = \frac{\acute{a}}{T_{RP}} \tag{4.11}$$

4.4.2 Investigation of safety distance algorithms

Now that the deceleration rate model has been detailed and shown and the calculated human reaction safety distance and the ADAS reaction safety distance have also been described, the algorithms for safety distance will now be presented and briefly described with their designated equation shown;

Mazda algorithm [27], [195], [194], [238] is a worst-case scenario model to ensure collisions do not occur and is shown in Equation 4.12. Where v_l, v_f, v_{rel} represent leading, following and relative vehicle velocities and $\acute{a}_f$, $\acute{a}_l$ represent each of the vehicle's deceleration. The algorithm assumes that the two vehicles are at a constant maintained velocity and that at T_2, the lead vehicle will begin braking with the designated deceleration rate. The following vehicle will begin braking after T_1 at its own given deceleration rate. R_{min} is used to represent a minimum range or a tolerance rate for safety, which is shown in the equation.

$$D_s(v_l, v_f, v_{rel}) = \frac{1}{2}[(\frac{{v_f}^2}{\acute{a}_f}) - (\frac{{v_l}^2}{\acute{a}_l})] + v_f T_1 + v_{rel} T_2 + R_{min} \tag{4.12}$$

SDA algorithm [27], [195], [194], [239] is a similar approximation of the conceptual idea of Mazda; however, it is based on the difference between the two stopping distances of the lead and the following vehicle, and it is usually a part of the ADAS system that utilises driver warning system incorporation. In this algorithm, T_R represents the driver's reaction time. Equation 4.13 is used to show this.

$$D_s(v_l, v_f) = v_f T_R + (\frac{{v_f}^2}{\acute{a}_f}) - (\frac{{v_l}^2}{\acute{a}_l}) \tag{4.13}$$

PATH [27], [195], [194], [240] is a modified version of the Berkeley algorithm based upon two vehicles, where the lead vehicle begins braking. The following

vehicle reacts to this action after T_r and brakes. This algorithm also uses R_{min} to represent a minimum range or a tolerance rate, similar to Mazda, as shown in Equation 4.14.

$$D_{\mathrm{s}}(v_{\mathrm{l}}, v_{\mathrm{f}}) = \frac{1}{2} + [(\frac{{v_{\mathrm{f}}}^2}{\acute{a}_{\mathrm{f}}}) - (\frac{{v_{\mathrm{l}}}^2}{\acute{a}_{\mathrm{l}}})] + v_{\mathrm{f}} T_{\mathrm{r}} + R_{\mathrm{min}} \tag{4.14}$$

In the specified algorithms, it is assumed that the vehicle velocity and deceleration are the same values, and therefore the relative speed will be 0 mph. The Berkeley example will also be applied to use two separate and selected values for deceleration. The deceleration value calculated from the simulations and the industry-standard value of 6.44 $\mathrm{m/s^2}$ [241], [242], [243]. The final method to be analysed is the Highway code guideline value that is used on UK roads, and this is given as a measurement of one metre per every mile per hour [4], [234]. For instance, at 30 mph, the safety distance gap should be approximately 30 metres. The calculation is compiled for each algorithm of the SDA, PATH and Mazda. The findings show that these algorithms are shown to work, but they all equate to the same safety distance as the findings that have been made for Human-based safety distance.

For this reason, only the relevant algorithms will be plotted. The PATH algorithm, Equation 4.7 and Equation 4.8 are used with the values of reaction time adjusted for the type being measured. These algorithms to be plotted will be five variations of safety distance which can be seen in Figure 4.14. This graph highlights how much quicker the ADAS based braking system would react compared to a typical human reacting to a warning produced by the other algorithms or from a visual reaction from human eyesight and manual braking alone.

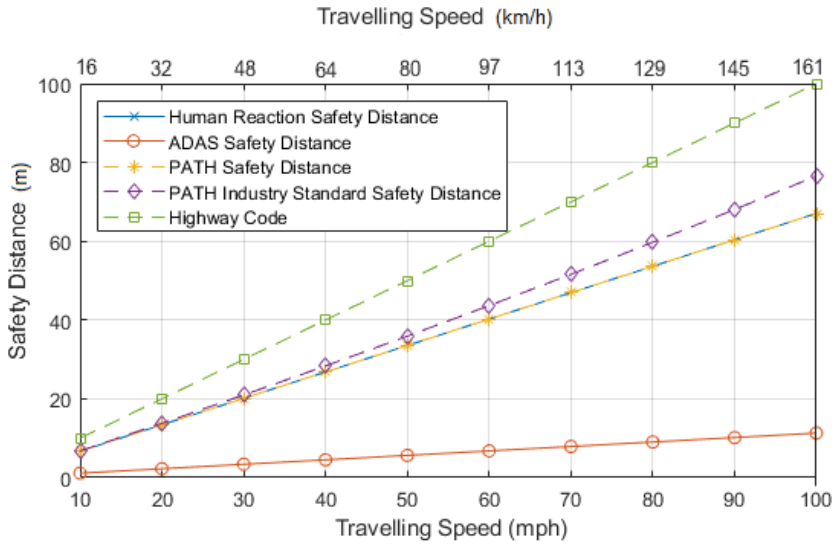

FIGURE 4.14: Safety distance comparison between different safety distance algorithms

4.4.3 Vehicle node density versus communication range

With the safety distance calculated for the various algorithms, the number of nodes in the range of the transmitting vehicle can now be predicted for each travelling speed required. This calculation will be based on the calculated safety distance and five metres set as a car length, a standard measurement for smaller vehicles.

Due to the use of omnidirectional antennas in the SDR-based DSRC, it is known the radiation pattern is a circle with the centre point being the antenna which has been shown in Chapter 3. To communicate to a vehicle of interest, the range of communication will be the safety distance plus one full car length. As this wireless emission is a circular pattern, the diameter is simply shown in Equation 4.15. However, a vehicle is also approximately five metres in length, and a centrally placed antenna would limit the circumference detrimentally. Therefore, to compensate, an additional five metres will be added to the diameter to represent the vehicle of interest shown as V_L. This equation will only be applicable in this simulation as it only considers average vehicle sizes. If more appropriate measurements are taken in real-world simulations, the vehicles would need to be varied, and compensation must be made. For instance, a custom radius distance would more appropriately represent other vehicles such as a bus or lorry. However, this would be a measurement known to the vehicle, so a simple adjustment to the equation would be needed.

$$d = (r * 2) + V_L \tag{4.15}$$

With the diameter calculated from the safety distance and Equation 4.15, the number of nodes within the diameter of the calculated safety distance for each algorithm can now be predicted and estimated. This calculation can be shown, for example, at 30 mph and using the PATH safety distance of 20.2 metres, the diameter of the range will be 45.4 metres. The number of nodes present in the communication range can be calculated with the range calculated. The calculation can be simplified into smaller terms such as the number of cars per lane, safety distance per car and the number of lanes. These terms will give an approximate minimum value. For the number of nodes, all vehicles will be considered to be maintaining the 20.2-metre spacing, with an approximate length of five metres per vehicle. Therefore, two nodes will be within the transmission range in one traffic lane. This number will be multiplied by the number of lanes required, leading to the classification that nine nodes will be within a range, including the central node.

This scenario is the best-case; a worst-case safety scenario would be that the minimum safety distance is not adhered to and vehicles would be more closely packed together. This scenario would lead to 11 cars per lane being within communication range and, by calculation, results in 33 vehicles in range at 30 mph. Equation 4.16 shows the best-case number of nodes and Equation 4.17 for maximum nodes, where d represents the diameter of communication range, r represents the radius of communication range, L is used to represent the number of lanes to be studied, and d_c shows the length of the studied vehicle.

$$Nodes_{\text{avg}} = ((d/(r + d_{\text{c}})) + 1) * L \tag{4.16}$$

$$Nodes_{\text{max}} = (d/d_{\text{c}}) * L \tag{4.17}$$

Figure 4.15 shows the result of the node calculation equation, and it shows that the ADAS has a vastly reduced number of nodes in the communication range compared to other equations. This reduced number is due to the lower operating reaction time.

As mentioned in previous sections, PATH and human reaction give identical measurement results so that these algorithms will be treated as the same for the simulation experiments, and this can also be seen in Figure 4.15. The worst performing is the general guidance given by the highway code and can deem this to be because it is rather a suggested guideline rather than a calculated algorithm. It should also be noted that the human reactions are not a reaction due to an emerging situation but rather the human reaction to the ADAS warnings provided by the DSRC communication system. In contrast, the ADAS reaction time is a reaction that is based on an automatic braking system provided and operated by DSRC. Figure 4.15 also

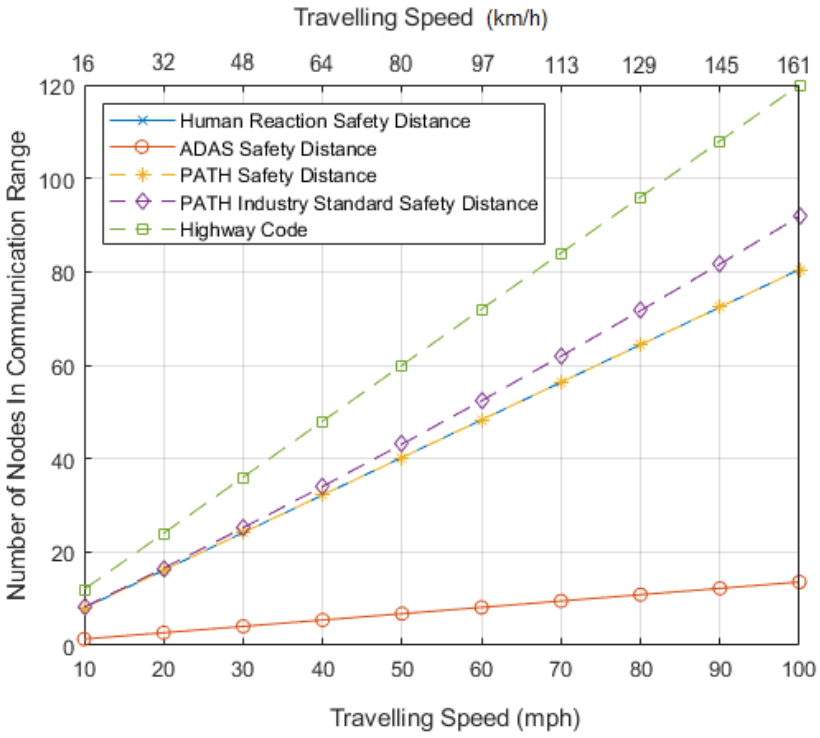

FIGURE 4.15: Node density comparison between different safety distance algorithms

shows that the incurred losses scale by increasing miles per hour, with changes only occurring in incremental stages as speed increases. This finding is useful for using and including an automatic gain control feature. The diameter would be kept identical until a threshold is reached, meaning the system would engage an increase or decrease to alter the gain to the required limit.

The number of nodes is calculated for each velocity, and a simulation is performed to find consecutive losses via density. The simulation has been conducted using MATLAB software and represents communication occurring between DSRC enabled vehicular nodes competing for channel access to broadcast safety messages. The simulations have been performed with varying numbers of communicating nodes to represent the number of nodes in the communication range for each travelling speed. The simulation provides the expected consecutive packet collision probability per node density/travelling speed when all vehicular nodes compete for DSRC channel access with BSM messages broadcasting safety data. According to standards, the simulation is based upon vehicular node density utilising DSRC communication, with associated equations and contains the parameters used in DSRC for MAC configuration. This configuration includes collision window timings, slot

TABLE 4.7: Node density, simulation parameters

Parameter	Value
Number of Simulations per cycle	5
Packets Per Node	1000
Transmission Rate	6 Mbps
Number of Nodes	Eq.15-16
Packet Size	256 bytes
Number of retransmissions	0
Contention Parameters (Safety Related)	Cwmin=3,Cwmax=7
Slot time	13us
MAC Sifs	32us
MAC Difs	58us
MAC Phy Header	32us

allocation, acknowledgements for packet reception that have been removed as they are not required for BSM. These standardised settings have been gathered through various sources [138], [163], [244]. Further information relating to the simulation and the settings have been collated from [70], [245], [246] and these relate to data rate settings and transmission scheme pre-sets. The simulation has kept as many variables the same as the tests in the distance-based experiments to maintain consistency, comparability and compatibility. Table 4.7 is used to emphasise important simulation parameters that have been used.

ADAS results will only be used as they are the most efficient to compare with distance-based losses, however the number of nodes for each type will be shown along with the respective probability of packet collisions. This is achieved through a simulation, comparing the number of nodes generated with Equation 4.16 and Equation 4.17. Figure 4.16 shows the simulated probability of consecutive packet collisions for the vehicular node of interest when a specific and calculated number of nodes are within its designated communication range at the specified ADAS/DSRC range. Figures 4.17, 4.18 and 4.19 show the results for the alternative algorithms, showing the probability of packet collisions.

The results show that the number of losses due to density is more severe than those incurred by the distance-based losses. The DSRC system suffers up to 15% losses, approximately 150 packets with 21 vehicular nodes in range. Compared to the distance-based, a maximum loss of 18 packets is observed. This result highlights the importance of the network's capabilities in terms of traffic load density and an adequate channel allocation scheme to reduce these losses to meet stringent requirements for safety-based systems. The results also highlight the reduced packet collision probabilities compared to those of Human/PATH, PATH with Industry standards and the highway code guidance. They also highlight the vast impacts produced by the large nodes that would need to be present in the required

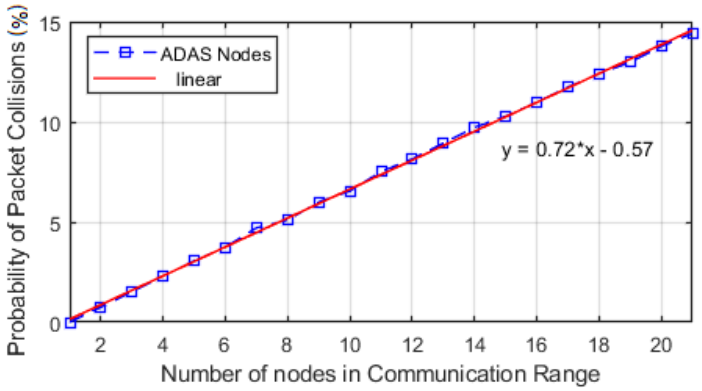

FIGURE 4.16: Node density, probability of collision with ADAS

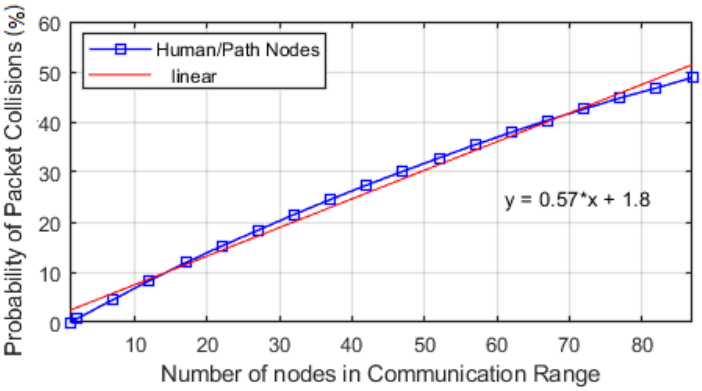

FIGURE 4.17: Node density, probability of collision with PATH/Human

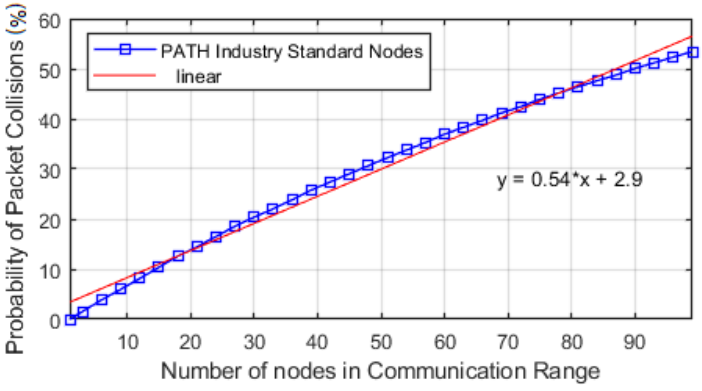

FIGURE 4.18: Node density, probability of collision with PATH/Industry Standard

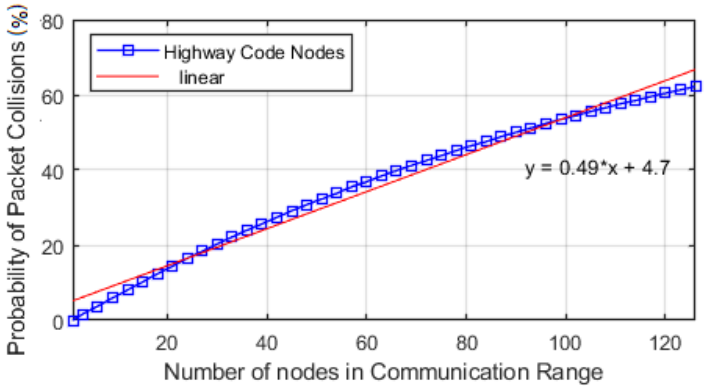

FIGURE 4.19: Node density, probability of collision with Highway Code

safety range.

Linear regression curve equations have been produced and shown. They enable the number of packets lost due to collisions to be calculated in a percentage (%) for each scenario and each different safety distance algorithm. These linear equations will be shown individually in Equation 4.18, 4.19, 4.20 and 4.21, where x represents the number of nodes.

$$ADAS = 0.72 * x - 0.57 \tag{4.18}$$

$$PATH = 0.57 * x + 1.8 \tag{4.19}$$

$$PATH_{IS} 0.54 * x + 2.9 \tag{4.20}$$

$$HC = 0.49 * x + 4.7 \tag{4.21}$$

TABLE 4.8: Losses per 1000 packets

Speed (mph)	Speed (km/h)	Human/PATH	PATH (IS)	ADAS	Highway Code
10	16.09	104	110	60	136
20	32.18	155	159	60	194
30	48.27	207	208	81	253
40	64.36	241	256	81	312
50	80.45	292	305	103	371
60	96.54	343	353	103	430
70	112.63	378	402	124	488
80	128.72	429	451	124	547
90	144.81	480	515	146	606
100	160.9	514	564	146	665

4.4.4 Investigation into consecutive losses for ADAS

The number of consecutive losses will need to be equated and shown for each travelling speed to show comparable results to the distance-based experiments. Linear regression formulas are used to show this, which have been developed through the simulation and then apply them to the number of nodes in the communication range found in Figure 4.15. These calculations will be shown up to 100 mph, and the values can be seen in Table 4.8 for each algorithm. These losses have been calculated using Equation 4.18, 4.19, 4.20 and 4.21, where x represents the number of nodes. The losses are then converted into losses per 1000 packets using Equation 4.22, where L_k represents the losses per 1000 and L_p represents the result from the previous equation used.

$$L_k = \frac{L_p * 1000}{100} \tag{4.22}$$

Table 4.8 shows the packet losses incurred due to density collisions are much higher than those produced by distanced distance-based, primarily due to nodes competing for transmission time slots. The table shows the number of consecutive losses per 1000 packets for each algorithm, with 100% losses being shown as per the linear equation, and the ADAS losses can be seen to be 124 at 70 mph. This loss level is considerably high for successive packet collisions in the vehicular network. For this reason, a scale is produced showing 1- 100% losses recorded as consecutive, as 100% losses are a rare occurrence. Figure 4.20 shows the results from calculating and extrapolating the packet losses based upon travelling speed. Table 4.9 shows the corresponding packet loss value to each percentage for clarification, and these have been rounded to the nearest whole packet, as partial loss packets are in this experiment considered fully lost packets and discarded.

The results will now be shown as stopping distance reduction for each algorithm, for each of the levels of the delays caused by each consecutive packet loss

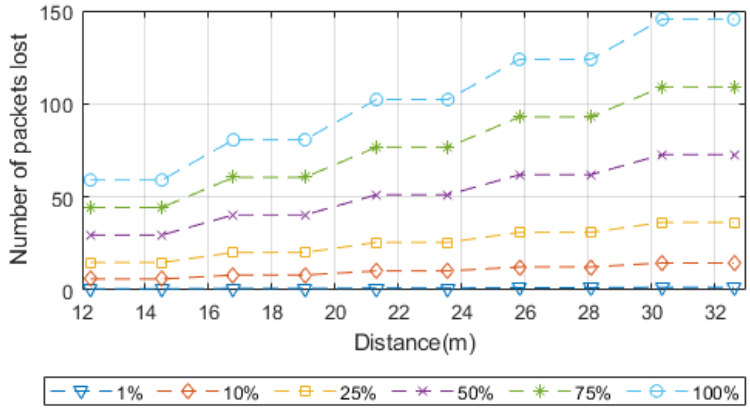

FIGURE 4.20: Percentage of consecutive packet losses for ADAS

TABLE 4.9: ADAS/DSRC percentage losses at different speeds

Speed (mph)	Speed (km/h)	1%	10%	25%	50%	75%	100%
10	16.09	1	6	15	30	45	60
20	32.18	1	6	15	30	45	60
30	48.27	1	9	21	41	61	81
40	64.36	1	9	21	41	61	81
50	80.45	2	11	26	52	77	103
60	96.54	2	11	26	52	77	103
70	112.63	2	13	31	62	93	124
80	128.72	2	13	31	62	93	124
90	144.81	2	15	37	73	110	146
100	160.9	2	15	37	73	110	146

percentage. The results will be shown for 30, 50 and 70 mph, respectively, using three different data rates, 10, 100 and 140 packets per second. These rates are the min, median and max from previous experiments and give the most useful comparisons. The algorithm used to calculate stopping distance in previous experiments is again utilised to keep comparability. However, the altered packet losses from density will be used instead of the distance-based. Figure 4.21, 4.22 and 4.23 show the results of this simulation.

4.4.5 Analysis of vehicle density losses on safety distance

The figures provided show similar results to that of distance-based losses. However, as can be seen, the losses are far greater, and thus, the distance needed to avoid potentially dangerous collisions is vastly reduced compared to distance-based. As DSRC aims for 99.9% reliability, the most appropriate result is in the 1% category or

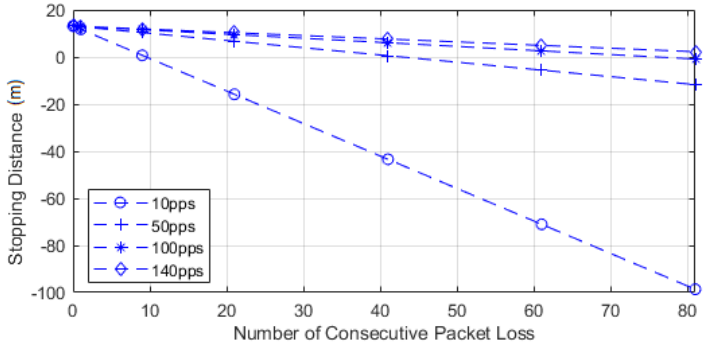

FIGURE 4.21: Reduction in stopping distance for ADAS at 30 mph (48.27km/h)

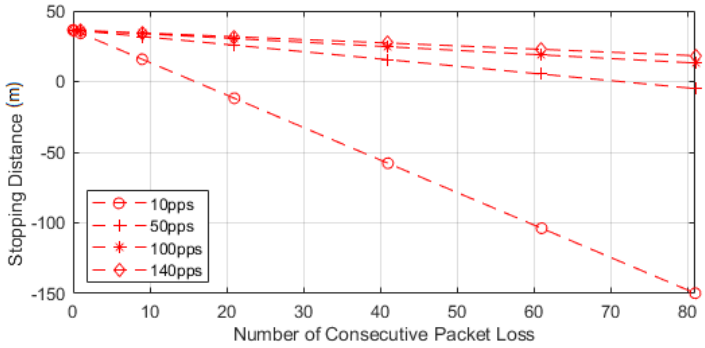

FIGURE 4.22: Reduction in stopping distance for ADAS at 50 mph (80.45km/h)

1-2 packet losses. If the losses are kept at this level, the stopping distance would not be affected substantially, but as the losses increase to even 10%, it is observed that a rate of 10 pps is unsafe to use. The use of 140 pps performs well at 70 mph, but at 30 mph, the 140 pps becomes unsafe to use due to unsafe reductions in the distance. This result also shows that DSRC needs to have high data rates if the reliability is reduced below 99%.

For a brief comparison, Figure 4.24 shows the PATH reaction at 70 mph and has the reaction time set to the standard human reaction as used previously of 1.5 seconds. This figure is only an example used to highlight DSRC systems' impact, showing how they assist and reduce vehicular stopping distances. It is acknowledged that the human driver would react from visually witnessing an emerging scenario, and therefore, the figures are highly improbable but not impossible. The only loss percentage that would not suffer significant degradation is at 1% consecutive loss, as shown in the following enhanced example in Figure 4.25. The result

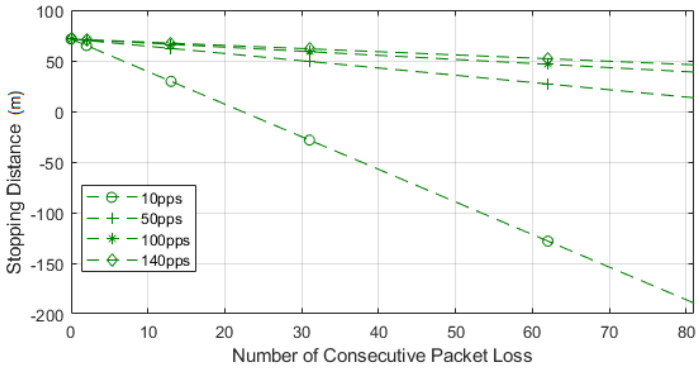

FIGURE 4.23: Reduction in stopping distance for ADAS at 70 mph (112.63km/h)

aligns with the assumption that reliability will be of utmost importance and should be guaranteed at 99.9%.

These tests highlight the importance of three main factors; reliability, data rate and latency. Other services would be able to cope with the loss of any of the three, but they are vital and must be ensured to the highest levels where safety is concerned.

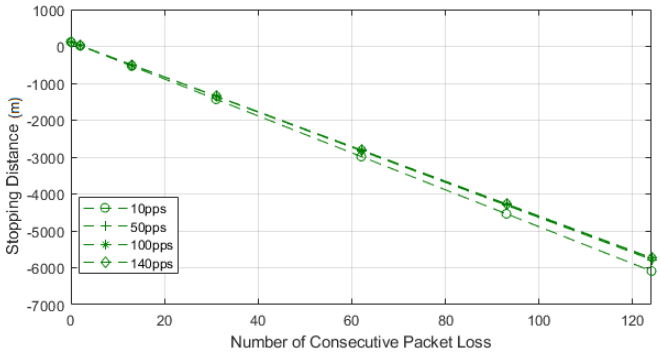

FIGURE 4.24: Reduction in Stopping Distance for PATH at 70 mph (112.63km/h)

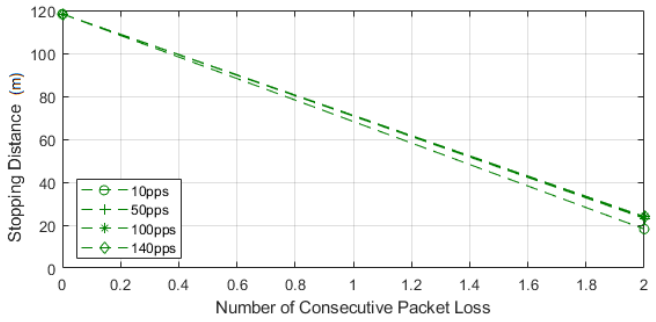

FIGURE 4.25: Enhanced view - reduction in stopping distance for PATH at 70 mph (112.63km/h)

4.5 Impact of losses caused by vehicle density and communication distance

The final part of the analysis is to employ a joint loss system between both distance reliant and density-based losses. This comparison will be brief as density losses contribute significantly more than distance losses.

4.5.1 Impact of joint losses on collision avoidance

Joint losses can be presented using both previous results for distance independent losses and the density-based losses, which are then combined in four different scenarios. These scenarios are shown at 70 mph and for four different data rates of 10, 5, 100 and 140 pps. The four differences being each simulation used 0%, 1%, 10% and 100% of the density-based losses. The algorithm used is the same as distance independent; however, it has been modified to consider two different packet loss scenarios. The results can be seen in Figure 4.26, 4.27, 4.28 and 4.29.

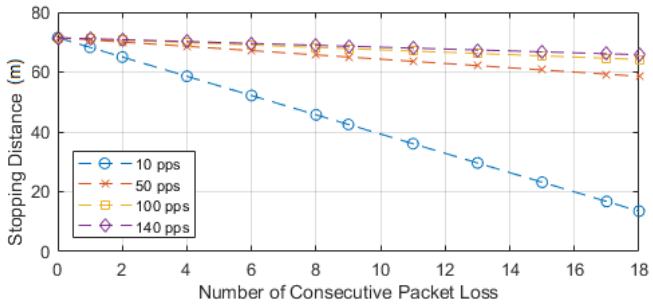

FIGURE 4.26: Stopping distance with joint loss, 0% density losses

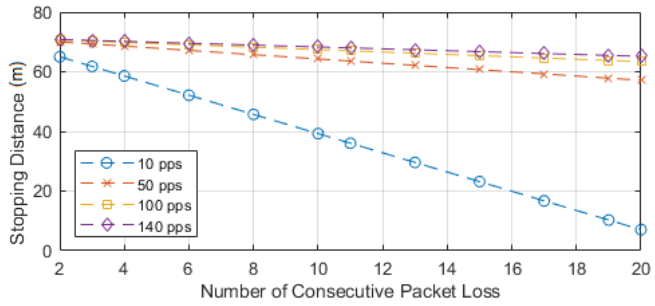

FIGURE 4.27: Stopping distance with joint loss, 1% density losses

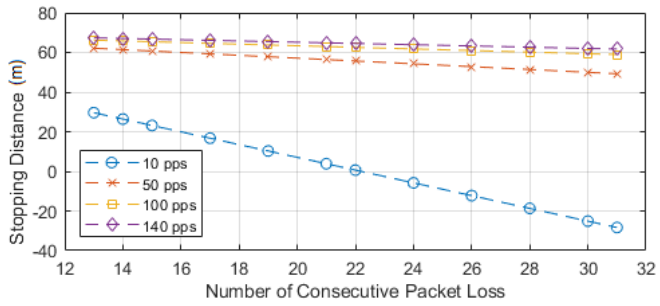

FIGURE 4.28: Stopping distance with joint loss, 10% density losses

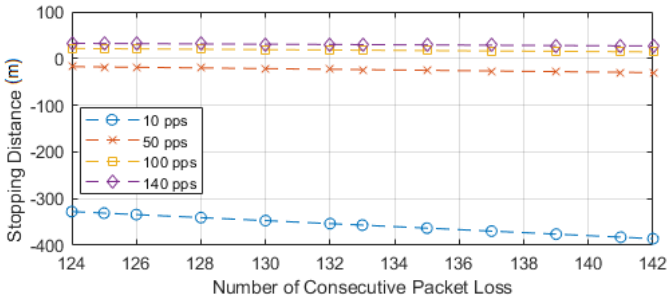

FIGURE 4.29: Stopping distance with joint loss, 100% density losses

From the figures produced, it can again be seen the biggest contributor to unsafe stopping distances is at any point over 1% density-based packet losses, and the second-highest is the use of low data rates such as 10 pps. In the 10% and 100% figures, the only data rates that do not become unsafe are those of 100 and 140 pps, and this is the stopping distance does not decrease highly, further proving the requirement of high data rates. As expected, and previously shown, the 10 pps perform extremely poorly when subjected to high-density collisions. In Figures 4.28 and 4.29

they reults again become a negative value, indicating a collision has occurred. Similar to the distance based results this result could stay at a zero value, but the negative values indicate the severity caused by delayed messages.

The final point to note is that with the requirement of 99.9% reliability, the simulated examples at density 1% and maximum distance loss of 18 packets consecutively, totalling approximately 20 consecutive packet losses, 140, 100 and 50 pps did not approach unsafe levels of distance.

4.5.2 Regression analysis for V2V link quality

Link quality is vital in wireless communications and is used as an indicator of the reliability or strength of a signal. Link quality can be quantified through regression based on the *PRR* and received power/RSSI results which will be shown.

The received power seen in chapter 4 in Figure 4.9 is used in combination with the losses recorded in the distance dependant experiment to create a simulated packet lost vs distance plot. In this example, the choice is made to use 140 pps as this is the max data rate capable of the SDR-based DSRC. A linear curve fitting is used to create a plot showing the trendline of losses at this data rate and is shown in Figure 4.30. Table 4.10 shows the correlated values up to 100 metres. This is done to highlight the relationship between the two, though this method is purely an example as the data is random and more substantial data would be required.

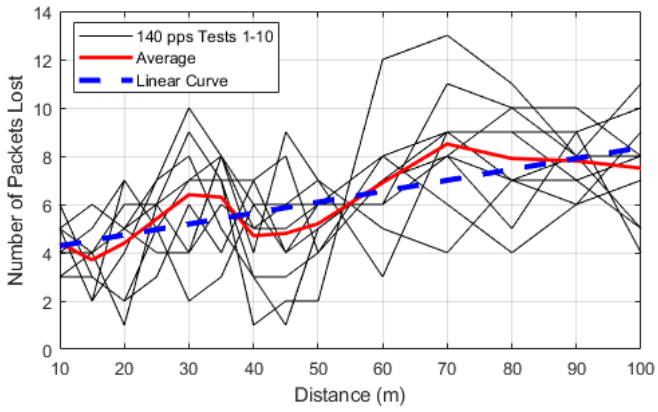

FIGURE 4.30: 140 pps curve fitting

The two curve fitting equations for 140 pps, Equation 4.23 and 4.24 will be used to create a symbolic value for a distance of 1000 metres through regression analysis. And this will be shown for both PRR and power individually, developed through a predicted number of losses per 100 packets. Figure 4.31 shows the predicted packet received rate in percentage for distances to 1000 metres, Figure 4.32 shows the power

TABLE 4.10: 140 pps regression table

Distance (m)	Average Packets Lost per 1000	Receieved Power (dBm)
10	4.4	-60.96105549
20	4.4	-71.12273766
30	6.4	-75.58207251
40	4.7	-70.33186672
50	5.2	-76.50693067
60	6.9	-83.42283966
70	8.5	-81.48620375
80	7.9	-80.0151403
90	7.8	-78.23006225
100	7.5	-78.50961634

estimation to 1000 metres, and Figure 4.33 shows the conversion to signal to noise ratio. A correlation graph can be produced from the plotted figures showing PRR versus power over distance correlated results, as shown in Figure 4.34 and is created with Equation 4.23 and 4.24.

$$y = 0.0453x + 3.8271 \tag{4.23}$$

$$y = -5.088ln(x) - 55.039 \tag{4.24}$$

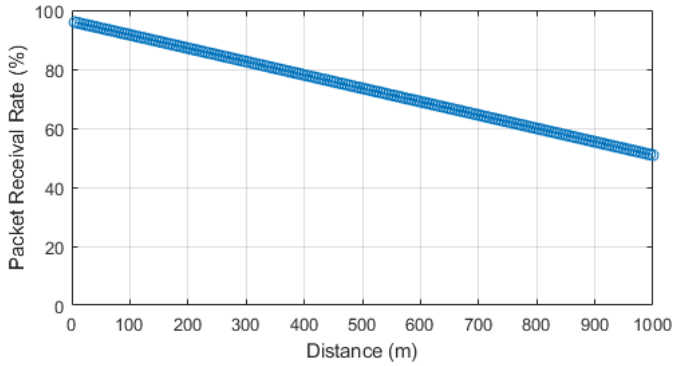

FIGURE 4.31: Regression PRR

In wireless networks such as WLAN, power levels are often referred to as RSSI and Table 4.11 shows some of the levels that are used to refer to signal quality taken from [247].

As shown in the correlation figure, the signal reaches bad quality or -70.02 dBm at 335 metres; at this point, V2V could be considered unreliable or maximum reliability range. This point will be where V2V is out of reliable range, a point at which relay nodes can be used, such as V2V or V2I. However, the signal does not leave the

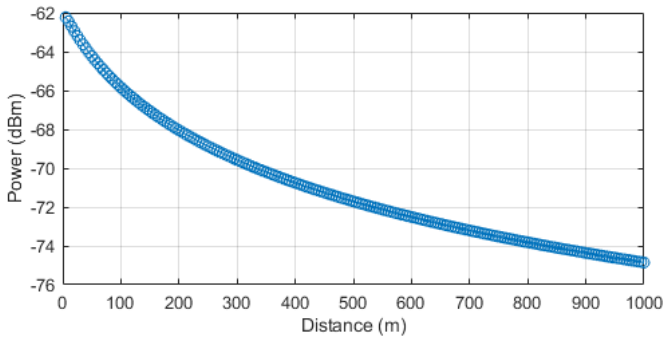

FIGURE 4.32: Regression power estimation

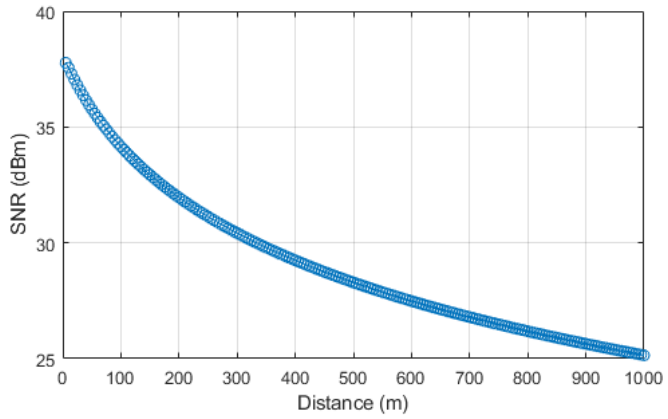

FIGURE 4.33: Regression SNR estimation

70 dBm range until 425 metres, indicating a signal would be on the edge between good and bad over this distance.

However, SNR must be considered in this case, where typically, the higher the SNR, the better the signal. In wireless above 20dbm is regarded as a good quality signal, and in Figure 4.33, at 335 metres, the SNR can be seen to be approximately 29.97 dBm, which indicates a good quality signal and at 425 metres the SNR is 28.99 dBm. This figure further shows that this range maintains good quality signal in terms of SNR. However, it is also demonstrated in Figure 4.34 that PRR is 80.997% at 335 metres, making this unreliable in terms of safety, but general message capabilities would still be established.

From the regression results, an assumption can predict the number of vehicles within this approximate 400-metre good quality range. Radius can be considered max range in one direction 400 metres, so the diameter is 800 metres. Using equation 4.17, the maximum number of nodes at this distance can be calculated to be 162

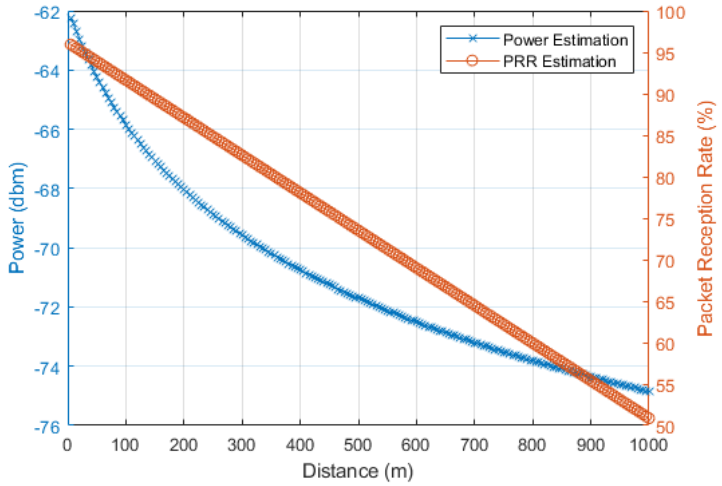

FIGURE 4.34: Regression PRR and power over distance

TABLE 4.11: Wi-Fi signal quality levels

Power (dBm)	Description
-30	Maximum signal strength, close to access point.
-50	Excellent signal strength.
-60	Good signal strength.
-67	Reliable signal strength, minimum for services requiring reliability.
-70	Weak signal strength, limited services.
-80	Unreliable signal strength supports connection but no activity.
-90	Bad Signal, No internet connectivity.

nodes in one lane and 486 nodes in a 3-lane highway environment. This large number of connectible nodes significantly increases the probability of collisions, thus why the range should be limited for safety services.

4.6 Summary and conclusions

This chapter proposes a model to use vehicular communication to increase safety through collision avoidance. Different methods are shown between human and SDR-based DSRC that highlight the reduction needed for stopping distance, meaning that vehicles can be alerted sooner and thus brake more efficiently, coming to a stop much farther in advance. This application is also shown as a beacon type message for VRU that will allow vehicles to be aware of their presence without seeing them visually. An awareness of the VRU can be as high as 120 seconds in advance at 70 mph.

Secondly, research was conducted into the various types of packet loss that can be present in vehicular communication. The losses were modelled based on the type of loss, distance or density based. This investigation was used to analyse the reliability of vehicular communication, focusing on 802.11p and safety distances. Distance-based losses were gathered from field test experiments and then divided into two simulations; distance dependant and distance independent. In addition to this, a simulation was designed to monitor the losses observed through vehicle density. The results from these experiments show how important reliability is in the context of vehicles and safety, especially for stopping distances. Real-world field test data is analysed, and results show how highly reliable communication could assist and even shorten the stopping distance via the significantly reduced reaction time. It was observed that autonomous or automatic braking systems would be a lot more efficient in reducing stopping distances, which will allow for more efficient traffic. In addition, the SDR-based DSRC transceiver is investigated for V2V collision avoidance, and the two scenarios produced show the increase in safety that can be provided with the latency and range attributes. This finding highlights a decrease in stopping distance with the SDR and an increased time to react with broadcast awareness messages.

A model for calculating the reduction to stopping distance when subjected to consecutive losses has also been produced and quantified. This investigation helps to highlight the importance of reliability when a system is based solely on communication, and no sensor data is utilised. The results also show that almost perfect packet reception must be guaranteed for safety when CAVs become more prevalent and prominent on the road. Lower data rates are not suitable for all safety needs. It was also proved that a method of reduced safety distance using the developed system could reduce the effect of tailgating. The safety distance algorithm that has been designed and modelled is viable in density-based simulations. Results show that this system can improve safety for vehicles, using the DSRC and adequate mathematical interpretation to maintain safe distances when driving and

equipped in conjunction with ADAS systems. The main detriment to DSRC is the collisions that can occur between vehicles, and that distance is a much smaller factor in comparison. With this said, it is presented that with the use of both DSRC and ADAS, the safety zone can be reduced, which would reduce the number of density collisions and, by proxy, increase road efficiency.

This chapter presents a model to provide collision avoidance with DSRC/802.11p communication, and results show a significant increase in stopping distance, which will lead to reduced rear end collisions. Furthermore, an empirical performance analysis for DSRC/802.11p under different packet loss situations is performed, with losses modelled and analysed. The results highlight that density is more of an issue than distance-based losses.

Chapter 5

Cooperative Connected Infrastructure and Smart Vehicles

5.1 Introduction

Many challenges remain for CAV, and these vary in nature, such as technological suitability [57], [248], location within the vehicle [249], adaptable technology [250], communication protocol [251], spectrum issues [252] market penetration and interoperability. There are also specific concerns on performance and operability between vehicles and infrastructure, commonly referred to as V2I, and how the cooperation between V2V and V2I communication can equate to a safer and more efficient driving system.

V2X is synonymous with the future of CAVs; for example, the issues of autonomous driving will rely on data from other vehicles to be aware of their intention and planned actions. This type of data will require low latency and high reliability to maintain up-to-date information, ultimately increasing road safety and reducing vehicle collisions. CAV design will need to be a robust system that is able to share data heterogeneously. The data shared will provide cooperative perception and mutual awareness regarding the actions of the road users, such as vehicles and pedestrians.

Many cases show that cooperation between connected vehicles alone cannot solve the issues for safety and complete autonomous driving, for example, adhering to the safe distance between vehicles or detection of pedestrians behind parked vehicles. Connected smart road infrastructure will be a key component towards solving these issues for CAVs that will offer a smarter and adaptive traffic system. Connected smart Road-infrastructure and Autonomous Vehicles (CRAV) [253] is a novel approach to connected vehicular technologies and their cooperation towards a safer transport system. The proposed CRAV framework operates by using a combination of V2V, V2I and local sensing to share information. Vehicles and infrastructure are vital in CRAV towards smart road infrastructure. It is a combined framework of

CAVs, pre-defined deep learning, roadside units (RSU) and camera sensing technology that has not yet been achieved. This new research approach is used with CV and AV due to the individual limitations of the different technologies when used independently. To the best of our knowledge, there are no current investigations concerning the design and evaluation of CRAV and no published results regarding the assessment and operability of a decoupled framework for autonomous vehicles that use V2X, pre-defined deep learning, camera based sensing and cooperative information sharing towards safety. CRAV makes use of these individual technologies towards cooperation for increased road awareness.

Connected smart road infrastructure and AVs (CRAV) is starting to receive attention, and pilot trials have reportedly begun [254], [255], [256]. CRAV holds excellent potential, but research on CRAV is still in its early stages. Research and investigation for CAV are complex and challenging due to cross-disciplinary technologies, including automotive, driving planning and control, vehicle communications, computer vision and artificial intelligence. The introduction of intelligent road and infrastructure technologies make CRAV research a more significant challenge. While field test systems could produce reliable results, they are costly and time-consuming to build. They are not scalable or flexible enough for pressure testing to valuable insights into difficult and dangerous scenarios.

Besides the traditional concepts used for CAV, there are areas of interest under investigation for CAV concepts, and one such area is the use of deep learning prerogatives. Deep learning is a large and well established technique with many available pre-trained models, this CRAV implementation makes use of pre-defined deep learning for object detection/recognition rather than develop a new method. Applications of deep learning have recently evolved into usage for vehicular needs [257] due to information importance in a highly dynamic vehicular environment. The concept for deep learning in a CAV environment is to use video technologies with object detection/recognition to enable mutual sharing of information concerning detections. This cooperation moves toward alerting road users of situations out of their awareness range.

The motivation for the developed CRAV framework is to demonstrate the safety increase that can be provided through a combined system using CAVs and infrastructure. Research is conducted into a new proposed cooperative framework between infrastructure and vehicles to offer smarter and safer driving. The advantages gained from combining V2X communication, pre-defined deep learning for object recognition, and sensing-based techniques will show the enhancements made for road safety and efficiency (RSE) and how these individual technologies combine to support each other. The deep learning applied in this chapter should be specified

as pre-defined and pre-trained models for object detection/recognition. The CRAV package helps identify these inherent advantages with a flexible approach unavailable to the best of knowledge. It will demonstrate the effectiveness of the proposed CRAV framework and identify the potentials of CRAV through investigations.

In Chapter 3 and Chapter 4, The approach was towards V2V communication for safety between vehicles. In this chapter, the consideration changes scope to encompass other road users as well as vehicles. This approach is achieved using V2I. V2I is a type of communication between vehicles and infrastructure and vice versa. The V2I system will incorporate communications between vehicles and infrastructure, in the form of roadside units (RSU). This communication approach is to solve safety issues for vulnerable road users using the same roads as vehicles. The main issue is that vehicles cannot detect VRUs if they are blocked from direct vision. However, RSUs may have better line of sight to the VRU and they possess the capability to share their local sensor information to make vehicles aware. The benefits will be an increased perception range using infrastructure data to be aware of situations not in the vehicles line of sight.

In this chapter, in section 5.1.1, an overview is given on current V2X/CAV systems and the state of modern concepts. The framework is designed and developed in section 5.2, along with an evaluation of CRAV components, and it is shown how they form the complete CRAV framework. The CRAV system architecture will be explained, detailing the current issues with modern CAV systems and the approaches CRAV uses to mitigate them. The framework will also identify the benefits of safer driving and mutual road awareness.

Following this, in section 5.3, the motivation for CRAV is detailed, focussing on the problems that CRAV will address regarding the safety of vehicles and VRUs. This proposed approach will be achieved using a developed CRAV framework. It will investigate the CRAV experimental procedures applied to demonstrate the applicability of cooperative, connected infrastructure towards a safer driving environment and show the benefits of CRAV RSU information sharing for detecting objects out of vision. This section will also highlight the benefits that CRAV will offer regarding increased safety compared to traditional local sensor approaches and the increased safety distances that can be achieved. CRAV results are evaluated to show how the RSU gives increased distance to react to a detected VRU with their shared knowledge, compared to vehicles using local sensors only.

In section 5.4, CRAV is modified to operate as a V2V/V2I relay, which provides a solution for the issue of vehicles equipped with different communication technologies. This method solves the problem of VRUs being out of the RSU vision and allows bidirectional cooperation between vehicles and infrastructure instead of the

one-way system previously used. This approach is of particular benefit for vehicles using different types of communication technology, with the RSU equipped with both. Section 5.5 further develops the previous investigations with the VRU given lateral movement in front of the vehicle instead of previous iterations with static VRUs. This novel approach predicts collision time and probability of collisions; identifying the RSU assistance offers increased safety at many different speeds with warnings provided for VRUs, the probabilities of collisions are reduced.

Section 5.6 proposes using a safety distance model known as Responsibility-Sensitive Safety (RSS) with the new concept of inclusion into CRAV, which has not been previously studied. This newly defined CRAV RSS algorithm is applied into the CRAV framework to demonstrate the benefits to safety distance when used with shared information. The CRAV RSS model is adapted to allocate adequate safety distance to the CAV. Then performance is assessed when vehicles use RSS, human or SDR-based DSRC-based reaction times. Alongside this, a new algorithm classified as AWD is developed and applied to measure actual distances between vehicle locations. These models are used to identify and demonstrate CRAV feasibility, with results highlighting the increased safety performance with AWD and RSS deployment. The CRAV framework provides high-quality results, specifically regarding the usage of pre-defined camera-based deep learning techniques, towards vehicle and VRU recognition, with algorithms used to identify warning distances and the likelihood of accidents. CRAV benefits are highlighted compared to on-board vehicle sensors and the issues they may encounter, finding that these models can significantly reduce road collisions.

5.2 Design and development of CRAV framework

This section will provide an overview of the current state of CRAV technologies, detail the developed CRAV framework, explain why this approach is taken, and briefly introduce the relevant technologies and concepts that form the framework.

5.2.1 Overview of the state of technologies

RSE is one of the core components leading the development of state-of-the-art vehicular solutions and the main contributors are connected vehicles, autonomous vehicles and camera based vision sensing technologies. In previous cases, the approaches for increased RSE performance were formed from traditional methods such as maintaining good adherence to driving standards, adopting and enforcing new road legislation, and expanding or simplifying road networks to increase capacity [258]. The adoption of CV and AV is a distinctly modern approach that directly

includes ADAS, platooning, collision avoidance, pre-crash sensing, and accident detection or mitigation [259].

Connected vehicles (CV) use communication technology known as Vehicle to Everything (V2X) to maintain connection, a state of information sharing between any connected road users, such as vehicles, infrastructure, or pedestrians. CV has also suffered detriments such as limited data rates and delayed message deliveries under highly demanding networks, which is unsuitable for CAV applications such as self-driving or automated chauffeuring [260]. Despite these shortcomings, this is one of the most promising evolutions for vehicles, and continued development is ongoing.

Advanced Driving Assistance Systems (ADAS) is a precursor to autonomous vehicles and is currently used to support vehicle drivers to offer information about the current driving situation and aid the vehicle's driver, primarily to reduce the number of road accidents to increase safety. The safety increase is achieved with the driver being informed to take appropriate actions or, in the case of partially automated, the vehicle can take preventative measures or intervene on the driver's behalf. As this technology continues to develop, the end goal is AV or self-driving vehicles, where all components of the driving situation are taken by the vehicle and supporting technologies. The leading support technologies for AV are sensing technologies such as LiDAR and RADAR. The combination of these allows various levels of automation. However, they too have limitations such as limited sensing range, line of sight blocking and channel issues such as adverse weather conditions. These limitations can harm the performance of adaptive cruise control, blind-spot detection, forward collision warning and lane change manoeuvres. Other areas vital for AVs are highly accurate GPS/GLONASS systems, robust and regularly updated high definition maps and enhanced driving systems that are intelligent enough to react to the ever-changing road networks and unexpected events. This approach requires highly accurate joint sensing systems that can be integrated with advanced data processing algorithms that are fast and robust. Recently approaches have been made to incorporate vision-based assistance into ADAS solutions, such as Tesla [261]. It has been envisioned as likely to encounter camera sensor issues but offers some benefits such as reverse assistance.

5.2.2 Cooperative CRAV for safe driving

CAV and CRAV implementation are highly challenging and diverse environments and evaluating these systems can prove difficult. While research works exist concerning CAVs, these investigations mainly comprise separate subsystems that form a functional part of the entire CAV backbone. Currently, no environment offers a

complete CAV system, with a full range of components such as V2X communication, local on-board camera sensing with computation, autonomous driving capabilities and computer vision with object detection or recognition. Widely used Simulators exist for V2X network components such as the network focused simulators NS-2 and NS-3 [262] or environments such as OMNET++ [263] and OPnet [264]. Then there are more vehicle focused simulators such as Vector Car2X [265] and iTetris [266]. These simulators can be combined with various traffic simulators such as SUMO Veins [267], Vissim [268] and MOVE [269]. These simulators with collaboration can express networks and traffic together, although they can be temperamental and difficult to combine. Additionally, cellular network simulators that represent C-V2X are available, too, such as Vienna LTE-A/5G [270], NYUSIM [271] and IS-Wireless [272].

Camera vision sensor-based simulations for CAVs and RSUs are vastly used in existing deep learning engines, including Facebook Pytorch [273], Google TensorFlow [274], MATLAB Deep Learning Toolbox [275], and MMDetection [276]. Existing projects are readily available within these systems but must be trained and compiled for individual needs. Many deep learning models exist already for object recognition or object detection.

Autonomous driving is another area that has seen significant software devised, such as CARSim [277] or the open-source project CARLA [278]. They, too, have their drawbacks as they are built on powerful gaming engines and require massive amounts of computer resources to operate. They are intelligent systems that cover the autonomous driving features to create specific scenarios or even city-wide driving simulations.

Simulated scenarios are significant for network planning, preliminary investigations and forming general ideas on performance characteristics. Simulators are an excellent way of monitoring a system in theory to predict performance. However, there are many factors that a simulated experiment cannot account for, such as interference, real-time operation, obstacles, reflections, refractions, environmental changes and weather conditions. With these issues, there comes a need for field or pilot tests. There have been some pilot tests reported for CRAV implementations, such as [254], [255], [256]. Still, due to the scale and slow nature of field tests, coupled with the need to test specific rare and dangerous use cases, an alternative approach must be found to implement and deeply evaluate a fully functioning CRAV system.

As discussed, the current availability of technologies to enable the future of CRAV and CAV driving architecture still faces many challenges and obstacles in terms of research and technology synthesis. Such problems can be simply poor

object detection, poor road layouts, or even incorrectly configured network issues. These are especially prevalent in field tests that are complex and time-consuming to troubleshoot and locate the exact issues. Further issues introduced by CRAVs are unreliable object detection results, which can pose threats if the receiving vehicle does not trust the information source. Mobile CAV systems are highly dynamic in terms of topology, and the connection times in these networks are short periods, proving challenging to cooperate, especially with minimal range. Object detection has an issue with object localisation, which means whilst an object can be detected and recognised, the RSU would have difficulty learning the location without reference from other connected users.

A significant problem for CRAV will be the fusion of the data between CAVs and RSUs, which would require specific attention to detail. The final and most crucial issue will be the allocation of CRAV towards enabling safe and efficient cooperative driving and road safety applications. Simulation procedures are also an issue to monitor, especially when operated in separate instances for each individual concept. This issue can be solved using a simulator that integrates all features into one framework and offers great benefits. They are much more flexible, cheaper, adaptable on the fly and operate faster.

5.2.3 CRAV framework

Many of the issues discussed are solvable problems using a comprehensive framework that is a complete model of a CRAV system. The system will be fast and scalable, with an interest in road safety applications. This framework supports cooperative CRAV systems with CAV, RSU and VRU. It is imperative to assess the benefits of CRAV, CRAV planning, and the increase in safety compared to non CRAV enabled road networks.

The realisation of a CRAV system will enable rapid design and set-up with additional support from available toolboxes and libraries will allow the operation to take much less time than separately compiled environments or real-world testing. Therefore, the designed CRAV framework will incorporate multiple subsystems into one intuitive framework. The framework will consist of a V2X communication system simulated at the packet level with adherence to communication protocols and local sensing, including vision-based that will be performed at the frame level, which will utilise the application of pre-trained deep learning models. In addition, the CAV movement and roadway simulation will be performed with a local trajectory programmed for speed, movement and location. Finally, the data fusion and object detection data tracks are performed using communication and local sensing from

the CAV, RSU and VRU. The results are then used to investigate and analyse cooperative road safety.

The approach to have a system framework that can fully utilise the various essential components for CRAV to gain credible insights and results to assist the safety of CAV is new. In this work, it is known as a decoupled framework, in which the separate blocks are initiated and compiled independently and then used cooperatively with one another. For example, V2X communication is simulated separately from the CAV driving scenario, allowing much faster simulations while requiring less computing power. This framework will enable many different safety scenarios to be expressly identified and analysed in multiple ways to explore the applicability and operation of each subsystem of CRAV and then jointly combined. This approach is novel in creating the framework design and how the results can be approached, evaluated and visualised. The applications towards safety can be looked at for vehicles and the safety of VRU. This approach is not commonly seen in multiple configuration systems or simulations with the inclusion of RSU vision-based VRU recognition. The data is then further disseminated to other road users.

Each subsystem will be briefly explained, including the functionality of the subsystems in the framework. An example of the CRAV framework can be seen in Figure 5.1.

- Simulation of V2X Communication: this subsystem is a simulation for V2X communication and is performed before the full CRAV system simulation is conducted. Within this subsystem, many options are available to modify the simulation regarding CAV layouts, such as the road network topology, CAV actor density, message type, bandwidth allocation, speed of the vehicle, starting location of actors, DSRC or cellular communication type and packet error rate. Additionally, the RSU and V2I components can be adjusted similarly to the CAVs. The simulation, in this case, will be performed at the packet level and follow standardised V2X communication algorithms. Different channel models can be specified for the different scenarios, such as weather differences or urban/highway driving. Following the specific parameters, the V2X simulation will produce statistical performance measurements for the packet delivery ratio and the delay against communication distance. The performance statistics are then used to create a V2X communication simulation profile and is stored for further use to be passed into the core CRAV. Additionally, these statistic attributes can be saved and viewed offline. The profile will contain performance curves at distances and packet error recorded.

- Object detection and tracking test: sensing and vision are crucial components

for intelligent and connected vehicles. Sensors such as LIDAR, RADAR, cameras, UWB and GPS are the most common and widely used in CAV frameworks. These sensing technologies can be equipped at CAV nodes and RSUs, and the object and tracking functions can be performed in separate runs conditionally. The object detection simulation is performed at the frame level with deep learning models in the scope of inference. The object detection results will be assessed in accuracy and confidential score. These attributes are then further evaluated against object distance, lighting, and weather conditions and collated with object categories, sizes, and object occlusion. All parameters can be specified depending on the application. For instance, choices can be made for registering VRU, such as a human pedestrian or cyclist, and then the speed of each can be computed. Similarly, as with the V2X subsystem, the results will create an object detection profile and be stored for further usage in the core CRAV. The profile will contain information such as performance curves for detection and occlusion.

- Core CRAV Simulation: The overall CRAV simulation is performed at the CRAV core as shown in Figure 5.1. and will use the two previous profiles created. V2X and object detection profiles will be taken as input files in the decoupled framework, and the performance curves are used to configure scenarios. This core will include some CRAV simulation settings and procedures that will be predetermined, such as the road layout, route trajectory, number of actors and the sensors installed at each actor. Within the CRAV core, additional parameters can be set for the road safety and driving application specifics.

With the configuration complete for the CRAV and subsystem profiles, the core CRAV simulation can start, which is completed in a predefined time step and will begin with regular updating of the actor's position, status and intention. Object detection and tracking will also be initialised and performed for each actor at each time step. This detection is completed by referring to the created object detection profile instead of constructing and applying a deep learning model for each frame. Then following this, the configuration for cooperation modes will be referenced for the road safety application. Depending on the design, the results for communication and sensing will be made available for sharing with neighbour nodes and internal actor usage. If communication is available and enabled, the interested actors will receive communicated data concerning the sensing and object detection, which is simplified to use the V2X communication profile. This profile will also determine the packet success rate, deciding if a message is received and added to the actor's results. If the message is received successfully, the neighbour actors will use the shared data comprised of the object detection and tracking information, and they

will fuse this to their local data. Depending on the core CRAV road safety application and settings, the cooperative sensing data will be used to make actions for cooperative driving.

The process of the core CRAV is completed at each time interval until a parameter is met that stops the scenario, and this is usually a predefined number of steps or when all actors reach their trajectory endpoint. The results will be output and displayed at the finalisation of the simulation using pre-configured settings. In this case, results for cooperative driving will be collected, collated and visualised.

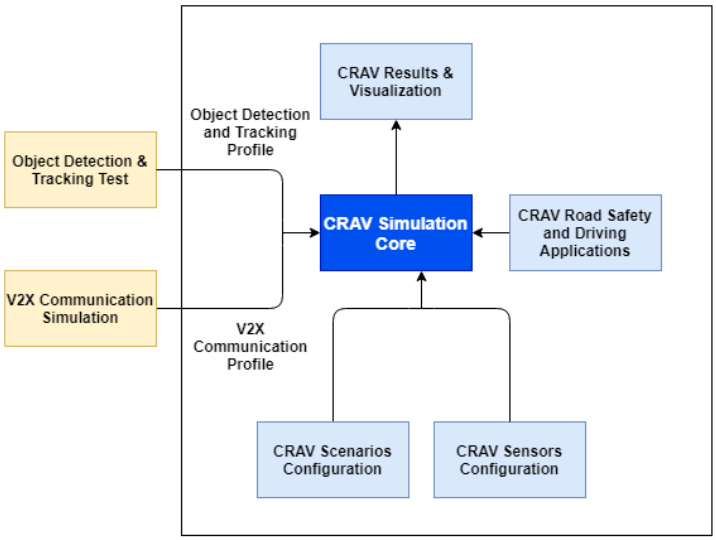

FIGURE 5.1: CRAV simulation block diagram [253]

5.3 CRAV for VRU detection

The CRAV implementation developed is a robust and capable framework that can be modified to suit the individual scenario needs, and this includes many types of visualisation for results. These needs encompass a potentially wide range of driving and safety applications, including cooperative and localised. The scenarios in this chapter have been designed to focus on safer driving to emphasise the impact of safety between the cooperative CRAV system and the approach whereby each actor uses only locally generated data. The simulation is built using Matrix laboratory (MATLAB) instead of NS-2/3 is due to the large number of available toolboxes and having a predefined autonomous driving toolbox, which NS-2/3 does not have. In these event driven simulations, the main toolbox used is the autonomous driving

toolbox [279], as it has preconfigured environments that can be altered depending on situation.

A general setting was applied for the investigations in this chapter, and then minor changes were performed and compiled for each scenario. The scenarios are event driven simulations and the core simulator settings will be explained, and then at each scenario, the modifications will be justified and explained for their relevance. Within each scenario, the steps and time intervals were maintained to be the same. The general settings for the framework will be defined in the initial CRAV scenario.

5.3.1 Investigation of CRAV: connected RSU and camera sensing

The initial scenario for the analysis of CRAV is performed to show the impact of the inclusion of RSU information into the vehicle tracks for a VRU when the vehicle actor's camera vision is initially blocked. This case study assesses a smart CRAV assisted VRU collision warning, and the impact is monitored for the CAV with and without RSU assistance. The initial settings of the simulation are built within a predefined roadway; the roadway is a 2-lane road with a width of 8 metres and is approximately 300 metres in length, although the dimensions can be altered. Then roadway is populated with an RSU, two CAV actors equipped with LTE-V2X communication radios and camera sensors, a parked bus and a VRU. The bus is positioned to obstruct CAV vision. The VRU is a pedestrian that is situated behind the bus in preparation to cross the roadway. Additional vehicles are used for road perception only.

The RSU is equipped with communication capability, two camera sensors facing different roadway directions and are fixed at a position of (95, -10). The two CAVs are travelling north on the road at a velocity (v) m/s. They are given a starting position of (-20,3) and (-10,3), respectively, whilst the non-important vehicle actors locations are randomised. The parked or stationary bus actor is given the (d,3) location, where d is a configurable variable that can be changed. In this case, it is positioned at locations from 5 to 65 at intervals of 20 metres. The bus is measured at 8.5 meters length, 2.5 meters width and 3.5m height. The VRU or pedestrian is located at (d+10,3.8), directly behind the bus location.

The concept of the scenario is for the RSU to monitor the road and observe the VRU and CAV locations. The CAVs use their camera sensors to monitor their road perception. If non-cooperative (Non-CRAV) is used, the vehicles will only use and update road information from their camera sensors, with no communication capability; however, if cooperation mode (CRAV) is enabled, the tracks from the communication with the RSU will be fused with the CAV local tracks, generated from camera sensors. This fusion generates information and warnings for the CAVs with the

VRU out of their perception range. The LTE-V2X settings have been compiled from [26] and maintain a 10MHz bandwidth and a communication curve of y=p(x)=1-0.3*d/x, where x represents max communication range of 150 metres. The results are visualised to measure the allowed time or distance between CAV and VRU colliding. An example of the defined CRAV scenario can be seen in Figure 5.2 and an example of the simulation running showing camera angle and range can be seen in Figure 5.3, the CAV camera sensors are always facing north which is entered as -15 with a range of 100 metres, and the RSU has two camera sensors with a range of 100 metres, however the RSU camera angles are set to 110 and 155. In some simulation examples the RSU camera yaw is altered to change the direction of camera vision, this is specified in each example.

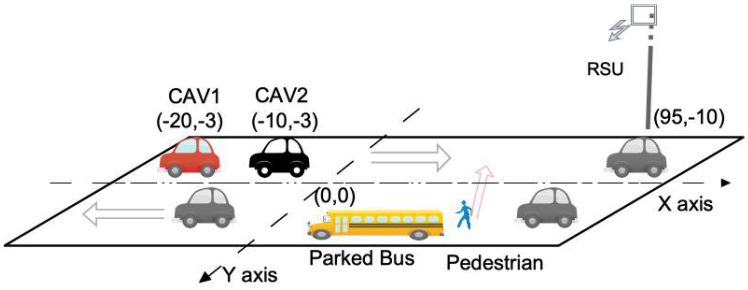

FIGURE 5.2: CRAV scenario example

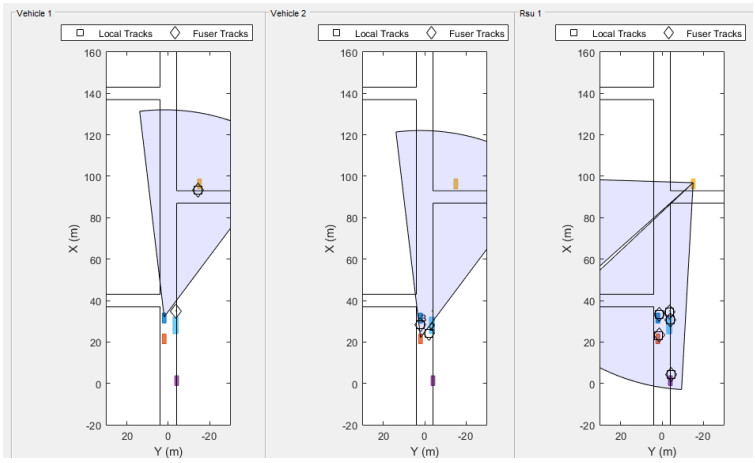

FIGURE 5.3: CRAV Simulation scenario example

5.3.2 VRU detection results with CRAV

After the parameters have been selected and entered, the CRAV procedure can be performed. In this scenario, velocity (v) has been chosen to be metres per second, and a different iteration was performed for five different speeds, 4.5, 9, 13, 18 and 22 m/s. The speed was altered for each simulation, and results were recorded for the remaining distance and time to VRU. In all experiments it should be stated that sensors are classified as camera sensors only and the RSU has a communication range of 100 metres. In the figures, the ARD is used to show how far in advance the CAV is aware of the VRU and the location of the bus is shown in the horizontal direction.

The results are shown as figures for 12 m/s and tabulated for the remaining speeds. Two figures are used, with one identifying the remaining distance in Figure 5.4 and the other showing the remaining time in Figure 5.5. In each figure, the results represent values for each CAV when the non-cooperative mode is used (local camera sensors only) and when CRAV cooperative mode is used (fused tracks from the RSU and local camera sensors). The local camera sensors for the CAV and the RSU are given a range of 100 metres and use object detection to identify pedestrians and vehicles through predefined detection profiles. The dotted lines represent the Non-coop mode, and the solid lines represent the cooperative fused tracks. Table 5.1 shows the allowed response distance (ARD) for CAV 1 and Table 5.2 shows the ARD for CAV 2.

The initial results are recorded at the location the VRU moves to from point 5-65 metres. The distance is a difference between the location of the CAV and the location of the RSU. This calculation is performed when CAV 1 and 2 detect the VRU with local camera sensors and when CAV 1 and 2 detect the vehicle from the RSU fused tracks. The distance is converted into time by dividing the distance measurement by the velocity of the CAV. The results are plotted directly using MATLAB simulation to represent the difference in detection between CAV camera sensors and RSU camera sensors fused with CAV data, which highlights the advantages of using RSU fused data.

The results show that when the CAVs rely on local camera sensors with object detection only and with no input from the RSU (non-coop mode), local detections for the VRU behind the bus occur at approximately 12-13 metres. This result means the allowed response distance is relatively low, and different bus and VRU locations do not alter the measured distance. This distance is not enough to come to a stop before potentially colliding with the pedestrian, except for the slowest case of 4.5 m/s, which is significantly lower than speed limits for UK roads. The second trend for non-coop mode shows that the increase in speeds would leave a significantly

TABLE 5.1: Allowed response CAV 1

		Allowed Response Distance (m)				Allowed Response Time (s)			
		Location of Bus							
	Speed	5	25	45	65	5	25	45	65
Sensor	4.5	12.822	12.638	12.799	12.534	2.849	2.808	2.844	2.785
	9	11.615	12.344	12.618	12.120	1.291	1.372	1.402	1.347
	12	12.350	11.976	12.895	12.265	1.029	0.998	1.075	1.022
	18	12.264	12.726	12.824	11.240	0.681	0.707	0.712	0.624
	22	11.391	11.142	11.069	10.931	0.518	0.506	0.503	0.497
RSU	4.5	18.692	39.050	58.699	78.626	4.154	8.678	13.044	17.472
	9	18.653	37.560	57.383	77.217	2.073	4.173	6.376	8.580
	12	19.237	36.274	55.185	75.132	1.603	3.023	4.599	6.261
	18	18.642	39.620	58.096	78.262	1.036	2.201	3.228	4.348
	22	16.562	37.412	55.703	75.909	0.753	1.701	2.532	3.450

TABLE 5.2: Allowed response CAV 2

		Allowed Response Distance (m)				Allowed Response Time (s)			
		Location of Bus							
	Speed	5	25	45	65	5	25	45	65
Sensor	4.5	12.304	12.544	12.017	12.536	2.734	2.788	2.671	2.786
	9	12.520	12.568	11.102	12.037	1.391	1.396	1.234	1.337
	12	12.588	12.273	11.695	12.739	1.049	1.023	0.975	1.062
	18	11.602	11.671	12.139	11.900	0.645	0.648	0.674	0.661
	22	12.339	12.116	12.234	9.858	0.561	0.551	0.556	0.448
RSU	4.5	28.692	49.050	68.699	88.626	6.376	10.900	15.266	19.695
	9	28.653	47.560	67.383	87.217	3.184	5.284	7.487	9.691
	12	29.237	46.274	65.185	85.132	2.436	3.856	5.432	7.094
	18	28.642	49.620	68.096	88.262	1.591	2.757	3.783	4.903
	22	26.562	47.412	65.703	85.909	1.207	2.155	2.986	3.905

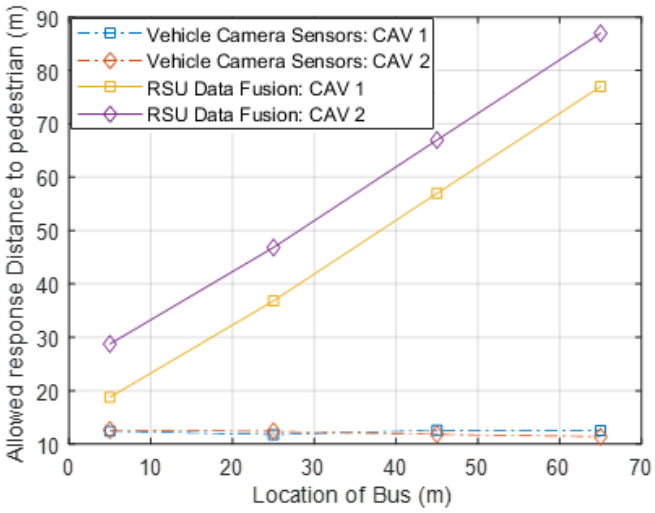

FIGURE 5.4: CRAV response distance 12 m/s

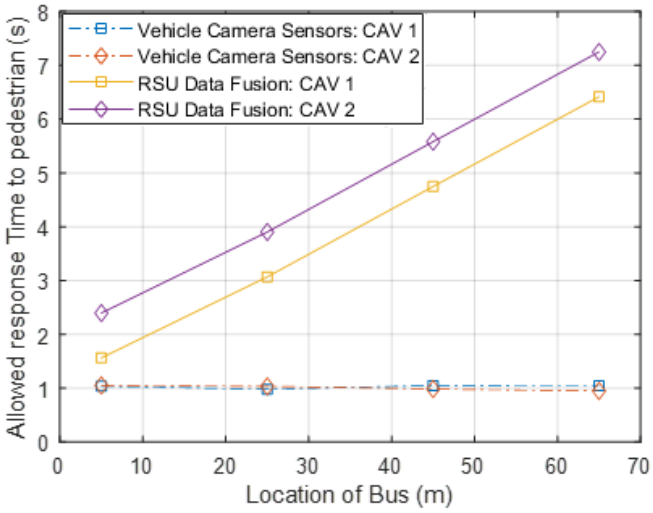

FIGURE 5.5: CRAV response time 12 m/s

smaller distance to react. In the time-related data in the tables, anything over 9 m/s leaves approximately one second or less to react, which is lower than the required reaction time for human drivers of 1.5 seconds. This low amount of time to react means that collisions with the VRU are highly likely, increasing as v increases.

This result is compared with the results from the fused tracks (coop mode) that have been cooperatively received from the RSU. In this scenario, there is an inherent advantage for the CAVs as the fused tracks provide knowledge of the VRU far

in advance of sensing them locally. This result means potential collisions would be reduced as the vehicle would be aware of its location and adjust speed to slow to a more appropriate velocity. The results also show that the first value for each speed for CAV 1 is approximately 20 metres, which will be as the CAV enters the communication range of the RSU. This finding shows that the communication range for the RSU plays a large part in the effectiveness of the fused tracks. Suppose the CAV is out of range until too late; the message is received too close to the VRU. The results also highlight that the allowed response distance with RSU increases linearly with the d value in response time. This result increases linearly with d as expected. However, it also shows that until the velocity approaches unsafe speeds for two-lane roads, which is 12 m/s, the time to react is over 1.5 seconds, which provides enough time for a human to react but not brake but still reduces the probability of fatalities.

Regarding CAV 2, allocating a gap between the vehicles also provides an extra distance to react, increasing the potential for avoiding chain-reaction collisions. The most prominent finding is that RSU holds an advantage over traditional camera sensing if data fusion is allowed and trusted. The use of RSU increases the distance for reaction than the traditional camera sensing method.

The results in Table 5.1 for CAV 1 show that at 4.5 m/s and using local camera sensors, is the only time in which the allowed response time is higher than 1.5 seconds, which is the reaction time of a human driver. Using the CRAV framework, the RSU supplies information to the extent of the communication range, set to a maximum camera range of 100 metres. This scenario relays information from RSU to CAVs. For each result at 18 and 22 m/s, respectively, the initial detection offers an increased reaction time but is still not high enough for a human driver to react. These results can be compared with the reaction time of a human driver and CAV SDR-based DSRC developed in this thesis in Chapter 3. Therefore, the results can be applied with a formula for both humans and autonomous reaction time, this will be taken from Chapter 4 and Equation 4.3. Figure 5.6 is used to show the distance remaining after the vehicle is notified of the pedestrian at 12 m/s, and the human driver makes a reaction. This is simulated for the distance that the driver is alerted from and the subtraction of the total stopping distance, this leaves a distance remaining before collision. A negative reading means that the vehicle would have collided with the VRU and shows how much extra distance would have been required. Where T_r=1.5s and the entire braking force is applied, this result highlights the additional distance that the RSU provides. This Figure shows that the remaining distance is negative with a human driver reacting to local sensors, indicating a crash has most likely occurred. For the RSU fused results, the human can react to the data

from the RSU earlier, and the only collision would be the initial detection for CAV 1.

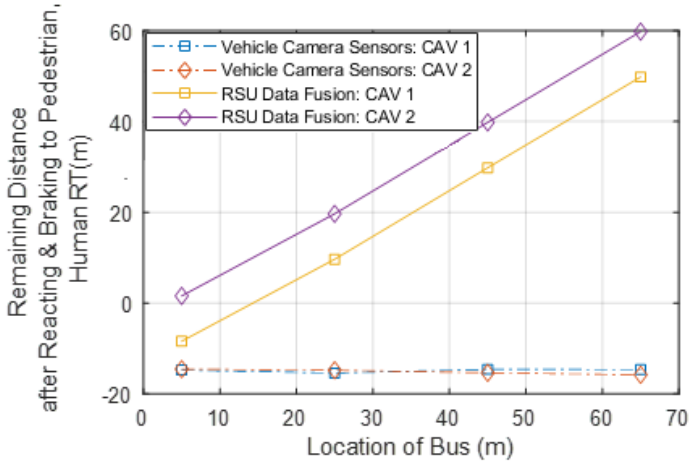

FIGURE 5.6: Remaining distance after reacting and braking 12 m/s and human reaction time

Following the results for a human reaction, the SDR-based DSRC reaction time for autonomous vehicles can be applied to the formula, and the results for this can be seen in Figure 5.7. and the reaction time is 2.9 ms taken from results in Chapter 3 for the SDR-based DSRC reaction time.

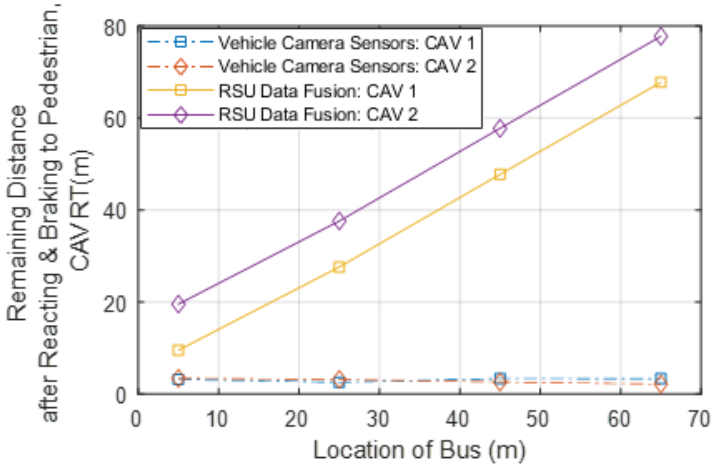

FIGURE 5.7: Remaining distance after reacting and braking 12 m/s and CAV reaction time

This experiment highlights the extra distance provided when using RSU to relay vision sensing data and shows that the CAV reaction time is vital as human reaction does not give enough time to react even with a warning message. Figure 5.7 also

indicates that with an autonomous reaction, the sensing from local cameras and autonomous features provides enough warning to brake to a complete stop. However, speeds higher than 12 m/s would start to decrease below 0. However, the speed limit for many UK roads is 30 mph, approximately 12 m/s.

With the reaction time of an autonomous vehicle and a velocity of 12 m/s, the CRAV framework shows the collisions could potentially be avoided as a vehicle still has enough time to react and come to a complete stop. This experiment highlights the extra distance provided when using RSU to relay data created by vision sensing and shows that the CAV reaction time is essential as human reaction does not provide adequate time to react.

These preliminary results demonstrate the effectiveness of the CRAV framework and how collisions can be reduced when this is applied. The RSU can notify CAVs of the existence of VRUs much earlier than a CAV with local sensors will be able to detect them. These results highlight the potential to use CRAV in different safety scenarios and address further possibilities.

5.4 CRAV and RSU relay for VRU detection

CRAV framework will not only rely on communication between the RSU and CAV for information to be fused, but it will also incorporate tracks shared from the CAV to the RSU. The scenario design has been modified to give the RSU a lower road position (55,-15), and the bus/VRU will move out of the detection range at points 65 and 85. CAV 1 (lead CAV) will use its camera sensors to identify the VRU and then share the data with the RSU. Following this, the RSU will add the information to its tracks and forward this to other interested vehicles in the communication range. V2V is a technology that would negate the need for the RSU to share data to CAVs that are following behind the lead CAV; however, if the two CAV road users have different communication equipment integrated, they will not be able to enable communication. This scenario would mean the vehicle would be equipped with either DSRC or C-V2X, With CAV 1 using DSRC and CAV 2 using C-V2X. The RSU is equipped with both and is required for efficient cooperation.

The RSU relay is beneficial for this scenario and can be seen in block form in Figure 5.8. The RSU is equipped with dual communication, and each CAV is assigned a different communication technology. The motivation is to observe the impact of RSU when CAVs are equipped with different communication technology and V2V is not available. The lack of V2V could be due to manufacturer choice, legacy vehicles or a system error.

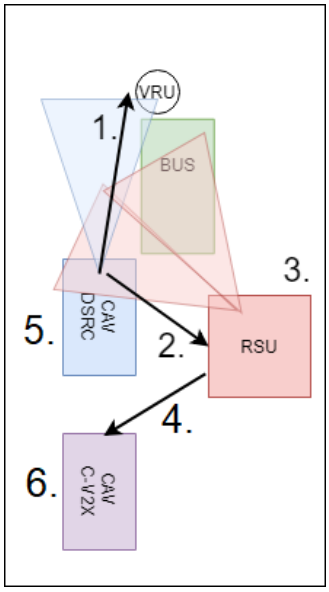

FIGURE 5.8: CRAV V2V block diagram

This CRAV investigation will identify the impact of the RSU towards cooperative shared tracks without direct communication between CAV nodes and will use the RSU as a relay point. This investigation will help determine the response of the RSU, and the benefits will be further explored as to how the use of V2I will assist in reducing collisions with VRUs.

This list shows the step-by-step procedure that takes place between the CAV 1, CAV 2 and the RSU, concerning the data transmission for detected VRUs on the road that have been positioned behind the bus. The arrows are used to dictate the direction of the communication and the numbers can be correlated to the steps seen below;

1. CAV 1 detects a VRU with camera sensors, adds a track to its fusion data
2. CAV 1 shares its fusion data with any interested parties, RSU receives fusion data
3. RSU checks if shared fusion data is new. The data received is not known (new data for RSU), so RSU adds a track to its local data and then adds local data to its fusion data
4. RSU shares its fusion data with interested parties. CAV 1 and CAV 2 receive RSU shared fusion data
5. CAV 1 checks if shared fusion data is new. The data received is already known (not new data for CAV 1), so it is not added to the CAV 1 local tracks

6. CAV 2 checks if shared data is new. The data received is not known (new data for CAV 2), so CAV 2 adds a track to its local data and then adds local data to its fusion data

The data fusion has been modified from previous iterations, and this is due to the RSU needing to incorporate tracks from CAV 1 and maintain the fusion tracks sent to CAV 1 and CAV 2. The tracks are still fused to CAV 1 to ensure that the initial detections for the VRU that the RSU can detect and CAVs cannot detect are still maintained. These steps ensure the tracks are bi-directional and updated from one user; this identifies that the tracks can be shared across the road network to non-directly connected recipients.

5.4.1 VRU detection results with CRAV and RSU relay

The results for this scenario have been conducted in the same method as the previous scenario. The most noticeable results will be those at VRU positions of 65 and 85 when the VRU is blocked from RSU camera vision. The plots have been kept to the distance remaining after braking for this set of results. A final point to note, is that to stop the sensing of CAV 2 before the VRU has added and transmitted the tracks, the gap between CAV 1 and CAV 2 has been slightly increased.

Figures 5.9 and 5.10 show results for 12 m/s, and they identify the successful reception of RSU to CAV messages at points 5-45 with the results the same as previously. However, at points 65 and 85, the trendline reaches the same level as the local sensors for CAV 1. This figure identifies that the RSU is unaware of the VRU, and CAV 1 cannot be alerted to the VRU presence. On the other hand, CAV 2 show that the received tracks from CAV 1 via the RSU are relayed, accepted and added to the fusion track. This finding is seen in the result where the RSU sensors for CAV 2 are higher than CAV 1, showing that CAV 2 is aware of the VRU without using its sensors. However, this resultant distance is proportionate to the distance between the CAVs. This result would mean that for CAV 2 not to cause a collision if CAV 1 brakes, the safety distance would need to be adequately calculated.

Regarding the remaining distance after reacting and braking, the local sensors are the same as before, where collisions are highly likely, the same for CAV 1 when the RSU does not relay information. For CAV 2, however, the distance between the CAVs is enough in this scenario and speed. A collision could be mitigated for both human and autonomous reactions, as shown with the positive value in both cases. It can be concluded that with the RSU and autonomous vehicles relaying, potential collision chains could be avoided for CAV 2 in both human and autonomous situations. Whereas for CAV 1, the local sensors and humans would still have collisions without using the RSU.

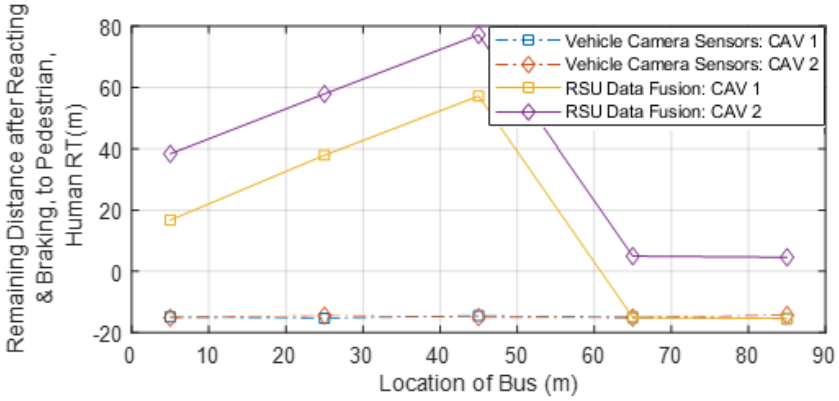

FIGURE 5.9: CRAV and V2V remaining distance, 12 m/s and human reaction time

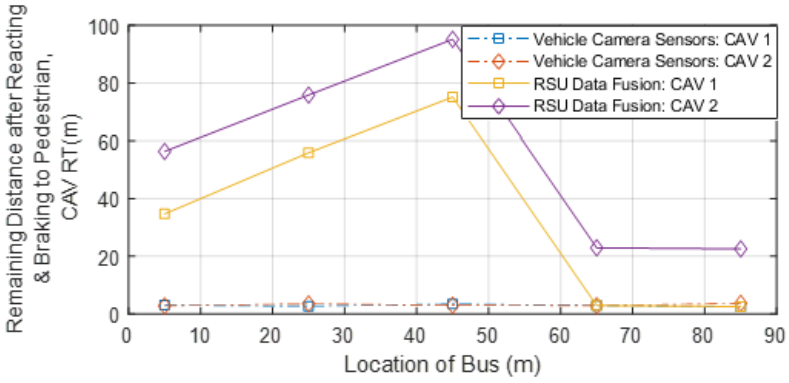

FIGURE 5.10: CRAV and V2V remaining distance, 12 m/s and CAV reaction time

This can be compared to 18 m/s in Figure 5.11 and Figure 5.12, where the remaining distance after reacting and braking is represented. These figures show that the increase in speed from 12 to 18 m/s leads to the human reaction times becoming likely to cause collisions by decreasing below 0. CAV 2 manages to have an approximate 10-metre distance safe space on the autonomous side, and CAV 1 and sensors again fall below 0. This result highlights the importance of a fully connected CRAV system and the importance of CRAV for chain accident mitigation.

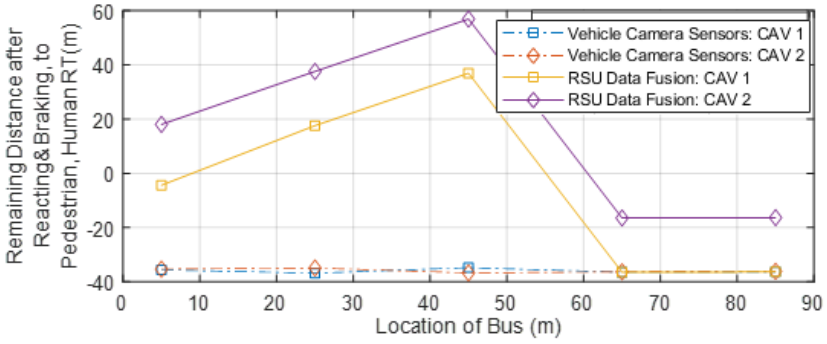

FIGURE 5.11: CRAV and V2V remaining distance, 18 m/s and human reaction time

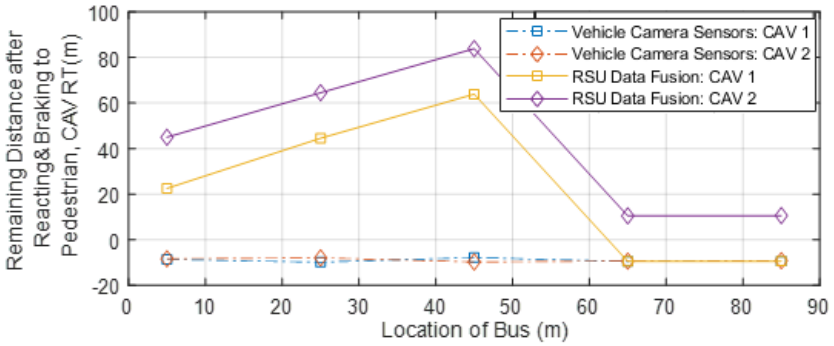

FIGURE 5.12: CRAV and V2V remaining distance, 18 m/s and CAV reaction time

5.5 CRAV connected RSU with mobile VRU

Previously the VRU has been specified as a static pedestrian behind a parked bus with the potential to attempt a crossing manoeuvre. It has been discovered that a collision is likely for high speeds if that occurs. The motivation in this scenario is to observe the potential collisions when the VRU is a moving pedestrian or bicycle, and they move from behind the bus to cross the roadway. This investigation will assess how sensors and fused RSU VRU detection data will assist in reducing potential collisions. As the previous results show, CAV 1 is specified to be moving longitudinally at a set speed and cannot detect the VRU behind the bus until it is much closer than with the assistance of the RSU. The VRU will be given a specified speed and will be moving latitudinally and the speeds of the VRU have been split into pedestrians or bicycles individually with a min, max and mean value. These have been extracted from previous works by Twisk et al. [280] and Forde et al. [281]. The values for the VRU velocities are seen in Table 5.3.

TABLE 5.3: VRU velocities

	Time m/s		
VRU Type	Min	Mean	Max
Pedestrian	0.67	1.45	3.35
Bicycle	4.12	4.94	5.76

The velocities for the VRU are used in conjunction with velocities for CAV and the detection distance to predict whether the vehicle will collide upon detecting the VRU. This method can also detect the difference in arrival time from the vehicle's perspective. This point will be known as the initial potential collision point and is the measurement of when the VRU and CAV will reach a point where they would collide, in this case as a head-on collision. The first point for this collision will be 0 when both independently reach the same location. The potential also exists as a speed difference whereby the VRU will cross the road before the CAV arrives; this will also be classed as a non-collision scenario. Figure 5.13 shows an example of the CRAV scenario along with the components used.

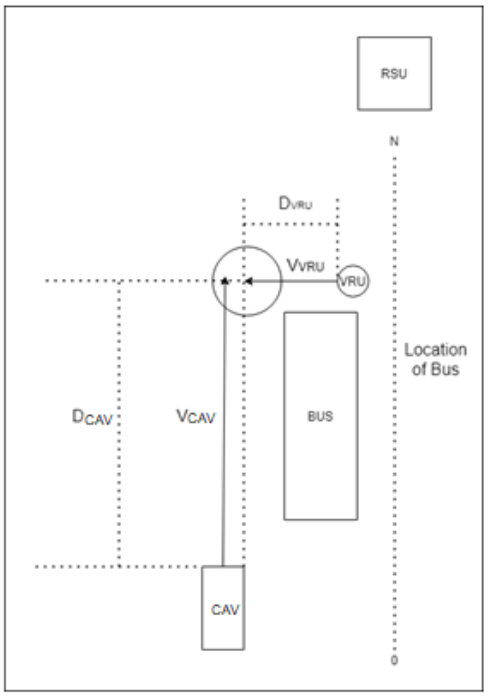

FIGURE 5.13: Diagram of mobile VRU scenario

The equation for calculating the prediction of collision time is taken from the combination of distances, velocities and times of the involved parties. This equation shown in Equation 5.1 represents the time of the predicted collision (T_{CP}) and

Figure 5.13 show the collision is judged at first contact between the vehicle (CAV) and VRU. If the VRU arrives ahead of the vehicle, the equation for the VRU crossing first must be used in addition. This extra equation is represented with (T_{CP2}) and Equation 5.2. If T_{CP} is less than zero this will indicate the VRU will attempt to cross the road before the CAV has arrived, this indicates a potential collision and thus Equation 5.2 will be used to calculate if the VRU will cross the distance needed before CAV will arrive or if it will be another collision situation.

$$T_{CP} = \frac{D_{CAV}}{V_{CAV}} - \frac{D_{VRU}}{V_{VRU}} = T_{CAV} - T_{VRU} \tag{5.1}$$

$$if, \begin{cases} T_{CP} > 0, & \text{VRU arrives first} \\ T_{CP} = 0, & \text{CAV and VRU arrive equal} \\ T_{CP} < 0, & \text{CAV arrives first} \end{cases}$$

$$if\ T_{CP} > 0, \text{ then }, T_{CP2} = \frac{D_S}{V_{VRU}} \tag{5.2}$$

Where, T_{CP} represents the time of the predicted collision, T_{CP2} represents the time to collision if VRU arrives first, D_{CAV} and D_{VRU} represent the distance needed to be travelled to reach the collision point for CAV and VRU respectively, V_{CAV} and V_{VRU} represent the velocity of the CAV and VRU respectively, T_{CAV} and T_{VRU} denote the time it will take to reach the collision point for the CAV and VRU respectively and D_s is used to denote the distance the VRU must travel before it has safely crossed the road.

This formula for T_{CP} is a difference of time between each VRU and CAV reaching the initial collision point, which will be the furthest edge of the vehicle closest to the VRU, which can also be calculated with the distance to the collision point and velocity of each respectively. If the VRU is arriving first, the vehicle's width must be considered. This calculation is needed because although the VRU may begin crossing, the CAV will still be travelling, and as such, the VRU could be moving at a slower speed, and collision could still occur. In the results, the negative value will indicate that a vehicle has arrived first and the pedestrian will not attempt to cross. If the value is positive, the VRU has arrived first, and then Equation 5.2 will need to be used. This extra equation is a measurement of the distance required to travel the car's width to safety, represented by D_s and the velocity of the VRU. In this example, the vehicle's width would also need to be assessed to indicate how long the VRU would take to pass the vehicle's width. This scenario uses a standard vehicle width estimation, and the width of the vehicle is set to 1.8 metres plus a safety gap of 0.5 metres, leaving the distance to be traversed by the pedestrian as 2.3 metres. The safety gap is added for the different sizes of potential VRUs.

The velocities shown in the Table 5.3 have been taken and split into a range of twenty values, and these cover a range from min to max as outlined and will be different for each scenario.

The results for this experiment will be split into a figure for each speed being 4.5, 12 and 22 m/s. The five curved lines represent the difference in arrival time between the VRU and CAV, and a black marker has been used to show the mean value. The lowest of the curved lines represents the CAV being equipped with sensors only for all values of the starting VRU location. The red line at value 0 indicates when the VRU and CAV collide and be classified as the initial collision point. The blue line is used as an indicator to show the stopping distance when travelling at the velocity shown for the CAV. The final line is the black curved line showing the T_{CP2} equation, and this represents how long it will take for the VRU to cross the distance previously specified of 2.3 metres.

5.5.1 CAV 1: the probability of collision with pedestrian VRU depending on longitudinal and latitudinal movement

In Figure 5.14, Figure 5.15 and Figure 5.16, the plots are presented for a pedestrian VRU and CAV 1 travelling at three different speeds. The figures are overlaid with various lines plotted to show the collision potential between the VRU and CAV, and the meaning of the figures needs to be explained.

The results of the plots will be explained to give insights into how the results should be understood and what they represent. The curved dotted lines are used as the basis for the results, and the other lines are used to present the different scenarios that can impact the probability of a collision. Initially, anything above the red line is considered a dangerous scenario where the VRU has reached the collision point first and has begun crossing. The black curved line and any values below are scenarios where the vehicle will collide with the VRU, and anything above is considered safe. The values below the blue line and above the red line represent additional unsafe scenarios where the VRU has arrived first and the CAV does not have enough time to come to a stop. In simple terms, the collision area can be considered any points that satisfy the conditions above the red line, below the blue line and below the black line, which are the scenarios where collisions can occur. The value represented as RSU location N, is the location of the RSU on the side of the road and N will be between 5 and 65. The mean value presented is a representation of the average pedestrian speed used which results in a mean T_{VRU}.

Initially, in these results, the velocity of 4.5 m/s is considered and is the slowest speed that has been evaluated. Due to the nature of the slower velocity, the area

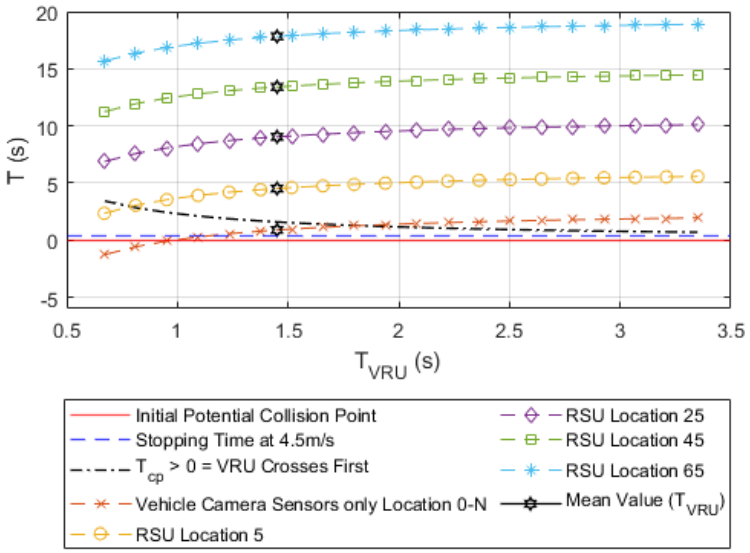

FIGURE 5.14: CRAV and Pedestrian VRU: potential collisions 4.5 m/s

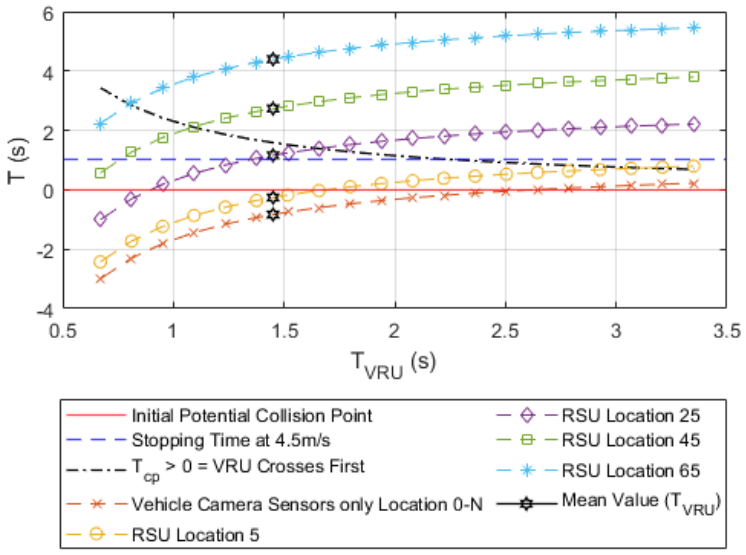

FIGURE 5.15: CRAV and Pedestrian VRU: potential collisions 12 m/s

between the collision point and the braking time is minimal, so the scope for collisions in this area is low. The time for the VRU to cross the T_{CP2} measurement is also unneeded, as this scenario where the pedestrian arrives first does not occur in an

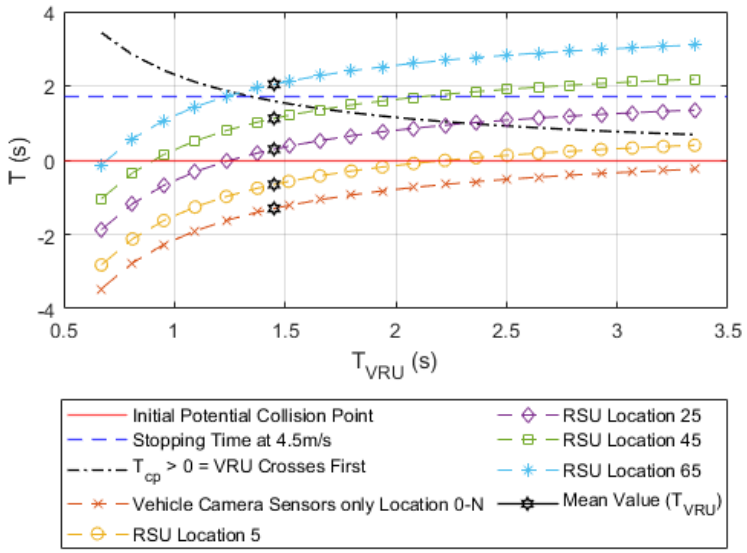

FIGURE 5.16: CRAV and Pedestrian VRU: potential collisions 22 m/s

unsafe area. The only profile that causes collisions in this velocity is the collisions between slow-moving pedestrians and the CAV when relying on sensors, and even in this case, the mean VRU speed is deemed safe. All RSU supported CAVs have no collision probability at any location.

In the results for 12 and 22 m/s, shown in Figure 5.15 and Figure 5.16 respectively, the collisions increase as the distance needed to stop increases. In the 12 m/s results, most collisions occur in the sensor, location 5 and location 10 areas. These collisions occur at different VRU speeds at each location, with sensors and location 5 occurring at higher VRU speeds and location 10 at slower VRU speeds. However, the mid-range and mean values are deemed safe. The VRU crossing first also occurs at 12 m/s, with some collisions avoided.

The highest collision probability can be seen in Figure 5.16 for 22 m/s, with collisions occurring at all locations with RSU assistance. Contrary to previous velocities, there are no collisions when sensors are used. Again, this is due to the increased stopping distance required and the higher velocity. In this case, the VRU crossing first again does omit some collisions but only when the VRU is travelling at higher speeds. In the case of locations 25 and 45, the mean value is also considered a collision point. This result highlights the level of reduced safety for this speed of CAV.

A probability can be plotted for the different speeds by taking these results and extracting the number of collisions. The results from Figure 5.14, Figure 5.15 and

Figure 5.16 can be used and the number of predicted collisions can be extracted and used to plot a probability in percentage. This result is seen in Figure 5.17 and is represented with number values on the x-axis, with one representing sensors and the others representing each RSU location, respectively. This plot is useful to show that the number of collisions at lower speeds is much lower than at higher speeds. However, an interesting result shows that at a higher speed of 22 m/s, the closer RSU locations lead to fewer collisions than 12 m/s. However, at the longer distance RSU locations, the collisions are much higher than 12 m/s. This result gives a beneficial insight that providing the CRAV system is in place, autonomous driving is in effect, and the VRU has been indicated to the CAV, many collisions can be avoided. At the minimum, this would allow the CAV to reduce speed before collisions, and according to studies [282], [283], [284], lower velocity collisions cause a reduction in collision fatalities.

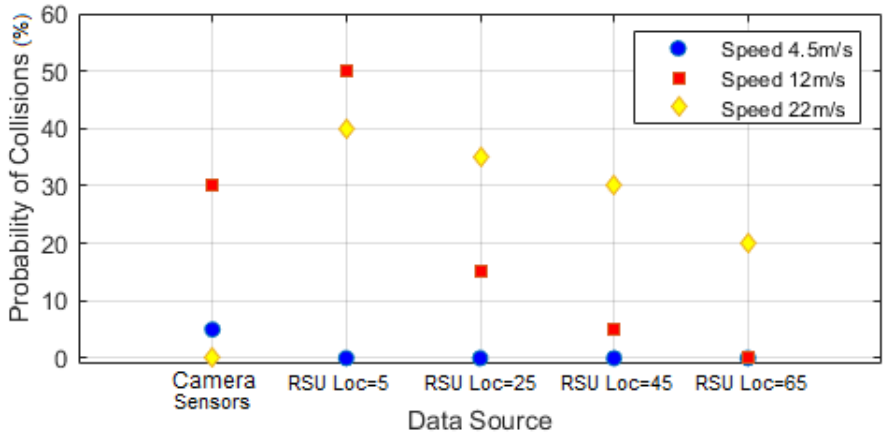

FIGURE 5.17: CRAV and Pedestrian VRU: collision probability CAV 1

5.5.2 CAV 2: the probability of collision with pedestrian VRU depending on longitudinal and latitudinal movement

An assessment of the performance of CAV 2 has not been evaluated. In Figure 5.18 the collision performance for CAV 2 following CAV 1 is shown. Velocity is set to 12 m/s with the same VRU speed range, and the calculations are performed in the same method. However, the difference is that the readings from the RSU will be slightly different due to the distance gap between the CAVs.

In the case of CAV 2, the overall number of collisions is not significantly different as with CAV 1; however, there is a slight reduction. The significant difference is that

the mean VRU velocity at location 5 is now classed as a collision point, so although collisions are reduced, the average velocity now poses a danger.

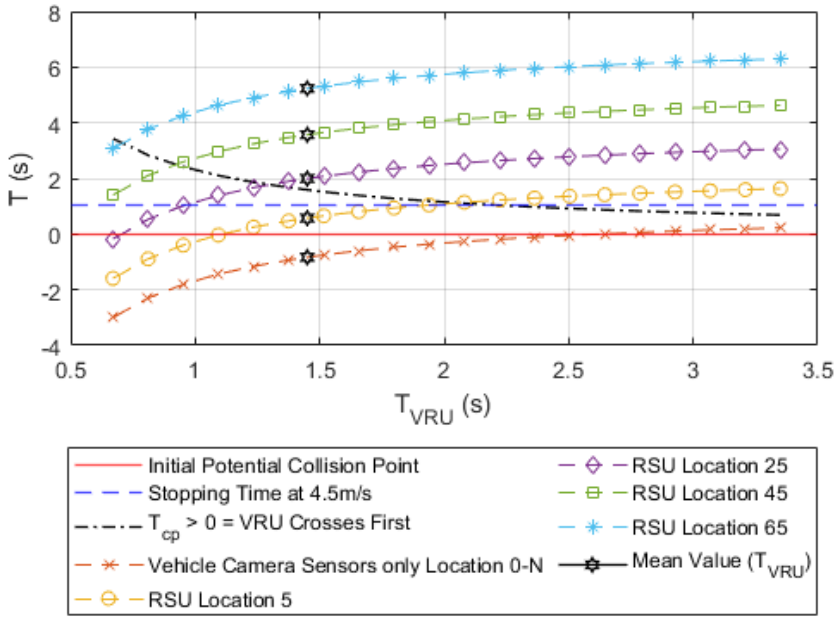

FIGURE 5.18: CAV 2 and Pedestrian VRU: potential collisions 12 m/s

CAV 1: the probability of collision with bicyclist VRU depending on longitudinal and latitudinal movement

The final comparison is with the VRU configured as a bicycle instead of a pedestrian. The values have been altered, and the parameters for the T_{CP} and T_{CP2} formula are altered to match bicycle studies. The range has also been selected from min to max through a range of 20 values.

Figure 5.19 shows the results of the bicycle evaluation when 12 m/s velocities are used for the CAV, and Figure 5.20 shows the collision probability for the same speeds as the pedestrian probability. In the case of bicycles, the results show that the collision probability is vastly reduced in all cases with RSU assistance. However, the shorter warning distance provided by sensors provides a higher collision probability than the pedestrian.

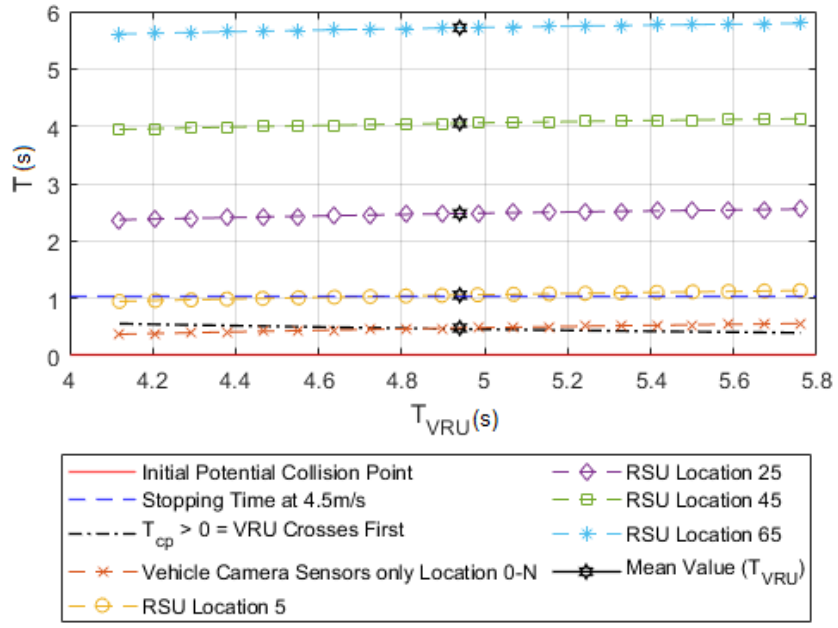

FIGURE 5.19: CRAV and Bicycle VRU: potential collisions 12 m/s

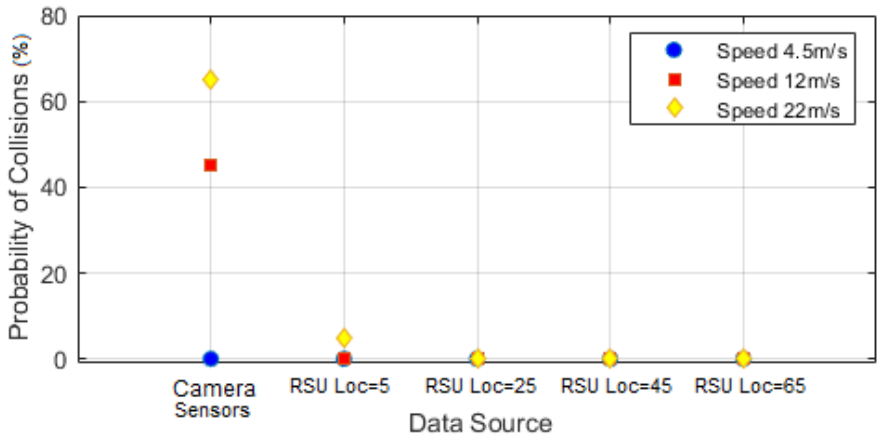

FIGURE 5.20: CRAV and Bicycle VRU: collision probability CAV 1

5.6 Development of AWD and RSS CRAV for collision avoidance

The motivation for this scenario is to compute an adequate distance for CAVs to adhere. As previously mentioned, this distance is referred to as a safety distance.

The reason for an adequate safety distance is that many road collisions are caused by the ineffective spacing between vehicles, which do not allow enough time to react [285], [286] and this is in part due to vehicles not obeying the speed limits [287].

The VRU is positioned on-road as an unavoidable object, such as an immobile pedestrian, a child, or a crashed car. In this case, Figure 5.21 shows the results at 12 m/s for the CRAV system. In the figures the Allowed Response Distance is used to show how far in advance the CAV is aware of the VRU and the location of the bus is shown in the horizontal direction.

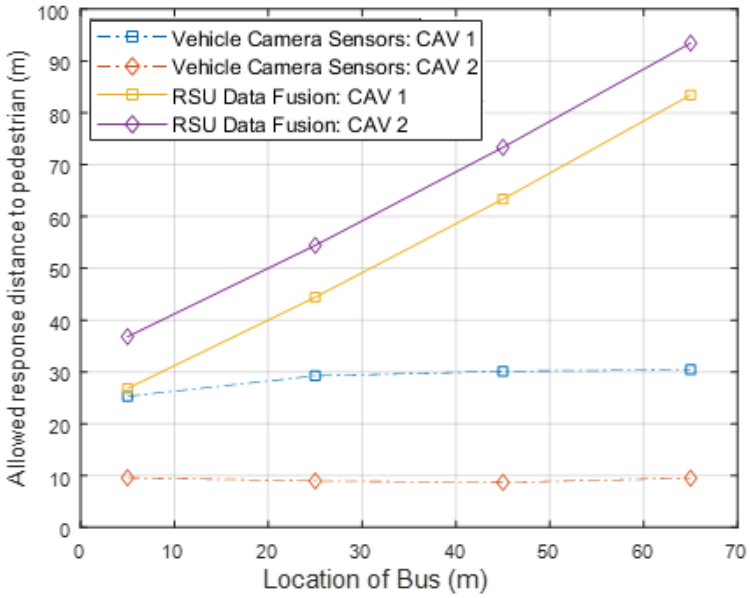

FIGURE 5.21: Obstruction blocking CAV 2 sensors

Figure 5.21 shows the detections for CAV 2. The results from the sensors are severely degraded due to the lead vehicle blocking the line of sight for the camera sensors on the following vehicle. The collisions could be mitigated by using an adequate safety gap between the vehicles instead of an arbitrarily estimated value. A recent mathematical model has been proposed known as the Responsibility-Sensitive Safety (RSS) model, and this model proposes a new way of providing safety for CAVs [288], [289], [290], [291]. RSS is currently being deployed in Intel and Mobileye's test fleet of automated vehicles and has a set of rules associated with it known as the five rules for autonomous safety [292], [293], [294].

The fundamental concept of these rules is to ensure a vehicle can follow implicit rules without using human common sense to verify and avoid causing collisions causing damage or injury to other parties. This framework is essentially a starting

TABLE 5.4: RSS Dmin formula

Vr	The longitudinal velocity of the rear vehicle
P	Response time
a max, accel	Max acceleration of the rear vehicle
a min, brake	Min braking of the lead vehicle
a max, brake	Max braking of the rear vehicle
Vf	The longitudinal velocity of the lead vehicle
where Vf can be considered 0 if lead vehicle/object stationary	

point for autonomous vehicle safety and defines an initial assessment and verification process for CAVs.

1. Do not collide with the vehicle in front (longitudinal distance)
2. Do not cut in without due care (lateral distance)
3. Right of way is given, not taken
4. Be cautious in areas with limited visibility
5. If a vehicle can avoid a collision without causing more collisions, it must do so

5.6.1 Algorithm development with RSS for collision avoidance

The rule of interest for safety distance is rule 1; Do not collide with the vehicle in front (longitudinal distance). For humans, this rule is usually given as an arbitrary measurement either in time or distance that is often different depending on the individual's advice. This advice usually means "leave a 2-3 second gap" or "leave enough space for two vehicles". However, this can cause issues as higher speeds mean larger gaps should be given to give enough time for a driver to react and stop. The RSS model proposes a mathematical algorithm to provide a minimum distance between two vehicles [206], [295]. If the rule is not met, the CAV will appropriately respond to reach the minimum value known as d_{min}. The equation for RSS can be seen in Equation 5.3 and each parameter in Table 5.4 [289].

$$d_{min} = [v_r p + \frac{1}{2} a_{max,accel} p^2 + \frac{(v_r + p a_{max,accel})^2}{a_{min,brake}} - \frac{v_f^2}{a_{max,brake}}] \tag{5.3}$$

The RSS model can be compared with the previous study of safety distance in [296] and Chapter 4. This result can be achieved for both a human reaction time and the SDR-based DSRC resultant reaction time. In this case, the formulas can be seen in Equation 5.4 and Equation 5.5. In this circumstance, for a non-moving obstacle for the lead vehicle, the obstacle can be considered to have a velocity of 0 as it is completely stationary.

TABLE 5.5: Stopping distance comparison

Speed (m/s)	SDR-based DSRC	RSS	Human	RSS+Human
4.5	2.613972221	4.895648	9.350947522	18.14128087
12	13.53035935	25.78248	31.49562682	54.39846065
18	28.16718035	54.1232	55.11516035	95.03545089
22	40.84064423	78.76083	73.77696793	127.8706031
26	55.84627703	107.9935	94.77113703	165.3008156
31	77.88332178	150.9962	124.2937318	218.5503848

$$D_{s,h} = a * T_{\mathrm{R}} \tag{5.4}$$

$$D_{s,a} = a * (T_{\mathrm{R}} + T_{\mathrm{RP}}) \tag{5.5}$$

Each of the attributes in this model has been taken as a value from previous work related to stopping distance and safety distance from earlier Chapter 4 to keep the results consistent. In some cases, further studies have been used for reference. The acceleration has been taken from an RSS study for different vehicles [297], [298]. The deceleration is taken from a study by Naumann et al. [299] on lane changes. Further information relating to the model is taken from [300].

The different safety distances can be compared directly, and with a lead vehicle velocity of 0, the equation results will show the stopping distance for the different models. This result will be compared for a range of speeds from 4.5 to 31 m/s, and the result is shown in Figure 5.22 and table format in Table 5.5.

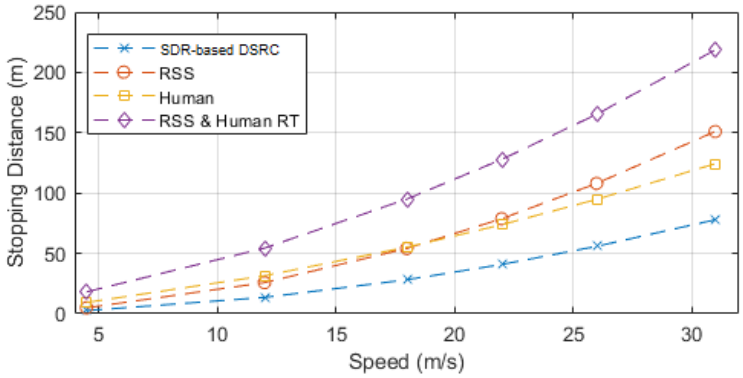

FIGURE 5.22: Stopping distance comparison of different models

Figure 5.22 shows the SDR-based DSRC has a slightly lower stopping distance than RSS, and human-based has an initially higher value than RSS. However, as the speed increases, the sharp gradient of RSS causes the value to go higher than the human-based reaction. The figure also shows that the RSS model has a much

sharper gradient as speed increases and that the Human with RSS has a higher value overall.

From this information, the 12 m/s data can be used in conjunction with the data for CAV 1 (Lead CAV) to show if a collision will occur. In this case, sensor detection data and the data for RSU alerts are extracted. As mentioned, this could be a crashed vehicle, or an obstruction caused by a pedestrian or other VRU. In this scenario, the lead vehicle is ahead of the following vehicle by 10 meters. The obstacle is positioned directly in the path of the approaching vehicles. Velocity is set to 12 m/s. The RSU and sensors are programmed to alert the vehicles of a detected obstacle. The 10-metre spacing is chosen as it is approximately the length specified for safe distances between vehicles travelling at 12 m/s or 26 mph.

5.6.2 Development of AWD algorithm

In addition to these parameters, an allocation must be made for the location of the sensors within the vehicle. A diagram representation of this can be seen in Figure 5.23 showing how the AWD is computed. Where, SL represents sensor location (camera), VL represents vehicle location (DSRC antenna) and LLV represents the length of lead vehicle.

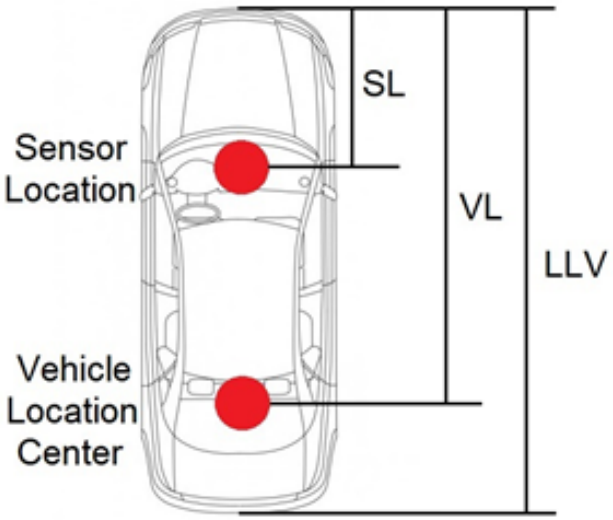

FIGURE 5.23: Diagram showing AWD

The flow chart for this can be seen in Figure 5.24. The equation for this more accurate warning distance can be seen in Equation 5.6 and is referred to as the Actual Warning Distance (AWD). In previous studies [202] and [191], the position of the CAV is assigned a value without a location reference. With safety concerns, this

measurement must be as accurate as possible hence this algorithm is designed to give an as close estimation to the location and distance measurements as possible. In this equation WD represents warning distance (from the data shared/camera data).

$$AWD = WD - (SL + VL + LLV + DBS) \tag{5.6}$$

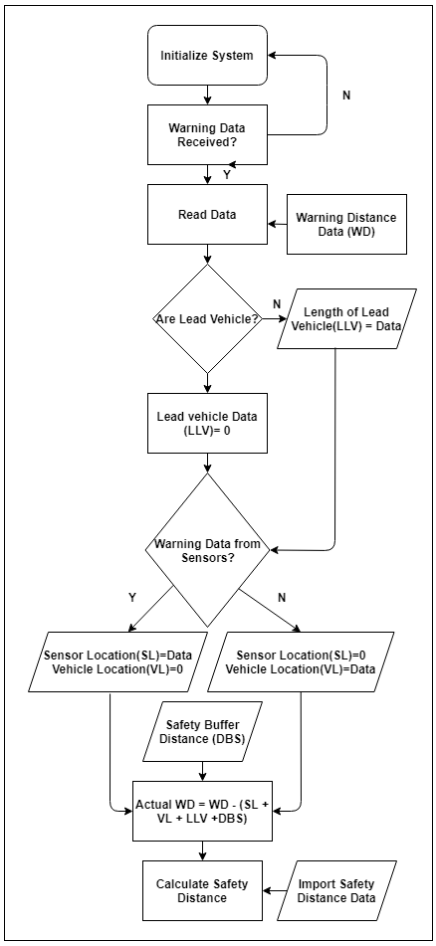

FIGURE 5.24: Flowchart for AWD decisions

In this experiment, VL, SL, DBS, and LLV represent individual distance measurements and vary depending on the circumstances to be evaluated. In this case, values are chosen to represent standard vehicles, and the locations of sensors and vehicle waypoint have been used as with previous scenarios, with LLV = 4.7m, VL=3.7m, SL=1.9m and DBS=0.5m. DBS, the distance for buffer safety, is used to give a gap for safety to ensure that a vehicle will be at a full stop before touching the obstacle/VRU, which is similar to an earlier experiment produced. Depending

on the data source used SL or VL will be equal to zero respectively and LLV will be zero if the vehicle is the lead vehicle.

Figure 5.25 is used to show a diagram for camera sensor-based AWD, and Figure 5.26 is a diagram for CAV based AWD. The diagrams show how the measurements and results are gathered for both CAV 1 and 2.

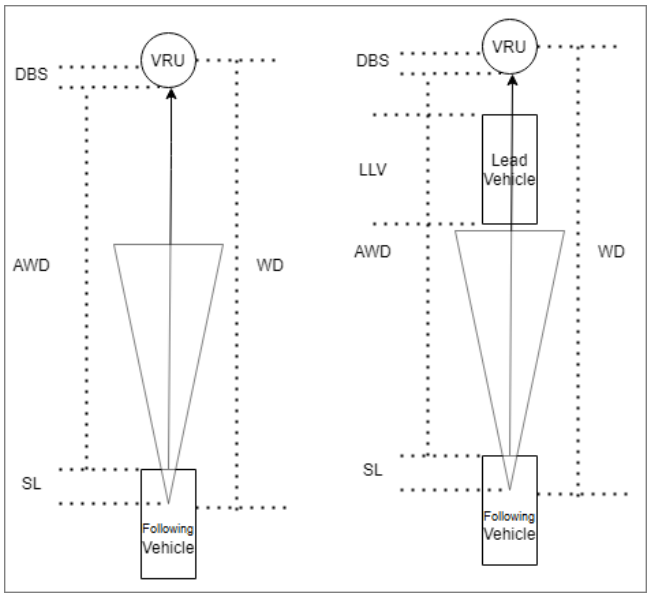

FIGURE 5.25: Diagram showing sensor based AWD

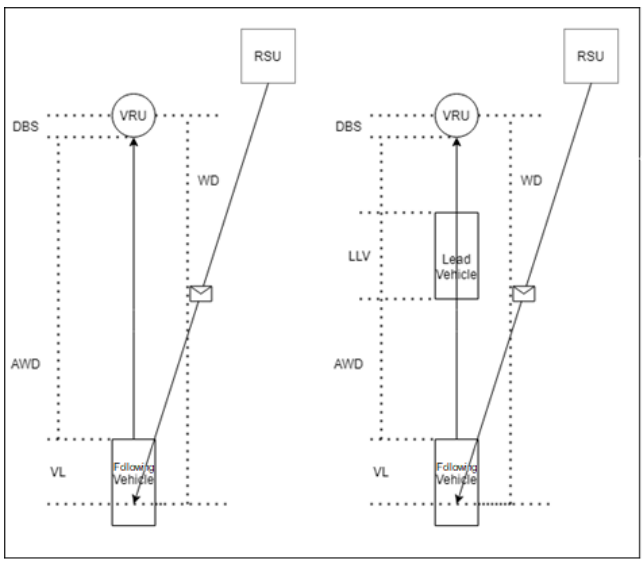

FIGURE 5.26: Diagram showing RSU based AWD

5.6.3 Collision avoidance results with CRAV and AWD

A more accurate representation of the remaining distance can be calculated using the AWD and stopping distance equations. Following the flowchart, values can be input for the lead or following vehicle, which will equate to a distance depending on the usage with the chosen stopping distance calculation.

The following figures show the comparison between the RSS, human and SDR-based DSRC models for CAV 1 in Figure 5.27 and CAV 2 in Figure 5.28 respectively. The plots show the stopping distance with AWD and RSS equation applied to the readings taken from MATLAB and are performed at 12 m/s. The equation used to find this result is shown in Equation 5.7, where DR represents the distance remaining, and the stopping distance SD will be dependent on 3 cases, where RSS stopping distance is represented with d_{min}, stopping distance from a human reaction time is shown with $D_{s,h}$ and a CAV/ADAS reaction time stopping distance is denoted with $D_{s,a}$. There are three cases specified in the equation for the value of SD, and these cases specified for SD will be represented by one of the values and can be changed to whichever is needed to represent the value of SD required. d_{min} for RSS based stopping distance, $D_{s,h}$ for human reaction based stopping distance and $D_{s,a}$ for autonomous reaction based stopping distance.

$$DR = AWD - SD = (WD - (SL + VL + LLV + DBS)) - SD \begin{cases} d_{min} \\ D_{s,h} \\ D_{s,a} \end{cases} \tag{5.7}$$

The results highlight important factors concerning various areas. In CAV 1, the only collisions observed following the RSS model and the AWD algorithm are vehicle sensors and one instance using the RSU relay at the earliest obstacle location. The collision at the earliest location is due to a much shorter warning time and, when coupled with the human reaction time, leads to a collision. It can also be seen that the sensor-based detections at the 5 locations in Figure 5.27 perform slightly better than the RSU relay. This finding is due to the developed AWD algorithm in Equation 5.7 more accurately measuring the location distance. It can be attributed to the sensor location being positioned closer to the front of the vehicle. In contrast, the fusion method uses a point of the car at the rear axle.

The second important in Figure 5.28 analysis is that CAV 2, the following vehicle, has a significantly higher number of collisions when using sensors only. This result is expected as CAV 1 is blocking the camera vision sensors of CAV 2. The collisions are also higher because the following distance that CAV 2 uses is not a large enough

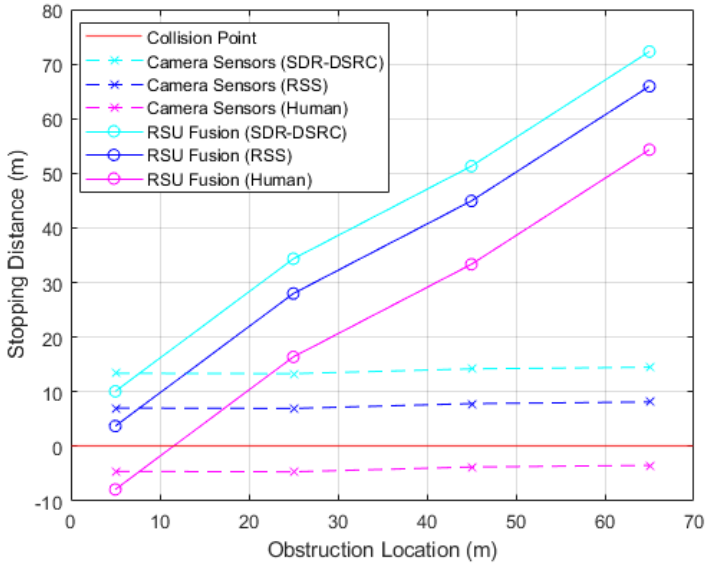

FIGURE 5.27: AWD results for CAV 1 (leading)

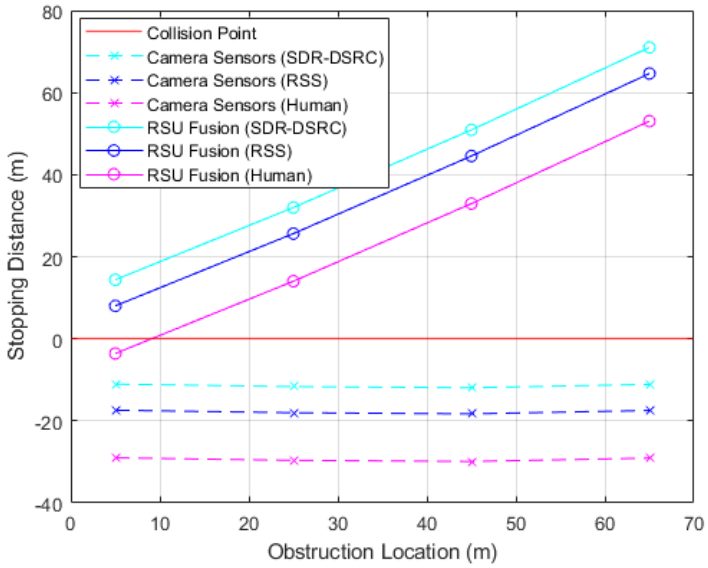

FIGURE 5.28: AWD results for CAV 2 (following)

distance, which doesn't allow CAV 2 to detect after CAV 1 has reacted to the emergency. This result means a collision is highly likely for CAV 2. The other interesting point to note for CAV 2 is that the only error from the RSU is the same as with CAV 1 in that the RSU with a human reaction time leads to a potential collision.

5.6.4 Collision avoidance results with CRAV, RSS and AWD

The result can also be validated by simulating the RSS model incorporated into the CAVs. However, this will be different as safety distance will consider the velocities of each vehicle instead of the non-moving obstacle. In this case, the safety distance for vehicles can be calculated for CAV 2 using the RSS formula, with assumptions made for CAV 1 and the operation of the brakes. In this scenario, AWD from Equation 5.7 is applied for CAV 1 as previously used; however, CAV 2 will now use RSS from Equation 5.3 to produce the safety distance between vehicles using both vehicles velocities. Figure 5.25 and 5.26 can be used to highlight obstruction location in position of the VRU, and the safety distance between Lead CAV 1 and following CAV 2 will be produced with Equation 5.7 and uses a reaction time to match the individual cases.

Using the RSS formula at 12 m/s, safety distance equals 13.12 metres. For example, the values taken for obstruction location at point 5 show that the lead vehicle (CAV 1) detects the obstacle at 22.9184 metres using AWD and sensors. The following vehicle (CAV 2) would only detect at 2.4923 metres using sensors. If CAV 1 applies its brakes immediately, it will take 19 metres to stop leaving a safety margin of 3 metres. CAV 2 would then begin braking after observing CAV 1 brake at a reaction time, and this for a human would be the standard 1.5 seconds. At 12 m/s, CAV 2 would travel 18 metres before braking, and this could cause collisions if the safety distance is too low.

A prime example of an inadequate safety distance would be a two-car length spacing of approximately 9 metres, which would leave a braking distance of (22+4.7+9)-18 =17.7m using Equation 5.7 and 12 m/s, where 22 meters is the warning distance, 4.7 metres is the length of the lead vehicle, 9 meters is the space between vehicles and 18 meters is the distance needed for complete braking. The resultant 17.7 meters is the total distance that would be left for braking, where a vehicle at 12 m/s would need 18 metres. This means an accident would occur between CAV 1 and CAV 2. Suppose the RSS formula is applied to the following vehicle in conjunction with the autonomous features. In that case, the safety distance will instead become 22+4.7+RSS, where RSS is equated with being 14.1 metres; this equates to a distance of 40.7 meters when a human again reacts the remaining distance 40.7 – 18 = 22.7 meters leaving a safe distance from the 18 metres needed to brake to a complete stop. This method does not implicitly adjust the sensor detection range for the obstruction; however, this is slightly increased due to the distance between vehicles. The increase can be seen in Figure 5.28 and shows a reduction for potential collisions with CAV 1.

The results are plotted for each vehicle's incorporated AWD and RSS. This simulation has been completed for various speeds from 4.5 to 31 m/s (10 to 70 mph) and these speeds are used as RSS can be applied in highway scenarios where the maximum UK speed limit is 31 m/s (70 mph). The results for 12 m/s and 22 m/s will be shown in Figure 5.29 and Figure 5.30 respectively. The additional results can be seen in Appendix B. These results show the allowed response distance for both CAV 1 and 2 for all locations previously used 5-65, this time with the incorporation of the RSS. RSS use means the distance between the CAV 1 and 2 will be increased from previous experiments.

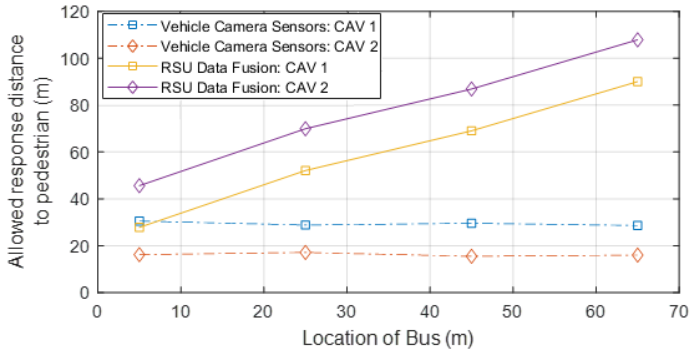

FIGURE 5.29: RSS and AWD results at 12 m/s

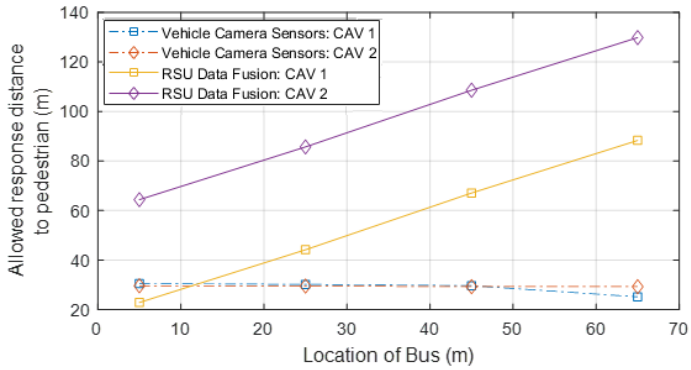

FIGURE 5.30: RSS and AWD results at 22 m/s

In these figures for all speeds, the results do not deviate below the zero-value collision point, and they also highlight the previous finding that the sensors of CAV 2 are blocked by CAV 1 and the value of distance remaining for CAV 2 to collide is still very low. This result emphasises the importance of the increased safety distance and at the same time also highlights the CRAV system benefits. At each speed, the RSU shared information ensures that the CAVs have a higher distance than those

of the sensors, particularly CAV 2, where there is a large distance increase due to the blocked cameras. Without using CRAV, the distances at higher speeds may be potentially dangerous.

An example speed of 12 m/s is used to identify potentially dangerous situations for CAVs to show the remaining safety distance after a driver or an autonomous vehicle is used to react at the detection of the obstacle for CAV 1. The previously shown equations are used for stopping distances for a human reaction and an autonomous reaction. In these figures, the results will show a standard stopping distance with sensors, a standard stopping distance using the RSU and the RSS stopping distance with sensors and the RSS stopping distance with RSU assistance. These figures can be seen in Figure 5.31 and Figure 5.32, for humans and autonomous reaction times respectively.

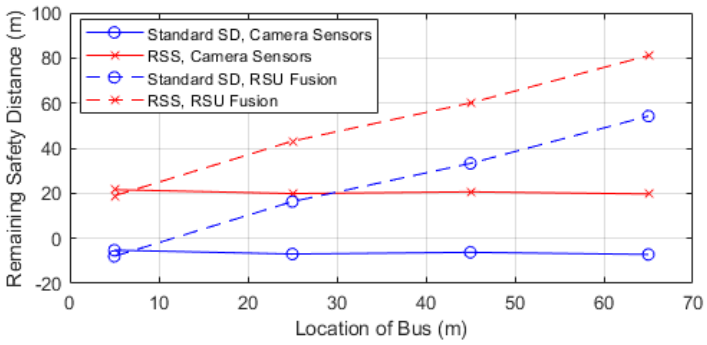

FIGURE 5.31: RSS and AWD results at 12 m/s and human reaction time

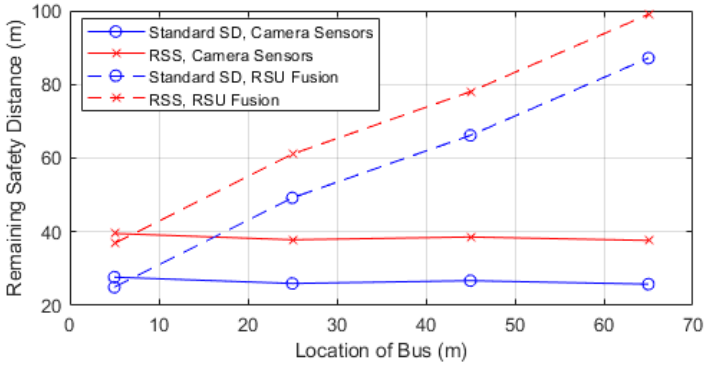

FIGURE 5.32: RSS and AWD results at 12 m/s and CAV reaction time

With the results for the remaining safety distance for a human reaction in Figure 5.31 for CAV 1, this figure shows that the sensors with a standard safety distance

are below the collision point, indicating collisions, and RSU with standard safety distance at the first location is also in the collision point. However, with the RSS safety distance and a human reaction, no values have deemed a collision at 12 m/s. All values in every scenario are not classed as collisions for the autonomous results in Figure 5.32, and the minimum distance is over 20 metres.

5.6.5 Probability of collision with CRAV, RSS and AWD

In this section, the probability of collision is calculated for CRAV, AWD and RSS. The scenarios are repeated at speeds from 4.5 to 31 m/s ten times, with the results collated and averaged out for each speed. The results are then extracted to account for the potential number of circumstances that could be potential collision scenarios. The results were then evaluated into a figure to show the potential number of collisions for CAV 1. The number of collisions was then converted into a probability of collision based on the resulting information, and the probabilities can be seen in Figure 5.33. This figure shows the collision probability between CAV 1 and the obstacle in the road at varying speeds, based upon a human standard reaction time and when equipped with CAV autonomous capabilities. Red shows human Reaction Time (RT), blue shows CAV RT. The probability results show an expected trend

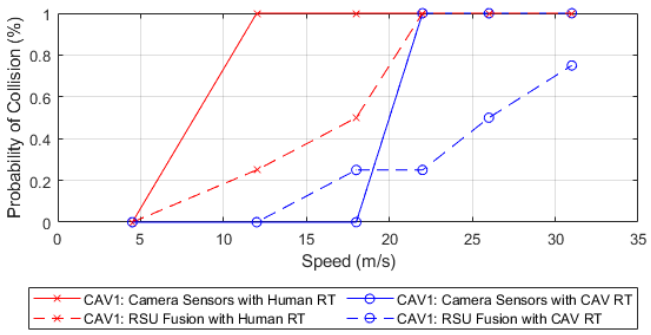

FIGURE 5.33: Probability of collision for CAV 1, with RSS and AWD

that sensor-based communications reach a 100% probability for collisions at relatively early speeds without autonomous capabilities. This result occurs at approximately 18 m/s or 40 mph with autonomous capabilities. This speed is acceptable as 30 mph is the UK speed limit on rural roads, but any road with higher limits will be in dangerous probability. The RSU based communication with human reaction reaches 50% probability at 18 m/s, which is exactly half of the camera sensor-based. It is expected that the RSU will perform better; however, this does reach 100% at speeds higher. The RSU with autonomous capabilities performs the best and, at its

peak speed of 31 m/s or 70 mph, reaches only a 75% probability, and the results show a 0% probability until 13 m/s or 30 mph. In general, the RSU results are better than sensor-based. However, a surprising find is that the sensors with autonomous reactions have a 0% probability at lower speeds, up to 18 m/s, which can be seen in Figure 5.33 and the solid blue line. This compared to the other results show a lower percentage compared to those with RSU fusion.

The previous figures were concerned with CAV 1 colliding with the obstacle in the road without any analysis for collisions of CAV 2 with CAV 1. The same procedure for CAV 1 was then compiled for CAV 2, investigating the probabilities of collisions with CAV 1 after reacting to the obstacle. This result makes use of the RSS and AWD formula in Equation 5.7 and, in addition, the stopping and safety distance equations for both human and autonomous reactions. The results for CAV 2 collision probabilities can be found for sensors and RSU in Figure 5.34, with varying speeds, safety distance type and reaction times.

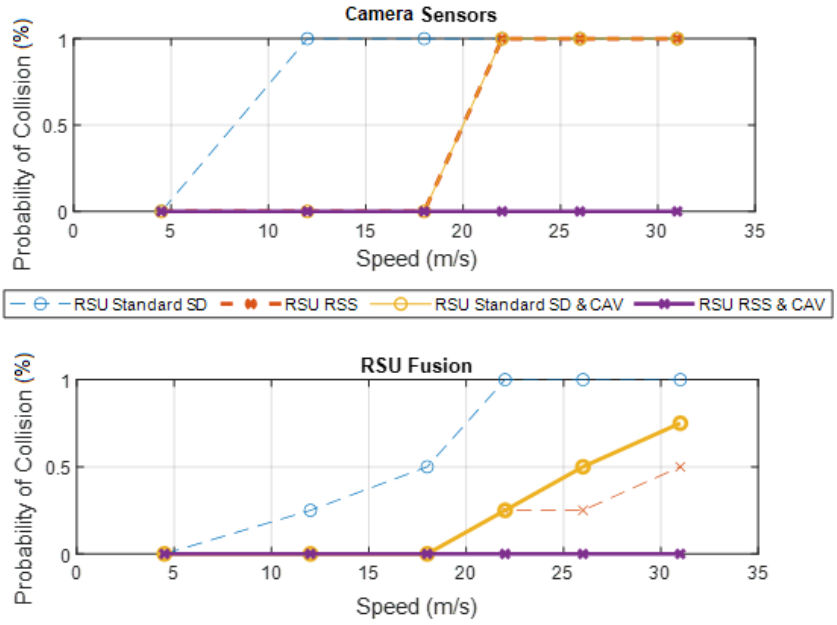

FIGURE 5.34: Probability of collision for CAV 2, with RSS and AWD

These results were then further evaluated for CAV 2, and regression analysis was used to create a collision probability for all speeds from 0 to 65 m/s. The regression was formulated from the previous results and the trendline equations utilised to plot a full range of speed analysis for the difference between the human and autonomous reaction times and is shown in Figure 5.35. The results for CAV 2 are split

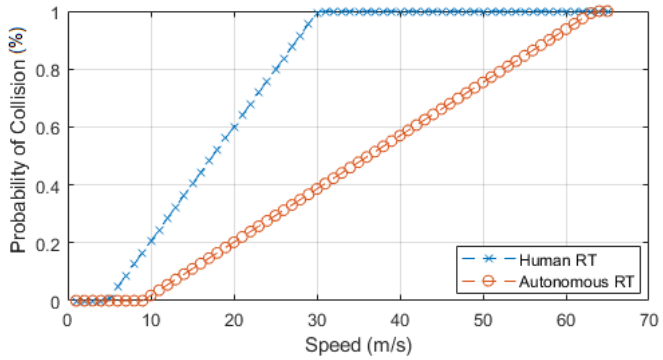

FIGURE 5.35: Regression probability of collision for CAV 2, with RSS and AWD

into two plots in one figure showing information for both sensors and RSU separately. The results are split into four categories in each. They represent the standard safety with and without autonomous assistance and the RSS model safety distance with and without autonomous assistance. In Figure 5.34 for the sensor results, the worst result is, as expected, the sensors without autonomous reaction, which reaches a 100% probability of collision after 13 m/s, which is quite low. Further to this, an interesting result is that the sensors with RSS and the sensors with standard safety distance/autonomous assistance have identical results. This result gives a new insight that the autonomous system and RSS with sensors have an approximate equal impact on the probability. In the result, which is a combination of RSS and CAV, the measurements campaigns show a 0% collision probability. The result is valuable in confirming that using the RSS model with an appropriate autonomous system can increase sensor usability. In previous scenarios the camera sensors proved to have reduced safety compared to RSU fusion and this is due to the inadequate safety distance used. This can be eliminated with the implementation of RSS.

In Figure 5.34 for RSU results, the same set of results was compiled from the relevant results. In this case, the results show that all scenarios are safer when using the CRAV system. With the CRAV RSU relay and a standard stopping distance and a human reaction, the possibility increases with each speed increase linearly with velocity, until 22 m/s, where the probability becomes 100. With the same but autonomous reaction, the results never reach a 100% possibility up to 70 mph; however, they are 0 until 18 m/s, and then they rise linearly with velocity until 75% at 31 m/s. When the standard safety distance is changed to the RSS model and a human reaction is used, the results are lower than with sensors and lower than the human reaction with RSS. In this case, the results only reach a peak of 50% at 31 m/s and are 0% until 18 m/s. Finally, as with sensors results, RSS and autonomous reaction

use lead to a 0% collision probability for all speeds. This result further proves that using RSS and autonomous reaction is key to avoiding accidents. The results show that CRAV relay is safer than the reliance only on local sensor data.

5.6.6 CAV 1: the probability of collision at different velocities

This set of results splits the remaining warning distance for each detection technology and reaction times to compare them directly. The split is for CRAV RSU relay and sensors initially and then split into human and autonomous CAV reactions. Then finally, the last split shows the probabilities for each at three different speeds, being 4.5, 12 and 22 m/s. The results will be shown for both CAV 1 and CAV 2 separately as before. The collision point is considered the point at which the CAV will collide with an obstruction that is positioned at the respective point on the road, which is indicated in the x-axis.

In Figure 5.36 the plot shows the collision point at 0, and all warning distances do not fall below this value indicating that sensors are suitable for this lower speed. It doesn't alter this with the use of CRAV RSU assistance or autonomous reactions. In Figure 5.37, the results are shown for 12 m/s, and in this case, the human reaction

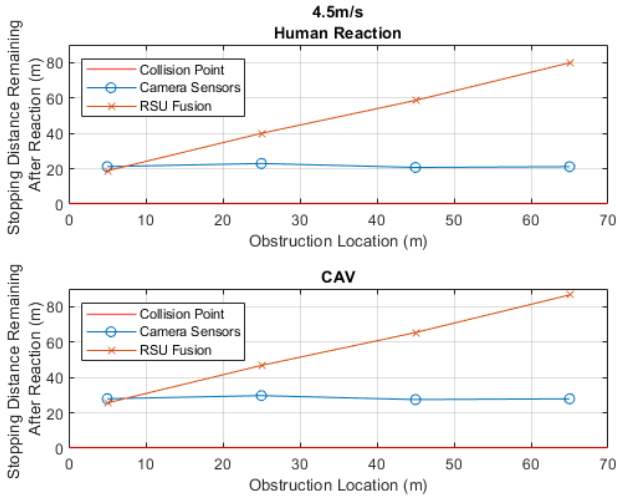

FIGURE 5.36: Probability of collision for CAV 1, with RSS and AWD at 4.5 m/s

with sensors and one instance of RSU relay encounter a collision with human reaction times. Therefore, at 12 m/s, sensors should not be used with human reaction times. And RSU relay with human reaction is slightly safer. However, the safest option is to use an autonomous reaction time with all results yielding no collisions for both sensors and RSU relay.

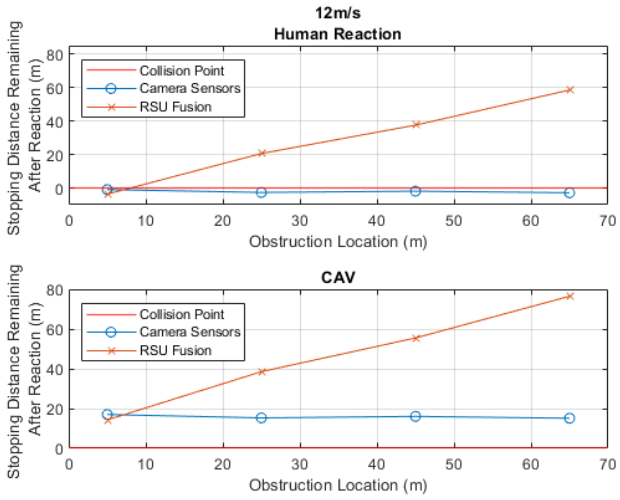

FIGURE 5.37: Probability of collision for CAV 1, with RSS and AWD at 12 m/s

At 22 m/s, the human reaction time results in Figure 5.38 show that all instances except one with the RSU result in a negative collision value indicating a collision are highly likely. In the case of autonomous reaction time, all sensor values yield a collision, and only the longer-range RSU relay offers the higher remaining distance. It can therefore be stated that RSU relay communication is also important at high speeds. Areas like motorways would require an RSU with an increased communication range to use precious data.

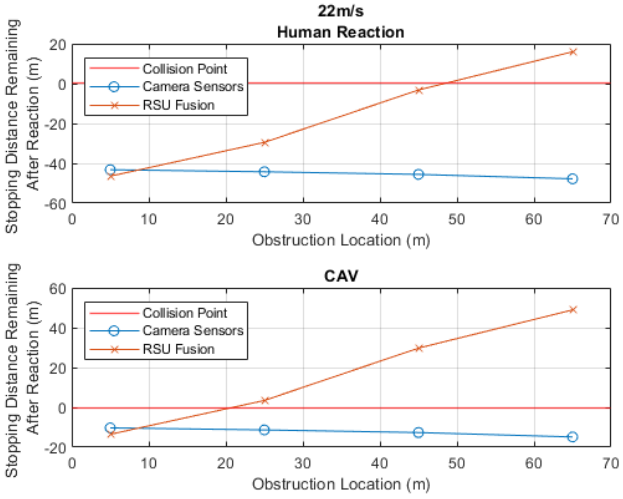

FIGURE 5.38: Probability of collision for CAV 1, with RSS and AWD at 22 m/s

5.6.7 CAV 2: probability of collision at different velocities

In these CAV 2 results, the plots contain more information than CAV 1 as these plots will also show RSS usage. This experiment uses the RSS distance to maintain a safe distance for following behind CAV 1 and the collision point for CAV 2 is deemed when CAV 2 will collide with CAV 1. Similarly, to the CAV 1 results, CAV 2 has no collisions at lower speeds with sensors and RSU. Results in Figure 5.39 again show sensors can be used solely at lower speeds. In the 12 m/s for CAV 2, the results in Figure 5.40 show that sensors with human reaction times cause a negative value; however, sensors with RSS are the opposite with no potential collisions. RSU and RSS also have no potential collisions. On the other hand, there are no negative values associated with the CAV reaction times and hence no potential collisions. The

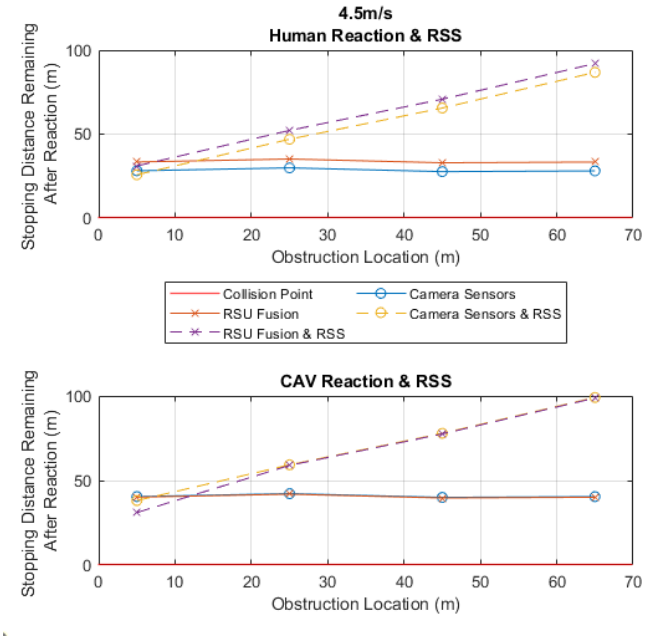

FIGURE 5.39: Probability of collision for CAV 2, with RSS and AWD at 4.5 m/s

results for 22 m/s are shown in Figure 5.41. In the case of human reaction times, the results show that all except the RSU and RSS result in a negative value, and collisions are probable. However, the RSU and RSS have one potential collision at the lowest detection range, emphasising the need for a more extended range for RSU communication. Regarding the CAV reaction, the only set of entirely negative results is sensors without RSS, with one instance of sensors with RSS having a negative collision probable value. Both RSU values with and without RSS result in no probability of collision indicated by the positive values at every location.

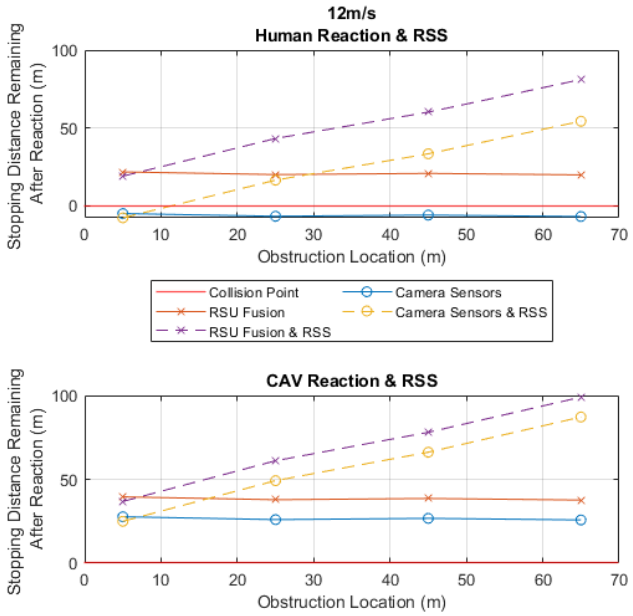

FIGURE 5.40: Probability of collision for CAV 2, with RSS and AWD at 12 m/s

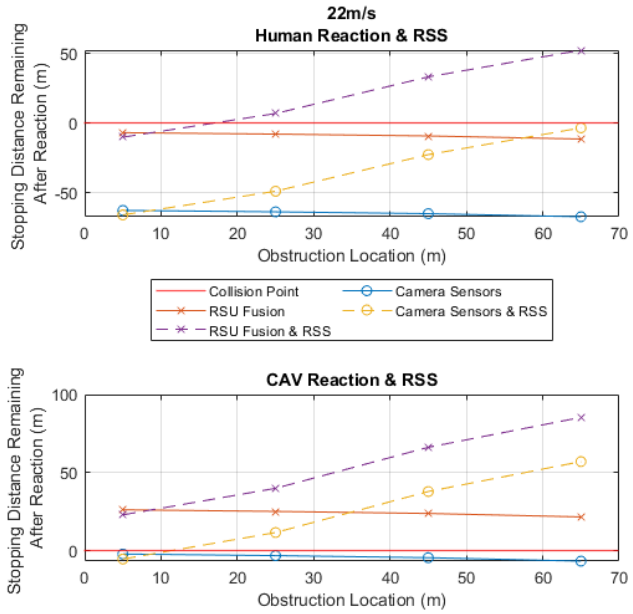

FIGURE 5.41: Probability of collision for CAV 2, with RSS and AWD at 22 m/s

5.6.8 Recommended application of AWD, RSS and reaction technology

With the application of the various techniques, models, technologies and algorithms at multiple speeds and for the difference between lead or following vehicle/CAV, a recommendation can be made for how and what types of these various features should be used in a particular scenario.

From these recommendations in Table 5.6, the key results can be summarised. Speed plays an essential role in the probability of collisions; as the velocity increases, the probability of collisions increases respectively. This increase can be mitigated at lower velocity values using sensor technologies for leading and following vehicles. As the velocity increases, the sensor technology cannot provide enough prior knowledge to avoid collisions if the reaction is completed by a human reaction in the lead vehicle. If this is achieved autonomously by the vehicle itself, sensors can still prevent collisions up to the velocity of around 12 m/s. However, the distance is relatively low, and this distance is vastly increased with the CRAV RSU fusion. As the velocity increases above 12 to 22 m/s, the use of sensors is completely unusable, and the use of CRAV is a lot safer; however, at this high speed, collisions may still occur, though they can be reduced with the use of autonomous reactions. This finding is an issue for the earliest alerts as a vehicle enters the RSU communication range as the warnings can be provided too late. Hence it is recommended to reduce speed in these scenarios.

For the following vehicle at 12 m/s, sensors are again unsuitable if used with human reaction times; however, collisions are avoided with the inclusion of the RSS model. With the use of autonomous reactions, all scenarios can be deemed safe. As the velocity is higher again at 22 m/s, the human reaction time again becomes unsuitable unless the CRAV RSU fusion is used with the addition of RSS. All collisions can be avoided at high speeds if the CAV is used with RSS and autonomous reaction.

To summarise the results, the most significant impact on collisions is speed. Camera sensors eliminate this slightly, but the biggest mitigator is CRAV RSU relays. The CRAV relay data is essential for these situations. Secondly, the use of inadequate safety distances causes many issues for the following vehicle, and if the RSS model is deployed with the CRAV system, safety is almost guaranteed. The final point is that human reactions are very limiting at large velocities, and autonomous reactions are essential as velocity increases.

These results display the increase in safety the CRAV has over traditional camera sensing, especially at higher velocities. The use of the RSS model is also validated to offer advantages to RSS, especially when the vehicles are autonomous.

TABLE 5.6: Recommended application of technologies

Speed (m/s)	Lead Vehicle	Following Vehicle
4.5	Sensors and RSU for Human or CAV acceptable. No RSS.	Sensors and RSU for Human or CAV acceptable. No RSS.
12	Sensors and RSU acceptable with CAV.	Sensors and RSU can be used with Human and RSS; if there is no RSS, the human driver should not be responsible. Sensors and RSU can be used with CAV; No RSS.
22	Sensors not suitable with Human or CAV. RSU can be used providing warnings are sent early speed should be reduced.	Sensors and RSU should not be used with Human Driver. Sensors and RSU can be used with CAV if RSS is used.

5.7 Summary and conclusions

In this chapter, a framework for cooperative CRAV was designed, developed and then evaluated. The CRAV investigation shows the inherent increase in safety possible with CRAV and RSU integration towards cooperative driving and mutual awareness. The research shows the importance of the RSU in the CRAV framework towards alerting road users of other vehicles or VRUs, this is particularly important for autonomous vehicles. The results in all sections show an increase in safety when the CRAV framework is used compared to traditional vision sensing methods. In addition, the scenarios examined emphasise the finding that autonomous CAV vehicles can be alerted to VRUs far in advance with CRAV. The results show a minimum awareness increase approximately 19 metres at minimum and 80 at maximum. Thus, the safety for CAVs and VRUs is vastly increased. This result is beneficial when the VRU is detected out of the direct vision of a CAV.

The findings show that V2I is highly important in safety and can provide many benefits that V2V cannot offer. This finding is particularly evident when the CAVs utilise different types of communication, as this may potentially occur with autonomous vehicles. The RSU can have dual communication and messages are relayed to vehicles based on the information it receives from others. Furthermore, the results show collision probabilities between different VRU types can be minimised using deep learning RSU vision perception. CAVs can avoid collisions at lower speeds with efficient warning system messages from an RSU. This result is also possible with sensors. However, as the speed of the CAV increases, the CRAV offers a lower collision probability than local sensors. The models developed in this section for both VRU arriving initially and VRU and CAV simultaneously provide a further increase in safety, showing a lower number of predicted collisions, with all findings

significantly safer when using autonomous vehicles compared to those operated by a human driver.

A new method of applying the RSS model into CRAV was also investigated to provide accurate safety spacing between CAVs. By assessing RSS and applying the algorithm to the CAVs, it was shown that using an adequately calculated safety distance prevented more collisions between CAVs and VRUs. The RSS approach increased the effectiveness of collision avoidance. Compared with human or autonomous CAV reaction, the stopping distance needed at 31 m/s is much lower, reducing a need of 220 metres to 150 metres.

A further addition is the use of the AWD algorithm, a new method of calculating the CAVs position from the type of technology applied. This algorithm provides accurate distances between vehicles, which assists in evaluating safety and distances between vehicles. The results from AWD and RSS show speeds up to 22 m/s can be made safer with the inclusion of these models. Recommendations are made to show the best technology for different speeds, with the higher speeds requiring more technology than lower speeds. The results highlight that human reaction at higher speeds cannot compete with CRAV with RSU assistance, for detecting and avoiding collisions with VRUs. Finally, when AWD is used for autonomous controlled CAVs, almost all collisions can be avoided at all speeds for CAV 1 with both RSU fusion and cameras. However, CAV 2 is only safe with autonomous operation at higher speeds, and only when RSS and AWD are applied.

Chapter 6

Conclusions and Future Work

6.1 Introduction

In the modern age of vehicular transport, the proposition of autonomous and connected cars is becoming a reality. Current research and development are setting a new precedent for this generation of transportation. The future of vehicles will undoubtedly encompass communication between vehicles and infrastructure to form a heterogeneous vehicular network. With the capability of connectedness, the possibility for a more efficient, more comfortable, and safer driving experience for road users is a reachable goal. The cooperation between vehicular nodes will rely on many technologies that will fuse a vehicle's data and offer cooperative communication to other vehicles to enable collaborative intelligent transport systems. Given the potential that CAVs encompass, industry and academia are investing ample time and funding in research and development. However, many areas still need to be investigated and finalised.

This chapter concludes the thesis with key findings discussed and speculated future research directions. To summarise, the thesis presents an essential work towards reliable vehicular communication with extensive results on SDR-based DSRC and fundamental performance towards V2V. The allocation of safety with V2V is developed, with results concerned the reliability and packet losses modelled. CRAV is designed and shown to increase safety for VRUs and vehicles, with increased safety distances and detections with RSU assistance provided earlier than those with local sensors.

6.2 Summary

In chapter 2, an extensive review detailing the many vital aspects of connected vehicles is presented. The modern automobile is rapidly becoming more connected towards self-driving autonomous vehicles. This connected nature will have many benefits such as safety, efficiency and quality of experience. The literature review in this chapter was conducted to investigate the types of wireless communication currently available for vehicle networks and identify the key technologies and how they perform. Further analysis is required on SDR-based DSRC in field test trials towards safety. Software-defined radios are a capable technology that has been reported to be capable of DSRC standards.

Following the literature review, an SDR-based DSRC platform is developed in chapter 3. The platform utilises open-source software and USRP SDR devices capable of providing DSRC connectivity by developing a modified 802.11p/DSRC compliant transceiver. This chapter is used to develop various experimental procedures and perform investigations into the capability of an inexpensive SDR-based DSRC implementation and investigate performance as a V2V transceiver. Based on results for latency, range, robustness, data rate and SNR, the study demonstrates that this modified SDR-based DSRC meets the requirements of DSRC and can perform to the high standards required of a V2V enabled link. Further to these field tests, experiments are conducted for an on-road field test where it is found that distance is not the most crucial factor to packet loss, and this is instead due to environmental or channel conditions. Finally, the SDR-based DSRC is shown to be capable of relaying video data over an 802.11p link via LoS and NLoS conditions.

V2V will be important for providing adequate collision avoidance in vehicular networks; however, packet delivery reliability could be an issue. Due to the nature of a mobile network, wireless communication conditions are continually changing. These changes can cause different types of losses from environmental conditions, the distance of communication, and vehicle density. In chapter 4, following the creation of the improved SDR-based DSRC transceiver and testing of the capabilities, a further study is conducted into stopping distance assistance capabilities and the cause and effect of different forms of loss in the V2V wireless channel. The SDR-based DSRC is shown to have capabilities that can increase safety through a decreased stopping distance needed and an increase in time for awareness. In addition, the different types of V2V communication losses are modelled, and simulations are performed for distance independent, distance dependant and density-based losses. The losses are evaluated to show impacts on stopping and safety distance. Algorithms are developed to produce a model that shows the impact of losses on collision avoidance via stopping distance. The experiment simulations show that

the most loss is caused by the density of nodes within the vehicle communication range. A model is developed to predict the number of nodes in the communication range which can be used to show expected losses through simulation. The impacts of the number of nodes are investigated. Distance-based losses are shown to be relatively low compared to those of density, highlighting that connectivity over distance is not a significant problem. This chapter demonstrates that the density of vehicles has a higher impact on safety distance than those caused by communication distance.

Connected and autonomous vehicles are valuable and promising technologies for increasing road efficiency and decreasing road accidents. However, currently, these technologies have shortcomings. In chapter 5, a new method of communication is investigated for cooperative sensing amongst CAVs and connected road infrastructure to improve road safety, which will be critical to the success of CAVs. This chapter presents a study of the modern state of the art technologies. It then proposes CRAV, a smart, scalable simulation framework that evaluates the increase in road safety that cooperative, connected smart road infrastructure can provide. The CRAV framework consists of decoupled subsystems for object detection and tracking, V2X communication and CRAV sensors and scenarios. Various use cases are investigated to evaluate the operation of CRAV and compare the impact with and without RSU on the detection of VRU. The use of RSU shows an immediate effect. It demonstrates that CRAV offers far greater recognition of VRUs for CAVs than using local sensors and significantly reduces the potential number of collisions. This finding is of particular importance when VRUs are outside of the visual detection of CAV local sensors.

Furthermore, the CRAV framework shows the benefits for RSU assistance when vehicles are equipped with different communication modes and the RSU is used as a V2V relay point to share information. Secondly, a new CRAV RSS model is developed and applied to show the impacts of rear-end collision avoidance at different speeds. Results show a smaller stopping distance requirement for CRAV reactions than human reactions, and a decrease in collisions with VRUs is evident when using this model. A second algorithm, AWD, is developed to provide an accurate warning distance based on more effective localisation. Applying the two algorithms leads to fewer collisions when CRAV and RSUs are used, showing the essential nature of infrastructure communication towards safety.

6.3 Future work

There exists a broad scope for future research into several areas that have not been covered in this study and warrant additional investigation. The following are some important areas that need additional research:

- An extensive field test utilising the SDR-based DSRC transceiver over long journeys with an exterior mounted antenna. The extra experiment will monitor performance in different road scenarios such as urban or highway environments. Extended field tests will further understand the DSRC channel performance in varied traffic scenarios.
- To design an automatic gain control (AGC) function block in GNURadio for the SDR-based DSRC. The AGC will be developed within the SDR-based DSRC transceiver and developed from received power results. This function will enable the communication system to remain connected without the need for the user to manually change or alter the gain settings within the GNURadio environment. It will allow simpler testing in future for other users.
- This research used a single omnidirectional antenna, and further tests could be modified to include two antenna types for different communication responsibilities. This approach could be extended to make a V2X transceiver comprised of cellular and Wi-Fi-based communication architectures. The antenna proposed is a directional antenna for directive broadcasts.
- Performance of in-depth analysis to investigate the causes of the losses seen in field tests, with a focus on different channel models and environmental conditions. This measurement campaign can include tunnels, rain, snow, fog, or densely built areas. Employing this approach will give further insights into performance under various conditions.
- Design a weighted algorithm for judging safety distance between vehicles. This algorithm can comprise a selection of LiDAR, V2V, GPS, and ultra-wideband (UWB) technologies. This algorithm will provide accurate distances between vehicles to enhance collision avoidance further.
- Further analysis of CRAV, focussing on different scenarios, such as overtaking, lane merging or platooning. This extended set of scenarios will identify further RSE applications and demonstrate the potential for CRAV implementation for additional safety-related scenarios.
- Utilise CRAV to assess the impacts to road network capacity with a varying number of connected users. This approach will allow the research into how

road capacity will perform when CRAV and a more efficient safety distance system is incorporated. Furthermore, this approach will correlate the use of autonomous systems and the increase in efficiency gained.

- Propose platooning integration with SDR-based DSRC, CRAV and RSS-AWD. The approach will include works from all chapters into one system for platooning to analyse how this lower cost and the model-based system can achieve collision avoidance and positioning.

Appendix A

Full GNURadio Transceiver Block

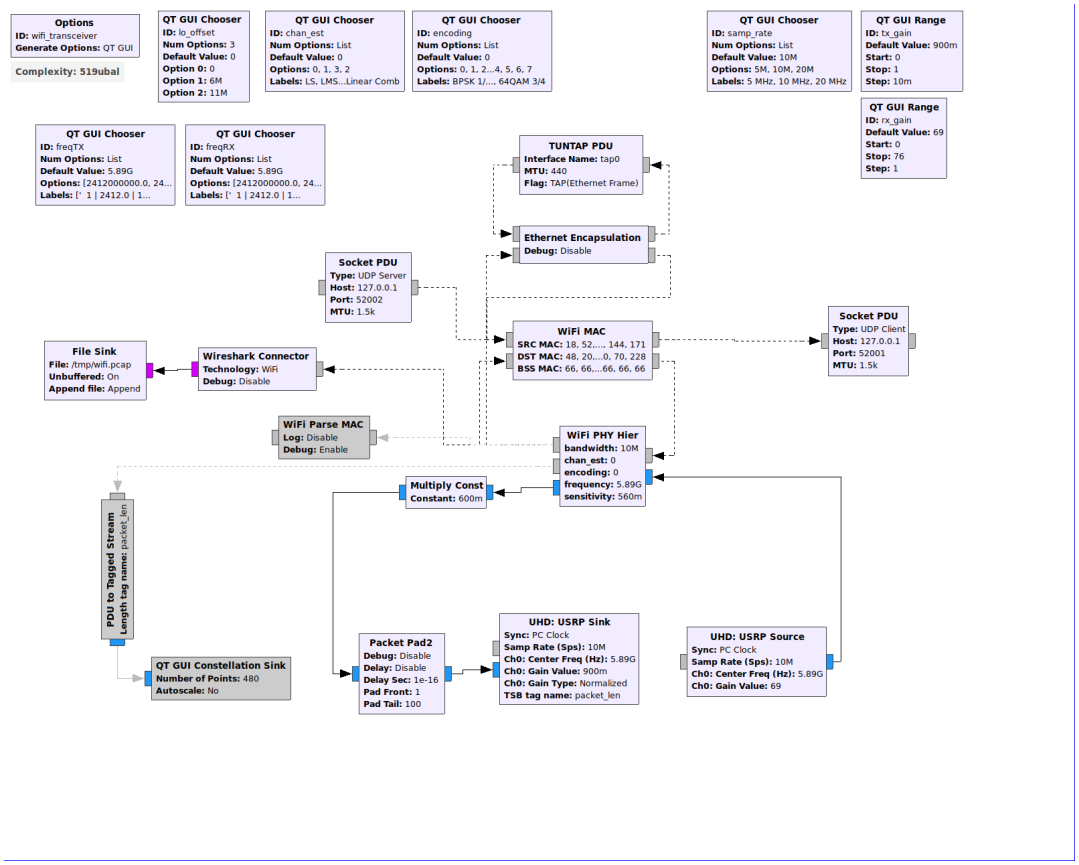

FIGURE A.1: Full GNURadio Transceiver Block

Appendix B

Extended Collision avoidance results with CRAV, RSS and AWD

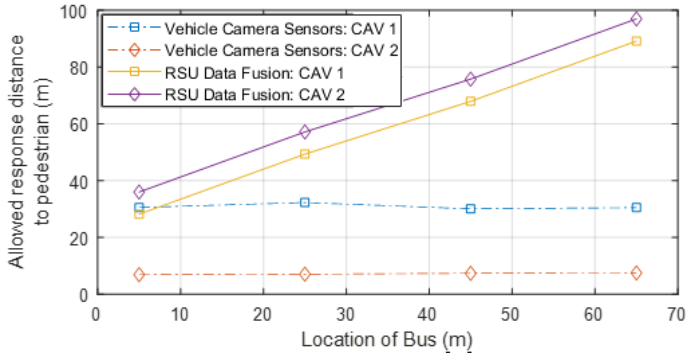

FIGURE B.1: RSS and AWD 4.5m/s results

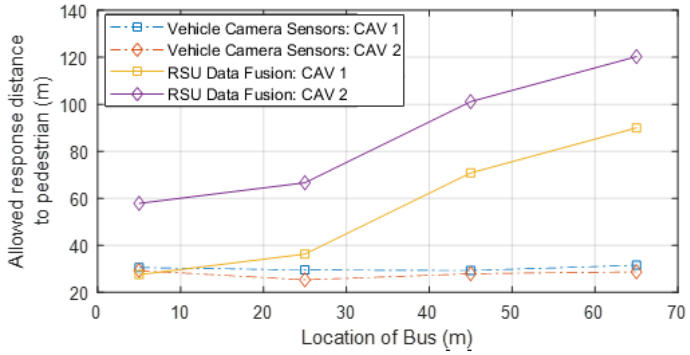

FIGURE B.2: RSS and AWD 18m/s results

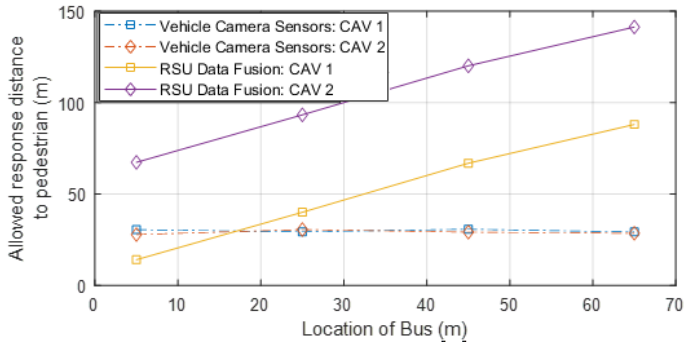

FIGURE B.3: RSS and AWD 26m/s results

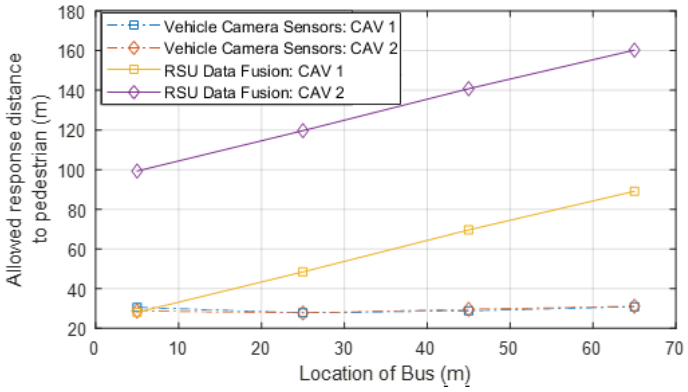

FIGURE B.4: RSS and AWD 31m/s results

Bibliography

[1] WHO, *Global status report on road safety 2015 | WHO | Regional Office for Africa*, 2015. [Online]. Available: https://www.afro.who.int/publications/global-status-report-road-safety-2015 (visited on 11/01/2021).

[2] W.H.O, *Road traffic injuries*, 2021. [Online]. Available: https://www.who.int/news-room/fact-sheets/detail/road-traffic-injuries (visited on 11/01/2021).

[3] ONS, "Reported road casualties in Great Britain: provisional results 2019," no. July, pp. 1–44, 2020. [Online]. Available: https://www.gov.uk/government/.

[4] RAC, *Economy lost £8 billion to traffic jams in 2018 - see the nationwide congestion rankings | RAC Drive*. [Online]. Available: https://www.rac.co.uk/drive/news/motoring-news/nationwide-congestion-rankings/ (visited on 11/01/2021).

[5] Inrix, *INRIX research shows Americans lose 97 hours per year to congestion | Roads & Bridges*. [Online]. Available: https://www.roadsbridges.com/inrix-research-shows-americans-lose-97-hours-year-congestion (visited on 11/01/2021).

[6] *Congestion Costs U.K. Nearly £8 Billion in 2018 - INRIX*. [Online]. Available: http://inrix.com/press-releases/scorecard-2018-uk/ (visited on 11/01/2021).

[7] *Details About the Fatal Tesla Autopilot Crash Released*. [Online]. Available: https://www.businessinsider.com/details-about-the-fatal-tesla-autopilot-accident-released-2017-6?r=US{\&}IR=T (visited on 11/01/2021).

[8] *Uber's self-driving operator charged over fatal crash - BBC News*. [Online]. Available: https://www.bbc.co.uk/news/technology-54175359 (visited on 11/01/2021).

[9] *Waymo's driverless cars were involved in 18 accidents over 20 months | VentureBeat*. [Online]. Available: https://venturebeat.com/2020/10/30/waymos-driverless-cars-were-involved-in-18-accidents-over-20-month/ (visited on 11/01/2021).

[10] *Florida Tesla crash which killed two will be investigated by federal board | Tesla | The Guardian*. [Online]. Available: https://www.theguardian.com/technology/2021/sep/18/florida-tesla-crash-autopilot-fire-national-federal-transportation-board (visited on 11/01/2021).

[11] A. Basaure1 and J. Benseny, "Smart city platform adoption for C-V2X services," *International Telecommunications Society (ITS), Calgary*, vol. 2020-June, 2020.

[12] *About C-ITS*. [Online]. Available: https://www.car-2-car.org/about-c-its/ (visited on 11/01/2021).

[13] A. Festag, "Cooperative intelligent transport systems standards in Europe," *IEEE Communications Magazine*, vol. 52, no. 12, pp. 166–172, 2014, ISSN: 01636804. DOI: 10.1109/MCOM.2014.6979970.

[14] R. Molina-Masegosa and J. Gozalvez, "LTE-V for Sidelink 5G V2X Vehicular Communications: A New 5G Technology for Short-Range Vehicle-to-Everything Communications," *IEEE Vehicular Technology Magazine*, vol. 12, no. 4, pp. 30–39, 2017, ISSN: 15566072. DOI: 10.1109/MVT.2017.2752798.

[15] The 5G Infrastructure Public Private Partnership, "5G Automotive Vision," pp. 1–67, 2015. [Online]. Available: https://5g-ppp.eu/white-papers/.

[16] N. Lu, N. Cheng, N. Zhang, X. Shen, and J. W. Mark, "Connected vehicles: Solutions and challenges," *IEEE Internet of Things Journal*, vol. 1, no. 4, pp. 289–299, 2014, ISSN: 23274662. DOI: 10.1109/JIOT.2014.2327587.

[17] J. B. Kenney, "Dedicated short-range communications (DSRC) standards in the United States," *Proceedings of the IEEE*, vol. 99, no. 7, pp. 1162–1182, 2011, ISSN: 00189219. DOI: 10.1109/JPROC.2011.2132790.

[18] Z. Xu, X. Li, X. Zhao, M. H. Zhang, and Z. Wang, "DSRC versus 4G-LTE for connected vehicle applications: A study on field experiments of vehicular communication performance," *Journal of Advanced Transportation*, vol. 2017, 2017, ISSN: 20423195. DOI: 10.1155/2017/2750452.

[19] S. Chen, J. Hu, Y. Shi, L. Zhao, and W. Li, "A vision of C-V2X: Technologies, field testing and challenges with Chinese development," *arXiv*, vol. 7, no. 5, pp. 3872–3881, 2020.

[20] Q. Technologies, "Leading the world to 5G:Cellular Vehicle-to-Everything (C-V2X) technologies," no. June, pp. 1–39, 2016.

[21] *DSRC Technology | 802.11p standard | ITS-G5 and ETSI ITS-G5, IEEE802.11p | Autotalks*. [Online]. Available: https://www.auto-talks.com/technology/dsrc-technology/ (visited on 08/21/2018).

[22] Y. L. Morgan, "Notes on DSRC & WAVE standards suite: Its architecture, design, and characteristics," *IEEE Communications Surveys and Tutorials*, vol. 12, no. 4, pp. 504–518, 2010, ISSN: 1553877X. DOI: 10.1109/SURV.2010.033010.00024.

[23] K. Abboud, H. A. Omar, and W. Zhuang, "Interworking of DSRC and Cellular Network Technologies for V2X Communications: A Survey," *IEEE Transactions on Vehicular Technology*, vol. 65, no. 12, pp. 9457–9470, 2016, ISSN: 00189545. DOI: 10.1109/TVT.2016.2591558.

[24] V. Manwar, S. N. Mane, and M. Sharma, "Intersection collision avoidance in vehicular ad hoc network," *IEEE International Conference on Computer Communication and Control, IC4 2015*, pp. 1–5, 2016. DOI: 10.1109/IC4.2015.7375598.

[25] V. Manwar and M. Sharma, "Intersection Collision Avoidance in Vehicular ad hoc Network," 2015.

[26] J. He, Z. Tang, Z. Fan, and J. Zhang, "Enhanced collision avoidance for distributed LTE vehicle to vehicle broadcast communications," *IEEE Communications Letters*, vol. 22, no. 3, pp. 630–633, 2018, ISSN: 10897798. DOI: 10.1109/LCOMM.2018.2791399.

[27] F. Bella and R. Russo, "A collision warning system for rear-end collision: A driving simulator study," *Procedia - Social and Behavioral Sciences*, vol. 20, pp. 676–686, 2011, ISSN: 18770428. DOI: 10.1016/j.sbspro.2011.08.075. [Online]. Available: http://dx.doi.org/10.1016/j.sbspro.2011.08.075.

[28] Z. Zhao, L. Zhou, Q. Zhu, Y. Luo, and K. Li, "A review of essential technologies for collision avoidance assistance systems," *Advances in Mechanical Engineering*, vol. 9, no. 10, pp. 1–15, 2017, ISSN: 16878140. DOI: 10.1177/1687814017725246.

[29] C. Zu, C. Yang, J. Wang, W. Gao, D. Cao, and F. Y. Wang, "Simulation and field testing of multiple vehicles collision avoidance algorithms," *IEEE/CAA Journal of Automatica Sinica*, vol. 7, no. 4, pp. 1045–1063, 2020, ISSN: 23299274. DOI: 10.1109/JAS.2020.1003246.

[30] *Tech talk: Audi, Traffic Light Information and the future of what—and how—to drive | Automotive World*. [Online]. Available: https://www.automotiveworld.com/news-releases/tech-talk-audi-traffic-light-information-and-the-future-of-what-and-how-to-drive/ (visited on 11/10/2021).

[31] *The DSRC vs 5G Debate Continues - EE Times Asia*. [Online]. Available: https://www.eetasia.com/the-dsrc-vs-5g-debate-continues/ (visited on 11/10/2021).

[32] *DSRC? 'It's become a faith-based thing' | ITS International*. [Online]. Available: https://www.itsinternational.com/its4/its7/its8/feature/dsrc-its-become-faith-based-thing (visited on 11/10/2021).

[33] B. Bloessl, "A Physical Layer Experimentation Framework for Automotive WLAN," no. June, 2018.

[34] G. R. M. Garratt, *The Early History of Radio: from Faraday to Marconi*. 1994. DOI: 10.1049/pbht020e.

[35] *A Brief History of Text Messaging*. [Online]. Available: https://www.mobivity.com/mobivity-blog/a-brief-history-of-text-messaging (visited on 11/11/2021).

[36] G. Maral and M. Bousquet, *Satellite Communications Systems: Systems, Techniques and Technology*, 8.9. 2011, vol. 56, p. 742, ISBN: 1119965098. [Online]. Available: https://books.google.com/books?id=PEsmLaDXzvsC&pgis=1.

[37] D. Tse and P. Viswanath, "The wireless channel," *Fundamentals of Wireless Communication*, pp. 10–48, 2012. DOI: 10.1017/cbo9780511807213.003.

[38] J. He, A. Radford, L. Li, Z. Xiong, Z. Tang, X. Fu, S. Leng, F. Wu, K. Huang, J. Huang, J. Zhang, and Y. Zhang, "Cooperative connected autonomous vehicles (CAV): Research, applications and challenges," *Proceedings - International Conference on Network Protocols, ICNP*, vol. 2019-Octob, no. 824019, 2019, ISSN: 10921648. DOI: 10.1109/ICNP.2019.8888126.

[39] *Connected devices will be 3x the global population by 2023, Cisco says - RCR Wireless News*. [Online]. Available: https://www.rcrwireless.com/20200218/internet-of-things/connected-devices-will-be-3x-the-global-population-by-2023-cisco-says (visited on 11/11/2021).

[40] *Noise-to-Signal Ratio - an overview | ScienceDirect Topics*. [Online]. Available: https://www.sciencedirect.com/topics/computer-science/noise-to-signal-ratio (visited on 01/04/2022).

[41] F. Fund, *Nyquist formula: relating data rate and bandwidth*, 2017. [Online]. Available: https://witestlab.poly.edu/blog/nyquist-formula-relating-data-rate-and-bandwidth/ (visited on 01/04/2022).

[42] *equal error rate - an overview (pdf) | ScienceDirect Topics*. [Online]. Available: https://www.sciencedirect.com/topics/computer-science/equal-error-rate/pdf (visited on 01/04/2022).

[43] *Free-Space Path Loss - Radartutorial*. [Online]. Available: https://www.radartutorial.eu/01.basics/Free-SpacePathLoss.en.html (visited on 01/04/2022).

[44] "The Drive to V2X : Technologies , Standards and Test," pp. 1–14,

[45] V. Mannoni, V. Berg, S. Sesia, and E. Perraud, "A comparison of the V2X communication systems: ITS-G5 and C-V2X," *IEEE Vehicular Technology Conference*, vol. 2019-April, 2019, ISSN: 15502252. DOI: 10.1109/VTCSpring.2019.8746562.

[46] *DSRC Technology | 802.11p standard | ITS-G5 and ETSI ITS-G5, IEEE802.11p | Autotalks*. [Online]. Available: https://www.auto-talks.com/technology/dsrc-technology/ (visited on 08/21/2018).

[47] B. Derviş, *C-ITS: Cooperative Intelligent Transport Systems and Services*, 2013. DOI: 10.1017/CBO9781107415324.004. arXiv: arXiv:1011.1669v3. [Online]. Available: https://www.car-2-car.org/about-c-its/ (visited on 02/02/2020).

[48] Car-2-car., *C-ITS: Cooperative Intelligent Transport Systems and Services*. [Online]. Available: https://www.car-2-car.org/about-c-its/ (visited on 02/02/2020).

[49] J. He, Z. Tang, T. O'Farrell, and T. M. Chen, "Performance analysis of DSRC priority mechanism for road safety applications in vehicular networks," *Wireless Communications and Mobile Computing*, vol. 11, no. 7, pp. 980–990, 2009, ISSN: 1530-8669. DOI: 10.1002/WCM.821. [Online]. Available: https://research.aston.ac.uk/en/publications/performance-analysis-of-dsrc-priority-mechanism-for-road-safety-a.

[50] I. Focus, "SUPPORT FOR VEHICLE-TO-EVERYTHING SERVICES BASED ON LTE," vol. 1, no. 2, pp. 60–80, 2012.

[51] S. Chen, J. Hu, Y. Shi, Y. Peng, J. Fang, R. Zhao, and L. Zhao, "Vehicle-to-Everything (v2x) Services Supported by LTE-Based Systems and 5G," *IEEE Communications Standards Magazine*, vol. 1, no. 2, pp. 70–76, 2017, ISSN: 2471-2825. DOI: 10.1109/MCOMSTD.2017.1700015. [Online]. Available: http://ieeexplore.ieee.org/document/7992934/.

[52] *SAE - Automated Driving*. [Online]. Available: https://www.sae.org/misc/pdfs/automated_driving.pdf (visited on 01/30/2018).

[53] L. Of, D. Automation, and A. R. E. Defined, "SuMMARy Of SAE InTERnATIOnAl'S lEVElS Of DRIVIng AuTOMATIOn fOR On-ROAD VEhIclES," 2014. [Online]. Available: http://www.sae.org/misc/pdfs/automated_driving.pdf.

[54] K. Scharring, S. Nash, and D. Wong, "Connected and Autonomous Vehicles: Position Paper," pp. 1–46, 2017. [Online]. Available: https://www.smmt.co.uk/wp-content/uploads/sites/2/SMMT-CAV-position-paper-final.pdf.

[55] *Levels of Autonomous Driving, Explained*. [Online]. Available: https://www.jdpower.com/cars/shopping-guides/levels-of-autonomous-driving-explained (visited on 04/25/2022).

[56] P. Salvo, I. Turcanu, F. Cuomo, A. Baiocchi, and I. Rubin, *Heterogeneous cellular and DSRC networking for Floating Car Data collection in urban areas*, 2017. DOI: 10.1016/j.vehcom.2016.11.004.

[57] K. Zheng, Q. Zheng, P. Chatzimisios, W. Xiang, and Y. Zhou, "Heterogeneous Vehicular Networking: A Survey on Architecture, Challenges, and Solutions," *IEEE Communications Surveys and Tutorials*, vol. 17, no. 4, pp. 2377–2396, 2015, ISSN: 1553877X. DOI: 10.1109/COMST.2015.2440103.

[58] A. Hosny, M. Yousef, W. Gamil, M. Adel, H. Mostafa, and M. S. Darweesh, "Demonstration of Forward Collision Avoidance Algorithm Based on V2V Communication," *2019 8th International Conference on Modern Circuits and Systems Technologies, MOCAST 2019*, no. 2, pp. 1–4, 2019. DOI: 10.1109/MOCAST.2019.8741580.

[59] W. Li, J. Wu, X. Ma, and Z. Zhang, "On reliability requirement for BSM broadcast for safety applications in DSRC system," *IEEE Intelligent Vehicles Symposium, Proceedings*, no. January, pp. 946–950, 2014. DOI: 10.1109/IVS.2014.6856434.

[60] A. Metzner and T. Wickramarathne, "Exploiting Vehicle-to-Vehicle Communications for Enhanced Situational Awareness," *Proceedings - 2019 IEEE Conference on Cognitive and Computational Aspects of Situation Management, CogSIMA 2019*, pp. 88–92, 2019. DOI: 10.1109/COGSIMA.2019.8724309.

[61] A. Sarker, H. Shen, M. Rahman, M. Chowdhury, K. Dey, F. Li, Y. Wang, and H. S. Narman, "A Review of Sensing and Communication, Human Factors, and Controller Aspects for Information-Aware Connected and Automated Vehicles," *IEEE Transactions on Intelligent Transportation Systems*, vol. 21, no. 1, pp. 7–29, 2020, ISSN: 15580016. DOI: 10.1109/TITS.2019.2892399. arXiv: 1903.08712.

[62] M. Zhao, A. Mammeri, and A. Boukerche, "Distance measurement system for smart vehicles," *2015 7th International Conference on New Technologies, Mobility and Security - Proceedings of NTMS 2015 Conference and Workshops*, 2015. DOI: 10.1109/NTMS.2015.7266486.

[63] M. Baek, D. Jeong, D. Choi, and S. Lee, "Vehicle trajectory prediction and collision warning via fusion of multisensors and wireless vehicular communications," *Sensors (Switzerland)*, vol. 20, no. 1, 2020, ISSN: 14248220. DOI: 10.3390/s20010288.

[64] X. Cheng, S. Member, L. Yang, and X. Shen, "D2D for Intelligent Transportation Systems : A Feasibility Study," *Intelligent Transportation Systems, IEEE Transactions on (Volume:16 , Issue: 4)*, vol. 16, no. 4, pp. 1784–1793, 2015, ISSN: 1524-9050. DOI: 10.1109/TITS.2014.2377074. [Online]. Available: https://www.scopus.com/inward/record.uri?eid=2-s2.0-84938102289&partnerID=40&md5=d14ea5ce6f5adc546e6199d0df1dbc1d.

[65] W. Sun, E. G. Strom, F. Brannstrom, Y. Sui, and K. C. Sou, "D2D-based V2V communications with latency and reliability constraints," *2014 IEEE Globecom Workshops, GC Wkshps 2014*, pp. 1414–1419, 2014. DOI: 10.1109/GLOCOMW.2014.7063632. arXiv: 1501.02973.

[66] N. Cheng, H. Zhou, L. Lei, N. Zhang, Y. Zhou, X. Shen, and F. Bai, "Performance Analysis of Vehicular Device-To-Device Underlay Communication," *IEEE Transactions on Vehicular Technology*, vol. 66, no. 6, pp. 5409–5421, 2017, ISSN: 00189545. DOI: 10.1109/TVT.2016.2627582.

[67] M. I. Ashraf, C. F. Liu, M. Bennis, and W. Saad, "Towards low-latency and ultra-reliable vehicle-to-vehicle communication," *EuCNC 2017 - European Conference on Networks and Communications*, 2017. DOI: 10.1109/EuCNC.2017.7980743. arXiv: 1704.06894.

[68] K. S. Nwizege, M. Bottero, S. Mmeah, and E. D. Nwiwure, "Vehicles-to-infrastructure communication safety messaging in DSRC," *Procedia Computer Science*, vol. 34, no. DPNoC, pp. 559–564, 2014, ISSN: 18770509. DOI: 10.1016/j.procs.2014.07.070. [Online]. Available: http://dx.doi.org/10.1016/j.procs.2014.07.070.

[69] M.-W. Li, T.-H. Wu, W.-Y. Lin, K.-C. Lan, C.-M. Chou, and C.-H. Hsu, "On the Feasibility of Using 802.11p for Communication of Electronic Toll Collection Systems," *ISRN Communications and Networking*, vol. 2011, pp. 1–11, 2011, ISSN: 2090-4355. DOI: 10.5402/2011/723814.

[70] F. Arena and G. Pau, "An overview of vehicular communications," *Future Internet*, vol. 11, no. 2, 2019, ISSN: 19995903. DOI: 10.3390/fi11020027.

[71] W.-y. Lin, M.-w. Li, K.-c. Lan, and C.-h. Hsu, "A Comparison of 802 . 11a and 802 . 11p for V-to-I Communication : A Measurement Study," pp. 559–570, 2011.

[72] D. Tian, H. Luo, J. Zhou, Y. Wang, G. Yu, and H. Xia, "A self-adaptive V2V communication system with DSRC," *Proceedings - 2013 IEEE International Conference on Green Computing and Communications and IEEE Internet of Things and IEEE Cyber, Physical and Social Computing, GreenCom-iThings-CPSCom 2013*, pp. 1528–1532, 2013. DOI: 10.1109/GreenCom-iThings-CPSCom.2013.271.

[73] M. Wang, X. Chen, B. Jin, P. Lv, W. Wang, and Y. Shen, "A novel v2v cooperative collision warning system using uwb/dr for intelligent vehicles," *Sensors*, vol. 21, no. 10, 2021, ISSN: 14248220. DOI: 10.3390/s21103485.

[74] S. Santini, A. Salvi, A. S. Valente, A. Pescape, M. Segata, and R. Lo Cigno, "A Consensus-Based Approach for Platooning with Intervehicular Communications and Its Validation in Realistic Scenarios," *IEEE Transactions on Vehicular Technology*, vol. 66, no. 3, pp. 1985–1999, 2017, ISSN: 00189545. DOI: 10.1109/TVT.2016.2585018.

[75] Nokia, "5G Radio Access - System Design Aspects," p. 16, 2015. [Online]. Available: http://networks.nokia.com/sites/default/files/document/nokia_5g_radio_access_white_paper.pdf.

[76] V. Vukadinovic, K. Bakowski, P. Marsch, I. D. Garcia, H. Xu, M. Sybis, P. Sroka, K. Wesolowski, D. Lister, and I. Thibault, "3GPP C-V2X and IEEE 802.11p for Vehicle-to-Vehicle communications in highway platooning scenarios," *Ad Hoc Networks*, vol. 74, pp. 17–29, 2018, ISSN: 15708705. DOI: 10.1016/j.adhoc.2018.03.004.

[77] S. Gao, A. Lim, and D. Bevly, "An empirical study of DSRC V2V performance in truck platooning scenarios," *Digital Communications and Networks*, vol. 2, no. 4, pp. 233–244, 2016, ISSN: 23528648. DOI: 10.1016/j.dcan.2016.10.003. [Online]. Available: http://dx.doi.org/10.1016/j.dcan.2016.10.003.

[78] G. Karagiannis, O. Altintas, E. Ekici, G. Heijenk, B. Jarupan, K. Lin, and T. Weil, "Vehicular networking: A survey and tutorial on requirements, architectures, challenges, standards and solutions," *IEEE Communications Surveys and Tutorials*, vol. 13, no. 4, pp. 584–616, 2011, ISSN: 1553877X. DOI: 10.1109/SURV.2011.061411.00019.

[79] C. Cooper, D. Franklin, M. Ros, F. Safaei, and M. Abolhasan, "A Comparative Survey of VANET Clustering Techniques," *IEEE Communications Surveys and Tutorials*, vol. 19, no. 1, pp. 657–681, 2017, ISSN: 1553877X. DOI: 10.1109/COMST.2016.2611524. arXiv: arXiv:1403.7012v1.

[80] O. S. Eyobu, J. Joo, and D. S. Han, "A broadcast scheme for vehicle-to-pedestrian safety message dissemination," *International Journal of Distributed Sensor Networks*, vol. 13, no. 11, 2017, ISSN: 15501477. DOI: 10.1177/1550147717741834.

[81] D. Jiang and L. Delgrossi, "IEEE 802.11p: Towards an international standard for wireless access in vehicular environments," *IEEE Vehicular Technology Conference*, pp. 2036–2040, 2008, ISSN: 15502252. DOI: 10.1109/VETECS.2008.458.

[82] G. Naik, B. Choudhury, and J. M. Park, "IEEE 802.11bd 5G NR V2X: Evolution of Radio Access Technologies for V2X Communications," *IEEE Access*, vol. 7, pp. 70 169–70 184, 2019, ISSN: 21693536. DOI: 10.1109/ACCESS.2019.2919489. arXiv: 1903.08391.

[83] B. Y. Yacheur, T. Ahmed, and M. Mosbah, "Analysis and Comparison of IEEE 802.11p and IEEE 802.11bd," *Lecture Notes in Computer Science (including subseries Lecture Notes in Artificial Intelligence and Lecture Notes in Bioinformatics)*, vol. 12574 LNCS, pp. 55–65, 2020, ISSN: 16113349. DOI: 10.1007/978-3-030-66030-7_5.

[84] F. Arena, G. Pau, and A. Severino, "A review on IEEE 802.11p for intelligent transportation systems," *Journal of Sensor and Actuator Networks*, vol. 9, no. 2, pp. 1–11, 2020, ISSN: 22242708. DOI: 10.3390/jsan9020022.

[85] W. Anwar, A. Trasl, N. Franchi, and G. Fettweis, "On the Reliability of NR-V2X and IEEE 802.11bd," *IEEE International Symposium on Personal, Indoor and Mobile Radio Communications, PIMRC*, vol. 2019-Septe, no. September, 2019. DOI: 10.1109/PIMRC.2019.8904104.

[86] Auto Alliance and Gloabla Automakers, "5.9 GHz DSRC Connected Vehicles for Intelligent Transportion Systems," 2013.

[87] ETSI, "ETSI EN 302 637-3 Intelligent Transport Systems (ITS); Vehicular Communications; Basic Set of Applications; Part 3: Specifications of Decentralized Environmental Notification Basic Service," *Etsi*, vol. 1, pp. 1–73, 2014.

[88] I. Parra, A. Garcia-Morcillo, R. Izquierdo, J. Alonso, D. Fernandez-Llorca, and M. A. Sotelo, "Analysis of ITS-G5A V2X communications performance in autonomous cooperative driving experiments," *IEEE Intelligent Vehicles Symposium, Proceedings*, no. Iv, pp. 1899–1903, 2017. DOI: 10.1109/IVS.2017.7995982.

[89] J. Manco, G. G. Baños, J. Härri, M. Sepulcre, and C. Sophiatech, "Prototyping V2X Applications in Large-Scale Scenarios using OpenAirInterface," pp. 151–154, 2020.

[90] *FCC Modernizes 5.9 GHz Band to Improve Wi-Fi and Automotive Safety | Federal Communications Commission*. [Online]. Available: https://www.fcc.gov/document/fcc-modernizes-59-ghz-band-improve-wi-fi-and-automotive-safety-0 (visited on 11/12/2021).

[91] P. Verma, N. Singh, and M. Sharma, "Modelling a vehicle-ID-based IEEE 802.11OCB MAC scheme for periodic broadcast in vehicular networks," *IET Communications*, vol. 12, no. 19, pp. 2401–2407, 2018, ISSN: 17518628. DOI: 10.1049/iet-com.2018.5488.

[92] M. Model, "Background terminology," pp. 1–4, 2014.

[93] Y. Li, "An Overview of the An Overview of the DSRC/WAVE Technology," vol. 15, no. March, pp. 9–21, 2015, ISSN: 00410861.

[94] N. Vivek, S. V. Srikanth, P. Saurabh, T. P. Vamsi, and K. Raju, "On field performance analysis of IEEE 802.11p and WAVE protocol stack for V2V and V2I communication," *2014 International Conference on Information Communication and Embedded Systems, ICICES 2014*, no. 978, pp. 1–6, 2015. DOI: 10.1109/ICICES.2014.7033960.

[95] C. Consortium, "Survey on ITS-G5 CAM statistics," pp. 1–35, 2018.

[96] R. Molina-Masegosa, M. Sepulcre, J. Gozalvez, F. Berens, and V. Martinez, "Empirical Models for the Realistic Generation of Cooperative Awareness Messages in Vehicular Networks," *IEEE Transactions on Vehicular Technology*, vol. 69, no. 5, pp. 5713–5717, 2020, ISSN: 19399359. DOI: 10.1109/TVT.2020.2979232.

[97] J. Santa, F. Pereñíguez, A. Moragón, and A. F. Skarmeta, "Experimental evaluation of CAM and DENM messaging services in vehicular communications," *Transportation Research Part C: Emerging Technologies*, vol. 46, pp. 98–120, 2014, ISSN: 0968090X. DOI: 10.1016/j.trc.2014.05.006.

[98] T. Petrov, M. Dado, P. Kortis, and T. Kovacikova, "Evaluation of packet forwarding approaches for emergency vehicle warning application in VANETs," *12th International Conference ELEKTRO 2018, 2018 ELEKTRO Conference Proceedings*, pp. 1–5, 2018. DOI: 10.1109/ELEKTRO.2018.8398258.

[99] J. Zhao, Y. Chen, and Y. Gong, "Study of connectivity probability of vehicle-to-vehicle and vehicle-to-infrastructure communication systems," *IEEE Vehicular Technology Conference*, vol. 2016-July, pp. 0–3, 2016, ISSN: 15502252. DOI: 10.1109/VTCSpring.2016.7504493.

[100] E. Lte, "Evolving LTE 5G future," pp. 1–17, 2017.

[101] *About 3GPP Home*. [Online]. Available: http://www.3gpp.org/about-3gpp/about-3gpp (visited on 01/30/2018).

[102] *3GPP - Ongoing Releases*. [Online]. Available: http://www.3gpp.org/images/articleimages/ongoing_releases_900px.JPG (visited on 01/30/2018).

[103] F. E. Release and E. Improvements, "3GPP Release 16 : Study Items and Road Map,"

[104] G. Araniti, C. Campolo, M. Condoluci, A. Iera, and A. Molinaro, "LTE for vehicular networking: A survey," *IEEE Communications Magazine*, vol. 51, no. 5, pp. 148–157, 2013, ISSN: 01636804. DOI: 10.1109/MCOM.2013.6515060.

[105] P. Luoto, M. Bennis, P. Pirinen, S. Samarakoon, K. Horneman, and M. Latva-aho, "System Level Performance Evaluation of LTE-V2X Network," pp. 445–449, 2016. arXiv: 1604.08734. [Online]. Available: http://arxiv.org/abs/1604.08734.

[106] M. Botte, L. Pariota, L. D'Acierno, and G. N. Bifulco, "An overview of cooperative driving in the european union: Policies and practices," *Electronics (Switzerland)*, vol. 8, no. 6, pp. 1–25, 2019, ISSN: 20799292. DOI: 10.3390/electronics8060616.

[107] S. A. Abdel Hakeem, A. A. Hady, and H. W. Kim, "5G-V2X: standardization, architecture, use cases, network-slicing, and edge-computing," *Wireless Networks*, vol. 26, no. 8, pp. 6015–6041, 2020, ISSN: 15728196. DOI: 10.1007/s11276-020-02419-8. [Online]. Available: https://doi.org/10.1007/s11276-020-02419-8.

[108] 5G Automotive Association, "The Case for Cellular V2X for Safety and Cooperative Driving," *5GAA Whitepaper*, pp. 1–8, 2016.

[109] E. Yaacoub and N. Zorba, "Enhanced connectivity in vehicular ad-hoc networks via V2V communications," *2013 9th International Wireless Communications and Mobile Computing Conference, IWCMC 2013*, pp. 1654–1659, 2013. DOI: 10.1109/IWCMC.2013.6583804.

[110] C. Paper and I. T. Society, "Www.econstor.eu," 2020.

[111] A. Festag, "Standards for vehicular communication—from IEEE 802.11p to 5G," *Elektrotechnik und Informationstechnik*, vol. 132, no. 7, pp. 409–416, 2015, ISSN: 0932383X. DOI: 10.1007/s00502-015-0343-0. [Online]. Available: http://dx.doi.org/10.1007/s00502-015-0343-0.

[112] C. Campolo and A. Molinaro, "Multichannel communications in vehicular Ad Hoc networks: A survey," *IEEE Communications Magazine*, vol. 51, no. 5, pp. 158–169, 2013, ISSN: 01636804. DOI: 10.1109/MCOM.2013.6515061.

[113] J. Choi and H. Kim, "A QoS-Aware Congestion Control Scheme for C-V2X Safety Communications," pp. 103–106, 2020.

[114] X. Liu and A. Jaekel, "Congestion control in V2V safety communication: Problem, analysis, approaches," *Electronics (Switzerland)*, vol. 8, no. 5, 2019, ISSN: 20799292. DOI: 10.3390/electronics8050540.

[115] M. Kloc, R. Weigel, and A. Koelpin, "SDR implementation of an adaptive low-latency IEEE 802.11p transmitter system for real-time wireless applications," *IEEE Radio and Wireless Symposium, RWS*, pp. 207–210, 2017, ISSN: 21642974. DOI: 10.1109/RWS.2017.7885989.

[116] P. Papadimitratos, A. La Fortelle, K. Evenssen, R. Brignolo, and S. Cosenza, "Vehicular communication systems: Enabling technologies, applications, and future outlook on intelligent transportation," *IEEE Communications Magazine*, vol. 47, no. 11, pp. 84–95, 2009, ISSN: 01636804. DOI: 10.1109/MCOM.2009.5307471.

[117] S. Zeadally, J. Guerrero, and J. Contreras, *A tutorial survey on vehicle-to-vehicle communications*, 2020. DOI: 10.1007/s11235-019-00639-8.

[118] J. Wang, J. Liu, and N. Kato, "Networking and Communications in Autonomous Driving: A Survey," *IEEE Communications Surveys and Tutorials*, vol. 21, no. 2, pp. 1243–1274, 2019, ISSN: 1553877X. DOI: 10.1109/COMST.2018.2888904.

[119] P. K. Singh, S. K. Nandi, and S. Nandi, "A tutorial survey on vehicular communication state of the art, and future research directions," *Vehicular Communications*, vol. 18, p. 100 164, 2019, ISSN: 22142096. DOI: 10.1016/j.vehcom.2019.100164. [Online]. Available: https://doi.org/10.1016/j.vehcom.2019.100164.

[120] M. Rizwan Ghori, A. Safa Sadiq, and A. Ghani, "VANET Routing Protocols: Review, Implementation and Analysis," *Journal of Physics: Conference Series*, vol. 1049, no. 1, 2018, ISSN: 17426596. DOI: 10.1088/1742-6596/1049/1/012064.

[121] D. W. Matolak and Q. Wu, "Channel models for V2V communications: A comparison of different approaches," *Proceedings of the 5th European Conference on Antennas and Propagation, EUCAP 2011*, pp. 2891–2895, 2011.

[122] V. Communications, "Vehicular Communications ;," vol. 1, no. May 2015, pp. 1–15, 2011.

[123] A. Balador, "Simulating IEEE 802.11 in VANETs," *Seminar at GRC – 12 December 2012*, vol. 2012, no. December, pp. 1–29, 2012.

[124] N. M. Abdelsamee, S. S. Alsaleh, and A. Algarni, "On Simulating Internet of Vehicles," *21st Saudi Computer Society National Computer Conference, NCC 2018*, pp. 1–9, 2018. DOI: 10.1109/NCG.2018.8593142.

[125] A. Jafari, S. Al-Khayatt, and A. Dogman, "Performance evaluation of IEEE 802.11p for vehicular communication networks," *Proceedings of the 2012 8th International Symposium on Communication Systems, Networks and Digital Signal Processing, CSNDSP 2012*, no. July, pp. 6–11, 2012. DOI: 10.1109/CSNDSP.2012.6292712.

[126] N. Baloch and L. Reggiani, "Study on communication reliability in VANETs," *ICIEECT 2017 - International Conference on Innovations in Electrical Engineering and Computational Technologies 2017, Proceedings*, 2017. DOI: 10.1109/ICIEECT.2017.7916566.

[127] J. W. Kim, J. W. Kim, and D. K. Jeon, "A cooperative communication protocol for QoS provisioning in IEEE 802.11p/wave vehicular networks," *Sensors (Switzerland)*, vol. 18, no. 11, pp. 1–19, 2018, ISSN: 14248220. DOI: 10.3390/s18113622.

[128] J. Wang, Y. Shao, Y. Ge, and R. Yu, "A survey of vehicle to everything (V2X) testing," *Sensors (Switzerland)*, vol. 19, no. 2, pp. 1–20, 2019, ISSN: 14248220. DOI: 10.3390/s19020334.

[129] T. Kosilo, J. Kolakowski, and Z. Walczak, "Project Safespot (Smart Vehicles on Smart Roads)," *2006 International Conference on Microwaves, Radar and Wireless Communications*, pp. 215–215, 2007. DOI: 10.1109/mikon.2006.4345145.

[130] K. Sjöberg, P. Andres, T. Buburuzan, and A. Brakemeier, "Cooperative Intelligent Transport Systems in Europe: Current Deployment Status and Outlook," *IEEE Vehicular Technology Magazine*, vol. 12, no. 2, pp. 89–97, 2017, ISSN: 15566072. DOI: 10.1109/MVT.2017.2670018.

[131] *InterCor Project: Interoperable corridors deploying cooperative intelligent transport systems*. [Online]. Available: https://intercor-project.eu/ (visited on 11/15/2021).

[132] *Hybrid TESTFEST - InterCor*. [Online]. Available: https://intercor-project.eu/intercor-hybrid-testfest/ (visited on 11/15/2021).

[133] *Cross-border Interoperability TESTFEST - InterCor*. [Online]. Available: https://intercor-project.eu/cross-border-interoperability-testfest/ (visited on 11/15/2021).

[134] G. Crockford, "Milestone 13 - Pilot Evaluation Report," 2020.

[135] J. He, K. Yang, and H. H. Chen, "6G Cellular Networks and Connected Autonomous Vehicles," *IEEE Network*, no. 1, pp. 1–8, 2020, ISSN: 1558156X. DOI: 10.1109/MNET.011.2000541. arXiv: 2010.00972.

[136] L. Bernadó, N. Czink, T. Zemen, and P. Belanović, "Physical layer simulation results for IEEE 802.11p using vehicular non-stationary channel model," *2010 IEEE International Conference on Communications Workshops, ICC 2010*, pp. 3–7, 2010. DOI: 10.1109/ICCW.2010.5503942.

[137] F. Bai and H. Krishnan, "Reliability analysis of DSRC wireless communication for vehicle safety applications," *IEEE Conference on Intelligent Transportation Systems, Proceedings, ITSC*, pp. 355–362, 2006. DOI: 10.1109/itsc.2006.1706767.

[138] H. J. Qiu, I. W. H. Ho, C. K. Tse, and Y. Xie, "A Methodology for Studying 802.11p VANET Broadcasting Performance with Practical Vehicle Distribution," *IEEE Transactions on Vehicular Technology*, vol. 64, no. 10, pp. 4756–4769, 2015, ISSN: 00189545. DOI: 10.1109/TVT.2014.2367037.

[139] M. Sepulcre, J. Gozalvez, and B. Coll-Perales, "Why 6 Mbps is Not (Always) the Optimum Data Rate for Beaconing in Vehicular Networks," *IEEE Transactions on Mobile Computing*, vol. 16, no. 12, pp. 3568–3579, 2017, ISSN: 15361233. DOI: 10.1109/TMC.2017.2696533.

[140] R. Tomar, "Analysis of Beaconing Performance in IEEE 802.11p on VANET," pp. 692–696, 2017.

[141] M. Mahipal, S. Batish, and A. Kakria, "Efficient Broadcasting Protocol for Vehicular Ad-hoc Network," *International Journal of Computer Applications*, vol. 49, no. 23, pp. 38–41, 2012. DOI: 10.5120/7946-1288.

[142] L. Stibor, Y. Zang, and H. J. Reumerman, "Evaluation of communication distance of broadcast messages in a vehicular ad-hoc network using IEEE 802.11p," *IEEE Wireless Communications and Networking Conference, WCNC*, pp. 254–257, 2007, ISSN: 15253511. DOI: 10.1109/WCNC.2007.53.

[143] S. N. Shaikh and S. R. Patil, "A robust broadcast scheme for vehicle to vehicle communication system," *Conference on Advances in Signal Processing, CASP 2016*, pp. 301–305, 2016. DOI: 10.1109/CASP.2016.7746184.

[144] X. Lei and S. H. Rhee, "Performance analysis and enhancement of IEEE 802.11p beaconing," *Eurasip Journal on Wireless Communications and Networking*, vol. 2019, no. 1, 2019, ISSN: 16871499. DOI: 10.1186/s13638-019-1381-9.

[145] C. Campolo, Y. Koucheryavy, A. Molinaro, and A. Vinel, "Characterizing broadcast packet losses in IEEE 802.11p/WAVE vehicular networks," *IEEE International Symposium on Personal, Indoor and Mobile Radio Communications, PIMRC*, no. September, pp. 735–739, 2011. DOI: 10.1109/PIMRC.2011.6140063.

[146] S. Gonzalez and V. Ramos, "A Simulation-Based Analysis of the Loss Process of Broadcast Packets in WAVE Vehicular Networks," *Wireless Communications and Mobile Computing*, vol. 2018, pp. 1–12, 2018, ISSN: 1530-8669. DOI: 10.1155/2018/7430728.

[147] F. Lyu, N. Cheng, H. Zhu, H. Zhou, W. Xu, M. Li, and X. Shen, "Towards Rear-End Collision Avoidance: Adaptive Beaconing for Connected Vehicles," *IEEE Transactions on Intelligent Transportation Systems*, pp. 1–16, 2020, ISSN: 1524-9050. DOI: 10.1109/tits.2020.2966586.

[148] B. Sikdar, "A broadcasting scheme for infrastructure to vehicle communications," *GLOBECOM - IEEE Global Telecommunications Conference*, no. January 2009, pp. 2509–2513, 2008. DOI: 10.1109/GLOCOM.2008.ECP.482.

[149] Y. A. Djilali, Y. Bakhtil, B. Kouninef, and B. Senouci, "Performances Evaluation Study of VANET Communication Technologies for Smart and Autonomous Vehicles," *International Conference on Ubiquitous and Future Networks, ICUFN*, vol. 2018-July, no. Ivc, pp. 79–84, 2018, ISSN: 21658536. DOI: 10.1109/ICUFN.2018.8436661.

[150] V. D. Khairnar and K. Kotecha, "Performance of Vehicle-to-Vehicle Communication using IEEE 802.11p in Vehicular Ad-hoc Network Environment," *International Journal of Network Security and Its Applications*, vol. 5, no. 2, pp. 143–170, 2013, ISSN: 09752307. DOI: 10.5121/ijnsa.2013.5212. arXiv: 1304.3357. [Online]. Available: http://arxiv.org/abs/1304.3357.

[151] S. Lee and A. Lim, "An empirical study on ad hoc performance of DSRC and Wi-Fi vehicular communications," *International Journal of Distributed Sensor Networks*, vol. 2013, 2013, ISSN: 15501329. DOI: 10.1155/2013/482695.

[152] M. Klapez, C. A. Grazia, and M. Casoni, "Application-Level Performance of IEEE 802.11p in Safety-Related V2X Field Trials," *IEEE Internet of Things Journal*, vol. 7, no. 5, pp. 3850–3860, 2020, ISSN: 23274662. DOI: 10.1109/JIOT.2020.2967649.

[153] S. E. Carpenter and M. L. Sichitiu, "Analysis of packet loss in a large-scale DSRC field operational test," *5th IFIP International Conference on Performance Evaluation and Modeling in Wired and Wireless Networks, PEMWN 2016*, 2017. DOI: 10.1109/PEMWN.2016.7842909.

[154] N. S. Rajput, "Measurement of IEEE 802.11p Performance for Basic Safety Messages in Vehicular Communications," *International Symposium on Advanced Networks and Telecommunication Systems, ANTS*, vol. 2018-Decem, pp. 1–4, 2018, ISSN: 21531684. DOI: 10.1109/ANTS.2018.8710108.

[155] X. Huang, D. Zhao, and H. Peng, "Empirical Study of DSRC Performance Based on Safety Pilot Model Deployment Data," *IEEE Transactions on Intelligent Transportation Systems*, vol. 18, no. 10, pp. 2619–2628, 2017, ISSN: 15249050. DOI: 10.1109/TITS.2017.2649538. arXiv: 1606.08365.

[156] R. A. Osman and X.-h. Peng, "QoS-Ensured Cooperative Vehicular Communications," vol. 11, no. 1, pp. 83–92, 2018.

[157] O. Chakroun and S. Cherkaoui, "Enhancing safety messages dissemination over 802.11p/DSRC," *Proceedings - Conference on Local Computer Networks, LCN*, no. 1, pp. 179–187, 2013. DOI: 10.1109/LCNW.2013.6758517.

[158] A. Rakhshan, "The Effect of Interference in Vehicular Communications on Safety Factors," *arXiv*, 2017, ISSN: 23318422. arXiv: 1706.05758.

[159] S. Sinha, *State of IoT 2021: Number of connected IoT devices growing to 12.3 B*, 2021. [Online]. Available: https://iot-analytics.com/number-connected-iot-devices/ (visited on 12/14/2021).

[160] *Software Updates Tesla UK*. [Online]. Available: https://www.tesla.com/en_GB/support/software-updates (visited on 12/14/2021).

[161] *USRP N210 Software Defined Radio (SDR) - Ettus Research*. [Online]. Available: https://www.ettus.com/product/details/UN210-KIT (visited on 08/09/2018).

[162] I. C. Chao, K. B. Lee, R. Candell, F. Proctor, C. C. Shen, and S. Y. Lin, "Software-defined radio based measurement platform for wireless networks," *IEEE International Symposium on Precision Clock Synchronization for Measurement, Control, and Communication, ISPCS*, vol. 2015-Novem, pp. 7–12, 2015, ISSN: 19490313. DOI: 10.1109/ISPCS.2015.7324672.

[163] W. Vandenberghe, I. Moerman, and P. Demeester, "Approximation of the IEEE 802 . 11p Standard Using Commercial Off-The-Shelf IEEE 802 . 11a Hardware," *ITS Telecommunications (ITST)*, pp. 21–26, 2011. DOI: 10.1109/ITST.2011.6060057.

[164] S. Ciccia, G. Giordanengo, and G. Vecchi, "Open-source implementation of an Ad-hoc IEEE 802.11 a/g/p software-defined radio on low-power and low-cost general purpose processors," *Radioengineering*, vol. 26, no. 4, pp. 1083–1095, 2017, ISSN: 12102512. DOI: 10.13164/re.2017.1083.

[165] *HackRF One - Great Scott Gadgets*. [Online]. Available: https://greatscottgadgets.com/hackrf/one/ (visited on 11/16/2021).

[166] F. Peng, S. Zhang, S. Cao, and S. Xu, "A Prototype Performance Analysis for V2V Communications using USRP-based Software Defined Radio Platform," 2018. arXiv: 1809.10413. [Online]. Available: http://arxiv.org/abs/1809.10413.

[167] N. B. Truong, Y. J. Suh, and C. Yu, "Latency analysis in GNU radio/USRP-based software radio platforms," *Proceedings - IEEE Military Communications Conference MILCOM*, pp. 305–310, 2013. DOI: 10.1109/MILCOM.2013.60.

[168] N. B. Truong and C. Yu, "Investigating latency in GNU Software Radio with USRP embedded series SDR platform," *Proceedings - 2013 8th International Conference on Broadband, Wireless Computing, Communication and Applications, BWCCA 2013*, no. August, pp. 9–14, 2013. DOI: 10.1109/BWCCA.2013.11.

[169] R. Gandhiraj and K. P. Soman, "Modern analog and digital communication systems development using GNU Radio with USRP," *Telecommunication Systems*, vol. 56, no. 3, pp. 367–381, 2014, ISSN: 15729451. DOI: 10.1007/s11235-013-9850-7.

[170] M. Engelhardt and A. Asadi, "The first experimental SDR platform for in-band D2D communications in 5G," *Proceedings - International Conference on Network Protocols, ICNP*, vol. 2017-Octob, pp. 2–3, 2017, ISSN: 10921648. DOI: 10.1109/ICNP.2017.8117580.

[171] A. Asadi and V. Mancuso, "Network-Assisted Outband D2D-Clustering in 5G Cellular Networks: Theory and Practice," *IEEE Transactions on Mobile Computing*, vol. 16, no. 8, pp. 2246–2259, 2017, ISSN: 15361233. DOI: 10.1109/TMC.2016.2621041.

[172] W. Zhang, S. Fu, Z. Cao, Z. Jiang, S. Zhang, and S. Xu, "An SDR-in-the-loop carla simulator for C-V2X-based autonomous driving," *IEEE INFOCOM 2020 - IEEE Conference on Computer Communications Workshops, INFOCOM WKSHPS 2020*, pp. 1270–1271, 2020. DOI: 10.1109/INFOCOMWKSHPS50562.2020.9162743.

[173] P Fuxjäger, a Costantini, D Valerio, P Castiglione, G Zacheo, T Zemen, and F Ricciato, "IEEE 802 . 11p Transmission Using GNURadio," *Spectrum*, vol. 94, no. 1, pp. 1–4, 2007, ISSN: 00359203. [Online]. Available: http://userver.ftw.at/$\sim$zemen/papers/Fuxjaeger10-WSR-paper.pdf.

[174] A. Kumar and S. Noghanian, "Wireless channel test-bed for DSRC applications using USRP software defined radio," *IEEE Antennas and Propagation Society, AP-S International Symposium (Digest)*, no. July 2013, pp. 2105–2106, 2013, ISSN: 15223965. DOI: 10.1109/APS.2013.6711711.

[175] P. Agostini, R. Knopp, J. Harri, and N. Haziza, "Implementation and test of a DSRC prototype on OpenAirInterface SDR platform," *2013 IEEE International Conference on Communications Workshops, ICC 2013*, pp. 510–514, 2013, ISSN: 2164-7038. DOI: 10.1109/ICCW.2013.6649287.

[176] D. Vlastaras, S. Malkowsky, and F. Tufvesson, "Stress Test of Vehicular Communication Transceivers Using Software Defined Radio," *2015 IEEE 81st Vehicular Technology Conference (VTC Spring)*, vol. 41, no. 2, pp. 1–4, 2015, ISSN: 15502252. DOI: 10.1109/VTCSpring.2015.7146111. [Online]. Available: http://ieeexplore.ieee.org/lpdocs/epic03/wrapper.htm?arnumber=7146111.

[177] *Wime Project*. [Online]. Available: https://www.wime-project.net/ (visited on 11/16/2021).

[178] B. Bloessl, M. Segata, C. Sommer, and F. Dressler, "Towards an Open Source IEEE 802.11p stack: A full SDR-based transceiver in GNU Radio," *IEEE Vehicular Networking Conference, VNC*, pp. 143–149, 2013, ISSN: 21579857. DOI: 10.1109/VNC.2013.6737601.

[179] ——, "An IEEE802.11a/g/p OFDM receiver for GNU radio," *SRIF 2013 - Proceedings of the 2nd, 2013 ACM SIGCOMM Workshop on Software Radio Implementation Forum*, pp. 9–15, 2013. DOI: 10.1145/2491246.2491248.

[180] B. Bloessl, S. Member, M. S. Member, C. S. Member, and F. D. Fellow, "Performance Assessment of IEEE 802.11p with an Open Source SDR-based Prototype - IEEE Journals and Magazine," vol. 1233, no. c, pp. 1–14, 2017, ISSN: 1536-1233. DOI: 10.1109/TMC.2017.2751474. [Online]. Available: http://ieeexplore.ieee.org/document/8031977/keywords.

[181] G. Arcos, "Accelerating an IEEE 802.11 a / g / p Transceiver in GNU Radio," 2016.

[182] Y. Xiang, S. Huang, M. Li, J. Li, and W. Wang, "Rear-End Collision Avoidance-Based on Multi-Channel Detection," pp. 1–11, 2019.

[183] B. R. Chang, H. F. Tsai, and C. P. Young, "Intelligent data fusion system for predicting vehicle collision warning using vision/GPS sensing," *Expert Systems with Applications*, vol. 37, no. 3, pp. 2439–2450, 2010, ISSN: 09574174. DOI: 10.1016/j.eswa.2009.07.036. [Online]. Available: http://dx.doi.org/10.1016/j.eswa.2009.07.036.

[184] J. Hérard, M. Lesemann, A. Aparicio, H. Eriksson, and J. Jacobson, "A comparative Study – Rearend Collision Avoidance," *Procedia - Social and Behavioral Sciences*, vol. 48, pp. 173–183, 2012, ISSN: 18770428. DOI: 10.1016/j.sbspro.2012.06.998.

[185] Y. Wang, X. Duan, D. Tian, G. Lu, and H. Yu, "Throughput and Delay Limits of 802.11p and its Influence on Highway Capacity," *Procedia - Social and Behavioral Sciences*, vol. 96, no. Cictp, pp. 2096–2104, 2013, ISSN: 18770428. DOI:

10.1016/j.sbspro.2013.08.236. [Online]. Available: http://dx.doi.org/10.1016/j.sbspro.2013.08.236.

[186] S. M. Mahmud, L. Ferreira, M. S. Hoque, and A. Tavassoli, "Application of proximal surrogate indicators for safety evaluation: A review of recent developments and research needs," *IATSS Research*, vol. 41, no. 4, pp. 153–163, 2017, ISSN: 03861112. DOI: 10.1016/j.iatssr.2017.02.001. [Online]. Available: https://doi.org/10.1016/j.iatssr.2017.02.001.

[187] Y. R. Liu and J. X. Guo, "Design of Improved Vehicle Collision Warning System Based on V2V Communication," *Proceedings of 2018 IEEE 8th International Conference on Electronics Information and Emergency Communication, ICEIEC 2018*, pp. 95–98, 2018. DOI: 10.1109/ICEIEC.2018.8473510.

[188] M. Yousef, A. Hosny, W. Gamil, M. Adel, H. M. Fahmy, M. Saeed Darweesh, and H. Mostafa, "Dual-mode forward collision avoidance algorithm based on vehicle-to-vehicle (V2V) communication," *Midwest Symposium on Circuits and Systems*, vol. 2018-Augus, no. 1, pp. 739–742, 2019, ISSN: 15483746. DOI: 10.1109/MWSCAS.2018.8623896.

[189] S. Agrawal and D. M. S.W.Varade, "Collision detection and avoidance system based on computer vision," *2nd International Conference on Communication and Electronics Systems (ICCES 2017) IEEE Xplore Compliant*, no. February, pp. 476–477, 2014.

[190] M. Gluhakovic, M. Herceg, M. Popovic, and J. Kovacevic, "Vehicle Detection in the Autonomous Vehicle Environment for Potential Collision Warning," *2020 Zooming Innovation in Consumer Technologies Conference, ZINC 2020*, pp. 178–183, 2020. DOI: 10.1109/ZINC50678.2020.9161791.

[191] M. Laurenza, G. Pepe, D. Antonelli, and A. Carcaterra, "Car collision avoidance with velocity obstacle approach: Evaluation of the reliability and performace of the collision avoidance maneuver," *5th International Forum on Research and Technologies for Society and Industry: Innovation to Shape the Future, RTSI 2019 - Proceedings*, pp. 465–470, 2019. DOI: 10.1109/RTSI.2019.8895525.

[192] N. Yakusheva, A. Proletarsky, and M. Basarab, "Pedestrian-Vehicle Collision Avoidance Strategy for NLOS Conditions," *2018 26th Telecommunications Forum, TELFOR 2018 - Proceedings*, pp. 1–4, 2018. DOI: 10.1109/TELFOR.2018.8612086.

[193] T. Yang, Y. Zhang, J. Tan, and T. Z. Qiu, "Research on forward collision warning system based on connected vehicle V2V communication," *ICTIS 2019 - 5th International Conference on Transportation Information and Safety*, pp. 1174–1181, 2019. DOI: 10.1109/ICTIS.2019.8883534.

[194] D. Lee and H. Yeo, "Real-Time Rear-End Collision-Warning System Using a Multilayer Perceptron Neural Network," *IEEE Transactions on Intelligent Transportation Systems*, vol. 17, no. 11, pp. 3087–3097, 2016, ISSN: 15249050. DOI: 10.1109/TITS.2016.2537878.

[195] J. W. Ro, P. S. Roop, and A. Malik, "A New Safety Distance Calculation for Rear-End Collision Avoidance," *IEEE Transactions on Intelligent Transportation Systems*, no. February, pp. 1–6, 2020, ISSN: 1524-9050. DOI: 10.1109/tits.2020.2975015.

[196] P Kalaivani, "Recognition (SCADAR) System," pp. 384–388, 2017.

[197] M. A. Javed and J. Y. Khan, "A cooperative safety zone approach to enhance the performance of VANET applications," *IEEE Vehicular Technology Conference*, no. July 2016, 2013, ISSN: 15502252. DOI: 10.1109/VTCSpring.2013.6691819.

[198] S. Banani, S. Gordon, S. Thiemjarus, and S. Kittipiyakul, "Verifying safety messages using relative-time and zone priority in vehicular ad hoc networks," *Sensors (Switzerland)*, vol. 18, no. 4, pp. 1–21, 2018, ISSN: 14248220. DOI: 10.3390/s18041195.

[199] F. Ye, M. Adams, and S. Roy, "V2V wireless communication protocol for rear-end collision avoidance on highways," *IEEE International Conference on Communications*, pp. 375–379, 2008, ISSN: 05361486. DOI: 10.1109/ICCW.2008.77.

[200] A. Tang and A. Yip, "Collision avoidance timing analysis of DSRC-based vehicles," *Accident Analysis and Prevention*, vol. 42, no. 1, pp. 182–195, 2010, ISSN: 00014575. DOI: 10.1016/j.aap.2009.07.019.

[201] G. Rakesh and M. Belwal, "Vehicle Collision Avoidance in a VANET environment by data communication," *Proceedings of the 3rd International Conference on Computing Methodologies and Communication, ICCMC 2019*, no. Iccmc, pp. 238–242, 2019. DOI: 10.1109/ICCMC.2019.8819797.

[202] D. Patel and R. Zalila-Wenkstern, "Collaborative Collision Avoidance for CAVs in Unpredictable Scenarios," *2020 IEEE 3rd Connected and Automated Vehicles Symposium, CAVS 2020 - Proceedings*, pp. 0–5, 2020. DOI: 10.1109/CAVS51000.2020.9334661.

[203] W. Yang, B. Wan, and X. Qu, "A Forward Collision Warning System Using Driving Intention Recognition of the Front Vehicle and V2V Communication," *IEEE Access*, vol. 8, pp. 11 268–11 278, 2020, ISSN: 21693536. DOI: 10.1109/ACCESS.2020.2963854.

[204] A. Bazzi, B. M. Masini, A. Zanella, and I. Thibault, "On the performance of IEEE 802.11p and LTE-V2V for the cooperative awareness of connected vehicles," *IEEE Transactions on Vehicular Technology*, vol. 66, no. 11, pp. 10 419–10 432, 2017, ISSN: 00189545. DOI: 10.1109/TVT.2017.2750803.

[205] G. Cecchini, A. Bazzi, B. M. Masini, and A. Zanella, "Performance Comparison Between IEEE 802.11p and LTE-V2V In-coverage and Out-of-coverage for Cooperative Awareness," *IEEE Vehicular Networking Conference (VNC)*, pp. 109–114, 2017.

[206] J. Li, Y. Zhang, M. Shi, Q. Liu, and Y. Chen, "Collision avoidance strategy supported by LTE-V-based vehicle automation and communication systems for car following," *Tsinghua Science and Technology*, vol. 25, no. 1, pp. 127–139, 2020, ISSN: 18787606. DOI: 10.26599/TST.2018.9010143.

[207] N. I. Shuhaimi, Heriansyah, and T. Juhana, "Comparative performance evaluation of DSRC and Wi-Fi Direct in VANET," *Proceedings - 2015 4th International Conference on Instrumentation, Communications, Information Technology and Biomedical Engineering, ICICI-BME 2015*, pp. 298–303, 2016. DOI: 10.1109/ICICI-BME.2015.7401382.

[208] B. A. Filippi, K. Moerman, P. D. Alexander, F. Schober, and Werner, "Why 802 . 11P Beats Lte and 5G for V2X," 2016.

[209] K. Peters, "Connected Future," vol. 8, no. 2, 2007.

[210] D. Tian, G. Wu, K. Boriboonsomsin, and M. J. Barth, "Performance Measurement Evaluation Framework and Co-BenefitTradeoff Analysis for Connected and Automated Vehicles (CAV) Applications: A Survey," *IEEE Intelligent Transportation Systems Magazine*, vol. 10, no. 3, pp. 110–122, 2018, ISSN: 19411197. DOI: 10.1109/MITS.2018.2842020.

[211] Z. Szendrei, N. Varga, and L. Bokor, "A SUMO-Based hardware-in-the-loop V2X simulation framework for testing and rapid prototyping of cooperative vehicular applications," *Lecture Notes in Mechanical Engineering*, vol. 0, no. 9783319756769, pp. 426–440, 2018, ISSN: 21954364. DOI: 10.1007/978-3-319-75677-6_37.

[212] H. Cao, S. Gangakhedkar, A. R. Ali, M. Gharba, and J. Eichinger, "A 5G V2X testbed for cooperative automated driving," *IEEE Vehicular Networking Conference, VNC*, 2017, ISSN: 21579865. DOI: 10.1109/VNC.2016.7835939.

[213] Cohda Wireless, *MK5 OBU Cohda Wireless*. [Online]. Available: https://www.cohdawireless.com/solutions/hardware/mk5-obu/ (visited on 11/26/2021).

[214] *bastibl (Bastian Bloessl) · GitHub*. [Online]. Available: https://github.com/bastibl/ (visited on 11/26/2021).

[215] *Apex II TG.35 - Wideband 4G LTE Hinged Dipole Terminal Antenna*. [Online]. Available: https://www.taoglas.com/product/apex-ii-tg-35-white-ultra-wide-band-4g-lte-dipole-terminal-antenna-90o-hinged-ra-smam/ (visited on 04/26/2022).

[216] *bastibl (Bastian Bloessl) · GitHub*. [Online]. Available: https://github.com/bastibl/ (visited on 11/26/2021).

[217] L. Chen, X. Xing, G. Sun, J. Qian, and X. Guan, "Cooperative BSM Dissemination in DSRC/WAVE Based Vehicular Networks," *Lecture Notes in Computer Science (including subseries Lecture Notes in Artificial Intelligence and Lecture Notes in Bioinformatics)*, vol. 11604 LNCS, pp. 55–66, 2019, ISSN: 16113349. DOI: 10.1007/978-3-030-23597-0_5.

[218] ETSI (European Telecommunications Standards Institute), "ETSI EN 302 637-2 - Part 2: Specification of Cooperative Awareness Basic Service V1.4.1 (2019-04)," *Etsi*, vol. 1, pp. 1–22, 2019.

[219] Cohda, "DSRC Field Trials," *Scenario*, pp. 1–12, 2017.

[220] Rohde and Schwarz GmbH Co, "Intelligent Transportation Systems Using IEEE 802.11p Application Note," p. 26, 2014. [Online]. Available: http://cdn.rohde-schwarz.com/pws/dl_downloads/dl_application/application_notes/1ma152/1MA152_3e_ITS_using_802_11p.pdf.

[221] W. Wang, Y. Li, J. Lu, Y. Li, and Q. Wan, "Estimating Rear-End Accident Probabilities with Different Driving Tendencies at Signalized Intersections in China," *Journal of Advanced Transportation*, vol. 2019, 2019, ISSN: 20423195. DOI: 10.1155/2019/4836908.

[222] S. Knowles Flanagan, J. He, and X. H. Peng, "Improving Emergency Collision Avoidance with Vehicle to Vehicle Communications," *Proceedings - 20th International Conference on High Performance Computing and Communications, 16th International Conference on Smart City and 4th International Conference on Data Science and Systems, HPCC/SmartCity/DSS 2018*, pp. 1322–1329, 2019. DOI: 10.1109/HPCC/SmartCity/DSS.2018.00220.

[223] House of Lords Science and Technology Select Committee, "Connected and Autonomous Vehicles: The future?," no. March, p. 66, 2017. [Online]. Available: https://www.publications.parliament.uk/pa/ld201617/ldselect/ldsctech/115/115.pdf.

[224] *Reported road casualties Great Britain, annual report: 2020 - GOV.UK*. [Online]. Available: https://www.gov.uk/government/statistics/reported-road-casualties-great-britain-annual-report-2020/reported-road-casualties-great-britain-annual-report-2020 (visited on 11/23/2021).

[225] R Nave, *Friction and Automobile Tires*, 2000. [Online]. Available: http://hyperphysics.phy-astr.gsu.edu/hbase/Mechanics/frictire.html (visited on 12/10/2021).

[226] *Highway Code stopping distances 'woefully short' as drivers' thinking time underestimated | The Independent*. [Online]. Available: https://www.independent.co.uk/news/uk/home-news/highway-code-car-stopping-distances-wrong-drivers-thinking-time-brake-rac-a7859061.html (visited on 08/24/2018).

[227] K. Lee and D. Kum, "Collision avoidance/mitigation system: Motion planning of autonomous vehicle via predictive occupancy map," *IEEE Access*, vol. 7, pp. 52 846–52 857, 2019, ISSN: 21693536. DOI: 10.1109/ACCESS.2019.2912067.

[228] Y. L. Chen, K. Y. Shen, and S. C. Wang, "Forward collision warning system considering both time-to-collision and safety braking distance," *International Journal of Vehicle Safety*, vol. 6, no. 4, pp. 347–360, 2013, ISSN: 14793113. DOI: 10.1504/IJVS.2013.056968.

[229] R. Layton and K. Dixon, "Stopping Sight Distance - Discussion Paper 1," no. April, 2012. [Online]. Available: http://cce.oregonstate.edu/sites/cce.oregonstate.edu/files/12-2-stopping-sight-distance.pdf.

[230] American Association of State Highway and Transportation Official (AASHTO), *A Policy on Geometric Design of Highways and Streets*. 2015, p. 12, ISBN: 9781560515081. [Online]. Available: /www.researchgate.net/publication/265571500.

[231] Y. L. Chen, S. C. Wang, and C. A. Wang, "Study on vehicle safety distance warning system," *Proceedings of the IEEE International Conference on Industrial Technology*, no. 2, 2008. DOI: 10.1109/ICIT.2008.4608344.

[232] Y. L. Chen and C. A. Wang, "Vehicle safety distance warning system: A novel algorithm for vehicle safety distance calculating between moving cars," *IEEE Vehicular Technology Conference*, pp. 2570–2574, 2007, ISSN: 15502252. DOI: 10.1109/VETECS.2007.529.

[233] *Road Vehicle Dynamics*. [Online]. Available: https://www.sae.org/publications/books/content/r-366/ (visited on 11/23/2021).

[234] *Highway Code, Driving Test Success, A safe Separation Distance*. [Online]. Available: https://www.drivingtestsuccess.com/blog/safe-separation-distance.

[235] A. Filippi, K. Moerman, V. Martinez, A. Turley, N. X. P. Semiconductors, O. Haran, and R. T. Autotalks, "LTE-V2V for safety applications,"

[236] A. K. Maurya and P. S. Bokare, "Study of Deceleration Behaviour of Different Vehicle Types," *International Journal for Traffic and Transport Engineering*, vol. 2, no. 3, pp. 253–270, 2012, ISSN: 2217544X. DOI: 10.7708/ijtte.2012.2(3).07.

[237] F. Terhar and C. Icking, "A New Model for Hard Braking Vehicles and Collision Avoiding Trajectories," no. c, pp. 28–33, 2019.

[238] Y. J. Zhang, F. Du, J. Wang, L. S. Ke, M. Wang, Y. Hu, M. Yu, G. H. Li, and A. Y. Zhan, "A Safety Collision Avoidance Algorithm Based on Comprehensive Characteristics," *Complexity*, vol. 2020, 2020, ISSN: 10990526. DOI: 10.1155/2020/1616420.

[239] W. Wu, L. Kong, and T. Xue, "Resource allocation algorithm for V2X communications based on SCMA," *Lecture Notes in Electrical Engineering*, vol. 463, pp. 1997–2004, 2019, ISSN: 18761119. DOI: 10.1007/978-981-10-6571-2_243.

[240] P. Dhawankar, P. Agrawal, B. Abderezzak, O. Kaiwartya, K. Busawon, and M. S. Raboacă, "Design and numerical implementation of V2X control architecture for autonomous driving vehicles," *Mathematics*, vol. 9, no. 14, 2021, ISSN: 22277390. DOI: 10.3390/math9141696.

[241] D. B. Fambro, R. J. Koppa, D. L. Picha, and K. Fitzpatrick, "Driver perception-brake response in stopping sight distance situations," *Transportation Research Record*, no. 1628, pp. 1–7, 1998, ISSN: 03611981. DOI: 10.3141/1628-01.

[242] A. Tassi, M. Egan, R. J. Piechocki, and A. Nix, "Modeling and Design of Millimeter-Wave Networks for Highway Vehicular Communication," *IEEE Transactions on Vehicular Technology*, vol. 9545, no. c, pp. 1–16, 2017, ISSN: 00189545. DOI: 10.1109/TVT.2017.2734684. arXiv: 1706.00298.

[243] C.-W. Kuo and M.-L. Tang, "Survey and empirical evaluation of nonhomogeneous arrival process models with taxi data," *Journal of Advanced Transportation*, vol. 47, no. June 2010, pp. 512–525, 2011, ISSN: 01976729. DOI: 10.1002/atr. [Online]. Available: http://onlinelibrary.wiley.com/doi/10.1002/atr.144/full.

[244] N. Uno, Y. Iida, S. Itsubo, and S. Yasuhara, "A microscopic analysis of traffic conflict caused by lane-changing vehicle at weaving section," *Proceedings of the 13th Mini-EURO Conference on Handling Uncertainty in the Analysis of Traffic and Transportation Systems*, pp. 143–148, 2003.

[245] A. Pressas, Z. Sheng, F. Ali, D. Tian, and M. Nekovee, "Contention-based learning MAC protocol for broadcast vehicle-to-vehicle communication," *IEEE Vehicular Networking Conference, VNC*, vol. 2018-Janua, pp. 263–270, 2018, ISSN: 21579865. DOI: 10.1109/VNC.2017.8275614.

[246] A. Pressas, Z. Sheng, P. Fussey, and D. Lund, "Connected vehicles in smart cities: Interworking from inside vehicles to outside," *2016 13th Annual IEEE International Conference on Sensing, Communication, and Networking, SECON 2016*, pp. 6–8, 2016. DOI: 10.1109/SAHCN.2016.7732976.

[247] *Wi-Fi Signal Strength: What is a Good Signal? – Glocomp Systems*. [Online]. Available: https://www.glocomp.com/wi-fi-signal-strength-what-is-a-good-signal/ (visited on 12/17/2021).

[248] M. N. Ahangar, Q. Z. Ahmed, F. A. Khan, and M. Hafeez, "A survey of autonomous vehicles: Enabling communication technologies and challenges," *Sensors (Switzerland)*, vol. 21, no. 3, pp. 1–33, 2021, ISSN: 14248220. DOI: 10.3390/s21030706.

[249] N. Adhikari and S. Noghanian, "Antenna location effects on the capacity of MIMO DSRC channels," *2014 United States National Committee of URSI National Radio Science Meeting (USNC-URSI NRSM)*, vol. 6, no. May 2013, pp. 1–1, 2014. DOI: 10.1109/usnc-ursi-nrsm.2014.6928032.

[250] J. E. Siegel, D. C. Erb, and S. E. Sarma, "A survey of the connected vehicle Landscape - Architectures, enabling technologies, applications, and development areas," *IEEE Transactions on Intelligent Transportation Systems*, vol. 19, no. 8, pp. 2391–2406, 2018, ISSN: 15249050. DOI: 10.1109/TITS.2017.2749459.

[251] A. Casteigts, A. Nayak, and I. Stojmenovic, "Communication protocols for vehicular ad hoc networks," *Wireless Communications and Mobile Computing*, vol. 11, no. 5, pp. 567–582, 2011, ISSN: 15308669. DOI: 10.1002/wcm.879.

[252] B. Canis and J. C. Gallagher, "Smart Cars and Trucks : Spectrum Use for Vehicle Safety," *Congressional Research Service*, no. November 2020, pp. 1–3, 2019.

[253] Z. Tang, J. He, S. K. Flanagan, P. Procter, and L. Cheng, "Cooperative connected smart road infrastructure and autonomous vehicles for safe driving," pp. 1–6, 2021. DOI: 10.1109/ICNP52444.2021.9651941.

[254] B. Coll-Perales, J. Schulte-Tigges, M. Rondinone, J. Gozalvez, M. Reke, D. Matheis, and T. Walter, "Prototyping and Evaluation of Infrastructure-Assisted Transition of Control for Cooperative Automated Vehicles," *IEEE Transactions on Intelligent Transportation Systems*, no. c, 2021, ISSN: 15580016. DOI: 10.1109/TITS.2021.3061085.

[255] J. Schindler, R. Markowski, D. Wesemeyer, B. Coll-Perales, C. Boker, and S. Khan, "Infrastructure supported automated driving in transition areas - A prototypic implementation," *2020 IEEE 3rd Connected and Automated Vehicles Symposium, CAVS 2020 - Proceedings*, 2020. DOI: 10.1109/CAVS51000.2020.9334555.

[256] M. Buchholz, J. Strohbeck, A. M. Adaktylos, F. Vogl, G. Allmer, S. C. Barros, Y. Lassoued, M. Wimmer, B. Hätty, G. Massot, C. Ponchel, M. Bretin, V. Sourlas, and A. Amditis, "Enabling automated driving by ICT infrastructure: A reference architecture," *arXiv*, 2020, ISSN: 23318422.

[257] J. Marchal, D. Gingras, and H. Pollart, "Vehicle Detection Assistance in Urban Intersection Using Data Exchange Between Road Infrastructure," no. c, pp. 59–66, 2019.

[258] Y. Y. Wang and H. Y. Wei, "Road capacity and throughput for safe driving autonomous vehicles," *IEEE Access*, vol. 8, pp. 95 779–95 792, 2020, ISSN: 21693536. DOI: 10.1109/ACCESS.2020.2995312.

[259] T. K. Lee, T. W. Wang, W. X. Wu, Y. C. Kuo, S. H. Huang, G. S. Wang, C. Y. Lin, J. J. Chen, and Y. C. Tseng, "Building a V2X Simulation Framework for Future Autonomous Driving," *2019 20th Asia-Pacific Network Operations and Management Symposium: Management in a Cyber-Physical World, APNOMS 2019*, pp. 1–6, 2019. DOI: 10.23919/APNOMS.2019.8892860.

[260] L. Studer, S. Agriesti, P. Gandini, G. Marchionni, M. Ponti, and B. Chiara, "Highway Chauffeur: state of the art and future evaluations : Implementation scenarios and impact assessment," *2018 International Conference of Electrical and Electronic Technologies for Automotive, AUTOMOTIVE 2018*, no. July, pp. 1–6, 2018. DOI: 10.23919/EETA.2018.8493230.

[261] *Autopilot | Tesla*. [Online]. Available: https://www.tesla.com/autopilot (visited on 11/17/2021).

[262] Ns-3, *Ns-3 | a Discrete-Event Network Simulator for Internet Systems*, 2021. [Online]. Available: https://www.nsnam.org/ (visited on 05/06/2022).

[263] J. Heidemann and U. S. C. Isi, *OMNeT++ Discrete Event Simulator*, 2002. [Online]. Available: https://omnetpp.org/%5Cnhttp://www.omnetpp.org (visited on 05/06/2022).

[264] OPNET, *OPNET Network Simulator - Opnet Projects*, 2012. [Online]. Available: https://opnetprojects.com/opnet-network-simulator/ (visited on 05/06/2022).

[265] *CANoe.Car2x | Vector*. [Online]. Available: https://www.vector.com/int/en/products/products-a-z/software/canoe/option-car2x/ (visited on 05/06/2022).

[266] *iTETRIS Platform*. [Online]. Available: http://ict-itetris.eu/ (visited on 05/06/2022).

[267] *Veins*. [Online]. Available: https://veins.car2x.org/ (visited on 05/06/2022).

[268] PTV Group, *Traffic Simulation Software | PTV Vissim*, 2020. [Online]. Available: https://www.ptvgroup.com/en/solutions/products/ptv-vissim/ (visited on 05/06/2022).

[269] K. C. Lan, "MOVE: A practical simulator for mobility model in VANET," *Telematics Communication Technologies and Vehicular Networks: Wireless Architectures and Applications*, pp. 355–368, 2009. DOI: 10.4018/978-1-60566-840-6.ch021. [Online]. Available: https://www.igi-global.com/chapter/move-practical-simulator-mobility-model/39536www.igi-global.com/chapter/move-practical-simulator-mobility-model/39536.

[270] *Vienna 5G Simulators – nt.tuwien.ac.at*. [Online]. Available: https://www.nt.tuwien.ac.at/research/mobile-communications/vccs/vienna-5g-simulators/ (visited on 05/06/2022).

[271] *NYUSIM Download Version 3.1*. [Online]. Available: https://wireless.engineering.nyu.edu/nyusim/ (visited on 05/06/2022).

[272] *ISWireless*. [Online]. Available: https://www.iswireless.com/ (visited on 05/06/2022).

[273] *PyTorch*. [Online]. Available: https://pytorch.org/ (visited on 05/06/2022).

[274] *TensorFlow*. [Online]. Available: https://www.tensorflow.org/ (visited on 05/06/2022).

[275] *Deep Learning in MATLAB*, 2020. [Online]. Available: https://www.mathworks.com/help/deeplearning/ug/deep-learning-in-matlab.html (visited on 05/06/2022).

[276] *Welcome to MMDetection's documentation! — MMDetection 2.24.1 documentation*. [Online]. Available: https://mmdetection.readthedocs.io/en/latest/ (visited on 05/06/2022).

[277] *VehicleSim Technical References*. [Online]. Available: https://www.carsim.com/publications/technical/modeling.php (visited on 06/16/2022).

[278] A. Dosovitskiy, G. Ros, F. Codevilla, A. López, and V. Koltun, "CARLA: An open urban driving simulator," *arXiv*, no. CoRL, pp. 1–16, 2017, ISSN: 23318422. arXiv: 1711.03938.

[279] I. The MathWorks, *Automated Driving Toolbox MATLAB*, 2021. [Online]. Available: https://www.mathworks.com/products/automateddriving.html (visited on 05/06/2022).

[280] D. Twisk, A. Stelling, P. Van Gent, J. De Groot, and W. Vlakveld, "Speed characteristics of speed pedelecs, pedelecs and conventional bicycles in naturalistic urban and rural traffic conditions," *Accident Analysis and Prevention*, vol. 150, no. November 2020, p. 105 940, 2021, ISSN: 00014575. DOI: 10.1016/j.aap.2020.105940. [Online]. Available: https://doi.org/10.1016/j.aap.2020.105940.

[281] A. Forde and J. Daniel, "Pedestrian walking speed at un-signalized midblock crosswalk and its impact on urban street segment performance," *Journal of Traffic and Transportation Engineering (English Edition)*, vol. 8, no. 1, pp. 57–69, 2021, ISSN: 20957564. DOI: 10.1016/j.jtte.2019.03.007. [Online]. Available: https://doi.org/10.1016/j.jtte.2019.03.007.

[282] D. Richards, "Relationship between Speed and Risk of Fatal Injury: Pedestrians and Car Occupants," *Road Safety Web Publication*, no. 16, pp. 19–22, 2010. [Online]. Available: http://www.dft.gov.uk/pgr/roadsafety/research/rsrr/theme5/researchreport16/doc/rswp16.doc.

[283] *Lower Speed Means Fewer Road Deaths | ITF*. [Online]. Available: https://www.itf-oecd.org/lower-speed-means-fewer-road-deaths (visited on 11/17/2021).

[284] *The Need for (Safe) Speed: 4 Surprising Ways Slower Driving Creates Better Cities | World Resources Institute*. [Online]. Available: https://www.wri.org/insights/need-safe-speed-4-surprising-ways-slower-driving-creates-better-cities (visited on 11/17/2021).

[285] K. Olejnik, "Permissible distance - Safety system of vehicles in use," *Open Engineering*, vol. 11, no. 1, pp. 303–309, 2021, ISSN: 23915439. DOI: 10.1515/eng-2021-0032.

[286] M. A. Berlin and S Muthusundari, "Safety Distance Calculation for Collision Avoidance in Vehicular Ad hoc Networks," *Scholars Journal of Engineering and Technology*, vol. 4, no. SJET, pp. 63–69, 2016, ISSN: 2347-9523. [Online]. Available: www.saspublisher.com.

[287] A. Vadeby and Å. Forsman, "Speed Distribution and Traffic Safety Measures," *Traffic Safety*, pp. 161–176, 2016. DOI: 10.1002/9781119307853.ch11.

[288] Lockergnome, *RSS Explained*, 2007. [Online]. Available: http://www.youtube.com/watch?v=g8G5dFddz8c.

[289] S. Shalev-Shwartz, S. Shammah, and A. Shashua, "On a Formal Model of Safe and Scalable Self-driving Cars," pp. 1–37, 2017. arXiv: 1708.06374. [Online]. Available: http://arxiv.org/abs/1708.06374.

[290] P. Koopman, B. Osyk, and J. Weast, "Autonomous vehicles meet the physical world: RSS, variability, uncertainty, and proving safety," *Lecture Notes in Computer Science (including subseries Lecture Notes in Artificial Intelligence and Lecture Notes in Bioinformatics)*, vol. 11698 LNCS, pp. 245–253, 2019, ISSN: 16113349. DOI: 10.1007/978-3-030-26601-1_17.

[291] D Leblanc, H Liu, X Yan, C Flannagan, and S. F. Umtri, "Metrics and Models to Evaluate Driving Safety,"

[292] "Implementing the RSS Model on NHTSA Pre-Crash Scenarios Implementing the RSS Model on,"

[293] *RSS Explained: the Five Rules for Autonomous Vehicle Safety | Intel Newsroom*. [Online]. Available: https://newsroom.intel.com/articles/rss-explained-five-rules-autonomous-vehicle-safety/gs.91n595 (visited on 11/17/2021).

[294] *Responsibility-Sensitive Safety (RSS) A Model for Safe Autonomous Driving - Mobileye*. [Online]. Available: https://www.mobileye.com/responsibility-sensitive-safety/ (visited on 11/17/2021).

[295] C. Chai, X. Zeng, I. Alvarez, and M. S. Elli, "Evaluation of Responsibility-Sensitive Safety (RSS) Model based on Human-in-the-loop Driving Simulation," *2020 IEEE 23rd International Conference on Intelligent Transportation Systems, ITSC 2020*, vol. 2020, no. 61803283, 2020. DOI: 10.1109/ITSC45102.2020.9294637.

[296] S. Knowles Flanagan, Z. Tang, J. He, and I. Yusoff, "Investigating and modeling of cooperative vehicle-to-vehicle safety stopping distance," *Future Internet*, vol. 13, no. 3, 2021, ISSN: 1999-5903. DOI: 10.3390/fi13030068. [Online]. Available: https://www.mdpi.com/1999-5903/13/3/68.

[297] S. Noei, M. Parvizimosaed, and M. Noei, "Longitudinal control for connected and automated vehicles in contested environments," *Electronics (Switzerland)*, vol. 10, no. 16, pp. 1–28, 2021, ISSN: 20799292. DOI: 10.3390/electronics10161994.

[298] P. S. Bokare and A. K. Maurya, "Acceleration-Deceleration Behaviour of Various Vehicle Types," *Transportation Research Procedia*, vol. 25, pp. 4733–4749, 2017, ISSN: 23521465. DOI: 10.1016/j.trpro.2017.05.486. [Online]. Available: http://dx.doi.org/10.1016/j.trpro.2017.05.486.

[299] M. Naumann, H. Konigshof, and C. Stiller, "Provably Safe and Smooth Lane Changes in Mixed Trafic," *2019 IEEE Intelligent Transportation Systems Conference, ITSC 2019*, pp. 1832–1837, 2019. DOI: 10.1109/ITSC.2019.8917461.

[300] S. Shalev-Shwartz, S. Shammah, and A. Shashua, "Vision Zero: on a Provable Method for Eliminating Roadway Accidents without Compromising Traffic Throughput," pp. 1–7, 2018. arXiv: 1901.05022. [Online]. Available: http://arxiv.org/abs/1901.05022.